Synthesis and evaluation of selective inhibitors of aldosterone synthase (CYP11B2) of the naphthalene and dihydronaphthalene type for the treatment of congestive heart failure and myocardial fibrosis

Dissertation

zur Erlangung des Grades

des Doktors der Naturwissenschaften

der Naturwissenschaftlich-Technischen Fakultät III

-Chemie, Pharmazie, Bio- und Werkstoffwissenschaften-

der Universität des Saarlandes

Marieke Voets

Saarbrücken 2006

Tag des Kolloquiums: 10. März 2006

Dekan: Prof. Dr. K. Hegetschweiler

Berichterstatter: Prof. Dr.R. W. Hartmann

Prof. Dr. U. Kazmaier

Acknowledgements

With these few words I would like to thank everyone who has contributed directly or indirectly to this work:

Prof. Dr. Rolf W. Hartmann, my promoter, who offered me the opportunity to do my research in his lab and supported me throughout.

The colleagues from CRO Pharmacelsus (Saarbrücken), and in particular Dr. C. Barassin, Dr. K. Biemel and Dr. S. Barassin for performing the pharmacokinetic studies and *in vivo* assays.

This work is the result of a stimulating scientific cooperation with Dr. Ursula Müller-Vieira, Dr. Iris Antes and Dr. Sarah Ulmschneider.

I would like to thank Martina Palzer and Anja Palusczak for performing numerous *in vitro* assays, and Christiane Scherer for performing Caco-2 experiments.

I'm very grateful to Dr. Sandrine Oberwinkler-Marchais, not only for sharing her scientific expertise, but especially for her kind friendship and continuing support.

Frau Tehrani and Lothar Jager provided excellent technical assistance, and thereby contributed significantly to the efficient work environment in the lab.

Dana Wienhold, Emmanuel Bey, Anja Palusczak and Adriane Stroba I would like to thank for their sympathy and friendship, providing welcome distraction during the 'long' working hours.

To my family, mama en papa, Karin and Tom, jullie stonden altijd klaar om mij met open armen te ontvangen in België. Dankjewel voor de niet aflatende steun, voor jullie oprechte interesse en luisterbereidheid gedurende mijn tijd tussen de Teutonen.

Rudi, jij stond altijd aan mijn zijde! Zonder je onvoorwaardelijke steun, de troostende woorden wanneer ze zo nodig waren en je gezelschap was mij dit nooit gelukt. De tijd met ons tweetjes in Saarland was onvergetelijk. Dankjewel.

Diese Arbeit enstand unter Anleitung von Prof. Dr. R. W. Hartmann in der Fachrichtung Pharmazeutische und Medizinische Chemie der Universität des Saarlandes von Juni 2002 bis Juni 2005.

So far the content of this thesis has been published in or submitted to the following journals:

Voets, M.; Müller-Vieira, U.; Marchais-Oberwinkler, S.; Hartmann, R. W. Synthesis of amidinohydrazones and evaluation of their inhibitory effect towards aldosterone synthase (CYP11B2) and the formation of selected steroids. *Arch. Pharm. Pharm. Med. Chem.* **2004**, *337*, 411-416.

Voets, M.; Antes, I.; Scherer, C.; Müller-Vieira, U.; Biemel, K.; Barassin, C.; Marchais-Oberwinkler, S.; Hartmann, R. W. Heteroaryl-substituted naphthalenes and structurally modified derivatives: Selective inhibitors of CYP11B2 for the treatment of congestive heart failure and myocardial fibrosis. *J. Med. Chem.* **2005**, *48*, 6632-6642.

Voets, M.; Antes, I.; Scherer, C.; Müller-Vieira, U.; Biemel, K.; Marchais-Oberwinkler, S.; Hartmann, R. W. Synthesis and evaluation of heteroaryl-substituted dihydronaphthalenes and indenes: Potent and selective inhibitors of aldosterone synthase (CYP11B2) for the treatment of congestive heart failure and myocardial fibrosis. *J. Med. Chem.* **2006**, *49*, 2222-2231.

Voets, M.; Müller-Vieira, U.; Hartmann, R. W. Selektive Hemmstoffe humaner Corticoidsynthasen, patent submitted in **2005**.

TABLE OF CONTENTS

III.   Results

Abbreviations

ACN	Acetonitrile
ACTH	Adrenocorticotropic Hormone
$AlCl_3$	Aluminium trichloride
Arg	Arginine
AUC	Area Under the Curve
BBr_3	Boron tribromide
$B(OMe)_3$	Trimethyl borate
$B(OiPr)_3$	Triisopropyl borate
BP	Blood Pressure
Calc.	Calculated
CC	Column Chromatography
CH_2Cl_2	Dichloromethane
Cl_{int}	Intrinsic hepatic clearance
C_{max} obs.	Maximal concentration measured in the plasma
CRH	Corticotropin Releasing Hormone
CuI	Copper(I) iodide
CuO	Copper(II) oxide
CYP11B1	11β-Hydroxylase
CYP11B2	Aldosterone synthase
CYP17	17α-Hydroxylase-C17,20-lyase
CYP19	Aromatase
DHEA	Dehydroepiandrosterone
DME	1,2-Dimethoxyethane
DMF	Dimethylformamid
DMSO	Dimethylsulfoxide
EtOH	Ethanol
h	Hour(s)
Het	Heterocycle
HPLC	High Performance Liquid Chromatography
HPTLC	High Performance Thin Layer Chromatography
IC_{50}	Inhibitor concentration which inhibits 50% of the enzyme activity
Im	Imidazole

*i*Pr	Isopropyl
IR	Infrared
I.S.	Internal Standard
LC-MS	Liquid Chromatography Mass Spectrometry
Leu	Leucine
MeOH	Methanol
Met	Methionine
mp	Melting point
NADPH	Nicotinamide Adenine Dinucleotide Phosphate (reduced form)
$NADP^+$	Nicotinamide Adenine Dinucleotide Phosphate (oxidized form)
n.d.	Not determined
n.i.	No inhibition
NMR	Nuclear Magnetic Resonance
Obs.	Observed
P_{app}	Apparent permeability coefficient
Phe	Phenylalanine
po	Peroral
PPA	Polyphosphoric acid
PPh_3	Triphenylphosphine
Pro	Proline
pTSA	*p*-Toluenesulphonic acid
Pyr	Pyridine
Pyrim	Pyrimidine
RIA	Radio Immuno Assay
RT	Room Temperature
SD	Standard Deviation
$t_{1/2}$	Half-life
t_{max}	Time point with the maximal plasma concentration measured
TLC	Thin Layer Chromatography
THF	Tetrahydrofuran
Thr	Threonine
R_f	Retention Factor
UV	Ultraviolet
Val	Valine

I. Introduction

1.1. Mineralo- and glucocorticoids

1.1.1. Physiology of mineralocorticoids and regulation by the renin-angiotensin-aldosterone system

The most important circulating mineralocorticoid, aldosterone, is secreted by the zona glomerulosa of the adrenal gland (100-150µg/day). A cytochrome P450 enzyme, CYP11B2 (aldosterone synthase, see 1.1.3.) catalyzes this synthesis by converting deoxycorticosterone to corticosterone and subsequently to aldosterone (Kawamoto *et al.*, 1992). Aldosterone plays a major role in the regulation of the salt and water household of the body. By binding to the epithelial mineralocorticoid receptors in the renal cortical collecting tubules, sodium resorption and potassium excretion are promoted. Water is retented at the same time leading to volume expansion. This is an osmotic effect directly related to increased sodium resorption. The effects of aldosterone are primarily mediated by augmented expression of Na^+/K^+ ATPase pumps on the basolateral membrane of epithelial cells, and probably non-genomic effects leading to increased apical permeability for Na^+ and increased luminal H^+ permeability (Ngarmukos *et al.*, 2001). Similar effects can also be seen in the gut, the salivary and sweat glands. Besides the classical adrenal biosynthetic pathway, extra-adrenal sites of aldosterone production have been identified in brain (Gomez-Sanchez *et al.*, 1997a), blood vessels (Hatakeyama *et al.*, 1994) and in heart (Silvestre *et al.*, 1998).

The adrenal aldosterone synthesis is regulated by the renin-angiotensin-aldosterone system (RAAS) (Stewart, 2002). This compensatory mechanism is activated when small changes in sodium or potassium balance or a decrease in blood pressure occur (Figure 1). Renin, a proteolytic enzyme, is released by the juxtaglomerular apparatus in the kidney and cleaves a dipeptide from the hepatic glucoprotein angiotensinogen, thereby forming the decapeptide angiotensin I. In turn, angiotensin I is converted to the octapeptide angiotensin II by the angiotensin-converting enzyme (ACE), which is localized in the vascular endothelium. Angiotensin II is a potent vasoconstrictor and can thus elevate blood pressure but it also stimulates the zona glomerulosa of the adrenal gland to synthesize and secrete aldosterone, which leads to sodium retention and potassium loss. Angiotensin II has also an important inhibitory effect on the secretion of renin that constitutes a negative feedback mechanism. Aldosterone secretion is also regulated by the plasma potassium concentration and to a much

lesser extent by ACTH. Hyperkalemia leads to direct stimulation of the zona glomerulosa cells whilst hypokalemia inhibits the aldosterone synthesis (Stewart, 2002).

Figure 1. The renin-angiotensin-aldosterone system (adapted from Aktories *et al.*, 2005)
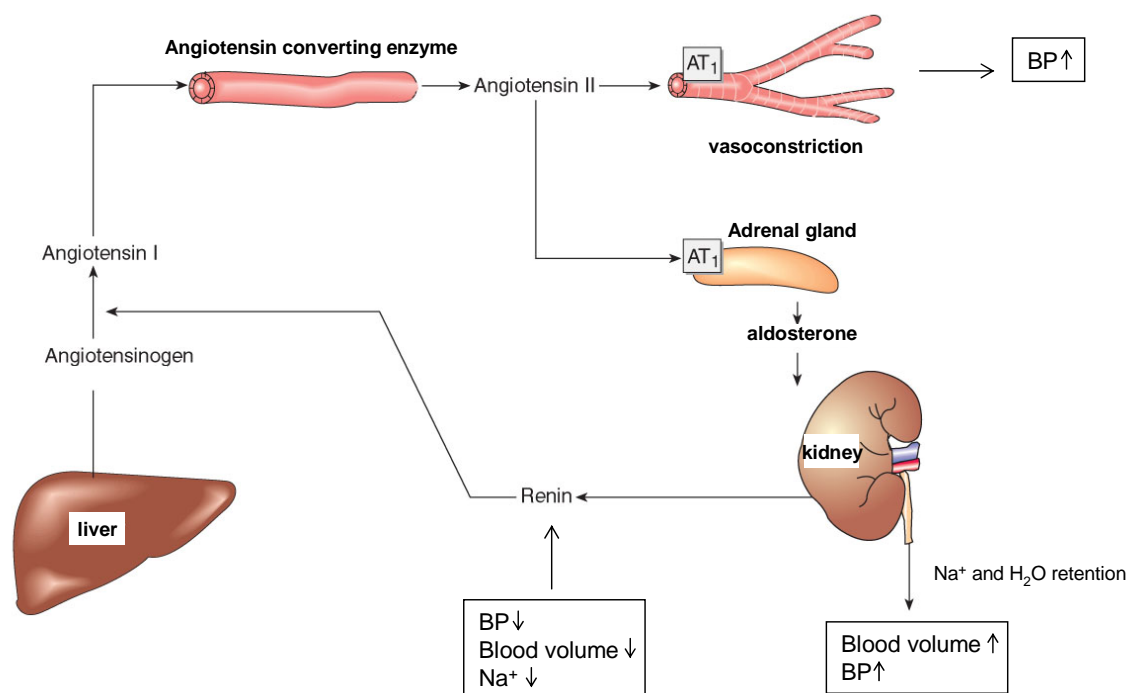
The mineralocorticoid receptors have similar affinity for both aldosterone and the glucocorticoid cortisol. Despite the fact that glucocorticoids are present at much higher concentrations in plasma, the mineralocorticoid receptors, however, clearly have specificity for aldosterone. Mineralocorticoid-responsive tissues, like kidney, colon and salivary gland, contain high concentrations of the enzyme 11β-hydroxysteroid dehydrogenase Type 2 (11β-HSD2), which converts cortisol to the inactive metabolite cortisone. As cortisone has a much lower affinity for the mineralocorticoid receptors, 11β-HSD2 inactivates the glucocorticoid and permits aldosterone to bind to and activate the mineralocorticoid receptor (Ngarmukos *et al.*, 2001). In conditions associated with a decreased activity of 11β-HSD2, cortisol accumulates and binds to the mineralocorticoid receptor, which leads to hypertension and hypokalemia. Such conditions include inhibition of 11β-HSD2 following liquorice ingestion, but also inherited impairment of 11β-HSD2 due to mutations in its HSD11B2 gene (Stewart, 2003).

1.1.2. Physiology of glucocorticoids and regulation of the glucocorticoid household

The most important glucocorticoid, cortisol, is synthesized and secreted by the zona fasciculata of the adrenal gland. A cytochrome P450 enzyme, CYP11B1 (11β-hydroxylase, see 1.1.3.) catalyzes this synthesis by converting deoxycorticosol to cortisol (Kawamoto *et al.*, 1992). The glucocorticoids act by binding to Type II glucocorticoid receptors in many cell types, like liver, muscle, adipose tissue and bone. Glucocorticoids have actions on glucose, protein and bone metabolism and possess anti-inflammatory and immunosuppressant actions.

Figure 2. The hypothalamic-pituitary-adrenal axis
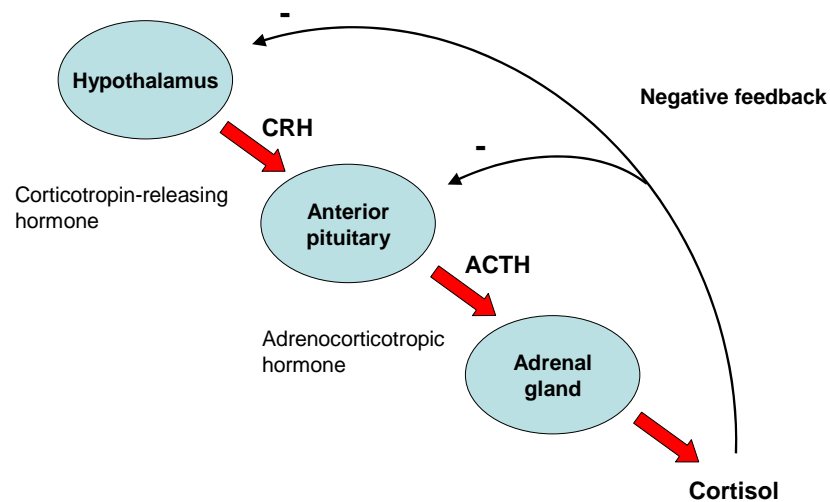
Glucocorticoids stimulate several processes that collectively serve to increase and maintain normal glucose concentrations in the blood. These include an increase in liver gluconeogenesis and an increase in amino acid degradation. In adipose tissue, cortisol stimulates lipolysis, resulting in the release of free fatty acids and glycerol. Glucocorticoids also regulate growth and development, particularly in fetal tissues. The presence of high concentrations of circulating glucocorticoids for long periods can lead to muscle wasting, inhibition of bone formation and delayed wound healing (Shupnik *et al.*, 1998). Cortisol synthesis and secretion are regulated by the pituitary hormone adrenocorticotropic hormone ACTH. Physiologically, ACTH concentration is increased in response to physical and environmental stresses. When the concentration of free cortisol in the blood is low, the hypothalamic-pituitary-adrenal axis is activated (Figure 2). The hypothalamic peptide

corticotropin-releasing hormone (CRH) acts on the pituitary to stimulate ACTH release. In turn, ACTH stimulates the zona fasciculata of the adrenal gland to produce cortisol. The hypothalamic-pituitary-adrenal axis loop is completed through cortisol-negative feedback: cortisol acts directly at the pituitary to decrease ACTH secretion and at the hypothalamus to suppress CRH release (Raff *et al.*, 2003).

1.1.3. Biosynthesis of the mineralo- and glucocorticoids

Cytochrome P450 enzymes.

The adrenal steroid hormones are produced in multi-step pathways that involve the participation of five cytochrome P450 enzymes. The name cytochrome P450 (CYP) derives from the fact that these enzymes have a heme group and an unusual spectrum (Omura *et al.*, 1964). The reduced form of the heme, when complexed with carbon monoxide, absorbs light strongly at 450 nm. The reason why cytochrome P450 absorbs in this range is the unusual ligand to the heme iron. Four ligands of the iron are provided by the pyrrole nitrogens of the porphyrine (Figure 3), the fifth coordination position is occupied by a thiolate group from a cysteine at the heme binding region of the active site. The substrate will occupy the sixth coordination position.

Figure 3. The protoporphyrine of P450
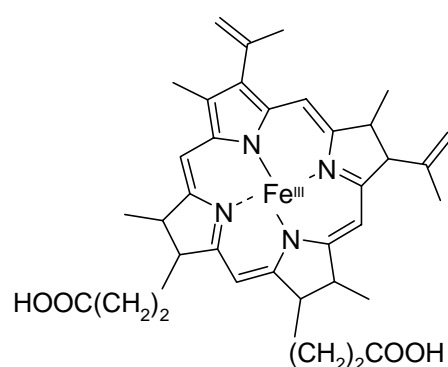
The CYP enzymes are expressed ubiquitously in different life forms: they have been found in animals, plants, fungi and bacteria. At the moment more than 2500 cytochrome P450 sequences are known (http://drnelson.utmem.edu/CytochromeP450.html). P450s in humans are either drug metabolizing enzymes or steroidogenic enzymes, e.g. enzymes involved in the biosynthesis of steroidal hormones.

The general molecular mechanism is activation and cleavage of molecular dioxygen. During the catalytic cycle a single oxygen is inserted into the substrate while the other oxygen atom leaves the reaction forming a water molecule, according Eq.1. This reaction requires the addition of two electrons (reduction) to the heme, delivered by a specific electron transfer system.

The Class-1-CYP-enzymes CYP11B1 (11β-hydroxylase) and CYP11B2 (aldosterone synthase), which are involved in the gluco- and mineralocorticoid synthesis, are membrane bound mitochondrial enzyme systems. Two soluble components, the flavoprotein adrenodoxin-reductase and the iron-sulphur protein adrenodoxin catalyze the electron transfer from NADPH to the P450 enzyme (Bureik *et al.*, 2002a) (Figure 4).

Figure 4. The electron transport pathway of Class-1-P450s (Bureik *et al.*, 2002a)
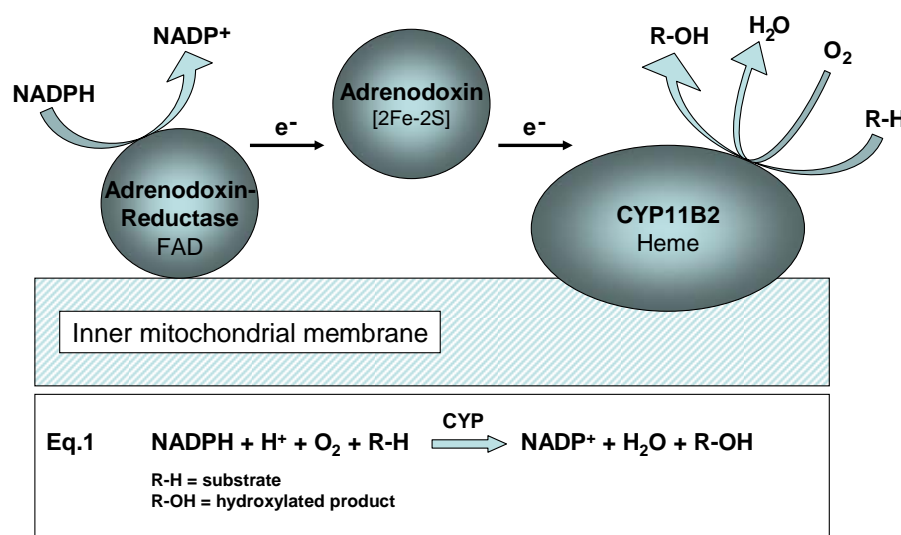
The P450 enzymes catalyze many types of reaction, including hydroxylations, epoxidations, sulfoxidations, *N*-oxidations, dealkylations and deaminations. The mechanism of hydroxylation is described in Figure 5. The binding of the substrate (R-H) to the sixth coordination position of the heme-iron (Fe^{3+}) triggers an electron transfer from the reductase protein, which causes the reduction of heme-iron. The reduced heme-iron (Fe^{2+}) is then able to coordinate molecular oxygen. Transfer of a second electron leads to the cleavage of the O-O bond, release of water and finally the transfer of one oxygen to the substrate (Meunier *et al.*, 2004).

Figure 5. Reaction cycle of the heme-iron of CYP enzymes
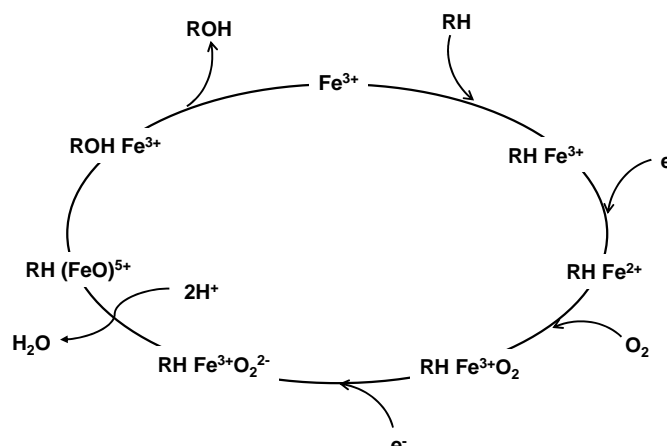
Biosynthesis of the corticoids.

The biosynthesis of the mineralo- and glucocorticoids is shown in Scheme 1. In case of the mineralocorticoids, the P450 enzyme cholesterol desmolase (CYP11A1, scc: side chain cleavage enzyme) hydroxylates and cleaves the side chain of cholesterol, the biosynthetic source of all steroidal hormones, to yield pregnenolone. This steroid is then transferred from the mitochondria to the smooth endoplasmatic reticulum, where 3β-hydroxy-steroid hydrogenase (3β-HSD) converts it into progesterone, followed by hydroxylation in position 21 by 21-hydroxylase (CYP21) to form 11-deoxycorticosterone (DOC). In the zona glomerulosa of the adrenal gland where the mineralocorticoid biosynthesis takes place, DOC is 11β-hydroxylated by aldosterone synthase (CYP11B2) to yield corticosterone. CYP11B2, located in the inner membrane of the mitochondria is the key enzyme of the mineralocorticoid synthesis. In a next step, CYP11B2 hydroxylates corticosterone in 18-position to form 18-hydroxycorticosterone. Finally, a second 18-hydroxylation and water release, catalyzed again by CYP11B2, results into the mineralocorticoid aldosterone.

The biosynthesis of the glucocorticoids starts also from cholesterol, which is converted into pregnenolone and subsequently, transformed into progesterone by 3β-HSD. This steroid is hydroxylated at position 17 by 17α-hydroxylase (CYP17) into 17α-hydroxyprogesterone and further hydroxylated at position 21 by CYP21 to form 11-deoxycortisol. In the zona fasciculata of the adrenal gland, 11-deoxycortisol is hydroxylated in position 11β by 11β-hydroxylase (CYP11B1), located inside the mitochondria, to yield the glucocorticoid cortisol. In contrast to CYP11B2, which can hydroxylate its substrate in 11β- and 18-position, CYP11B1, the key enzyme of the glucocorticoid synthesis, can only insert a hydroxyl group in 11β-position (Kawamoto *et al.*, 1992).

6

Scheme 1. The biosynthesis of corticoids

Cholesterol

Desmolase
(P450 scc)

Pregnenolone →CYP17→ **17α-Hydroxypregnenolone**

3β-HSD

Progesterone →CYP17→ **17α-Hydroxyprogesterone**

CYP21

11-deoxycorticosterone   **11-deoxycortisol**

CYP11B2   CYP11B1

corticosterone   **cortisol**

CYP11B2

18-hydroxycorticosterone   CYP11B2   **aldosterone**

7
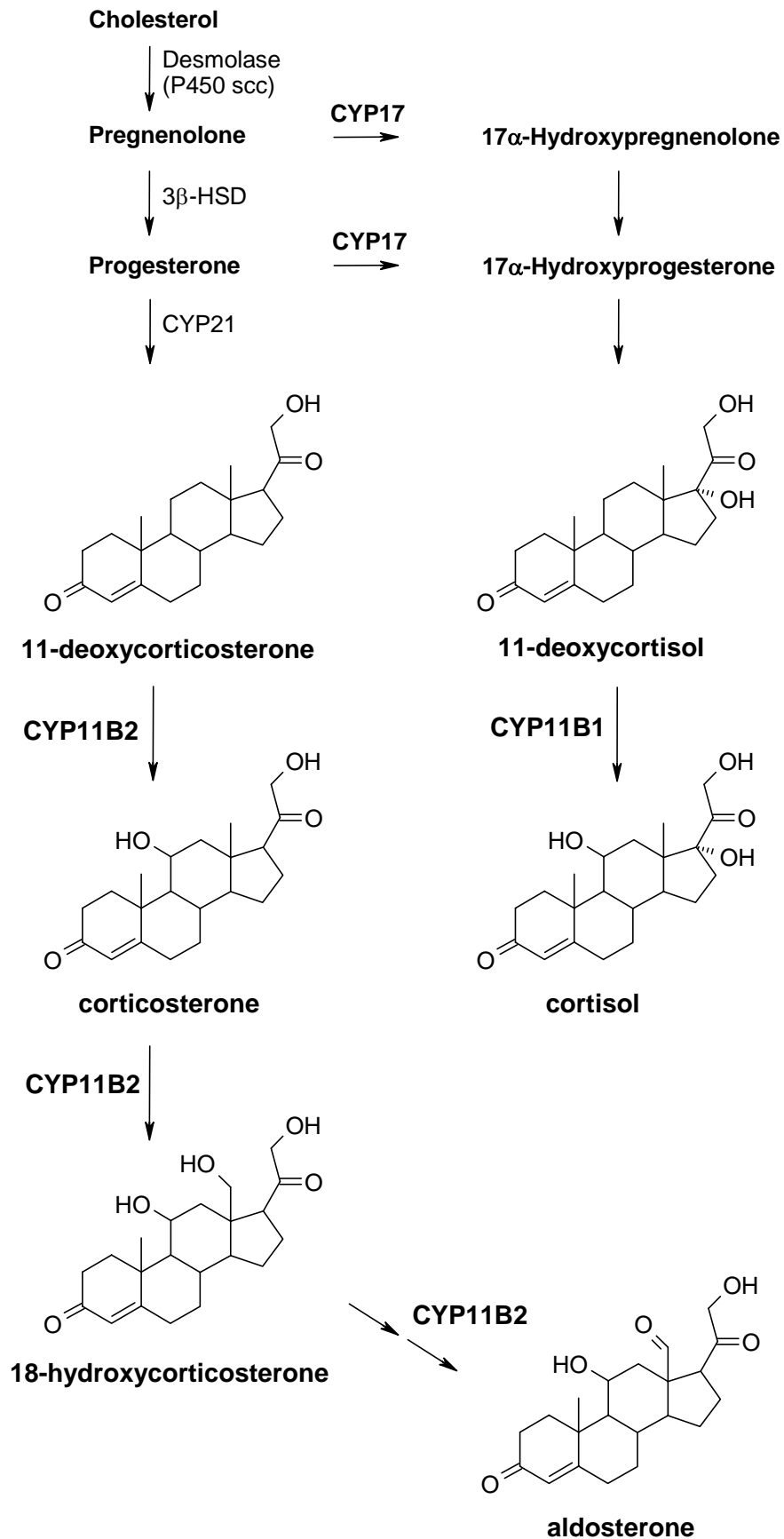
CYP11B1 and CYP11B2, the key enzymes of the corticoid biosynthesis.

Steroid 11β-hydroxylase (CYP11B1) is the key enzyme of the glucocorticoid biosynthesis. In the zona fasciculata of the adrenal gland, it catalyzes the 11β-hydroxylation of deoxycortisol into cortisol. Cortisol is the main glucocorticoid in the human and regulates energy mobilization and, thus, the stress response.

Aldosterone synthase (CYP11B2) is the key enzyme of the mineralocorticoid biosynthesis. This P450 enzyme catalyzes in the zona glomerulosa of the adrenal gland the conversion from 11-deoxycorticosterone to corticosterone by 11β-hydroxylation, and two hydroxylations in 18 position to give the most potent mineralocorticoid aldosterone. An intermediate of these last steps is 18-hydroxycorticosterone. As mentioned before, aldosterone is involved in the regulation of the salt and water household and thus the regulation of the blood pressure. CYP11B1 and CYP11B2 are both mitochondrial P450 enzymes bound to the inner mitochondrial membrane.

The genes encoding CYP11B1 and CYP11B2 are tandemly arranged on chromosome 8, approximately 45 kB apart from each other. They are about 94% identical at gene level (Taymans *et al.*, 1998). Despite this high homology, these enzymes show clearly different catalytic properties. Both CYP11B1 and CYP11B2 hydroxylate deoxycortisol and deoxycorticosterone in 11 position. However, CYP11B1 is a pure 11β-hydroxylase and can not hydroxylate in position 18. CYP11B2 does have the 11β-hydroxylase and the 18-hydroxylase activity for the aldosterone synthesis, and is also capable of hydroxylating cortisol in position 18 (Kawamoto *et al.*, 1992).

An interesting feature is the interspecies differences of these enzymes. In human, rat and mouse the corticoid synthesis is carried out by two different enzymes, as explained above. In bovine, porcine and frog, however, the gluco-and mineralocorticoid synthesis is catalyzed by a single enzyme CYP11B (Bureik *et al.*, 2002a).

The 3D-structures of CYP11B1 and CYP11B2 are unknown, since the membrane anchor prevents the proteins from crystallizing. Alternatively, homology modelling methods in which the known structures of bacterial or human P450s are being used as template, have been developed to gain insight in the 3D-structure of the active site of these enzymes (Belkina *et al.*, 2001; Ulmschneider *et al.*, 2005a; Voets *et al.*, 2005).

1.2. Pathophysiology of the renin-angiotensin-aldosterone system

1.2.1. Congestive heart failure

Congestive heart failure is described as any condition in which the heart is unable to adequately pump blood throughout the body. These conditions cause symptoms as shortness of breath, fatigue, weakness and swelling (oedema) of the legs. The most common cause is coronary artery disease and hypertension. In the United States, each year 400.000 new cases are being diagnosed. The prevalence of the disease increases with age from 1-2 per cent in 50-60 year olds to over 10 per cent in those aged 80. There is a poor prognosis with 30 per cent mortality within one year, increasing to 60-70 per cent mortality after five years (Sani, 2004).

Figure 6. Pathophysiological action of aldosterone
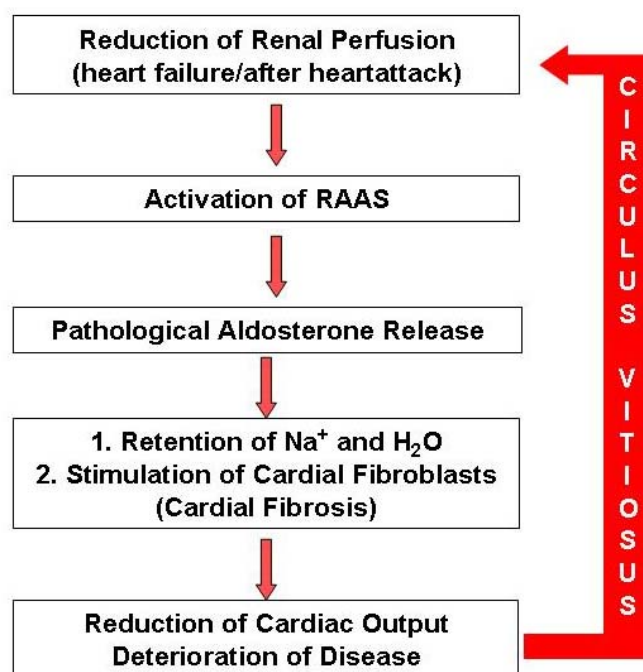
Congestive heart failure is considered to be a neurohormonal imbalance. Chronic activation of neurohormonal pathways such as the renin-angiotensin-aldosterone system leads to elevated plasma aldosterone levels, which correlate with mortality in chronic heart failure (Sani, 2004). The renin-angiotensin-aldosterone system is pathologically activated in patients with congestive heart failure to compensate for myocardial cell dysfunction and to normalise the output and function of the heart (Figure 6). Aldosterone and angiotensin II induce sodium and water retention and increased blood pressure, which lead to a further reduction of the cardiac

output. The renal perfusion is again reduced and this leads to the further release of renin ("circulus vitiosus"). This prolonged activation of the RAAS exerts adverse effects on the heart dysfunction and leads to the progression of heart failure disease (Brilla, 2000a).

1.2.2. Myocardial fibrosis

A second important effect of the pathophysiological activation of the RAAS is the stimulation of cardiac fibroblasts. Aldosterone binds to and activates mineralocorticoid receptors present in cardiomyocytes and fibroblasts in the heart. This leads to fibroblast growth and proliferation and an increased production of collagen type I and type III (Khan *et al.*, 2004). Collagen is synthesized in the fibroblasts as procollagen, which contains polypeptide extensions at its amino- and carboxy-terminal end. These peptides are removed from the procollagen by procollagen-specific proteinases, allowing the rigid collagen to integrate into the growing fibrils. The production and deposition of collagens in the cardiac fibroblasts leads to myocardial fibrosis (Lijnen *et al.*, 2000). The heart becomes stiffer and less elastic, which results in the deterioration of the heart function.

The collagen synthesis is stimulated by various growth factors, e.g. endothelin 1 (ET-1) and transforming growth factor (TGF)-β_1. Aldosterone increases the expression of ET-1 in cardiac fibroblasts. Moreover, angiotensin II decreases the activity of the matrix metalloproteinase MMP 1 which is the key enzyme of the interstitial collagen degradation (Brilla, 2000b). In this way, either effector hormone of RAAS, aldosterone and angiotensin II, induces the collagen synthesis also in an autocrine manner.

Besides the classical adrenal biosynthetic pathway, extra-adrenal sites of aldosterone production have been identified in the heart (Silvestre *et al.*, 1998). In addition to the effects of aldosterone release after RAAS activation, this cardial biosynthesis of aldosterone can have pathophysiological importance too. The myocardial expression of CYP11B2, the key enzyme of aldosterone synthesis, is increased in patients with heart failure or after myocardial infarction. This increase is associated with increased myocardial fibrosis (Satoh *et al.*, 2002). In healthy humans however, only a very small amount of CYP11B2 expression was detected. In rats, it is described that aldosterone, produced locally in the myocardium, triggers myocardial fibrosis as well (Weber *et al.*, 1990). So, in addition to the indirect effects of aldosterone on the failing heart from sodium retention, hypervolemia and hypertension,

aldosterone exerts also direct effects on the heart. The myocardial aldosterone system is regulated by the same stimuli as the adrenal system, e.g. K^+ and angiotensin II.

1.2.3. Therapy options for congestive heart failure and myocardial fibrosis

Long-term activation of the RAAS has detrimental effects on the cardiovascular system of congestive heart failure patients. Treatments that interfere or block the RAAS may improve the output of the heart and relieve the symptoms.

The major clinically useful site of enzyme inhibition is the angiotensin-converting enzyme (ACE), which promotes blood pressure elevation by converting angiotensin I to the vasoconstrictor angiotensin II (AT-II). ACE Inhibitors dilate the arteries, making it easier for the heart to pump blood throughout the body. Angiotensin receptor blockers, on the other hand, block the angiotensin II receptors and show similar action as the ACE inhibitors. Although ACE inhibitors reduce the AT-II activity, usual doses of these inhibitors do not completely block the production of aldosterone. In fact, increased levels of aldosterone may be seen after several months of therapy (Struthers, 1996). This phenomenon is called "aldosterone escape". It shows that some aldosterone production is independent of ACEs and can occur at extra-adrenal sites, such as for instance in the heart.

Beta-blockers have been shown to block renin release and conversion of prerenin to renin. They also relax the heart and reduce the vigor of its contractions. Other drugs for the treatment of heart failure are diuretics, which cause the kidneys to excrete excess amounts of salt and water in the urine, and digoxin, which increases the contractility of the heart. However, these drugs are not able to remove myocardial fibrosis, which plays an important role in the malfunction of the myocardium and the further progression of the heart disease.

1.2.4. Clinical studies with aldosterone receptor antagonists: RALES and EPHESUS

Due to the high mortality rate of heart failure patients and the knowledge about the aldosterone-induced changes of the heart, new therapy options were investigated. In 1999, results of the Randomized Aldactone Evaluation Study (RALES) showed the importance of the treatment with the aldosterone receptor antagonist, spironolactone (Aldactone®). In a double-blind study, patients with severe heart failure were treated with spironolactone, in addition to standard treatment including ACE inhibitors, diuretics and digoxin. Previous results showed that these therapeutics were not able to inhibit the aldosterone synthesis

completely (Aldosterone escape, see 1.2.3.). When spironolactone was added additionally (25mg/day), mortality among patients was reduced by 30%, hospitalization by 35%. Due to these results, the trial was discontinued in order to treat the placebo group with the effective spironolactone (Pitt *et al.*, 1999). Additionally, other studies show that spironolactone can oppose the promotion of cardiac fibrosis by aldosterone (Brilla *et al.*,1993, Zannad *et al.*, 2000) The spironolactone treatment reduced circulating levels of procollagen Type I and III peptides (Macfayden *et al.*,1997). The antagonist, however, showed progestational and antiandrogenic side effects, like gynecomastia and impotence in men and hirsutism and menstruational disturbances in women, because of its high affinity for the androgen and progesterone receptors. Moreover, a correlation between the use of spironolactone and hyperkalemia-associated mortality was observed: Juurlink demonstrated that after publication of the RALES study, the rate of prescriptions of spironolactone and hyperkalemia-associated mortality increased by a factor of 5 and 3, respectively (Juurlink *et al.*, 2004).

Eplerenone (Inspra®), a selective aldosterone receptor antagonist, has been used in the EPHESUS study (Eplerenone Post-acute myocardial infarction Heart failure Efficacy and Survival study). Eplerenone has a higher degree of selectivity for the aldosterone receptor and a low binding affinity for progesterone, androgen and glucocorticoid receptors. Patients received either placebo or eplerenone (43mg/day) within two weeks of a myocardial infarction. The study showed a decrease of sudden death by 21% and a 23% reduction in hospitalization. Due to eplerenone's higher level of selectivity, the EPHESUS study showed no increased side effects, although there was an increased incidence of hyperkalemia (Pitt *et al.*, 2003).

Figure 7. The aldosterone antagonists used in the RALES and EPHESUS studies

spironolactone

eplerenone
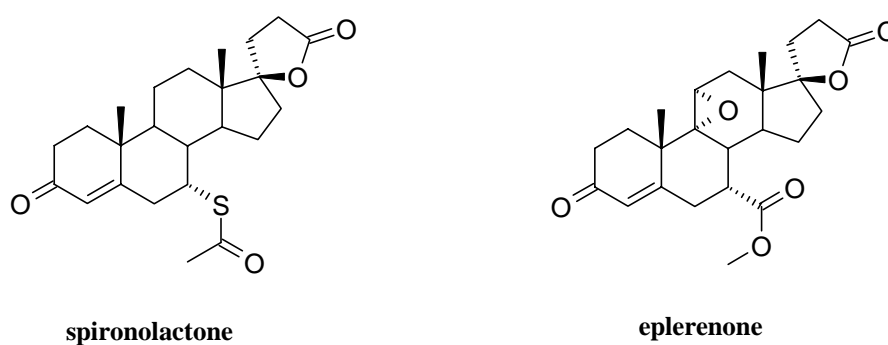
1.2.5. New therapy for the treatment of congestive heart failure and myocardial fibrosis.

The results of the RALES and EPHESUS studies show the importance of the aldosterone receptor antagonists. Blockade of aldosterone receptors substantially reduces the risk of both morbidity and death among patients with severe heart failure. The treatment with spironolactone, however, was accompanied with severe side effects because of its poor selectivity for the aldosterone receptor. Eplerenone turned out to be more selective, but the hyperkalemia-associated mortality, described for spironolactone, can be expected to occur as well. Another crucial point is that treatment with aldosterone antagonists does not reduce the high aldosterone levels in the blood.

A new therapeutic option for the treatment of congestive heart failure and myocardial fibrosis could be the blockade of the aldosterone biosynthesis, preferably by inhibition of the key enzyme CYP11B2. It should be clinically advantageous to reduce aldosterone formation rather than leaving the pathologically elevated aldosterone levels unaffected and interfering one step later at the receptor level. Non steroidal inhibitors are to be preferred because they are expected to have fewer side effects on the endocrine system than the steroidal antagonists. It is crucial that the CYP11B2 inhibitors do not affect 11β-hydroxylase (CYP11B1), the key enzyme of the glucocorticoid synthesis. To find inhibitors with selectivity towards CYP11B2 is challenging, as CYP11B1 and CYP11B2 have a sequence homology of more than 93% (Taymans *et al.*, 1998).

The CYP11B2 inhibitors could also be an interesting and promising tool for treatment of post-myocardial infarction patients. After a myocardial infarction, the myocardial aldosterone production is increased and this leads to the formation of fibrotic scar tissue, which impairs the heart function. As aldosterone antagonists were able to prevent myocardial fibrosis after myocardial infarction by blocking the cardiac aldosterone action (Silvestre *et al.*, 1999), selective CYP11B2 inhibitors could also play an important role here.

1.3.   Evaluation of new CYP11B2 inhibitors

1.3.1. Screening system for the identification of CYP11B2 inhibitors

Adequate test systems are necessary to evaluate new compounds as possible aldosterone synthase inhibitors and to determine the selectivity of these new CYP11B2 inhibitors. In the past, our working group used mitochondria from bovine adrenal cortex (Hartmann *et al.*, 1995) and tissue preparations of rat adrenal glands (Wächter *et al.*, 1996). This latter method

used ACTH stimulated rat adrenal fragments in potassium containing buffer (Häusler *et al.*, 1989). However, interspecies differences exist between human CYP11B2 and bovine CYP11B. As explained before, bovine CYP11B catalyzes the synthesis of both gluco- and mineralocorticoids and is therefore not the appropriate target enzyme to test possible CYP11B2 inhibitors. On the other hand, rat CYP11B2 has more resemblance to the human enzyme but the homology between rat CYP11B2 and human CYP11B2 (69.6%) is even less than the homology between the human and the bovine enzyme (74.3%). Thus, only the humane enzyme can be used for the testing of possible CYP11B2 inhibitors since the use of enzymes of other species can not predict the inhibitory activity towards human CYP11B2 and the selectivity towards CYP11B2. Therefore, the evaluation of inhibitors requires test systems using the human enzymes CYP11B2 and CYP11B1.

Two cell lines derived from V79 chinese hamster cells were established to express human CYP11B1 and CYP11B2. They were called V79MZh11B1 and V79MZh11B2, respectively (Denner *et al.*, 1995a). V79 cells have been proven to be suitable mammalian cells for stable expression of microsomal cytochrome P450 of human origin. Most importantly, these cells lack any endogenous cytochrome P450 activity (Denner *et al.*, 1995b). Because of the time-consuming handling of the cells and the high costs, these cell lines cannot be used for high-throughput screening. However, comparing the inhibitor's effect on two different enzymes using identical conditions is an appropriate strategy to evaluate the selectivity of the inhibitor.

Recently, our working group demonstrated the functional expression of human CYP11B2 in the fission yeast *S. Pombe* (Ehmer *et al.*, 2002). The integration of human CYP11B2-cDNA into the chromosomal DNA of *Schizosaccheromyces pombe* led to a stable recombinant yeast line PE1. Although Class-1-CYP-enzymes depend for their activity on an electron transport chain that consists of the two proteins Adx and AdR, coexpression of these proteins is not needed for efficient substrate conversion by fission yeast cells. The explanation for this phenomenon is the presence of the yeast specific protein etp1, which is capable of transferring electrons on mammalian cytochromes P450 (Bureik *et al.*, 2002b). Using this expression system, an assay could be established for the rapid, cheap and effective screening of potential CYP11B2 inhibitors.

Potent and selective inhibitors could be detected using the above described screening procedures: in a first step, candidate compounds are tested in the fission yeast system; then, the selectivity of the most potent compounds is evaluated in V79MZh11B2 and V79MZh11B1. While recombinant fission yeast provides a low-cost system, V79 cells constitute a mammalian system that is closer in the physiology to human adrenal cells.

1.3.2. Inhibitors of the aldosterone biosynthesis

Only few inhibitors of aldosterone biosynthesis are known at the moment. Mespirenone, a derivative of the aldosterone receptor antagonist spironolactone, proved to be a potent and quite specific steroidal inhibitor of the adrenal mineralocorticoid synthesis (Weindel *et al.*, 1991). The production of aldosterone was inhibited about 40% at a concentration of 100 μM in rat adrenal glands. Thus, in addition to its antagonistic effects on the receptor level, mespirenone is also able to inhibit the aldosterone synthesis.

The aromatase inhibitor fadrozole (CGS 16949A), which is in use for the treatment of breast cancer, is able to reduce aldosterone and corticosterone levels *in vitro* using rat adrenal gland fragments. It inhibits the aldosterone biosynthesis 100 times more than the corticosterone synthesis (Häusler *et al.*, 1989). *In vivo*, however, the corticoid biosynthesis is only inhibited at doses ten times higher than used in the breast cancer treatment (Demers *et al.*, 1990).

In 1994, Soll described some non steroidal inhibitors of the aldosterone biosynthesis (Soll *et al.*, 1994). The aldosterone biosynthesis inhibitory activity of guanabenz-related amidinohydrazones were evaluated in rat adrenal glomerulosa cells. The most potent compound (Figure 8) exhibited an IC_{50} value of 16 nM.

Figure 8. Steroidal and non steroidal inhibitors of the aldosterone biosynthesis

mespirenone

fadrozole

guanabenz derivative
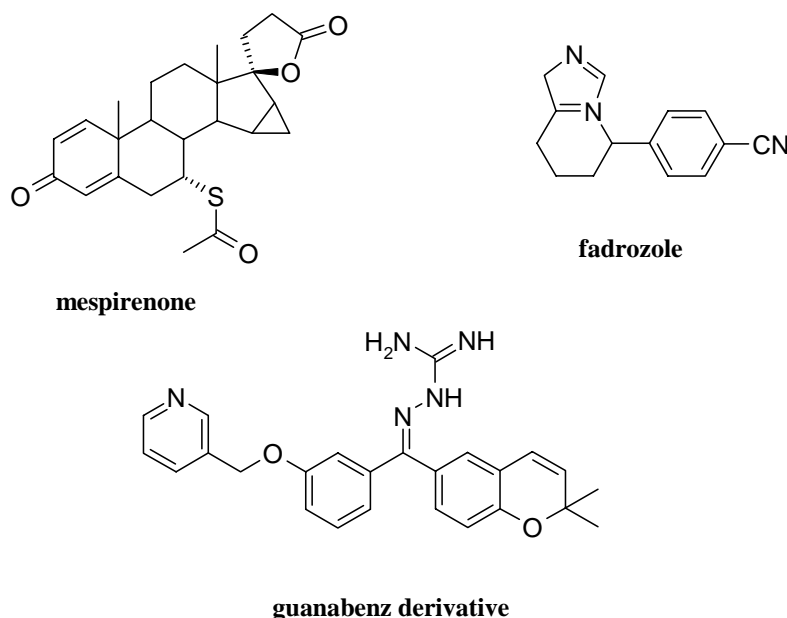
1.3.3. Inhibitors of aldosterone synthase

Until now, only a few steroidal inhibitors of aldosterone synthase are described in the literature. The 18-methyl substituted derivatives of progesterone, 18-vinylprogesterone (18-

VP) and 18-ethynylprogesterone (18-EP) were developed to bind covalently to the heme group of the P450 enzyme CYP11B2 (Defaye *et al.*, 1996). These "suicide" inhibitors have a steroidal structure, based on the natural substrate of the enzyme. They are able to inhibit the 18-hydroxylation of corticosterone to aldosterone. However, these compounds have not been tested towards the human CYP11B2.

Figure 9. Steroidal CYP11B2 inhibitors (Defaye *et al.*, 1996)

18-VP   **18-EP**
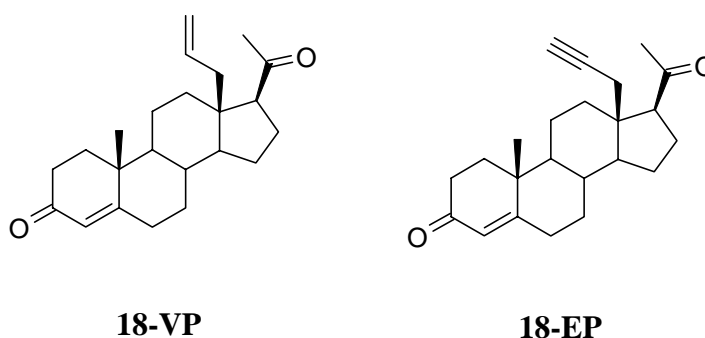
For the discovery and structural optimization of non steroidal CYP11B2 inhibitors, our in house library of compounds, which have been synthesized as potential inhibitors of P450 enzymes like CYP19, CYP17 and CYP5, was screened for inhibition of aldosterone synthase. This search resulted in several hits. Among them were the *E*-and *Z*-isomers of the unsubstituted (imidazolylmethylene)tetrahydronaphthalene and -indane (Figure 10). This class of compounds **A** was further investigated but turned out to show little or no selectivity (Ulmschneider *et al.*, 2005a). Recently, our working group found that exchange of the imidazole ring by a pyridyl moiety increased potency and especially selectivity (Ulmschneider *et al.*, 2005b). These (pyridylmethylene)tetrahydronaphthalenes and -indanes **B** proved to be potent and selective CYP11B2 inhibitors. The imidazole compounds **A** are the lead structures, from which we started in the current work.

Figure 10. Non steroidal CYP11B2 inhibitors

A   **B**

16
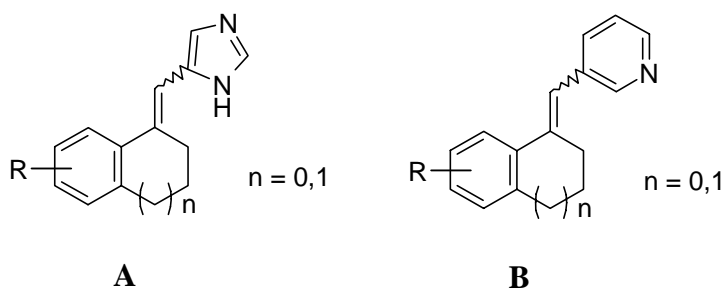
II. Aim and working strategy

2.1. Aim of this work

Chronic elevations in plasma aldosterone levels play an important role in the development and progression of congestive heart failure and myocardial fibrosis. The treatment of these cardiovascular diseases with aldosterone antagonists resulted in a reduction of mortality in heart failure patients, but was also accompanied by severe side effects.

A new pharmacological approach for the treatment of congestive heart failure and myocardial fibrosis was recently suggested by our working group, i.e. inhibition of aldosterone biosynthesis with non steroidal, selective CYP11B2 inhibitors (Ehmer *et al.*, 2002; Hartmann *et al.*, 2003). By reducing the aldosterone secretion, these inhibitors could prevent or diminish fibrotic remodelling of the failing heart and facilitate its action due to their diuretic effects.

The structure of the active site of the target enzyme is not yet elucidated, so a "key-lock" design of inhibitors is not possible. Unlike other P450 enzymes there are almost no CYP11B2 inhibitors known. Until now, only our working group described non steroidal CYP11B2 inhibitors, which are used in this work as lead compound (Ulmschneider *et al.*, 2005a; Ulmschneider *et al.*, 2005b). It is known that the concept of heme iron complexing compounds is appropriate to discover highly potent and selective inhibitors. These compounds interact with the substrate binding site in the apoprotein moiety and complex the heme iron which is located in the active site. This complexation mechanism does not only increase binding affinity of the inhibitors, but also prevents oxygen activation of the heme which is required for the catalytic process.

By modifying the lead structure, we want to enhance potency and selectivity and explore the active site of the CYP11B2 enzyme. Thus, the aim of this work was to develop *in vivo* highly active and selective non steroidal CYP11B2 inhibitors, which can be used as a novel treatment of congestive heart failure and myocardial fibrosis.

2.2. Working strategy

The working strategy used in this work is depicted in Figure 11. Starting point is the design of potential inhibitors, followed by the synthesis of the compounds and the evaluation of biological activity and probing selectivity *in vitro* and *in vivo*.

17

Figure 11. Rational drug design, synthesis and evaluation of potential drugs
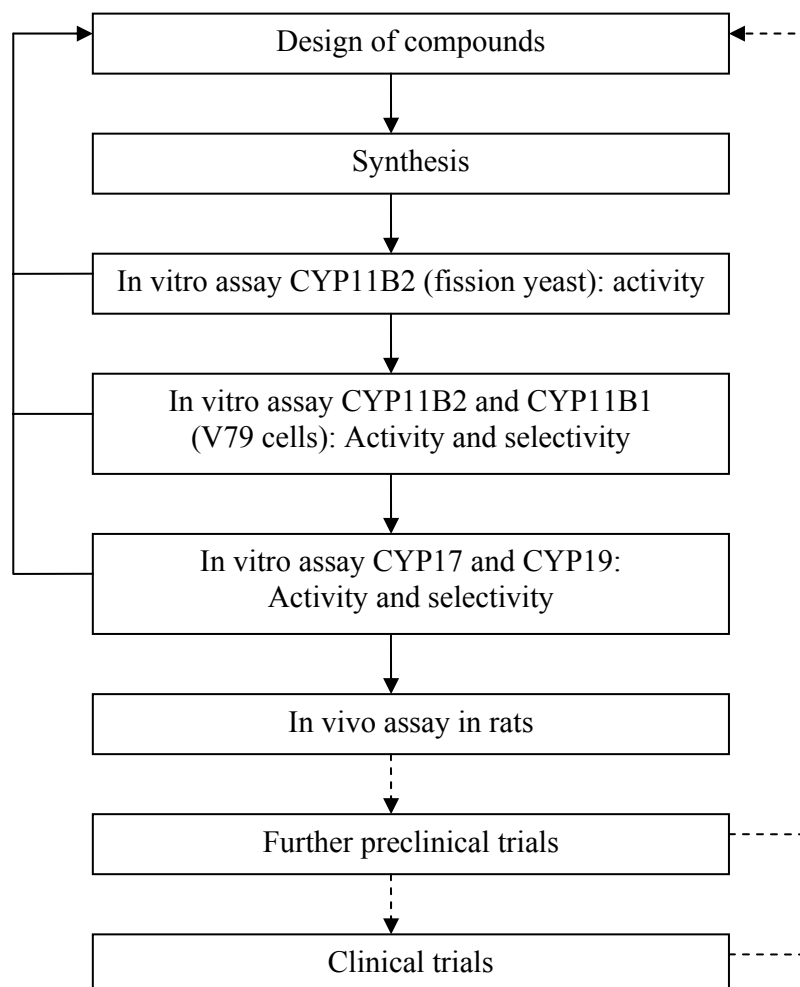
Our compounds have been designed and synthesized based on the lead structures found by screening the in-house compound library. Changing the core of our lead compound, whilst considering the fact that CYP inhibitors should contain a heme iron complexing functional group, led to new classes of compounds.

After synthesis, the potencies have to be evaluated *in vitro* towards human CYP11B2 using a human CYP11B2 expressing fission yeast system. When the compounds show good inhibitory activity they will be tested towards human CYP11B2 and CYP11B1 in V79 cells to obtain more information on activity and selectivity. The compounds will also be evaluated towards other related P450 enzymes (CYP 17, 17α-hydroxylase-C17,20-lyase and CYP19, aromatase) to check further selectivity. In a last step only highly active and selective CYP11B2 inhibitors will be tested *in vivo* to determine their ability to reduce aldosterone levels in the body.

2.3. Inhibitors of CYP11B2

Figure 12. General structures

R = H, OMe, OCH$_2$-3-Pyr
n = 0,1

R = H, OMe, OCH$_2$-3-Pyr
R' = H, OMe
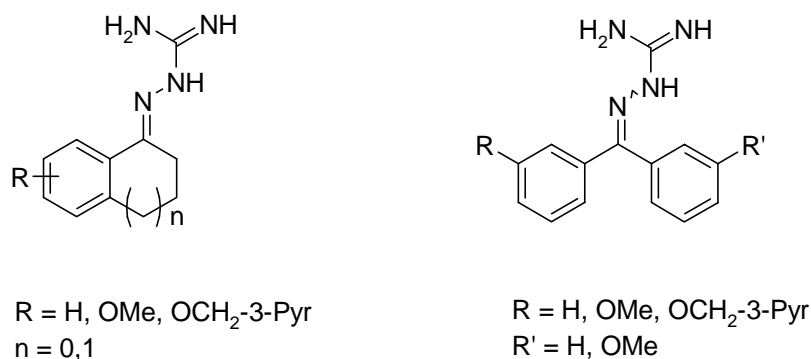
First, we have synthesized amidinohydrazones to test whether the aminoguanidine moiety is a good alternative for nitrogen containing heterocycles to obtain strong complexation with the heme group of the CYP enzyme (see 3.1.).

Figure 13. General structures

R = H, OMe
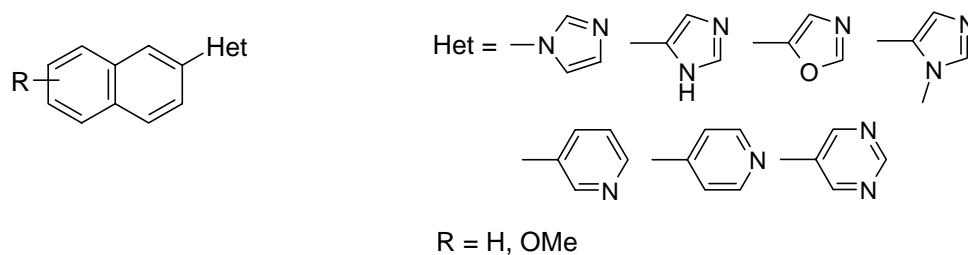
By modifying the lead compound, we found a new class of compounds, the heteroaryl substituted naphthalenes. Different azole and pyridine substituted naphthalenes, such as imidazoles, oxazoles, 3- and 4-pyridines and 5-pyrimidines, were synthesized to investigate which nitrogen containing heterocycle is most appropriate to coordinate with the heme iron (see 3.2.).

Figure 14. General structures

R = H, Br, Cl, CN, OH,
OMe, OEt, OPr, OBn
COOMe, CONHR

X,Y = CH, N
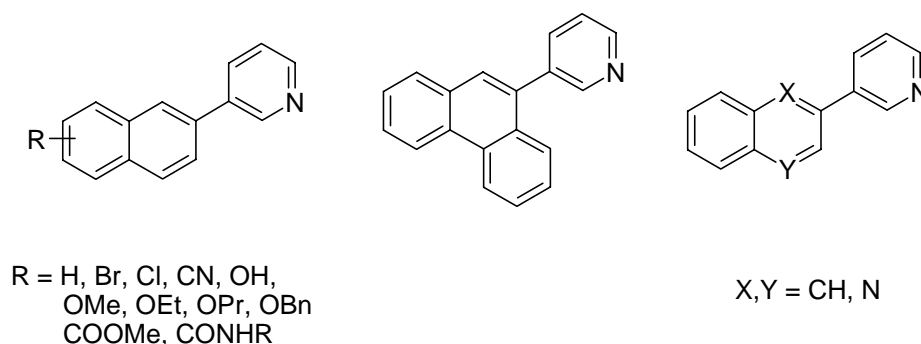
Additionally to the comparative study outlined above, we evaluated the role of the core and of the substituents in a series of 3-pyridine substituted naphthalenes. The influence of the chain length, the size and the position of the substituents on the naphthalene core was investigated (see 3.3.). Molecular dynamics studies were performed to explain interesting structure-activity relationships.

Figure 15. General structures

R = H, OMe
Het = 1-Im, 3-Pyr, 4-Pyr
n = 0,1

R',R" = H, Me, Et
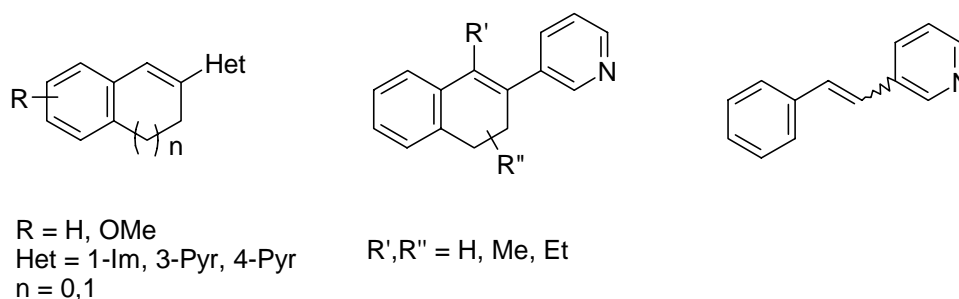
The inhibitors described in chapter 3.4. were derived from the highly active 3-pyridine substituted naphthalenes. Instead of aromatic naphthalenes, we synthesized 3-pyridine substituted 3,4-dihydronaphthalenes, indenes and styryls. Additionally, docking studies revealed the importance of hydrophobic interactions between the inhibitors and the binding pocket of aldosterone synthase.

Chapter 3.5. focused on the *in vivo* experiments of active and selective CYP11B2 inhibitors in rats. In addition, pharmacokinetic properties of active compounds were investigated *in vitro* and *in vivo*. Metabolic stability assays and Caco-2 cell permeation studies were performed on 3-pyridine substituted (dihydro)naphthalenes and indenes.

III. Results

3.1. Synthesis and biological evaluation of amidinohydrazones as inhibitors of CYP11B2

3.1.1. Introduction

A number of non steroidal inhibitors of the aldosterone synthesis have been described (Soll *et al.*, 1994). These compounds are non-azole substances carrying an amidinohydrazone group. This class of compounds is based on the α_2-adrenergic receptor agonist guanabenz **I**, which is able to inhibit the synthetic pathway of aldosterone at high concentrations. The inhibitors were evaluated in an isolated rat adrenal glomerulosa cell preparation in which the aldosterone biosynthesis was stimulated by angiotensin II. The most potent compound **II** inhibited the aldosterone formation with an IC_{50} of 16 nM. It was, however, not investigated if these compounds are specific CYP11B2 inhibitors.

Figure 16. Inhibitors of aldosterone biosynthesis

I
Guanabenz

II
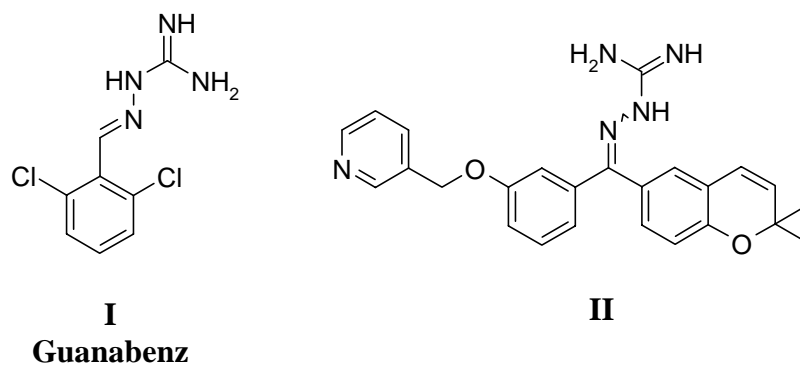
As explained before, P450 inhibitors contain a functional group, mostly a nitrogen containing heterocycle, capable of forming a coordinate bond with the heme iron of the enzyme. In order to investigate whether amidinohydrazone derivatives are CYP11B2 inhibitors and whether the non-azole moiety is a good alternative for the nitrogen containing heterocycle, we prepared a series of amidinohydrazones (Figure 17). A combination of the core of our lead structure **III** (Ulmschneider *et al.*, 2005a) and the amidinohydrazone moiety yielded compounds **1-8,12-13.** The benzophenone derivatives **9-11** were synthesized to mimic the active compound **II**. In the following we describe the syntheses of compounds **1-13** as well as their evaluation as inhibitors of human CYP11B2.

Figure 17. General structures

| | III | 1-8 12-13 | 9-11 |

$n = 0,1$ $n = 0,1$

III

1-8
12-13

9-11
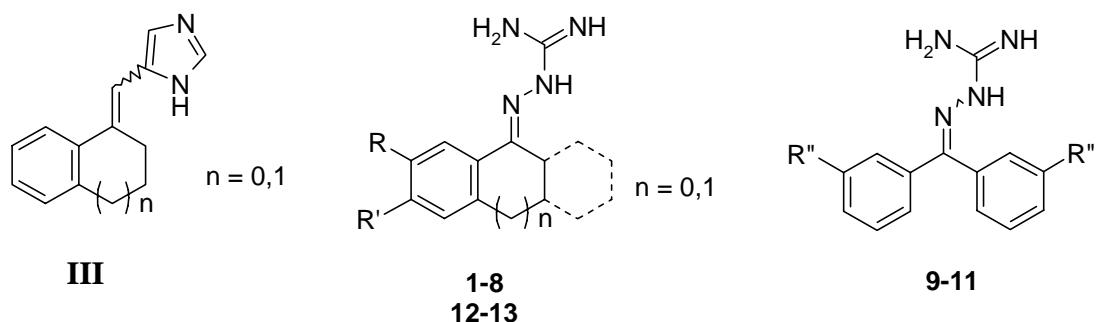
3.1.2. Synthesis

The amidinohydrazone compounds were prepared from the appropriate ketones, by condensation with aminoguanidine nitrate in methanol in the presence of sulfuric acid (method 1).

Scheme 2[a]. Synthesis of amidinohydrazones **1-8**

1-8a

1-8

	R	R'	n
1	H	H	0
2	H	H	1
3	OCH_3	H	0
4	OCH_3	H	1
5	H	OCH_3	1
6	pyridine-CH_2O	H	0
7	pyridine-CH_2O	H	1
8	H	pyridine-CH_2O	1
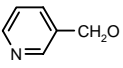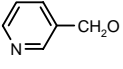
[a] : method 1: aminoguanidine nitrate, H_2SO_4, methanol, 50°C, 3 h - overnight.

Compounds **1-5** were synthesized from commercially available ketones **1-5a**. The pyridinyl compounds **6-8** were prepared from the corresponding methoxy substituted precursors **3-5a**. Demethylation with AlCl$_3$ in toluene gave the hydroxylated compounds **6-8b** (method 2). Subsequent reaction with picolyl chloride and K$_2$CO$_3$ as base gave the pyridinyl ketones **6-8a** (method 3), which reacted with aminoguanidine nitrate to give the desired pyridine compounds **6-8** (Scheme 3).

Scheme 3ª. Synthesis of 3-pyridyl ketones **6-8a**

3a R=OCH$_3$, R'=H, n=0	**6b** R=OH, R'=H, n=0	**6a** R=OCH$_2$-3-Pyr, R'=H, n=0
4a R=OCH$_3$, R'=H, n=1	**7b** R=OH, R'=H, n=1	**7a** R=OCH$_2$-3-Pyr, R'=H, n=1
5a R=H, R'=OCH$_3$, n=1	**8b** R=H, R'=OH, n=1	**8a** R=H, R'=OCH$_2$-3-Pyr, n=1
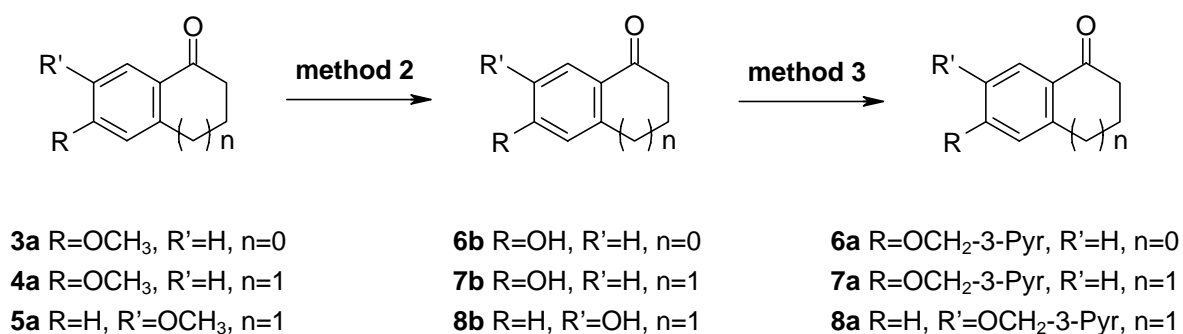
[a] : method 2: AlCl$_3$, toluene, reflux, 2 h; method 3: picolyl chloride hydrochloride, K$_2$CO$_3$, DMF, 100°C, 3 h.

The compounds **1-8** were characterized using proton NMR and the geometry of the hydrazone function was determined with Nuclear Overhauser Effect experiments. Only the isomer with the guanidine function anti to the aromatic ring could be detected. This anti-configuration, which is in analogy with results found by single-cristal X-ray diffraction of the 6-methoxytetralone derivative **4** (Pitzele *et al.*, 1988), might be related to steric hindrance.

The benzophenone derivatives **9-11** were prepared from (3-methoxyphenyl) phenyl-methanone **9a** (Negash *et al.*, 1997) and bis(3-methoxyphenyl)methanone **10a** (Riechers *et al.*, 1996). The pyridine analogue **11a** was synthesized, starting from the methoxy compound **9a**. Demethylation with BBr$_3$ gave the hydroxylated compound **11b** (method 4), which reacted with picolyl chloride and K$_2$CO$_3$ to give the pyridine compound **11a** (method 3). Condensation of the benzophenones **9-11a** with aminoguanidine nitrate (method 1) or sulfate (method 5) yielded the wanted compounds **9-11** as a mixture of isomers (ratio1:1). The two isomers have very close R$_f$ values and could not be separated using column chromatography.

Scheme 4[a]. Synthesis of the diphenylmethylene compounds **9-11**

9a R=H, R'=OCH$_3$
10a R=R'=OCH$_3$
method 4 ⌐ **11a** R=H, R'=OCH$_2$-3-Pyr.
method 3 ⌐ **11b** R=H, R'=OH

9 R=H, R'=OCH$_3$
10 R=R'=OCH$_3$, HNO$_3$-salt
11 R=H, R'=OCH$_2$-3-Pyr.
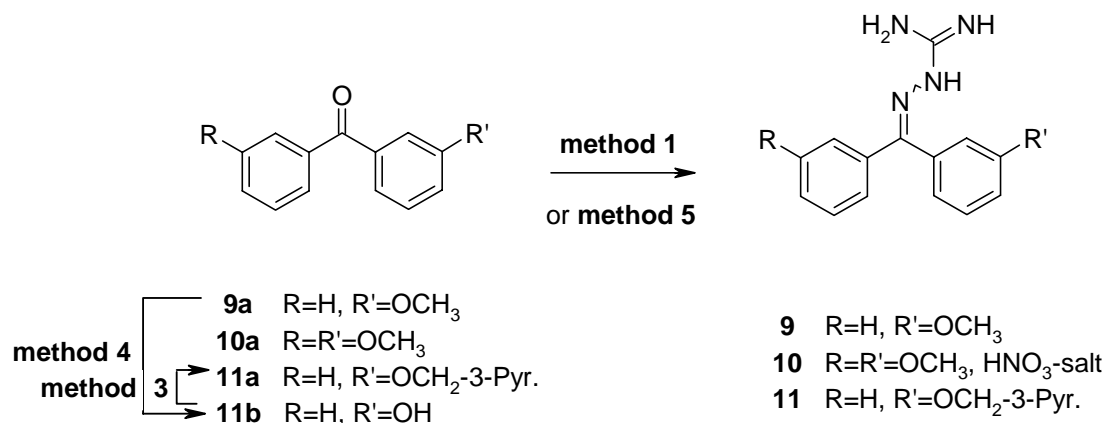
[a] : method 1: aminoguanidine nitrate, H$_2$SO$_4$, methanol, 50°C, 3 h - overnight; method 3: picolyl chloride hydrochloride, K$_2$CO$_3$, DMF, 100°C, 3 h; method 4: BBr$_3$, CH$_2$Cl$_2$, -78°C, overnight; method 5: aminoguanidine hemisulfate, H$_2$SO$_4$, methanol, reflux, 24 h.

The tricyclic amidinohydrazone compound **12** and semicarbazone **13** were prepared from the condensation of 9H-fluorenone **12a** with aminoguanidine nitrate and semicarbazide hydrochloride, respectively (method 1 or method 6).

Scheme 5[a]. Synthesis of the tricyclic compounds **12-13**

12a

12 X=NH, H$_2$SO$_4$ salt
13 X=O, HCl salt
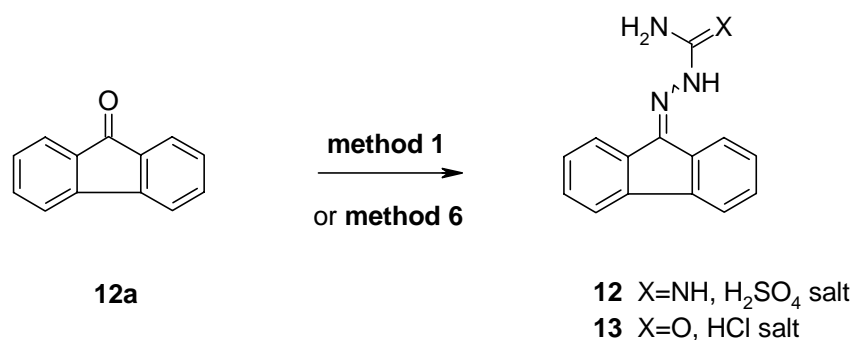
[a] : method 1: aminoguanidine nitrate, H$_2$SO$_4$, methanol, 50°C, 3 h - overnight;
method 6: semicarbazide hydrochloride, NaOAc, H$_2$O, RT, overnight.

3.1.3. Biological results and discussion

The inhibitory activity of compounds **1-13** and fadrozole as a reference was determined *in vitro* using CYP11B2 expressing fission yeast. The fission yeast was incubated with [^{14}C]-deoxycorticosterone as substrate in the presence of the inhibitor at a concentration of 500 nM. The percent inhibition values are presented in Table 1.

Table 1. Inhibition of human CYP11B2 by amidinohydrazones **1-13**

Compound	% inhibition[a] human CYP11B2[b]
1	n.i.
2	n.i.
3	1.3
4	n.i.
5	1.0
6	10.9
7	10.6
8	3.2
9	2.8
10	3.1
11	n.i.
12	n.i.
13	n.i.
fadrozole	68

[a] Mean value of four determinations, standard deviation less than 10%. [b] *S. pombe* expressing human CYP11B2; substrate: deoxycorticosterone, 100 nM; inhibitor, 500 nM. n.i. = no inhibition.

The amidinohydrazones did not show any inhibitory effects towards human CYP11B2, except for the pyridine compounds **6** and **7**. These two compounds showed a 10% inhibition of the target enzyme CYP11B2.

These results might be due to the fact that the amidinohydrazone compounds are not able to reach the active site of the target enzyme in the yeast cell. The expression of CYP11B2 in yeast can cause in some cells the formation of inclusion bodies between the inner and the

outer membrane of the mitochondria (Bureik *et al.*, 2002b), making it more difficult for the compounds to enter the cells. To investigate this theory, we used human cells in a further experiment. Similarly to the assay described by Soll (Soll *et al.*, 1994) using rat zona glomerulosa primary cells, the pyridine compound **11** was tested for its effect towards the adrenocortical tumor cell line NCI-H295R (Gazdar *et al.*, 1990; Rainey *et al.*, 1994). This cell line is derived from an invasive human adrenocortical tumour and is able to produce all the adrenocortical steroids, e.g. mineralocorticoids, glucocorticoids and adrenal androgens. The steroid concentrations were measured after exposition of the cells to the selected compound. Compound **11**, which is very similar to the most active compound described by Soll *et al.*, had no effect on the formation of aldosterone, cortisol or the androgens, androstenedione and DHEA (Table 2).

Table 2. Effect of compound **11** on the formation of selected steroids in the adrenocortical tumor cell line NCI-H295R

Steroid secretion	Compound **11**	Control
Aldosterone (pg/ml)	1364.4 ± 165.8	1360.5 ± 157.2
Cortisol (ng/ml)	38.43 ± 2.64	38.56 ± 1.14
Androstenedione (ng/ml)	3.06 ± 0.38	3.49 ± 0.33
DHEA (ng/ml)	11.31 ± 0.62	10.36 ± 0.44

An explanation for this inactivity could be the fact that the amidinohydrazones are strong bases. Under physiological conditions, the compounds are protonated and may not be able to permeate the cell membrane. Experiments using cell free homogenate were not performed, because we are only interested in potential inhibitors that can pass the cell membranes.

We can conclude that our amidinohydrazone compounds are not able to penetrate cells and/or to inhibit CYP11B2 intracellularly. Neither do they show an effect on human steroidogenic CYP enzymes within the cell. The amidinohydrazone moiety is not a good alternative for the azole group, which is an important structural feature of CYP inhibitors. Its aromatic nitrogen is able to complex the heme iron of the CYP enzyme and its pK_b-value is more or less in the range of physiological pH. This enables the compound to permeate cell membranes as a base.

3.2. Synthesis and biological evaluation of heteroaryl substituted naphthalenes as inhibitors of CYP11B2.

3.2.1. Introduction

We recently reported that amidinohydrazones are not able to inhibit CYP11B2 (Voets *et al.*, 2004, see 3.1.). These compounds were not able to penetrate cells because of their unfavorable pK_b-values and/or to inhibit CYP11B2 intracellularly. In search of a new approach, we returned to the azole substituted lead structure **III**. We changed the core structure of **III** by moving its exocyclic double bond into the ring. In this way we found a new class of compounds, the heteroaryl substituted naphthalenes **IV** (Figure 18).

Figure 18. From lead structure **III** to a new class of inhibitors **IV**
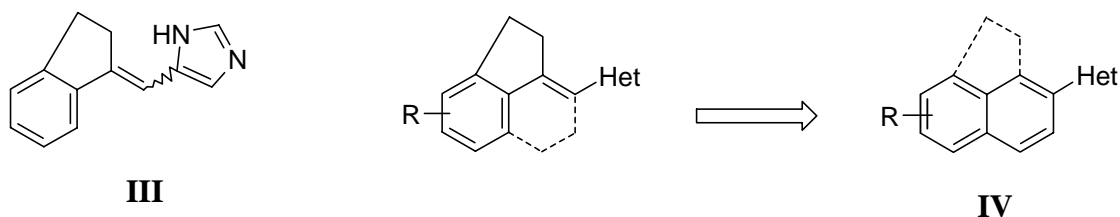
Different azole and pyridine substituted naphthalenes, such as 1- and 5-imidazoles, 5-oxazoles, 3- and 4-pyridines and 5-pyrimidines, were synthesized to investigate which nitrogen containing heterocycle is most appropriate to coordinate with the heme iron of our target enzyme. This section contains the syntheses and the biological evaluation of these heteroaryl substituted compounds **14-23** (Figure 19).

Figure 19. General structures
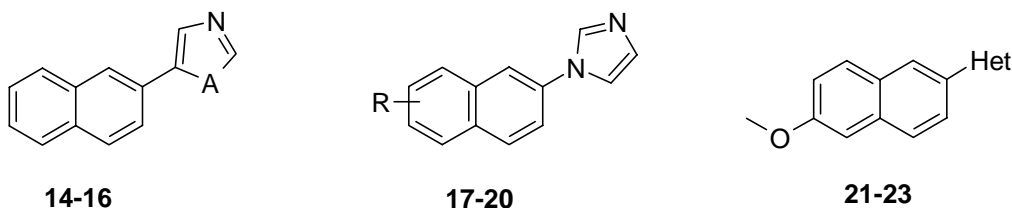
3.2.2. Synthesis

5-Naphthalen-2-yl-1*H*-imidazole **14** was prepared by reacting 2-bromo-1-(2-naphthyl)ethanone **14a** with formamide at high temperatures (method 8) (Bredereck *et al.*, 1953). The bromocompound **14a** was synthesized through bromination of 2-acetonaphthone **14b** with tetrabutylammonium tribromide (method 7). The reaction of tosylmethylisocyanide (tosmic) with *N*-methylimine **15a** or the aldehyde **16a** yielded the *N*-methylimidazole **15** or the oxazole **16**, respectively (method 9).

Scheme 6[a]. Synthesis of azole substituted naphthalenes **14-16**

14 A = NH
15 A = NMe
16 A = O

15a A = NMe
16a A = O
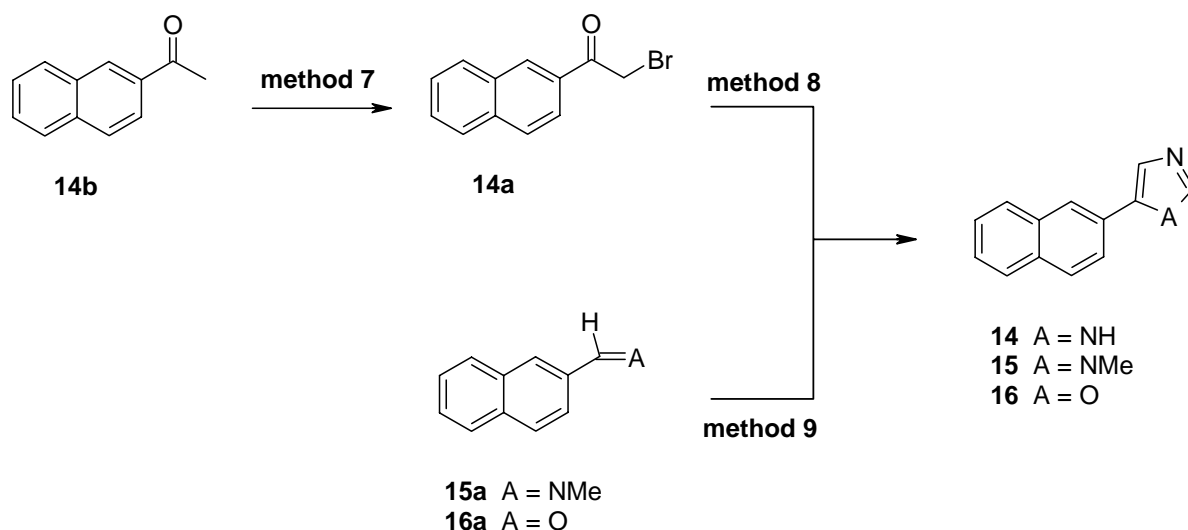
[a] : method 7: tetrabutylammonium tribromide, CH_2Cl_2/methanol, RT, 1 h; method 8: formamide, 185°C, 2 h; method 9: tosmic, K_2CO_3, RT, overnight.

The reaction of the naphthylboronic acid **17-19a** with imidazole in the presence of a copper salt yielded the 1-imidazole substituted naphthalenes **17-19** (method 11-12) (Lam *et al.*, 1998; Lan *et al.*, 2004). The boronic acids **17a** and **19a** were commercially available. 2-Methoxy-3-naphthylboronic acid **18a** was prepared by treating 2-methoxynapthalene **18b** with *n*BuLi and B(OCH$_3$)$_3$ (method 10). The 1-imidazole substituted quinoline **20** was prepared by coupling 3-bromoquinoline **20a** with imidazole in the presence of CuO (method 13) (Kauffmann *et al.*, 1982).

Scheme 7^a. Synthesis of 1-imidazole substituted naphthalenes **17-20**

17a R = H
18a R = 3-OMe
19a R = 6-OMe

17-20

18b

20a
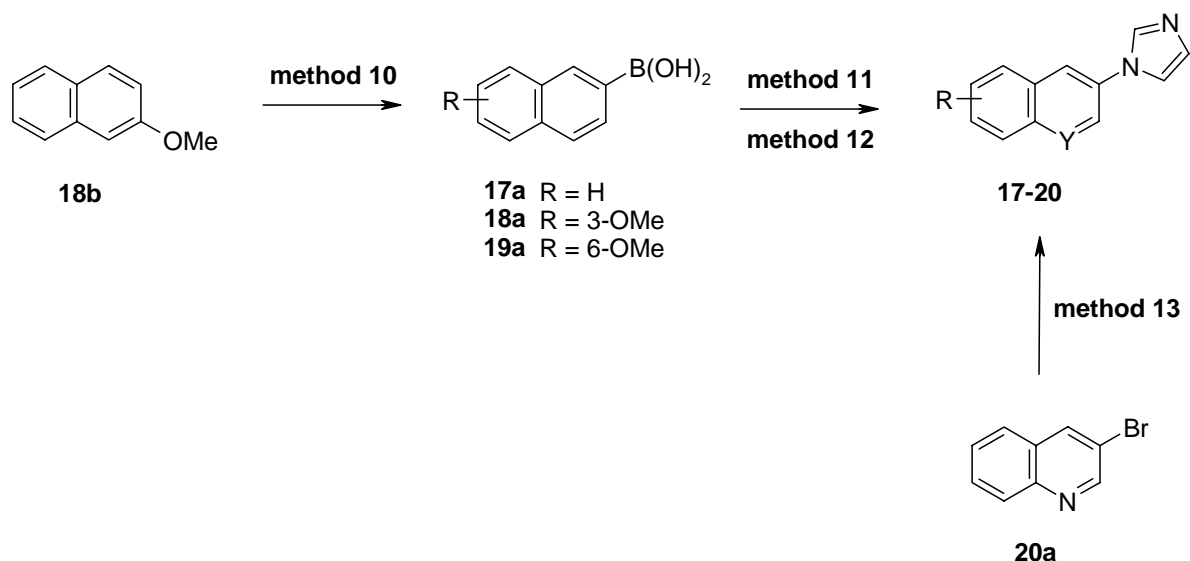
^a : method 10: 1) *n*BuLi, THF, -20 °C – RT, 2 h 2) B(OCH$_3$)$_3$, -60 °C, 1 h, RT, overnight 3) HCl, RT, 20 min; method 11: imidazole, Cu(OAc)$_2$, CH$_2$Cl$_2$, RT, 48 h; method 12: imidazole, CuI, methanol, reflux, 3 h; method 13: imidazole, CuO, K$_2$CO$_3$, nitrobenzene, reflux, 24 h.

A general method for introducing a pyridyl or pyrimidyl group on the naphthalene ring is the Pd-catalyzed cross-coupling of bromonaphthalenes with suitable pyri(mi)dyl containing nucleophilic coupling partners. In this case we used the Suzuki coupling.

The first step of the synthesis of the wanted compounds **21-23** was the preparation of the heteroarylboronic acids **24-26**. *n*Butyllithium was added to a mixture of bromopyri(mi)dine **24-26a** and triisopropyl borate, followed by an acid quench (method 15) (Li *et al.*, 2002). The next step was the Suzuki coupling of the 2-bromo-6-methoxynaphthalene **21a** with the heteroarylboronic acids **24-26** in the presence of potassium carbonate and tetrakis(triphenylphosphine)palladium as a catalyst (method 14) (Miyaura *et al.*, 1995).

Scheme 8ᵃ. Synthesis of pyri(mi)dine substituted naphthalenes **21-23**
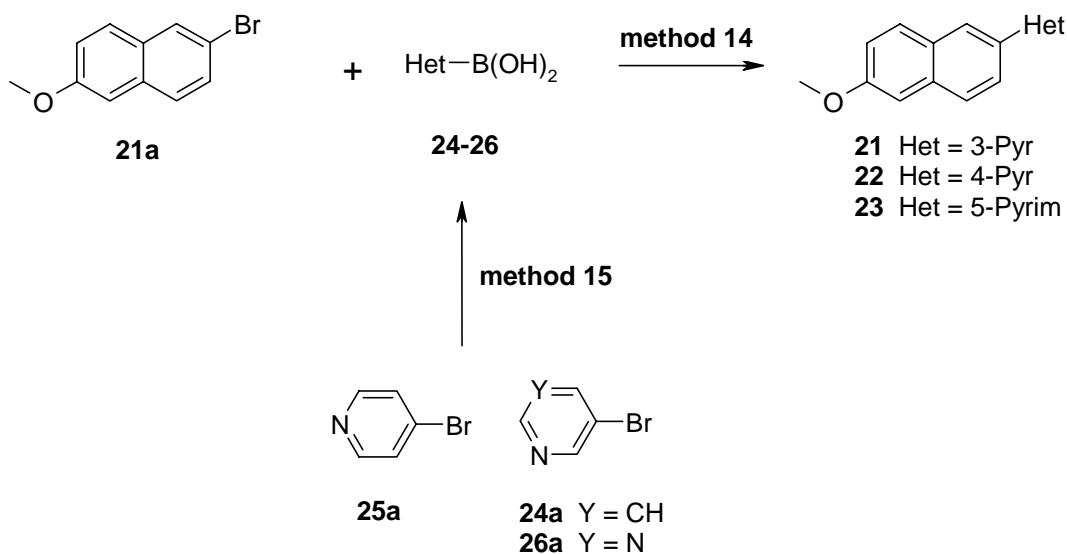
ᵃ : method 14: NaCO$_3$, Pd(PPh$_3$)$_4$, DME, 80°C, overnight; method 15: 1) B(OiPr)$_3$, nBuLi, toluene/
THF, -70°C, 0.5 h 2) HCl, -20°C - RT.

3.2.3. Biological evaluation

For the determination of the inhibitory activity of compounds **14-23** and fadrozole as a reference, CYP11B2 expressing fission yeast was used. The fission yeast was incubated with inhibitor and [^{14}C]-deoxycorticosterone as substrate. The product formation was monitored by HPTLC using a phosphoimager. The percent inhibition values are shown in Tables 3 and 4. The compounds, showing more than 60% inhibition in *S. Pombe*, as well as a few other compounds with less activity, were tested om V79 MZh cells expressing either CYP11B1 or CYP11B2 (Ehmer *et al.*, 2002) to get information about activity and selectivity in mammalian cells. The same substrate and similar conditions for incubation, extraction and analytics were used as described for the yeast assay. The IC$_{50}$ values at a concentration of 500 nM are also presented in Tables 3 and 4.

Table 3. Inhibition of human adrenal CYP11B1 and CYP11B2 by azole substituted
compounds **14-20**

14-16

17-20

Compound	A	R	% inhibition[a] CYP11B2[b]	IC$_{50}$-value (nM)[c]		Selectivity factor[f]
				V79 11B1[d] CYP11B1	V79 11B2[e] CYP11B2	
14	NH		41	207	296	0.7
15	NMe		28	n.d.	n.d.	-
16	O		11	805	12	66
17		H	80	1317	38	35
18		3-OMe	87	81	19	4
19		6-OMe	49	849	218	4
20		Y=N	17	6338	604	10
fadrozole			68	10	1	10

[a] Mean value of four determinations, standard deviation less than 10%. [b] *S. pombe* expressing human CYP11B2; substrate: deoxycorticosterone, 100 nM; inhibitor, 500 nM. [c] Mean value of four determinations, standard deviation less than 20%. n.d. = not determined. [d] Hamster fibroblasts expressing human CYP11B1; substrate: deoxycorticosterone, 100 nM. [e] Hamster fibroblasts expressing human CYP11B2; substrate: deoxycorticosterone, 100 nM. [f] IC$_{50}$ CYP11B1/ IC$_{50}$ CYP11B2.

As seen in Table 3, the azole substituted naphthalenes **14-16** and **19-20** exhibited moderate to low potency in the yeast assay (11-49%). Only the unsubstituted and 3-methoxy substituted 1-imidazolyl naphthalenes **17** and **18** showed a pronounced inhibitory activity (80-87%) higher than the reference fadrozole (68%). These compounds **17** and **18** were also very active towards CYP11B2 in V79 cells with IC$_{50}$ values of 38 nM and 19 nM, respectively. The compounds **14, 19** and **20**, which showed moderate to low activity in the yeast assay, exhibited higher IC$_{50}$ values in the V79 assay in the range between 218 and 604 nM. The IC$_{50}$ values were thus in good accordance with the values of the yeast assay. The only exception was the oxazolyl compound **16**, which was very potent in the mammalian cell assay (IC$_{50}$ = 12 nM) and showed almost no activity in the yeast assay (11% inhibition). This oxazole

31

substituted compound **16** turned out to be the most selective inhibitor of this series with a selectivity factor of 66. This means that **16** is 66 times more potent towards CYP11B2 than CYP11B1 and is much more selective than the reference fadrozole (selectivity factor = 10). The other azole substituted naphthalenes **17-20** displayed a variety of moderate to low selectivity factors ranging from 4 to 35. Interestingly, the 5-imidazolyl compound **14** exhibited a selectivity factor of 0.7.

Table 4. Inhibition of human adrenal CYP11B1 and CYP11B2 by pyri(mi)dine substituted compounds **21-23**

21-23

Compound	Het	% inhibition[a] CYP11B2[b]	IC$_{50}$-value (nM)[c] V79 11B1[d] CYP11B1	IC$_{50}$-value (nM)[c] V79 11B2[e] CYP11B2	Selectivity factor[f]
21	3-Pyr	91	1577	6	263
22	4-Pyr	n.i.	n.d.	n.d.	-
23	5-Pyrim	29	n.d.	n.d.	-
fadrozole		68	10	1	

[a] Mean value of four determinations, standard deviation less than 10%. [b] *S. pombe* expressing human CYP11B2; substrate: deoxycorticosterone, 100 nM; inhibitor, 500 nM. n.i. = no inhibition [c] Mean value of four determinations, standard deviation less than 20%. n.d. = not determined. [d] Hamster fibroblasts expressing human CYP11B1; substrate: deoxycorticosterone, 100 nM. [e] Hamster fibroblasts expressing human CYP11B2; substrate: deoxycorticosterone, 100 nM. [f] IC$_{50}$ CYP11B1/ IC$_{50}$ CYP11B2.

When we compare the pyri(mi)dine substituted compounds, we notice the high activity of the 3-pyridine substituted compound **21** (Table 4). In the yeast assay, compound **21** inhibited the target enzyme CYP11B2 with 91%. In the V79 cell assay, it has a very low IC$_{50}$ value of 6 nM. Additionally, the 3-pyridine substituted compound is surprisingly selective with a selectivity factor of 263. The 4-pyridine and 5-pyrimidine substituted compound **22** and **23**, on the other hand, showed moderate or no inhibition at all.

For the compounds which displayed activity towards CYP11B2, the selectivity towards other steroidogenic CYP enzymes, the estrogens producing CYP19 (aromatase) and the androgens forming CYP17 (17α-hydroxylase-C17,20-lyase), was investigated (Table 5).

Table 5. Inhibition of human CYP19 and human CYP17 by heteroaryl substituted compounds **14-23**

				IC$_{50}$-value (nM)^a	% inhibition^c [IC$_{50}$-value (nM)]
Compound	A	R	Het	human CYP19^b	human CYP17^d
14	NH			n.d.	n.d.
15	NMe			n.d.	n.d.
16	O			n.d.	n.d.
17		H		2821	13
18		3-OMe		129	4
19		6-OMe		n.d.	n.d.
20		Y=N		n.d.	n.d.
21			3-Pyr.	586	72 [667]
22			4-Pyr.	n.d.	n.d.
23			5-Pyrim.	n.d.	n.d.
fadrozole				30	5
ketoconazole				n.d.	40

^{a} Mean value of four determinations, standard deviation less than 20%. n.d. = not determined ^{b} human placental CYP19; 1mg/ml of protein; substrate: androstenedione, 500 nM. ^{c} Mean value of four determinations, standard deviation less than 10%. n.d. = not determined. ^{d} E.coli expressing human CYP17; 5 mg/ml; substrate: progesterone, 2.5 μM; inhibitor, 2.5 μM.

The IC$_{50}$ values of the compounds for CYP19 were determined *in vitro* using human placental microsomes and [1β-^{3}H]androstenedione as substrate as described by Thompson and Siterii

(Thompson and Siterii, 1974) using our modification (Hartmann and Batzl, 1986). The compounds **17** and **21** exhibited very low inhibitory activity with IC_{50} values of 2821 nM and 586 nM. Only compound **18** had an IC_{50} value of 129 nM, which is still much higher than the IC_{50} value of the reference fadrozole ($IC_{50} = 30$ nM).

The percent inhibition values of the compounds towards CYP17 were determined *in vitro* using progesterone as substrate an the 50.000g sediment of *E.coli* recombinantly expressing human CYP17 (Hutschenreuter *et al.*, 2004). The 1-imidazole substituted compounds **17** and **18** exhibited a weaker (4-13%) inhibition as the reference ketoconazole (40%) at a concentration of 2.5 μM. This is not a strong inhibition taking into consideration that potent CYP17 inhibitors are much more active than ketoconazole (IC_{50} ketoconazole = 4.5 μM; IC_{50} **SA40** = 36 nM; factor = 125) (Hutschenreuter *et al.*, 2004). The 6-methoxy compound **21** showed a higher activity towards CYP17 with an IC_{50} value of 667 nM.

3.2.4. Discussion and conclusion

The (imidazolylmethylene)tetrahydronaphthalenes and –indanes described by our working group (Ulmschneider *et al.*, 2005a), proved to be potent and moderate selective CYP11B2 inhibitors. With the aim of further increasing activity and most of all selectivity towards aldosterone synthase, we modified the lead compound **III** (Figure 18). Instead of exocyclic double bond bearing (imidazolylmethylene)tetrahydronaphthalenes and indanes, we synthesized a series of heteroaryl substituted naphthalenes **14-23**.

An important requirement for strong CYP inhibitors is a nitrogen containing heterocycle which can complex with the heme iron of the target enzyme. This complexation mechanism does not only increase binding affinity of the inhibitors, but also prevents oxygen activation of the heme which is required for the catalytic process. Different heteroaryl substituted naphthalenes were synthesized and tested for their potency towards CYP11B2. The 3-pyridine substituted compound **21** turned out to be very active and highly selective with an IC_{50} value of 6 nM and a selectivity factor of 263. The replacement of this group by other heterocyclic moieties, like 4-pyridine, 5-pyrimidine, 1- and 5-imidazole and 5-oxazole, resulted in a decrease or loss of activity. Only the 1-imidazole substituted compounds **17** and **18** were very active. Their selectivity towards CYP11B2, however, was quite low (selectivity factor = 35 and 4).

An explanation for the difference in binding affinities (potency) between the 3-pyridine and 4-pyridine compounds **21** and **22** has been postulated before (Ulmschneider *et al.*, 2005b). For an optimal orbital overlap of the pyridyl nitrogen and the heme iron, the pyridyl moiety should be located perpendicular with respect to the plane of the heme group. In case of the 4-pyridine compounds, the distorsion of this geometry weakens the interaction and results in low inhibitory activities.

Another interesting point is that the 5-imidazolyl compound **14** has a selectivity factor of 0.7. It is 1.5 times more active towards CYP11B1 than towards CYP11B2. This is an indication that it might be possible to find selective inhibitors of CYP11B1 as well. These inhibitors could be used for the treatment of Cushing's syndrome and the metabolic syndrome, which are diseases related to increased cortisol levels.

We can conclude from this present chapter that the 3-pyridyl moiety is ideal with respect to activity and selectivity. Additionally, the 3-pyridine substituted naphthalene affected the sex hormone producing enzymes CYP17 and CYP19 only marginally. The other heteroaryl substituted compounds displayed lower activity and/or selectivity towards CYP11B2. Therefore, 6-methoxy-3-pyridyl naphthalene **21** will be used as a new lead compound in the following chapters.

3.3. Synthesis and biological evaluation of 3-pyridine substituted naphthalenes and quinolines as inhibitors of CYP11B2.

3.3.1. Introduction

By comparing the inhibitory activities of different heteroaryl substituted naphthalenes, we found that the 3-pyridine substituted naphthalene is a promising new lead for the development of novel aldosterone synthase inhibitors (see 3.3.). In order to investigate this 3-pyridine compound in detail, a series of different substituents was introduced on different positions of the naphthalene ring. Additionally, some 3-pyridine substituted quino(xa)lines **46-48** were tested to evaluate the role of the naphthalene core (Figure 20).

Figure 20. General structures

27-44　　　　　　　45　　　　　　　46-48
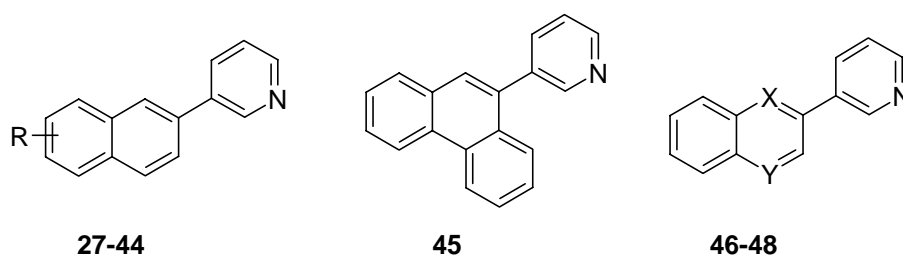
3.3.2. Synthesis

The 3-pyridine substituted naphthalenes **27-28,30-39,41-42,45** were synthesized by the route shown in Scheme 9. The key step of this synthesis is the Suzuki cross-coupling of bromo- or triflate-naphthalenes with the 3-pyridylboronic acid **24** in the presence of sodium carbonate and tetrakis(triphenylphosphine)palladium as a catalyst (method 14).

The triflates **33a,37-39a** were prepared by treating the corresponding naphthols **33b,37-39b** with trifluoromethanesulfonic anhydride and dry pyridine at 0°C (method 16) (Mewshaw *et al.*, 2003). The naphthols **33b** and **38b** were commercially available. The 1,5-dichloro-6-methoxy compound **37b** was synthesized following a literature procedure (method 17) (Mewshaw *et al.*, 2003) and the 1-chloro-7-methoxy naphthol **39b** by treating **39c** with *N*-chlorosuccinimide (method 18).

Scheme 9ᵃ. Synthesis of 3-pyridyl compounds **27-28,30-39,41-42,45**
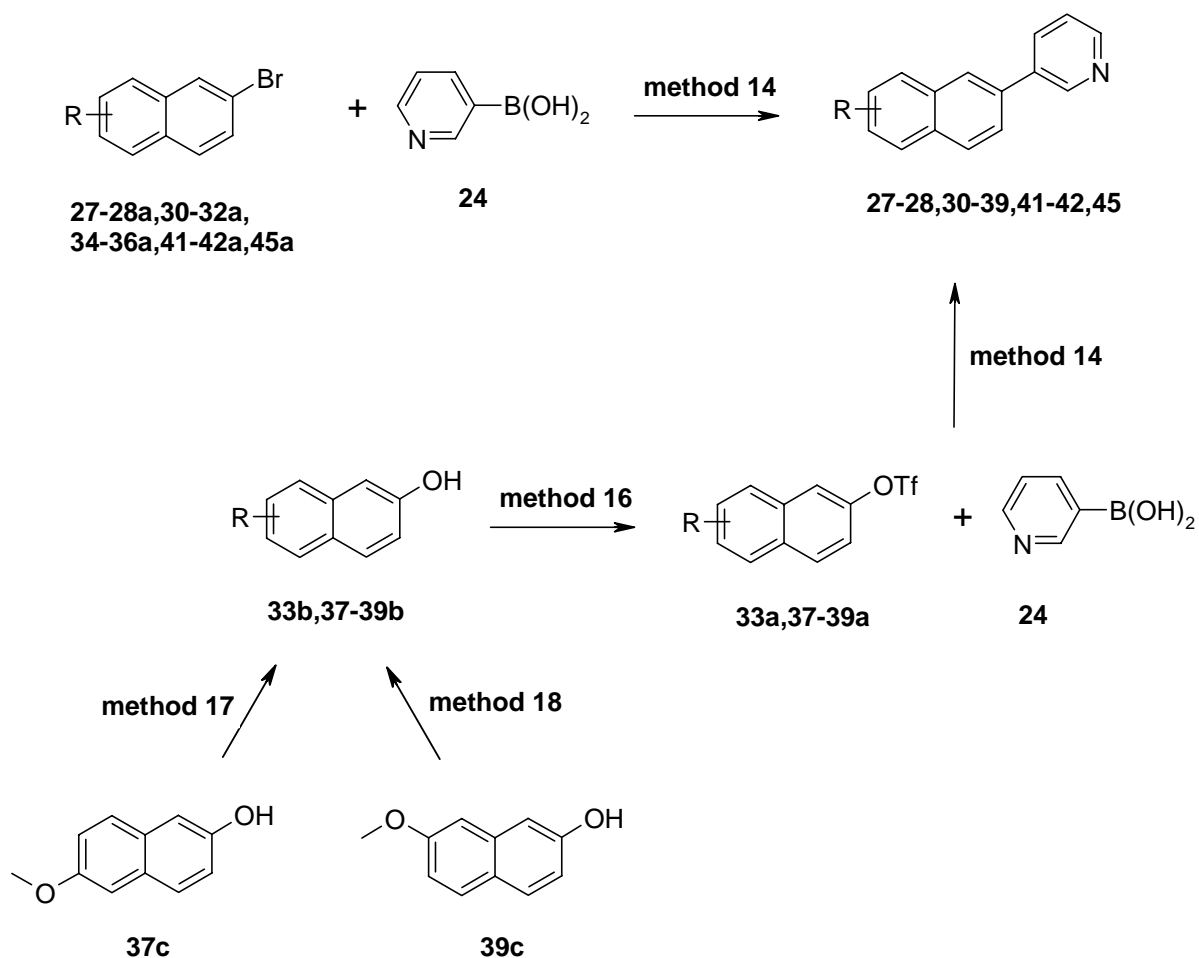
no	R	no	R	no	R
27	H	**33**	6-CN	**38**	7-OMe
28	6-Br	**34**	5-Cl-6-OMe	**39**	1-Cl-7-OMe
30	6-OEt	**35**	5-Br-6-OMe	**41**	6-COOMe
31	6-OPr	**36**	5-(3-Pyr)-6-OMe	**42**	6-OMe-7-COOMe
32	6-OBn	**37**	1,5-diCl-6-OMe	**45**	phenanthrene

ᵃ : method 14: NaCO₃, Pd(PPh₃)₄, DME, 80°C, 2.5 h - overnight; method 16: trifluoromethanesulfonic
anhydride, dry pyridine, 0 - 5°C, 30 min, RT, overnight; method 17: *N*-chlorosuccinimide, ACN,
RT, overnight; method 18: *N*-chlorosuccinimide, ACN, reflux, 3 h.

The bromonaphthalenes **30-32a** were prepared by treating 6-bromo-2-naphthol **49** with potassium carbonate and an alkyl halogenide (method 19). The dihalogenated naphthalenes **34-35a** were synthesized by reacting 2-bromo-6-methoxynaphthalene **21a** with *N*-bromo- or *N*-chlorosuccinimide (method 20).

Scheme 10[a]. Synthesis of compounds **30-32a, 34-35a**

30a R=Et
31a R=Pr
32a R=Bn

49

21a

34a X=Cl
35a X=Br
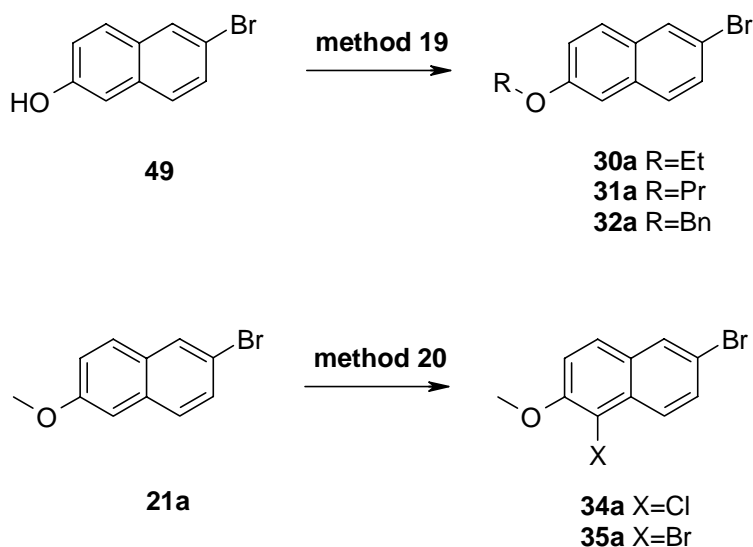
[a] : method 19: RX, K$_2$CO$_3$, DMF, reflux, 3 h; method 20: *N*-chlorosuccinimide or *N*-bromosuccinimide, THF, reflux, 3 h, RT, overnight.

The synthesis of the ester **42a** is shown in Scheme 11 (Murphy *et al.*, 1990). Treatment of 3-hydroxy-2-naphthoic acid **42d** with bromine in glacial acetic acid gave the 4,7-dibromo compound **42c** (method 21), which was then selectively debrominated at the 4-position with tin and glacial acetic acid to yield the bromo compound **42b** (method 22). In a last step **42b** was refluxed with Me$_2$SO$_4$ and K$_2$CO$_3$ to give the wanted ester **42a** (method 23).

Treatment of the 6-methoxy substituted naphthalene **21** with BBr$_3$ at −78°C gave the hydroxylated compound **29** (method 24). The cross-coupling of 2-methoxy-3-naphthylboronic acid **18a** with 3-bromopyridine **24a** yielded the 3-methoxy compound **40** (method 14). The conversion of the ester **41** to the amides **43** and **44** was performed in a one step reaction following a literature procedure (Jagdmann *et al.*, 1990). The methyl ester was treated with formamide and sodium methoxide in anhydrous DMF (method 25) (Scheme 12).

Scheme 11ᵃ. Synthesis of compound **42a**
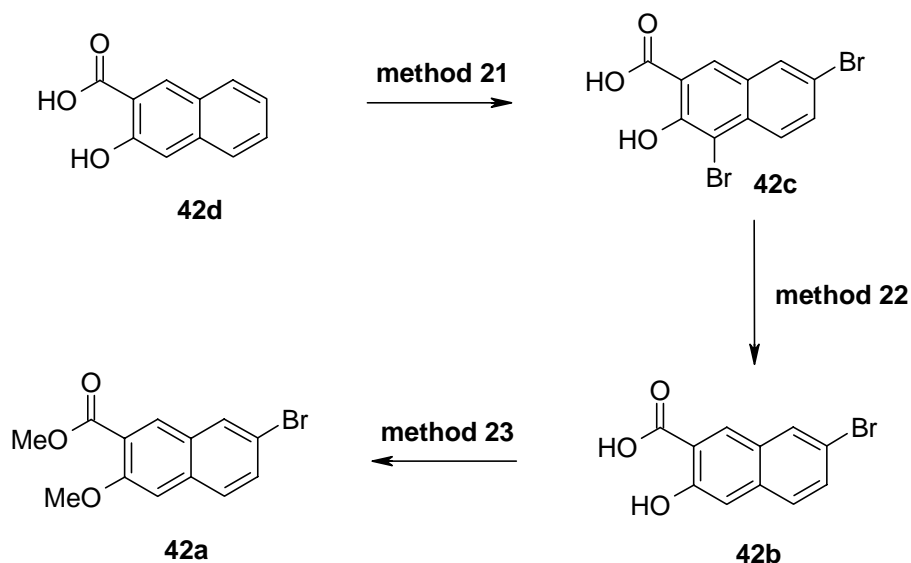
ᵃ : method 21: Br₂, glacial acetic acid, 0°C - reflux, 2 h; method 22: Sn, glacial acetic acid, reflux, 3 h; method 23: Me₂SO₄, K₂CO₃, acetone, reflux, 4 h.

Scheme 12ᵃ. Synthesis of compounds **29,40,43-44**
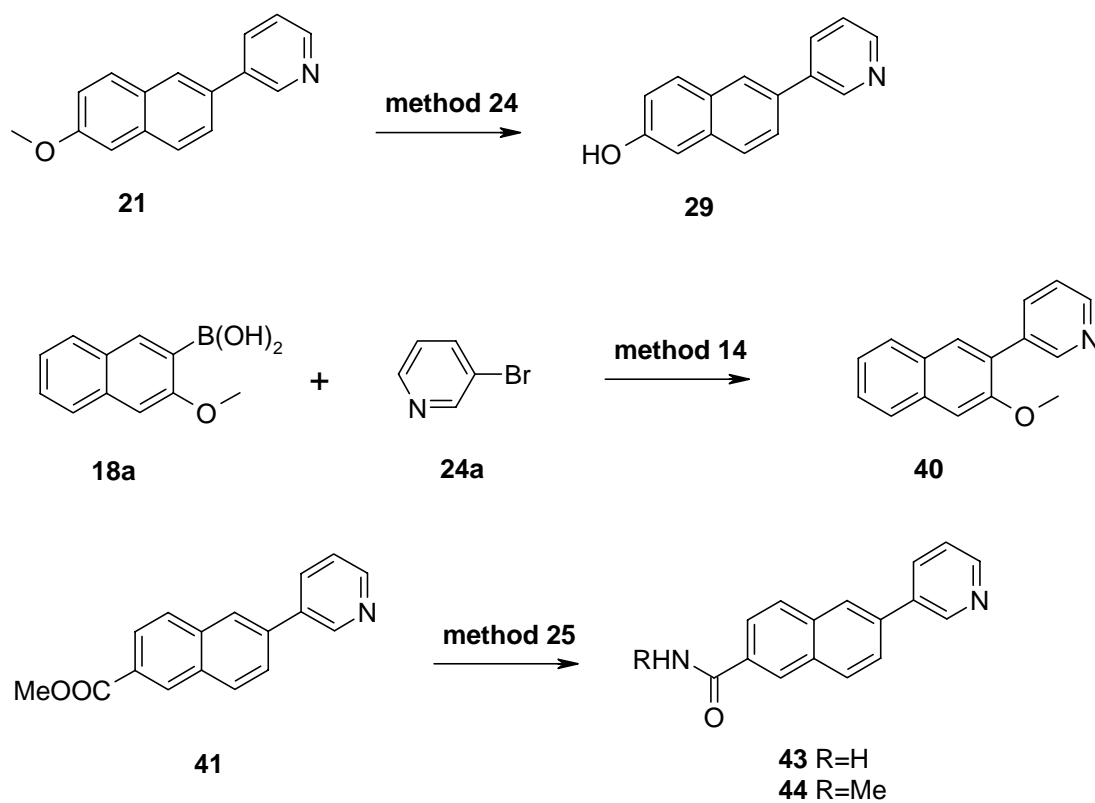
ᵃ : method 24: BBr₃, CH₂Cl₂, -78°C, 30 min, RT, overnight; method 14: NaCO₃, Pd(PPh₃)₄, DME, 80°C, 4 h; method 25: RNHCHO, NaOMe, dry DMF, 100°C, 1 h.

The first step in the synthesis of the quinoline and quinoxaline analogues **46-48** (Scheme 13) was the preparation of the brominated compounds **46-48a**. The hydroxyl compounds **47-48b** were treated with POBr$_3$ to yield compounds **47-48a** (method 26) (Young *et al.*, 1951). The 3-bromoquinoline **46a** was commercially available. Subsequently, the bromo compounds were coupled with 3-pyridylboronic acid **24** to give the 3-pyridine substituted quino(xa)lines **46-48** (method 14).

Scheme 13^a. Synthesis of compounds **46-48**

47b X=N, Y=CH
48b X,Y=N

46-48a

24

method 26

method 14

46-48
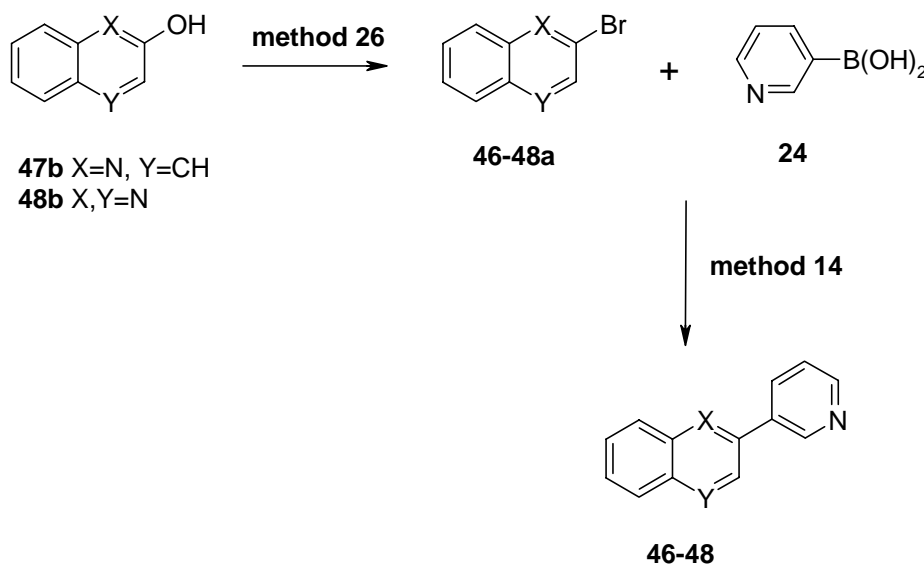
^{a} : method 26: POBr$_3$, 155°C, 4 h; method 14: NaCO$_3$, Pd(PPh$_3$)$_4$, DME, 80°C, overnight.

3.3.3. Biological evaluation

The inhibitory activities of the compounds **27-48** towards human CYP11B2 were determined using human CYP11B2 expressing fission yeast. After incubation with [^{14}C]-deoxycorticosterone as substrate in the presence of the inhibitor at a concentration of 500 nM, the product formation was monitored by HPTLC using a phosphoimager. The percent inhibition values are shown in Table 6.

Most of the 3-pyridine substituted naphthalenes showed a pronounced inhibitory activity similar to or higher than the reference fadrozole (68%). The 3-methoxy and 7-methoxy compounds **40** and **38** and the quinolines **46** and **47** had only moderate activity (≈ 40%), while compounds **43, 44, 45** and **48** showed little or no activity at all (< 27%). Introduction of a methoxy or ethoxy group in 6-position did not change potency (**21** and **30**), but larger

substituents like propoxy diminished inhibitory activity (**31**) or resulted in complete loss of potency as shown for the benzyloxy compound **32**. The same tendency can be seen for the substituents in 5-position. The 5-chlorinated and 5-brominated compounds **34** and **35** showed high inhibitory activities, but introducing a large 3-pyridyl substituent in the 5-position (**36**) diminished the potency drastically. The additional ring in the phenanthrene compound **45** was also too large as this compound exhibited a low potency (27%). The shift of the methoxy substituent from the 6- into the 7-position resulted in a moderate inhibitor (**38**). However, introducing an additional chloro substituent in the 1-position of compound **38** increased the activity significantly (**39**).

Table 6. Inhibition of human adrenal CYP11B1 and CYP11B2 by 3-pyridine substituted compounds **27-48**
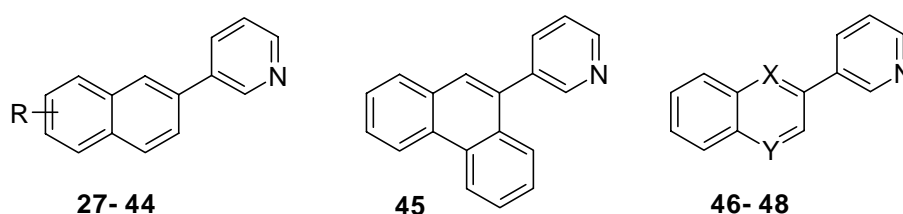
Compound	R	% inhibition[a]	IC$_{50}$-value (nM)[c]		Selectivity factor[f]
		CYP11B2[b]	V79 11B1[d] CYP11B1	V79 11B2[e] CYP11B2	
21	6-OMe	91	1577	6	263
27	H	92	5826	28	208
28	6-Br	85	2939	15	196
29	6-OH	88	2671	23	116
30	6-OEt	86	5419	12	451
31	6-OPr	36	n.d.	n.d.	-
32	6-OBn	3	n.d.	n.d.	-
33	6-CN	98	691	3	238
34	5-Cl-6-OMe	86	2517	13	192
35	5-Br-6-OMe	68	4481	33	136
36	5-(3-Pyr)-6-OMe	9	n.d.	n.d.	-
37	1,5-diCl-6-OMe	82	4898	28	174
38	7-OMe	46	n.d.	n.d.	-

Compound	R	% inhibition[a] CYP11B2[b]	IC$_{50}$-value (nM)[c] V79 11B1[d] CYP11B1	IC$_{50}$-value (nM)[c] V79 11B2[e] CYP11B2	Selectivity factor[f]
39	1-Cl-7-OMe	85	2724	29	94
40	3-OMe	30	n.d.	n.d.	-
41	6-COOMe	74	10505	72	145
42	6-OMe-7-COOMe	n.d.	>10000	>10000	-
43	CONH$_2$	n.i.	n.d.	n.d.	-
44	CONHMe	n.i.	n.d.	n.d.	-
45		27	7553	n.d.	-
46	X=CH,Y=N	40	n.d.	n.d.	-
47	X=N,Y=CH	53	n.d.	n.d.	-
48	X,Y=N	13	n.d.	n.d.	-
fadrozole		68	10	1	10

[a] Mean value of four determinations, standard deviation less than 10%. [b] *S. pombe* expressing human CYP11B2; substrate: deoxycorticosterone, 100 nM; inhibitor, 500 nM. n.i. = no inhibition [c] Mean value of four determinations, standard deviation less than 20%. n.d. = not determined. [d] Hamster fibroblasts expressing human CYP11B1; substrate: deoxycorticosterone, 100 nM. [e] Hamster fibroblasts expressing human CYP11B2; substrate: deoxycorticosterone, 100 nM. [f] IC$_{50}$ CYP11B1/ IC$_{50}$ CYP11B2.

The most potent compounds, showing more than 60% inhibition in *S. pombe*, were tested for activity and selectivity in V79 MZh cells expressing either CYP11B1 or CYP11B2. [^{14}C]-Deoxycorticosterone was used as substrate and the products were monitored as in the yeast assay. In Table 6 the IC$_{50}$ values are presented.

All the compounds exhibited very high activity towards CYP11B2 with IC$_{50}$ values in the range of 3 nM to 72 nM. The 6-cyano compound **33** was the most potent CYP11B2 inhibitor with an IC$_{50}$ value of 3 nM. In addition, these active compounds were highly selective by showing only low inhibition of CYP11B1 (IC$_{50}$ = 691-10505 nM). It was very surprising that all of them were much more selective than the reference fadrozole which displayed a selectivity factor of 10. The most selective compounds **33** and **30** were 238-fold and even 451-fold more selective for CYP11B2.

Using the CYP11B2 expressing V79 cells, the 6-cyano compound **33** was tested for its type of CYP11B2 inhibition. The conversion of the substrate deoxycorticosterone to corticosterone by CYP11B2 was measured at five substrate concentrations (50 nM – 2 μM) in the absence or presence of inhibitor at different concentrations (3 – 15 nM). Using the Lineweaver-Burk equation: $1/v = 1/V_{max} + K_m/V_{max}$ [S], the plots at different inhibitor concentrations were

obtained as shown in Figure 21. Plotting $1/v$ against $1/[S]$ gives rise to an Y-intercept of $1/V_{max}$. The intercept on the x-axis equals $-1/K_m$ and the slope of the line is K_m/V_{max}. The K_m is defined as the substrate concentration which gives rise to a velocity equal to half of the maximal reaction velocity. As the inhibitor concentration increased, the K_m increased giving rise to a value designated as $K_{m,obs}$. The slope of the line and the X-intercept changed, while the Y-intercept was unaffected. This is the typical hallmark of competitive inhibition. The inhibitor competes with the substrate to bind in the active site. As the inhibitor binds to the enzyme, it forms an enzyme-inhibitor complex which cannot be converted to product.

Figure 21. Lineweaver-Burk plots for the conversion of deoxycorticosterone to corticosterone in the presence of different concentrations of compound **33**
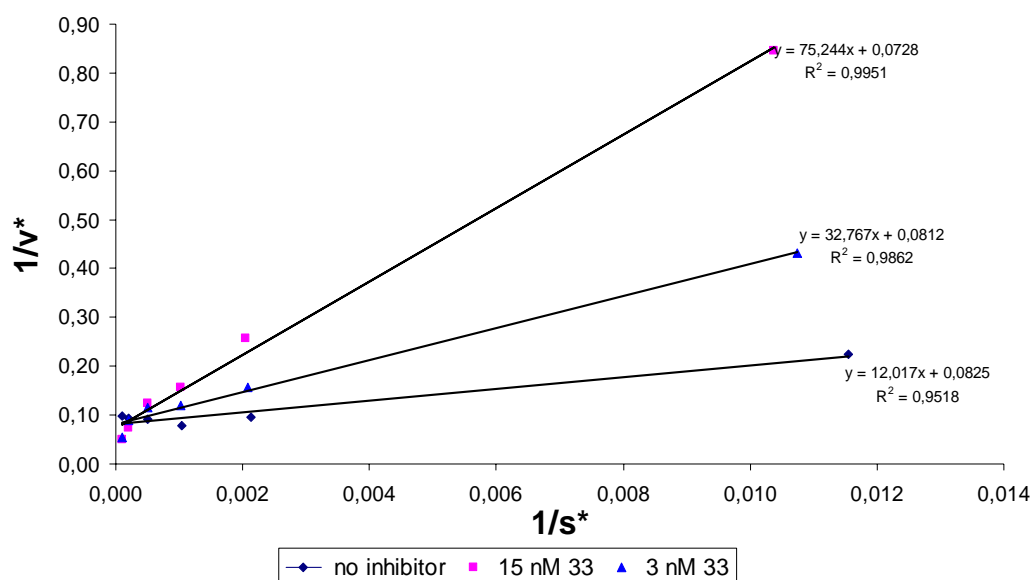
The dissociation constant for inhibitor binding, K_i, could be determined using the equation $K_i = [I] / K_{m,obs} / K_m - 1$, where $[I]$ is the inhibitor concentration (nM) and $K_{m,obs}$ is the K_m value in presence of inhibitor. The 6-cyano compound **33** exhibited a K_i value of 1.9 nM (K_m value deoxycorticosterone = 185 nM). Assuming that the other inhibitors of this class are also competitive inhibitors, we can calculate the corresponding K_i values from the respective IC_{50} values using the equation of Cheng and Prusoff: $K_i = IC_{50}/1 + [S]/K_m$ (Cheng and Prusoff, 1973). Thus, the 6-ethoxy compound **30** and the dichloro compound **37** revealed K_i values of 8 nM and 18 nM, respectively.

Table 7. Inhibition of human CYP19 and human CYP17 by 3-pyridine substituted compounds **27-48**

Compound	R	IC$_{50}$-value (nM)^a human CYP19^b	% inhibition^c [IC$_{50}$-value (nM)]^c human CYP17^d
27	H	5727	40
28	6-Br	>36000	46
29	6-OH	>36000	65
30	6-OEt	6638	53
31	6-OPr	n.d.	n.d.
32	6-OBn	n.d.	n.d.
33	6-CN	>36000	73 [686]
34	5-Cl-6-OMe	1805	32
35	5-Br-6-OMe	9107	38
36	5-(3-Pyr)-6-OMe	n.d.	n.d.
37	1,5-diCl-6-OMe	970	83 [233]
38	7-OMe	n.d.	n.d.
39	1-Cl-7-OMe	>36000	94 [27]
40	3-OMe	n.d.	n.d.
41	6-COOMe	1252	12
42	6-OMe-7-COOMe	n.d.	n.d.
43	CONH$_2$	n.d.	n.d.
44	CONHMe	n.d.	n.d.
45		n.d.	n.d.
46	X=CH,Y=N	n.d.	n.d.
47	X=N,Y=CH	n.d.	n.d.
48	X,Y=N	n.d.	n.d.
fadrozole		30	5
ketoconazole		n.d.	40

^{a} Mean value of four determinations, standard deviation less than 20%. n.d. = not determined ^{b} human placental CYP19; 1mg/ml of protein; substrate: androstenedione, 500 nM. ^{c} Mean value of four determinations, standard deviation less than 10%. n.d. = not determined. ^{d} E.coli expressing human CYP17; 5 mg/ml; substrate: progesterone, 2.5 μM; inhibitor, 2.5 μM.

Selectivity towards the steroidogenic CYP enzymes, CYP19 and CYP17, was also evaluated (Table 7). The IC_{50} values of the compounds for CYP19 were determined *in vitro* using human placental microsomes and [1β-^{3}H]androstenedione as substrate. The compounds exhibited very low to no inhibitory activity with IC_{50} values in the range between 970 nM and >36000 nM. The percent inhibition values of the compounds towards CYP17 were determined *in vitro* using progesterone as substrate and the 50.000g sediment of *E.coli* recombinantly expressing human CYP17. Most of the compounds showed a similar inhibition at a concentration of 2.5 μM as the reference ketoconazole (40%). The ester **41** displayed a weaker inhibition (12%). The 6-methoxy substituted naphthalene **33** showed a higher activity towards CYP17 (IC_{50} = 686 nM) and the chloro substituted compounds **37** and **39** exhibited IC_{50} values of 223 and 27 nM, respectively.

The most selective CYP11B2 inhibitor **30** was further tested toward two crucial human hepatic CYP enzymes, CYP3A4 being responsible for 75% of the drug metabolism and CYP2D6 for which a genetic polymorphism is described. No inhibitory effect could be observed (CYP3A4, ketoconazole IC_{50} = 50 nM, **30** no inhibition at 50 nM; CYP2D6, quinidine IC_{50} = 20 nM, **30** no inhibition at 20 nM) (Voets *et al.*, 2005).

3.3.4. Docking and molecular dynamics studies

Docking and molecular dynamics studies were performed by Dr. Iris Antes (Max Planck Institut, Saarbrücken) to explain very interesting structure-activity relationships of three pairs of imidazole and pyridine compounds (Table 8).

While in the case of the unsubstituted pyridyl and imidazolyl derivatives (**27** and **17**) both compounds were very potent inhibitors, introduction of a OCH_3-group in the 3 or 6 position leads to a strong decrease of activity for one compound of the pairs. In case of the 3-methoxy compounds the pyridyl derivative lost activity dramatically whereas for the 6-methoxy compounds it was the imidazolyl compound which exhibited a strong drop of activity.

Because there are no X-ray structures available for CYP11B2, due to its membrane bound nature, a 3D model was built using the X-ray structure of human CYP2C9 as template (Williams *et al.*, 2003). The use of mammalian cytochrome P450 structures as templates has already shown to improve the quality of resulting 3D structural models considerably (Kirton *et al.*, 2002).

45

Table 8. IC$_{50}$ values for CYP11B2 inhibition and Fe(heme)-N(inhibitor) distances after docking and molecular dynamics of selected compounds.

21,27,40   17-19
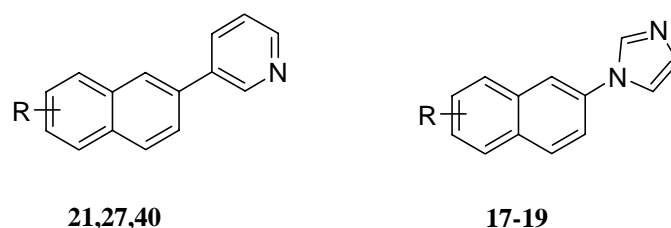
Compound	R	IC$_{50}$-value (nM) V79 11B2 CYP11B2	Fe-N distance (Å) after docking	Fe-N distance (Å) after MD^a
27	H	28.4	2.48	2.63
17	H	38.5	2.38	2.13
21	6-OMe	6.2	2.27	2.48
19	6-OMe	218.0	2.29	7.36
40	3-OMe	>500	2.52	10.58
18	3-OMe	19.1	2.08	2.52

^{a} Time for MD simulations: 1ns

After docking of the inhibitors into the protein structure, molecular dynamics simulations were performed with the inhibitor-protein complexes. In Figure 22 (a-f) the starting and the final positions after 1ns of molecular dynamics of the compounds in the binding pocket are shown. In all pictures the starting structures of the locations of the important binding pocket residues are presented. To enhance the clarity of the presentations the final locations of the residues after the simulation are only shown if a large movement was observed (Figure 22(d) and 22(e)). In all other cases the final positions were almost identical to the starting positions.

Figure 22 (See next page). Selected residues of the energy minimized structures of CYP11B2 complexed with the compounds **27** (a), **17** (b), **21** (c), **19** (d), **40** (e) and **18** (f). For the inhibitors the starting (orange) and end (yellow) positions of the MD simulations are shown. In (d) and (e) the end conformations of Met230 and Leu227 are also given.

46
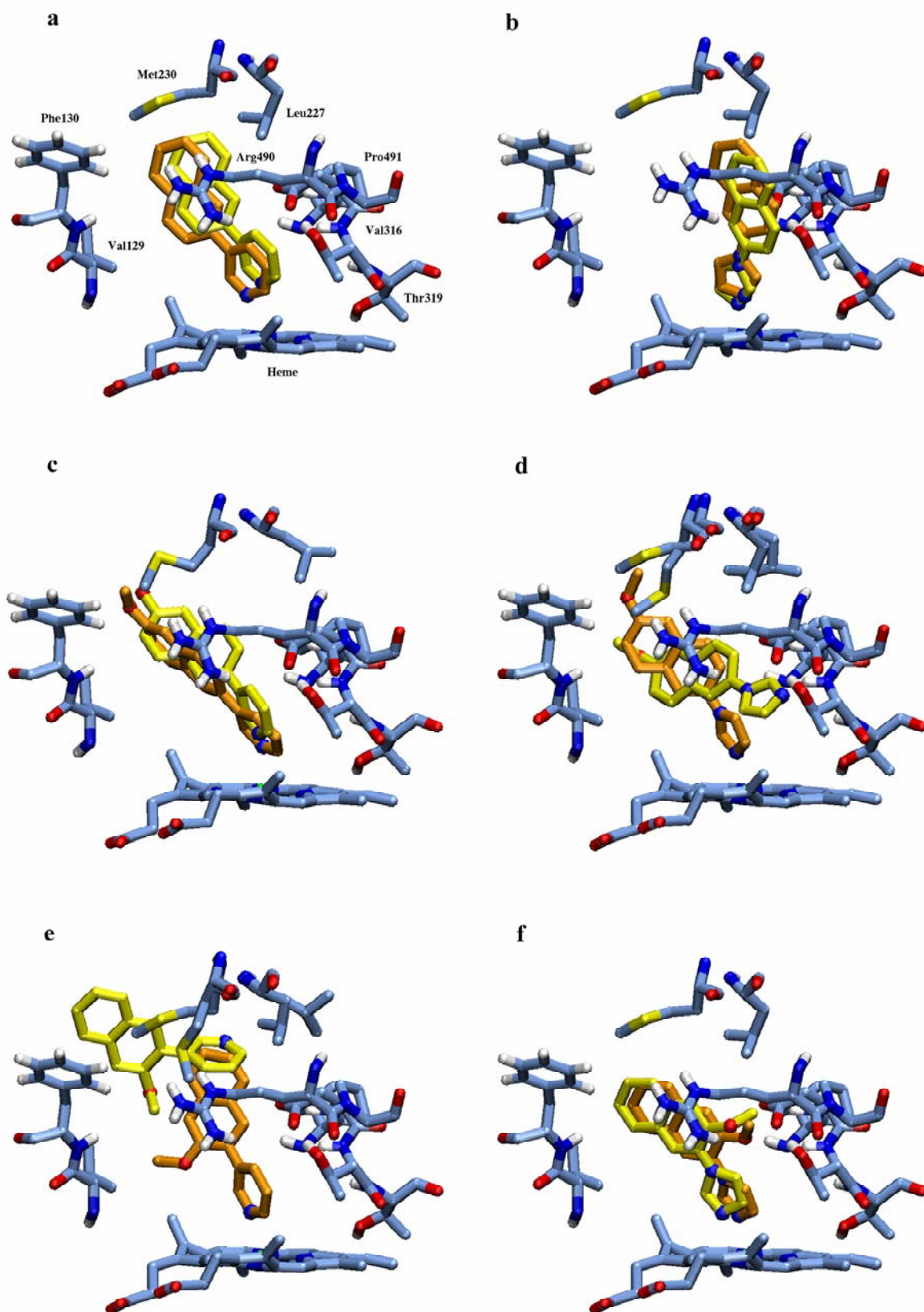
Regarding the location of the inhibitors, the ligands remained close to the docked position except for compounds **19** and **40** (Figure 22(d) and 22(e)), the compounds which had shown little to no activity in the binding experiments. In these cases large movements were observed: at the end of the simulations the compounds had moved away from the heme and the Fe-N contact was broken.

To gain a deeper insight into these phenomena, the binding modes of the compounds in the original positions were studied. One major difference was observed for compound **19** and **40** in comparison to the other compounds. The requirement for a strong inhibitor binding is a Fe-N interaction which is almost perpendicular with respect to the plane of the heme. In the case of compound **19** and **40** this leads to positions much closer to the I-helix (partially shown in Figure 22: Val316-Thr319) than observed for the other inhibitors. These positions are energetically obviously unfavourable because the hydrophilic/hydrophobic regions in the I-helix are located close to the aromatic regions of the ligands. Thus, during the simulation the compounds, while minimizing unfavourable contacts, reorient themselves and subsequently lose contact with the heme group.

In addition it was observed, that the methoxy group of compound **18** fits perfectly into a hydrophobic groove formed by the amino acid residues of Thr318 (CH_3 group), Arg490 (CH_2-CH_2 chain), and Pro491 as shown on the right side of Figure 22(f). In case of compound **40** the larger size of the pyridyl ring and especially the different geometry of the complex due to the binding of the nitrogen to the heme prohibits that the methoxy group fits in this pocket. Thus, the methoxy group is turned by nearly 180 degrees, leading to the above described unfavorable position of the inhibitor.

3.3.5. Discussion and conclusion

In this chapter, the 6-methoxy 3-pyridine substituted naphthalene **21**, which is a very active and selective CYP11B2 inhibitor (see 3.2.), was used as the new lead compound. A series of different substituents was introduced on the 3-pyridine substituted naphthalene core to get more insight into this new class of compounds. The influence of the chain length, the size and the position of the substituents on the naphthalene core was investigated. In addition, some quino(xa)line compounds have been synthesized to evaluate the role of the naphthalene ring.

The structure-activity relationships obtained revealed that the naphthalene core is more appropriate than the (iso)quinoline or quinoxaline moiety. The corresponding compounds **46-48** displayed low or no activity at all. Obviously, a nitrogen atom at this position is unfavourable for an optimal interaction with the active site.

Substitution in the 6-position of the naphthalene core is appropriate to have high activity and selectivity. Only in case of space-filling substituents, like propoxy or benzyloxy (**31,32**), the activity drops drastically. Further substitution in the 5-position did not result in lower potency, as long as this substituent was not too large as for compound **36**. A loss in activity was observed when substituents are introduced in 3- or 7-position (**38,40**). The phenanthrene compound **45**, showing a low activity towards CYP11B2, was probably too large to fit adequately into the active site of the target enzyme.

In this study, we demonstrated that 3-pyridine substituted naphthalenes showed *in vitro* a highly selective inhibition of CYP11B2 versus CYP11B1, despite the high homology between the two enzymes. These compounds showed even better selectivity profiles than the (pyridylmethylene)tetrahydronaphthalenes and –indanes (Ulmschneider *et al.*, 2005b). The best 3-pyridyl compounds described in this work were more than 190-fold more selective for CYP11B2 (**27,28,33,34**). In the case of the 6-ethoxy compound **30** an exceptional 451-fold stronger inhibition was observed. The other steroidogenic CYP enzymes CYP17 and CYP19 and the drug-metabolizing enzymes CYP3A4 and CYP2D6 were not affected. Only the 1-chloro-7-methoxy compound **39** turned out to be a potent CYP17 inhibitor.

Additionally, the 6-cyano compound **33** was tested for its type of CYP11B2 inhibition and turned out to be a competitive inhibitor with a K_i value of 1.9 nM (K_m value deoxycorticosterone = 185 nM).

The results of the molecular dynamics studies showed that for the highly potent compounds **17**, **18**, **21** and **27** the docked positions remained stable throughout the simulations. For the two less potent compounds **19** and **40** however, major rearrangements of the inhibitors in the complex were observed leading to the breaking of their Fe-N interactions. A closer analysis of the ligand interactions with the binding pocket revealed that in the case of **19** and **40** the formation of a close Fe-N interaction leads to unfavourable contacts between the ligands and the I-helix of the protein. As it is known that a strong Fe-N interaction is a prerequisite for strong inhibitor binding, it can be concluded that the reason for the little inhibitory potency of **19** and **40** is mainly sterical. In addition, this study shows that the protein model of CYP11B2, which has been improved continuously (Ulmschneider *et al.*, 2005a, Ulmschneider *et al.*, 2005b, Voets *et al.*, 2005), demonstrates some predictive value.

In summary, we have obtained a new class of non steroidal highly active and selective inhibitors of aldosterone synthase. The most active CYP11B2 inhibitor was the 6-cyano compound **33** (IC_{50} = 3 nM). The 6-ethoxy compound **30** turned out to be a very active and the most selective inhibitor (IC_{50} = 12 nM) showing a selectivity factor of 451

3.4. Synthesis and biological evaluation of heteroaryl substituted dihydronaphthalenes and indenes as inhibitors of CYP11B2.

3.4.1. Introduction

By modifying our lead compound, the (imidazolylmethylene)tetrahydronaphthalenes and indanes **III**, we found a new class of 3-pyridine substituted naphthalenes **IV**, which showed *in vitro* a highly selective inhibition of CYP11B2 versus CYP11B1, despite the high homology between the two enzymes (Voets *et al.*, 2005, see 3.3.). We changed the core structure of **III** by moving its exocyclic double bond into the ring. The naphthalene compounds showed the best selectivity profiles of all the CYP11B2 inhibitors described until now in the literature.

Figure 23. From lead structure **III** to a new class of inhibitors **V**
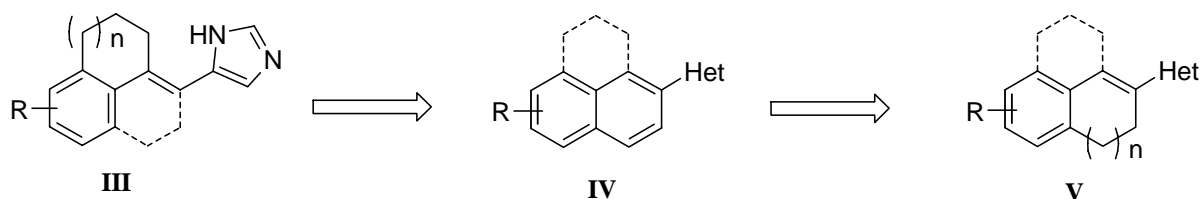
Instead of introducing an unsaturated bridge into the ring, which yielded the aromatic naphthalene compounds, we now introduce a saturated bridge to mimic the aliphatic ring in the lead compound **III**. This modification leads to a new class of CYP11B2 inhibitors, the heteroaryl substituted dihydronaphthalenes and indenes **V** (Figure 23).

Figure 24. General structures
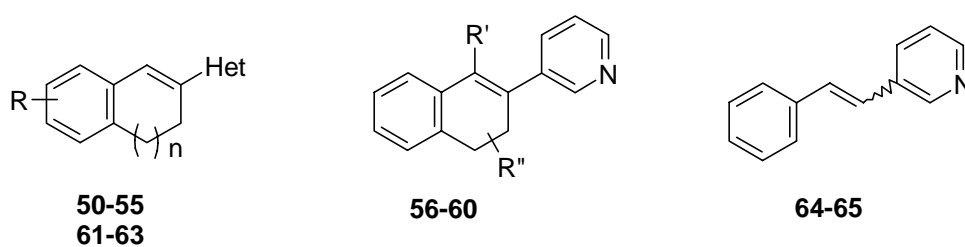
In this chapter, the synthesis of a series of dihydronaphthalenes and indenes (Figure 24) and their biological activity towards the human CYP enzymes CYP11B2, CYP11B1, CYP17 and

CYP19 are described. Molecular modelling and docking studies using our homology modelled CYP11B2 structure were performed to understand some interesting structure-activity relationships.

3.4.2. Synthesis

The pyridine substituted indenes and dihydronaphthalenes **50-51,53-55,59** were synthesized by the route shown in Scheme 14.

Scheme 14[a]. Synthesis of compounds **50-51,53-55,59**
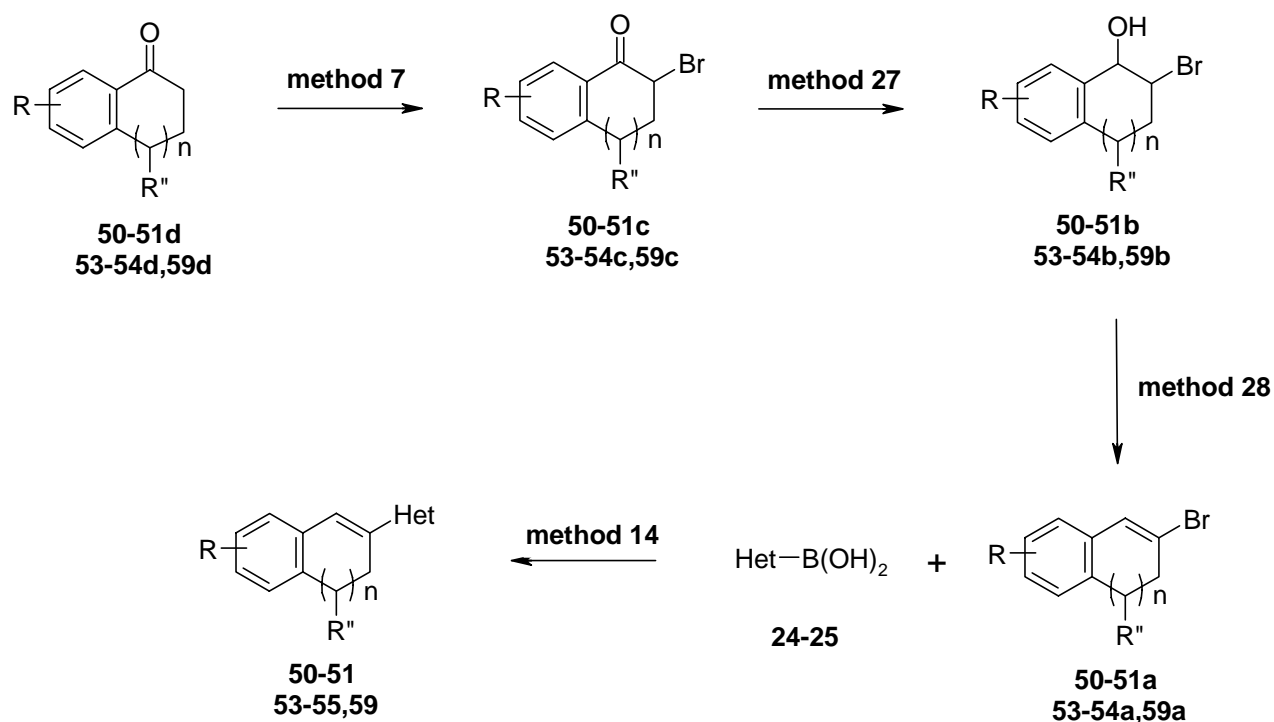
no	n	R	R''	Het	no	n	R	R''	Het
50	0	H	-	3-Pyr	**54**	1	7-OMe	H	3-Pyr
51	1	H	H	3-Pyr	**55**	1	6-OMe	H	4-Pyr
53	1	6-OMe	H	3-Pyr	**59**	1	H	Me	3-Pyr

[a] : method 7: tetrabutylammonium tribromide, CH_2Cl_2/methanol, RT, 1 h; method 27: $NaBH_4$, MeOH, 0°C – RT, 1 h; method 28: pTSA, toluene, reflux, 2 h; method 14: $NaCO_3$, $Pd(PPh_3)_4$, DME, 80°C, 2 h – overnight.

The α-bromoketones **50-51,53-54,59c**, synthesized by reacting the corresponding ketones **50-51,53-54,59d** with tetrabutyl ammonium tribromide (method 7), were reduced with $NaBH_4$ (method 27). The resulting alcohols **50-51,53-54,59b** were refluxed in toluene with a catalytic amount of pTSA to yield the dehydrated compounds **50-51,53-54,59a** (method 28). The last step was the Suzuki cross-coupling with a pyridylboronic acid in the presence of sodium carbonate and tetrakis(triphenylphosphine)palladium as a catalyst (method 14).

Scheme 15^a. Synthesis of compounds **52,58,60**
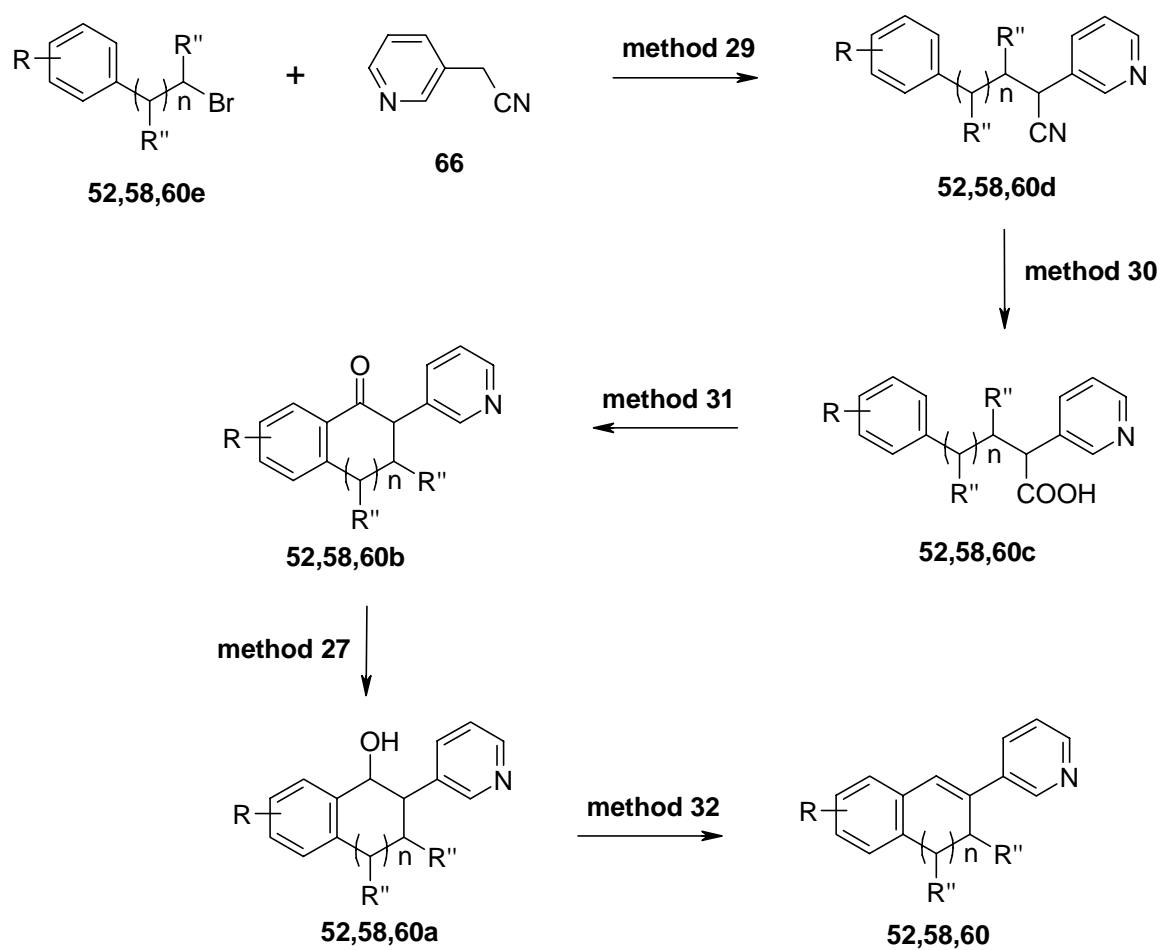
no	n	R	R"
52	0	5-OMe	H
58	1	H	3-Me
60	1	H	4-Et

^{a} : method 29: $NaNH_2$, DMF, 0 - 80°C, 6 h; method 30: NaOH, H_2O/EtOH, reflux, 48 h; method 31: PPA, 110°C, 20 min; method 27: $NaBH_4$, MeOH, 0°C – RT, 1 h; method 32: CH_3COOH, H_2SO_4, 100°C, 1 h.

An alternative synthetic pathway was used for the synthesis of the 3-pyridine substituted compounds **52,58,60** (Scheme 15). The alkylation of 3-pyridylacetonitrile **66** with the brominated alkyl derivatives **52,58,60e** produced the nitriles **52,58,60d** (method 29). Hydrolysis with NaOH yielded the acids **52,58,60c** (method 30), which were cyclized to the corresponding indanones and tetralones **52,58,60b** by treatment with PPA (method 31). The reduction with NaBH$_4$ to the alcohols **52,58,60a** (method 27) was followed by the dehydration with sulfuric and acetic acid (method 32) to give the wanted indenes and dihydronaphthalenes **52,58,60**.

Scheme 16^a. Synthesis of compounds **56-57**
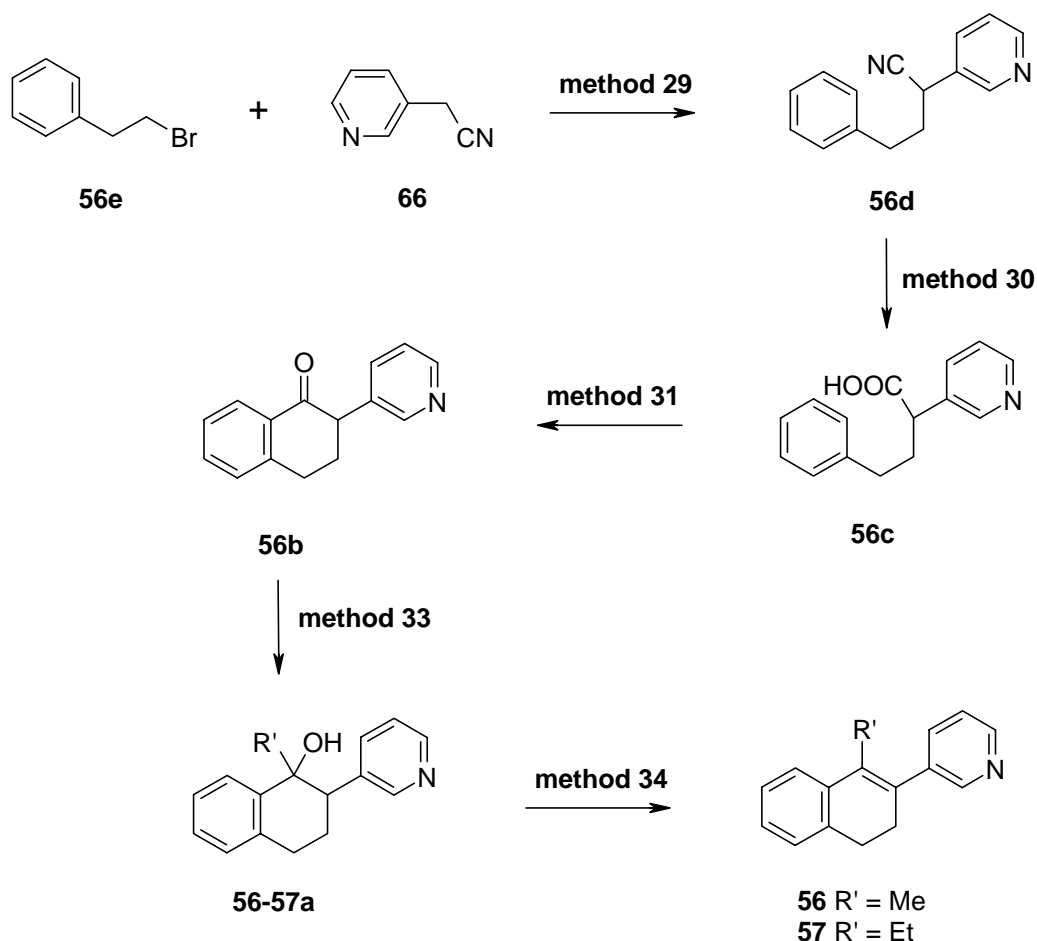
^{a} : method 29: NaNH$_2$, DMF, 0-80°C, 6 h; method 30: NaOH in H$_2$O, EtOH, reflux, 48 h; method 31: PPA, 110°C, 20 min; method 33: R'MgX, toluene, reflux, 3 h, RT, overnight; method 34: HCl, 100°C, 2 h.

The Grignard reaction of the tetralone **56b** with an alkyl magnesium halogenide (method 33) and the following dehydration of the resulting alcohols **56-57a** with HCl (method 34) yielded the 1-alkyl substituted dihydronaphthalenes **56-57** (Scheme 16). The 3-pyridine substituted tetralone **56b** was prepared as described above. The alkylation of 3-pyridylacetonitrile **66** with phenethyl bromide **56e** produced the nitrile **56d** (method 29). Hydrolysis with NaOH yielded the acid **56c** (method 30), which was cyclized to the corresponding tetralone **56b** by treatment with PPA (method 31).

The synthesis of the 1-imidazole substituted indene and dihydronaphthalenes **61-63** is shown in Scheme 17. The α-bromoketones **50-51,53c** were stirred with imidazole for 24 hours to give the imidazole **61-63b** (method 35). The reduction with NaBH$_4$ to the alcohols **61-63a** (method 27) and the subsequent acid-catalyzed dehydration (method 32) yielded the 1-imidazolyl compounds **61-63**.

Scheme 17[a]. Synthesis of compounds **61-63**
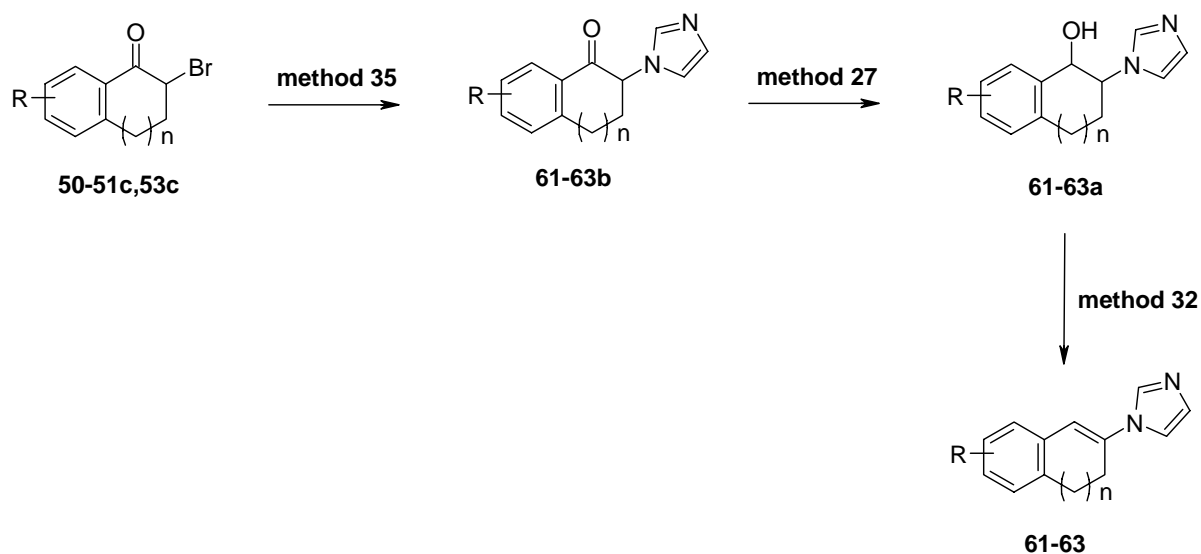
no	n	R
61	0	H
62	1	H
63	1	6-OMe

[a] : method 35: imidazole, DMF, RT, 24 h; method 27: NaBH$_4$, MeOH, 0°C – RT, 1 h; method 32: CH$_3$COOH, H$_2$SO$_4$, 100°C, 1 h.

The (*E*) and (*Z*)-3-styrylpyridine **64** and **65** were synthesized by a modified Wittig reaction (Scheme 18). The benzylalcohol **64b** was transformed into the phosphonium salt **64a** (method 36), which reacted with 3-pyridine carbaldehyde **67** in the presence of K_2CO_3 as a base and 18-crown-6 as phase-transfer catalyst (method 37). The resulting E/Z mixture was separated by column chromatography.

Scheme 18[a]. Synthesis of compounds **64-65**

64 E-isomer
65 Z-isomer
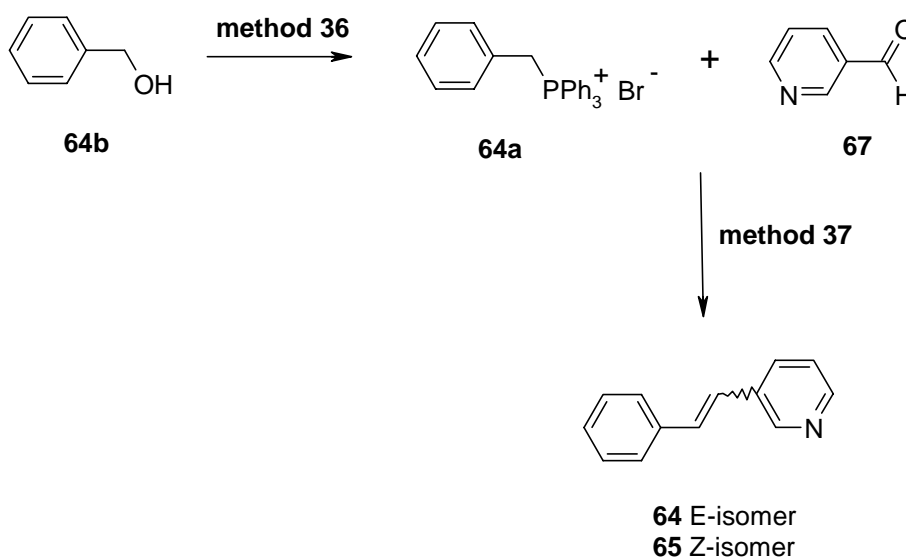
[a] : method 36: $PPh_3 \cdot HBr$, toluene, reflux, 14 h; method 37: K_2CO_3, 18-crown-6, CH_2Cl_2, reflux, 14 h.

3.4.3. Biological evaluation

For the determination of the inhibitory activity towards human CYP11B2, CYP11B2 expressing fission yeast was incubated with [14C]-deoxycorticosterone as substrate and the inhibitor at a concentration of 500nM. The percent inhibition values are shown in Table 9.

Most of the 3-pyridine substituted derivatives showed a higher inhibitory activity than the reference fadrozole (68%). Only the 7-methoxy compounds **54** exhibited a moderate activity (51%). The 1-imidazolyl compounds **61**, **62** and **63** also displayed moderate activity (25-54%). The 4-pyridine substituted naphthalene **15**, on the other hand, had almost no activity (15%) at all. In general the 3-pyridine substituted indenes exhibited a slightly lower activity than the 3,4-dihydronaphthalenes. The shift of the methoxy substituent from 6- into 7-position of the 3,4-dihydronaphthalene core reduced activity resulting in a moderate inhibitor (**54**).

Table 9. Inhibition of human adrenal CYP11B1 and CYP11B2 by heteroaryl substituted

compounds **50-55** and **61-63**

Compound	n	R	% inhibition[a] CYP11B2[b]	IC$_{50}$-value (nM)[c] V79 11B1[d] CYP11B1	V79 11B2[e] CYP11B2	Selectivity factor[f]
50	0	H	90	2391	13	184
51	1	H	95	1729	7	247
52	0	5-OMe	66	5684	4	1421
53	1	6-OMe	98	578	2	275
54	1	7-OMe	51	n.d.	n.d.	-
55	1	6-OMe	15	2529	2834	1
61	0	H	33	n.d.	n.d.	-
62	1	H	34	639	334	2
63	1	6-OMe	35	763	411	2
fadrozole			68	10	1	10

[a] Mean value of four determinations, standard deviation less than 10%. [b] *S. pombe* expressing human CYP11B2; substrate: deoxycorticosterone, 100 nM; inhibitor, 500 nM. [c] Mean value of four determinations, standard deviation less than 20%. n.d. = not determined. [d] Hamster fibroblasts expressing human CYP11B1; substrate: deoxycorticosterone, 100 nM. [e] Hamster fibroblasts expressing human CYP11B2; substrate: deoxycorticosterone, 100 nM. [f] IC$_{50}$ CYP11B1/ IC$_{50}$ CYP11B2.

The most potent compounds, showing more than 60% inhibition in S. pombe, and a few less potent compounds were tested for activity and selectivity in V79 MZh cells expressing either CYP11B1 or CYP11B2. [14C]-Deoxycorticosterone was used as substrate and the products were monitored as in the yeast assay. In Table 9 the IC50 values are presented. All the compounds with more than 60% inhibition in the yeast assay exhibited very high activity towards CYP11B2 with IC50 values in the range of 2 nM to 13 nM. They were also highly selective by showing only moderate inhibition of CYP11B1 (IC50 = 578-5684 nM). The most selective compounds **51** and **53** were over 240-fold more selective for CYP11B2 in contrast to the reference fadrozole which displayed a selectivity factor of 10. The 5-methoxy substituted indene **52** had an exceptional selectivity factor of 1421.

Selected compounds with less than 60% inhibition in the yeast assay (**55, 62** and **63**), also showed only moderate or no activity at all in the CYP11B2 expressing V79 cells (IC_{50} values in the range between 334 nM to 2834 nM).

Table 10. Inhibition of human adrenal CYP11B1 and CYP11B2 by 3-pyridine substituted compounds **56-60** and **64-65**

56-60   **64-65**

Compound	R'	R"	% inhibition[a] CYP11B2[b]	IC$_{50}$-value (nM)[c]		Selectivity factor[f]
				V79 11B1[d] CYP11B1	V79 11B2[e] CYP11B2	
56	Me	H	94	1268	7	166
57	Et	H	81	2117	30	71
58	H	3-Me	84	503	5	97
59	H	4-Me	82	1291	13	99
60	H	4-Et	20	1615	176	9
64	E-isomer		25	n.d.	n.d.	-
65	Z-isomer		54	288	735	0.4
fadrozole			68	10	1	10

[a] Mean value of four determinations, standard deviation less than 10%. [b] *S. pombe* expressing human CYP11B2; substrate: deoxycorticosterone, 100 nM; inhibitor, 500 nM. [c] Mean value of four determinations, standard deviation less than 20%. n.d. = not determined. [d] Hamster fibroblasts expressing human CYP11B1; substrate: deoxycorticosterone, 100 nM. [e] Hamster fibroblasts expressing human CYP11B2; substrate: deoxycorticosterone, 100 nM. [f] IC_{50} CYP11B1/ IC_{50} CYP11B2.

Introduction of a methyl substituent in 1-, 3- or 4-position of the 3,4-dihydronaphthalene moiety did not change potency (**56, 58, 59**), but a larger ethyl substituent in 4-position resulted in a loss of activity (**60**). The 1-ethyl compound **57**, however, still exhibited high activity in the yeast assay as well as in the V79 cells. The open styryl structures **64** and **65** showed moderate activity (25-54% inhibition) (Table 10).

An interesting finding is that the Z-isomer **65** exhibited little selectivity for CYP11B1 as compared to CYP11B2 with a 2.5-fold lower IC50 for the 11β-hydroxylase.

For selected compounds **50-53**, the Ki values were calculated using the equation of Cheng and Prusoff as described in 3.3.3. These CYP11B2 inhibitors revealed Ki values of 8.4, 4.6, 2.6 and 1.3 nM, respectively (Km value deoxycorticosterone = 185 nM).

Tests for selectivity towards other steroidogenic CYP enzymes (CYP19 and CYP17) were performed as well (Tables 11 and 12). The IC50 values of the compounds for CYP19 were determined in vitro using human placental microsomes and [1-3H]androstenedione as substrate. All the compounds showed very low or no inhibitory activity with IC50 values in the range between 814 and >36000 nM, thus being much less active than the reference fadrozole (IC50 = 30 nM), a rather specific aromatase inhibitor used for the treatment of breast cancer.

Table 11. Inhibition of human CYP19 and human CYP17 by heteroaryl substituted compounds **50-55** and **61-63**

Compound	n	R	Het	IC_{50}-value (nM)[a] human CYP19[b]	% inhibition[c] IC_{50}-value (nM)[c] human CYP17[d]
50	0	H	3-Pyr	>36000	2
51	1	H	3-Pyr	4073	37
52	0	5-OMe	3-Pyr	>36000	7
53	1	6-OMe	3-Pyr	814	62
54	1	7-OMe	3-Pyr	n.d.	n.d.
55	1	6-OMe	4-Pyr	n.d.	n.d.
61	0	H	Im	n.d.	n.d.
62	1	H	Im	n.d.	n.d.
63	1	6-OMe	Im	n.d.	n.d.
fadrozole				30	5
ketoconazole				n.d.	40

[a] Mean value of four determinations, standard deviation less than 20%. n.d. = not determined [b] human placental CYP19; 1mg/ml of protein; substrate: androstenedione, 500 nM. [c] Mean value of four determinations, standard deviation less than 10%. n.d. = not determined. [d] E.coli expressing human CYP17; 5 mg/ml; substrate: progesterone, 2.5 μM; inhibitor, 2.5 μM.

The percent inhibition values of the compounds towards CYP17 were determined in vitro using progesterone as substrate and the 50.000g sediment of E.coli recombinantly expressing human CYP17. The indenes **50** and **52** and the 3- and 4-methyl 3,4-dihydronaphthalenes **58**

and **59** displayed a weaker inhibition at a concentration of 2.5 µM as the reference ketoconazole (40%), which is an antimycotic and an unspecific inhibitor of several CYPs. The 3,4-dihydronaphthalenes **51**, **53** and **57** showed a similar or slightly higher inhibition (37-62%). The most potent CYP17 inhibitor was the 1-methyl substituted compound **56** exhibiting an IC50 value of 1085 nM. Thus, the tested compounds are all very weak CYP17 inhibitors, having moderate to very low percent inhibition values.

Table 12. Inhibition of human CYP19 and human CYP17 by 3-pyridine substituted compounds **56-60** and **64-65**

Compound	R'	R''	IC$_{50}$-value (nM)^a human CYP19^b	% inhibition^c IC$_{50}$-value (nM)^c human CYP17^d
56	Me	H	6045	69 [1085]
57	Et	H	1507	57
58	H	3-Me	1787	27
59	H	4-Me	3551	23
60	H	4-Et	n.d.	n.d.
64	E-isomer		n.d.	n.d.
65	Z-isomer		n.d.	n.d.
fadrozole			30	5
ketoconazole			n.d.	40

^{a} Mean value of four determinations, standard deviation less than 20%. n.d. = not determined ^{b} human placental CYP19; 1mg/ml of protein; substrate: androstenedione, 500 nM. ^{c} Mean value of four determinations, standard deviation less than 10%. n.d. = not determined. ^{d} *E.coli* expressing human CYP17; 5 mg/ml; substrate: progesterone, 2.5 µM; inhibitor, 2.5 µM.

3.4.4. Molecular modelling and docking studies

Docking and protein modelling studies were performed by Dr. Iris Antes (Max Planck Institut, Saarbrücken) to explain some interesting structure-activity relationships of two imidazolyl and one pyridyl compound (Table 13). In Chapter 3.2., compound **17** was found to be a highly active inhibitor of CYP11B2. In this chapter, we observed that the corresponding dihydronaphthalene compound **61** shows a much lower activity. However, the 3-pyridine dihydronaphthalene **51** is again highly active.

Table 13. IC$_{50}$ values for CYP11B2 inhibition of selected compounds

Compound	Structure	IC$_{50}$-value (nM) V79 11B2 CYP11B2
17		38.5
51		6.9
61		333.9
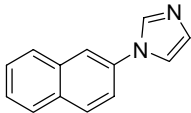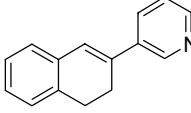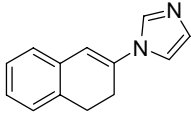
To understand the differences in activity, the three compounds were docked into the CYP11B2 model and molecular dynamics simulations of the docked complexes of compounds **51** and **61** were performed. During the 1ns simulations compound **61** moved away from the heme cofactor, whereas compound **51** stayed close to its docked position. In Chapter 3.3., a correlation was found between the stability of the docked poses during molecular dynamics simulations and their IC$_{50}$ values, which is confirmed here. Subsequently, our docking results were further analyzed in order to explain the different stabilities.

Figure 25. Structure of the CYP11B2 binding pocket with the docked inhibitors **51** (a), **61** (b) and **17** (c).
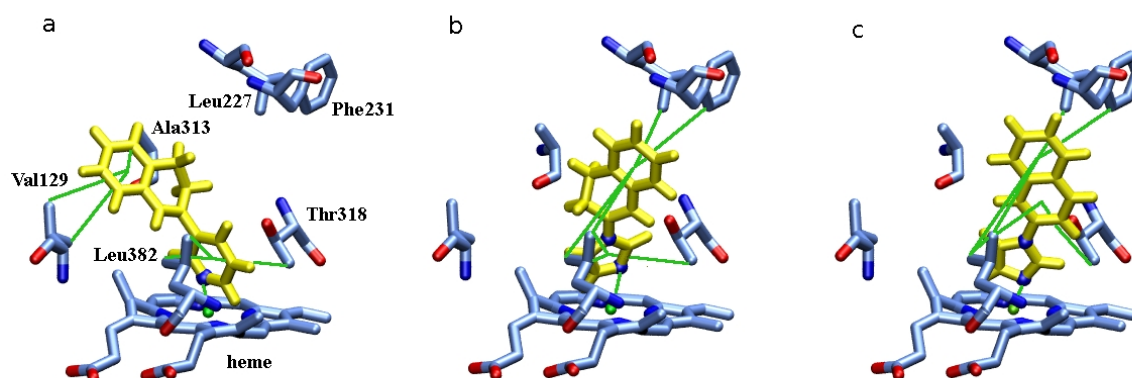
In Figure 25(a-c), the best scoring docking poses for the three compounds and the amino acids of the binding pocket are shown. The ligand-protein interactions are indicated by green lines added to the pictures. Figure 25(b) shows the least active compound **61**. Besides the Fe-N interaction with the heme group, it forms aromatic-hydrophobic interactions between its phenyl and imidazolyl ring and the binding pocket side chains (with Leu227/Phe231 and Leu382/Thr318, respectively). The corresponding highly active naphthalene compound **17**, shown in Figure 25(c), forms strong phenyl-CH_3 interactions with both aromatic rings of the naphthalene (with Leu382, Thr318, Leu227, and Phe231). The imidazole moiety is only forming the Fe-N interaction. In Figure 25(a), the docked complex of compound **51** is presented. This compound binds quite similar to compound **61**. However, due to the larger size of the pyridine ring and the different geometry, the ligand interacts with other amino acids (with Val129 and Ala313 instead of Leu227, Phe231 and Leu382) of the binding pocket and is thus placed differently in the pocket. Its Fe-N interaction is less distorted compared to compound **61**. As a consequence, the IC_{50} value is strongly increased.

Figure 26. Superimposition of the pyridine substituted compounds **51,53,56,58,59** (grey) and the imidazole substituted compounds **61-63** (yellow).

The differences in the orientation of the pyridyl and imidazolyl compounds in the binding pocket can be explained by superimposition of these two classes of compounds. From Figure 26 it is clear that, when the lone pairs of the heterocyclic nitrogens are pointing in the same direction, the corresponding dihydronaphthalene cores are located with a different angle towards the plane of the heme, which in case of the pyridyl compound is more favorable.

3.4.5. Discussion and conclusion

In this study, we describe the discovery of highly active and selective inhibitors of CYP11B2 based on the modification of the lead structure **III**. Instead of 3-pyridine substituted naphthalenes, we synthesized 3-pyridine and 1-imidazole substituted 3,4-dihydronaphthalenes and indenes. To evaluate activity and selectivity of the synthesized compounds, inhibition data for CYP11B2 and CYP11B1 were compared.

From the data presented in Tables 9 and 10 following structure-activity relationships could be deduced. In order to obtain the necessary complexation with the heme iron, the 3-pyridyl moiety was ideal with respect to activity and selectivity. The 1-imidazole substituted compounds were less active and replacement with a 4-pyridyl group resulted in almost no activity at all. The 3-pyridine substituted dihydronaphthalenes exhibited in general a slightly higher activity than the corresponding indanes. The styryl compounds, on the other hand, showed low activity. Whilst substitution in the 7-position of the dihydronaphthalene structure diminished activity, the unsubstituted and 6-methoxy dihydronaphthalene compounds were very active. Small alkyl substituents in the 1, 3 and 4-position did not influence the high activity of this class of compounds. The 4-position, however, seems to be limited in space as an ethyl group in this position decreases the activity drastically.

Most of the 3-pyridine substituted dihydronaphthalenes and indenes turned out to be very active and highly selective CYP11B2 inhibitors. The 6-methoxy substituted dihydronaphthalene **53** was the most active inhibitor with an IC_{50} value of 2 nM. The 5-methoxy substituted indene **52** was a very potent (IC_{50} value = 4 nM) and the most selective compound with a remarkable selectivity factor of 1421. This compound displays the highest selectivity towards CYP11B2 described until now. Interestingly, compound **65** turned out to be a slightly selective CYP11B1 inhibitor, being 2.5 times more active towards CYP11B1 than CYP11B2. An important point to mention is that all the compounds show only effect towards other steroidogenic CYP enzymes like CYP17 and CYP19 at very high concentrations.

Comparing the docking poses of **17**, **51**, and **61**, we made the following observations. Due to the loss of aromaticity in the second ring of the bicycle, the dihydronaphthalene compound **61** can make fewer interactions in the core region than the naphthalene **17**. To compensate this

weakening of the interactions, the compound forms additional aromatic/hydrophobic interactions via its imidazole ring. To obtain this interactions, the heterocycle shifts with respect to the Fe-atom of the heme-cofactor, weakening the Fe-N interaction. However, the requirement for a strong inhibitor binding is a Fe-N interaction, which is almost perpendicular with respect to the plane of the heme. This orientation leads to an optimal binding orbital geometry. Thus due to the distortion of this interaction, the imidazole compound **61** is not as active as the others. Although the 3-pyridine dihydronaphthalene **51** has the same ligand-protein interactions as **61**, it is a strong inhibitor. Due to the size of the pyridyl ring, the ligand is docked differently and the distortion of the Fe-N interaction is much smaller than in compound **61**. This docking study shows that there exists a specific "network" of hydrophobic interaction groups in the binding pocket, which has to be complemented by the inhibitor in a way that the geometry of the Fe-N interaction is retained. Only then strong binding is possible. This is very interesting, because such specific interactions normally consist of hydrogen bonds and the hydrophobic interactions are thought to play only a minor role for the exact positioning of the ligand.

3.5. *In vivo* experiments of CYP11B2 inhibitors

3.5.1. Concept of the *in vivo* experiments

In the previous chapters, we described the discovery of *in vitro* highly active and selective inhibitors of CYP11B2. However, these compounds can only offer a new therapeutic option for the treatment of congestive heart failure and myocardial fibrosis if they show the same potency *in vivo*. The pharmacokinetic properties of a compound are crucial parameters for determining its *in vivo* potency. The study of pharmacokinetics refers to the journey of the drug from its point of entry to the site of action. Absorption, distribution, metabolism and elimination are the different phases of this process. Although a lot of *in vitro* models exist to predict these events, the use of an animal model is inevitable to obtain answers to a very important question in this project. Are the *in vitro* very active and highly selective compounds able to decrease the aldosterone levels in the blood? This would provide a *proof of principle* to the concept of the therapeutic treatment of cardiovascular diseases with CYP11B2 inhibitors. Furthermore, it is important to evaluate the selectivity of these inhibitors *in vivo*.

For the *in vivo* study, we used the animal model of Häusler *et al.*, which is designed to test inhibitors of the gluco- and mineralocorticoid biosynthesis. Adult male rats received a subcutaneous injection of ACTH, to stimulate the gluco- and mineralocorticoid biosynthesis over 18 h. The test compound was orally administered and after 2 h, the animals were decapitated and blood was collected. The plasma gluco- and mineralocorticoid levels were determined using RIA (Häusler *et al.*, 1989).

To investigate the *in vivo* action of our *in vitro* very potent CYP11B2 inhibitors, some small modifications were made. The test compounds were administered intraperitoneally because their bioavailability had not been investigated yet. To eliminate a stress reaction of the animals, decapitation was replaced by cervical dislocation. It is important that the test animals are free of stress, as stress stimulates the glucocorticoid biosynthesis. Because of their high activity and selectivity *in vitro*, it was decided to test the 6-methoxy substituted naphthalene **21** and dihydronaphthalene **53** in this animal model. Fadrozole, for which the Häusler model had been optimized, was used as a reference substance.

3.5.2. The *in vivo* action of fadrozole

In a first step, the *in vivo* action of the reference fadrozole in the modified animal model was investigated. ACTH-stimulation led to the elevation of both the corticosterone and aldosterone plasma concentration. Then, fadrozole was given in two different doses (4 and 0.4 mg/kg). The results showed that fadrozole in a concentration of 4 mg/kg was able to reduce the plasma aldosterone and corticosterone concentrations (64 and 52 % inhibition respectively), whereas no significant reduction of gluco- or mineralocorticoids was observed at a lower dose of 0.4 mg/kg (Figure 27). These results were in good correlation with the data described by Häusler (Häusler *et al.*, 1989)

Figure 27. Action of fadrozole on the aldosterone and corticosterone plasma level
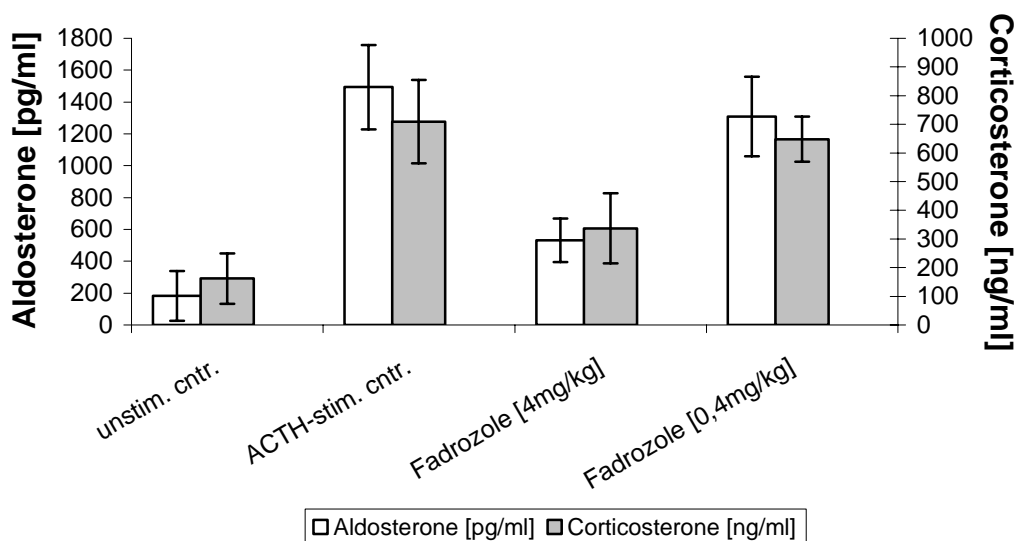
3.5.3. The *in vivo* action of CYP11B2 inhibitors

The compounds **21** and **53** were selected from the library of inhibitors, described in previous chapters, to be tested *in vivo*. They exhibited *in vitro* very high activity towards CYP11B2 with IC_{50} values of 2 and 6 nM. Additionally, they were highly selective inhibitors with selectivity factors of 263 and 275, respectively. The doses of the selected compounds were calculated by comparing their IC_{50} values with the IC_{50} value of fadrozole in the V79 CYP11B2 *in vitro* assay. Fadrozole exhibited in this assay an IC_{50} value of 1 nM. As a dose of

4 mg/kg of fadrozole showed activity in the first *in vivo* test, a dose of 4mg/kg of test compound pro 1 nM of its IC_{50} value was used in the animal test. This means that for compound **53**, which has an IC_{50} value of 2.1 nM, the calculated dose for the *in vivo* test is 4 mg/kg × 2.1 = 8.4 mg. The action of the compounds is shown in Figure 28.

Figure 28. Action of selected inhibitors on the aldosterone and corticosterone plasma level
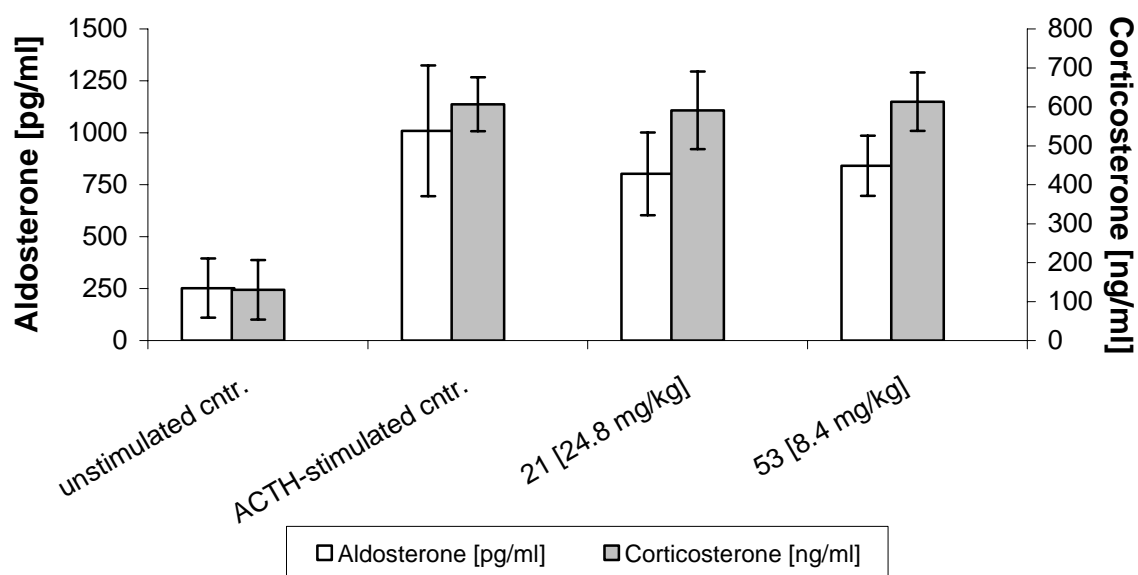
The *in vitro* active and selective inhibitors **21** and **53** showed *in vivo* a small reduction of the aldosterone plasma level (17.1 and 13.1% inhibition, respectively). The corticosterone level was not influenced by the test compounds. Although both of the compounds displayed some selectivity, no statistically significant inhibition of aldosterone could be observed.

3.5.4. Metabolic stability and metabolite identification

In order to find out why the *in vitro* active CYP11B2 inhibitors showed only little activity *in vivo*, metabolic studies were performed in cooperation with Pharmacelsus CRO, Saarbrücken. The reason for the low *in vivo* activity of the inhibitors could be their fast metabolism. The test compounds bear a pyridine ring, which can be easily oxidized to the corresponding *N*-oxide. This would be in accordance with the finding that some 1-[4(5)-imidazolylmethylene]indanes showed *in vivo* activity in the same animal model (Müller-Vieira, 2005). Instead of a pyridyl moiety they bear a metabolically more stable imidazole ring

66

The 6-methoxy substituted compounds **21** and **53** were tested for their metabolic stability in rat liver microsomes, which are subcellular fractions containing many drug metabolizing enzymes, e.g. cytochrome P450s, flavinmonooxygenases, carboxylesterases and epoxide hydrolase. Therefore they are widely used as *in vitro* model system in order to investigate the rate to which a compound is metabolized by the hepatic enzymes. The test compounds were added to the liver microsomes and samples were taken at various time points. The remaining percentage of parent compound was determined by LC/MS. The assay showed that the naphthalene **21** has a half-life of 93 minutes, the dihydronaphthalene **53** a half-life of 67 minutes. This is an indication that these compounds are metabolically stable, knowing that the reference compounds verapamil and testerone only have half-lifes of a few minutes (Figure 29).

Figure 29. Metabolic stability of **21** (MV23) and **53** (MV45) after incubation in rat liver microsomes
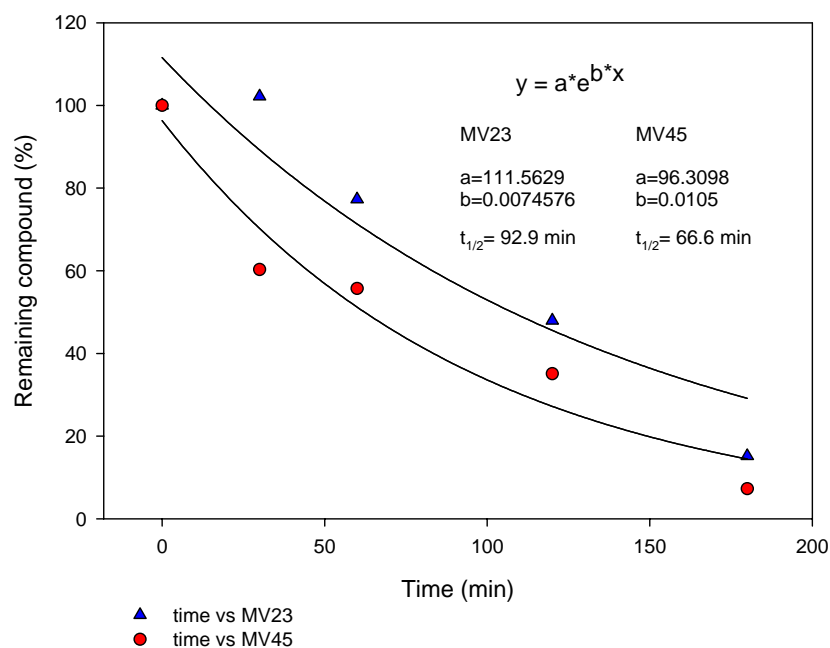
In addition, the possible major metabolites of the test compounds **21** and **53** were detected and characterized by LC-MS/MS to obtain information on the metabolic pathway of the compounds. The metabolites were identified by comparison of the ion chromatograms at the time points t=0 min and t=180 min, under consideration of the expected metabolites according

to predicted gains and losses in molecular mass of the parent compound. Once possible metabolites are detected, they are subjected to further analysis by MS/MS.

Metabolite identification of compound 21

Possible major metabolites with the $[M+H]^+$ at *m/z* 222 and 252 were detected in the full scan run (Figure 30) and proceeded for further MS/MS analysis (Figure 31). The MS/MS fragmentation of methoxy compound **21** (**1**) shows a product ion spectrum of *m/z* 236 and fragment ions of *m/z* 221, 204 and 193. The fragmentation spectrum of (**3**) at retention time 2.8 min shows for the parent ion at *m/z* 222 fragment ion of *m/z* 204 and 194 which suggests that **21** has undergone demethylation resulting in the formation of the corresponding naphthol **29**.

Figure 30. UV (230 nm) and product ion MS/MS chromatograms of compound **21** (**1**) and its metabolites (**2a,b** and **3**) detected in rat liver microsomes incubated for 180 min
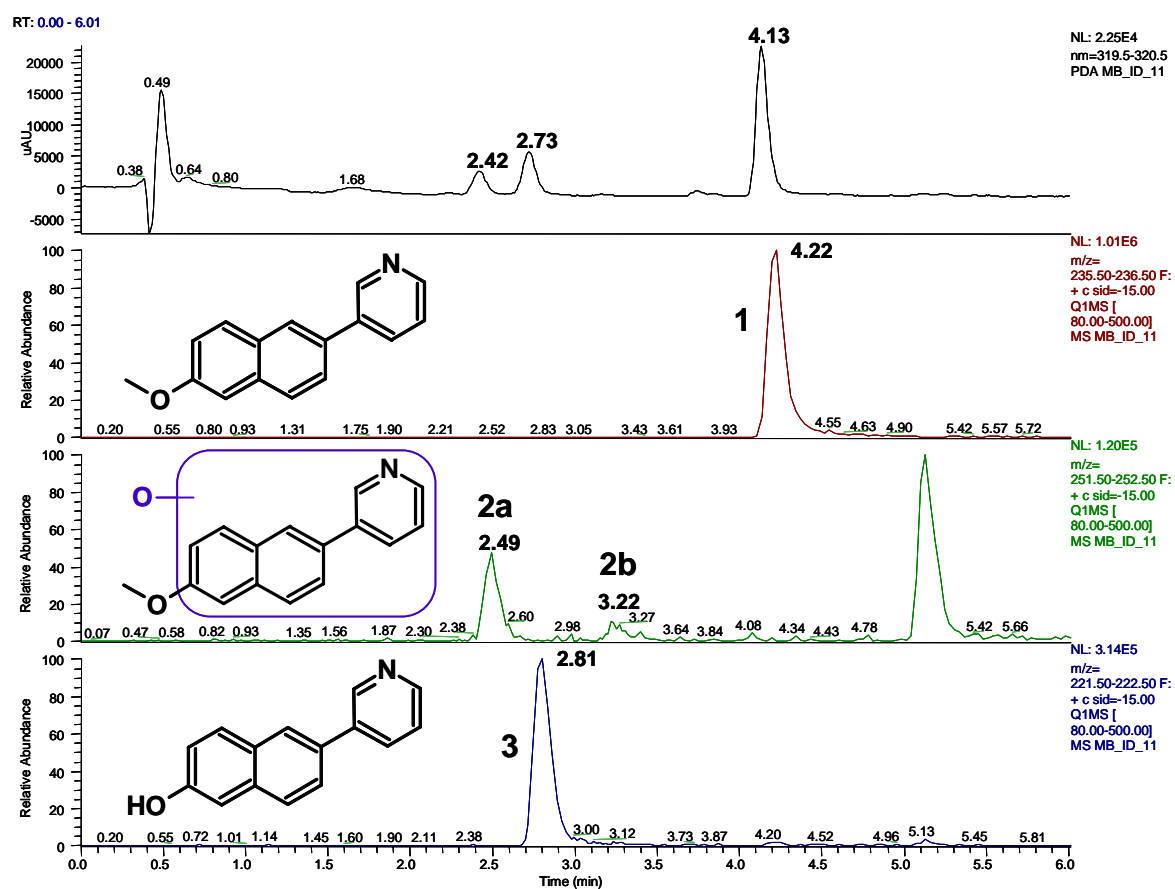
The quasimolecular ions at *m/z* 252 for (**2a**) and (**2b**) and the fragment ions of *m/z* 220 and 237 indicate that these two new signals at retention times 2.5 and 3.2 min bear an additional

oxygen atom in their (6-methoxy-2-naphthyl)pyridine structure. This demonstrates that oxidation has occurred either hydroxylating the naphthalene ring or forming an *N*-oxide.

Figure 31. MS/MS spectra of the [M+H]$^+$ of **21** (**1**) (*m/z* 236) and the metabolites **2a,b** (*m/z* 252) and **3** (*m/z* 222). The dash lines indicate possible sites of fragmentation
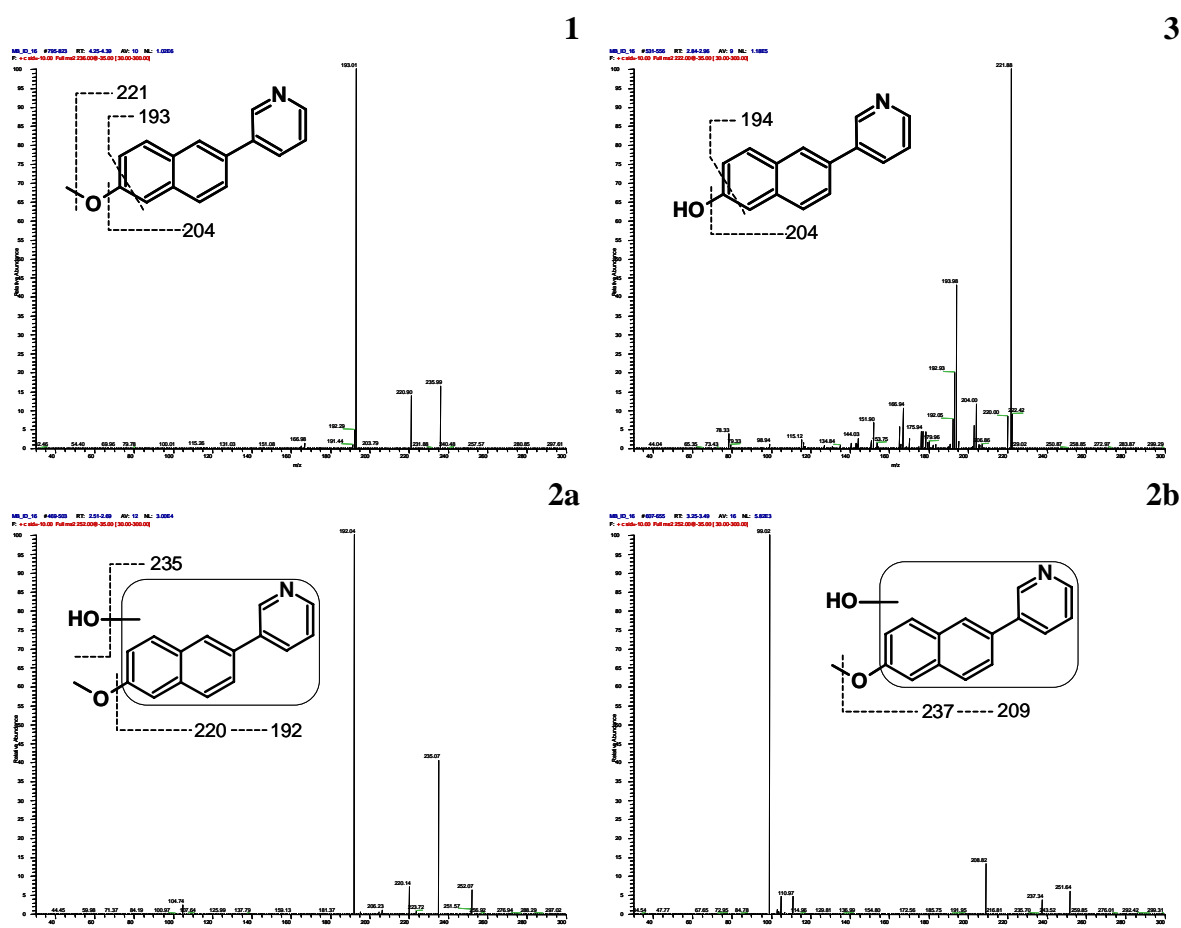
It was found that the metabolic fate of the dihydronaphthalene **53** is similar to that of the naphthalene **21**. Possible metabolites were detected in the full scan run and proceeded for further MS/MS analysis. The fragmentation of the metabolite with the [M+H]$^+$ at m/z 224 suggests that **53** has undergone O-demethylation resulting in the formation of the corresponding naphthol **68**. Two other major metabolites **69a,b** with the [M+H]$^+$ at m/z 254 bear an additional oxygen atom in their dihydronaphthalene structure, indicating that oxidation occurred. The proposed metabolic pathway of compound **53** is illustrated in Scheme 19.

Scheme 19. Proposed metabolic pathway of compound **53**

53

Demethylation   Oxidation

68   **69a-b**
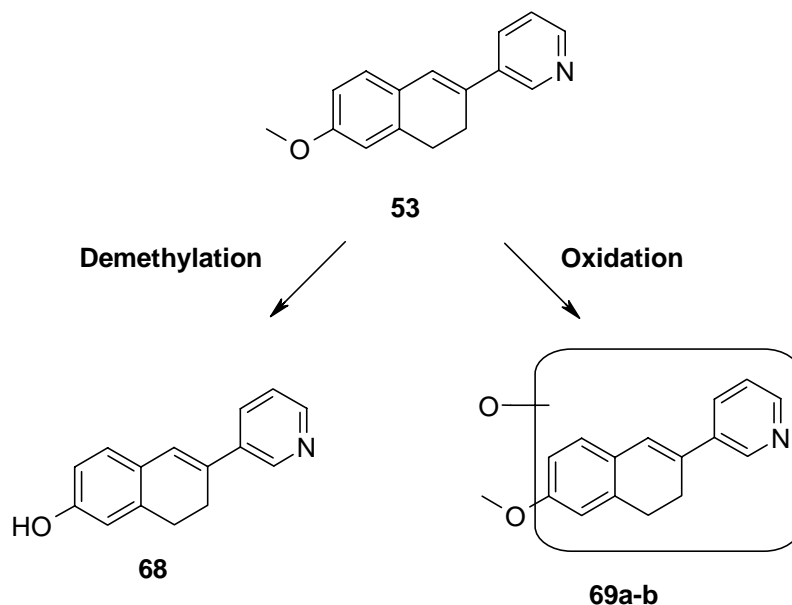
3.5.5. Permeability screening using Caco-2 monolayers

Another crucial parameter for *in vivo* potency is oral absorption. The prediction of peroral drug absorption *in vivo* was performed by Christiane Scherer (Universität des Saarlandes) using a generally accepted *in vitro* model, Caco-2 monolayers (Yee, 1997). Caco-2 cells are derived from human adenocarcinoma colon cells and spontaneously differentiate when grown on porous polycarbonate membranes to form monolayers possessing functions similar to intestinal enterocytes. The higher the measured transport in Caco-2 cells, the higher is the expected peroral absorption.

The *in vivo* test compounds **21** and **53** and other selected compounds (**17,27-30,33-35,37,39,41,50-52,56-59**) (structures in Table 14) which showed high activity and selectivity were screened for peroral drug absorption using Caco-2 monolayers. In order to increase the throughput of the Caco-2 assay, a multiple dosing approach was developed for the test compounds (cassette dosing). The feasibility of the application of compound mixtures was tested for **21, 27, 37** and **53** in comparison to the permeability of single dosing. The rest of the compounds were only tested as a mixture because no inherent interactions were expected. Four reference compounds were used in each assay for validation of the transport properties of the Caco-2 cells. By this approach, compounds can be marked as low (P_{app} (10^{-6} cm/sec) < 1), medium (1 < P_{app} (10^{-6} cm/sec) < 10) or highly (P_{app} (10^{-6} cm/sec) > 10) permeable.

Table 14. Caco-2 cell permeation in a multiple dosing approach

| | 17 | | 21,27-30,33-35,
37,39,41 | | 50-53 | | 56-59 |

Compound	R	n	R'	R''	P_{app} (10^{-6} cm/sec)[a,b]
17					14.7 ± 0.6
21	6-OMe				7.9 ± 0.6
27	H				2.9 ± 0.7
28	6-Br				1.2 ± 0.1
29	6-OH				17.4 ± 1.0
30	6-OEt				3.6 ± 0.9
33	6-CN				10.8 ± 0.4
34	5-Cl-6-OMe				1.5 ± 0.1
35	5-Br-6-OMe				1.0 ± 0.3
37	1,5-diCl-6-OMe				$2.5 \pm 0\,3$
39	1-Cl-7-OMe				0.5 ± 0.05
41	6-COOMe				0
50	H	0			6.6 ± 0.5
51	H	1			14.6 ± 0.6
52	5-OMe	0			12.5 ± 0.2
53	6-OMe	1			13.5 ± 0.6
56			Me	H	3.4 ± 0.1
57			Et	H	21.6 ± 1.6
58			H	3-Me	14.7 ± 0.6
59			H	4-Me	16.3 ± 3.0
atenolol					0.1 ± 0.03
ketoprofene					25.7 ± 0.5
testosterone					9.4 ± 0.2
erythromycin					< LOD

[a] Permeability of research compounds was ranked according to reference compounds: atenolol, ketoprofene, testosterone and erythromycin; LOD = limit of detection; [b] Mean value of three determinations.

Most of the tested compounds were medium to highly permeable. Only the halogenated naphthalenes (**28,34,35,37,39**) had a lower permeability. The 6-hydroxy naphthalene **29** and the 4-ethyl dihydronaphthalene **57** turned out to be most permeable compounds with P_{app} values of 17.4 and 21.6 10^{-16} cm/sec, respectively. The ester **41**, on the other hand, was not permeable at all (Table 14).

3.5.6. Lipophilicity and solubility

The logP values of the compounds **14-23, 27-48** and **50-65** were calculated to obtain more information about lipophilicity, which is related to absorption and bioavailability (Table 15). The significance of logP is captured by the Rule-of-5, which states that a molecule will be poorly absorbed if its logP value exceeds 5 (Lipinski *et al.*, 1997). All the inhibitors had logP values in the range between 1.7 and 5.0. Only the benzyloxy compound **32** and the ethyl substituted dihydronaphthalenes **57** and **60** exhibited a less favourable logP of 5.5.

Table 15. LogP and solubility values of compounds **14-23, 27-48** and **50-65**

Compound	logP[a]	Solubility[a,b] (mol/l)	Compound	logP[a]	Solubility[a,b] (mol/l)
14	2.69 ± 0.51	$2.9\ e^{-4}$	**30**	4.34 ± 0.26	$3.7\ e^{-5}$
15	3.11 ± 0.25	$3.3\ e^{-4}$	**31**	4.87 ± 0.26	$1.7\ e^{-5}$
16	3.72 ± 0.33	$1.4\ e^{-4}$	**32**	5.46 ± 0.27	$4.4\ e^{-6}$
17	3.21 ± 0.57	$2.8\ e^{-4}$	**33**	3.33 ± 0.29	$1.6\ e^{-4}$
18	3.13 ± 0.81	$9.7\ e^{-5}$	**34**	4.35 ± 0.36	$7.6\ e^{-6}$
19	3.13 ± 0.81	$2.2\ e^{-4}$	**35**	4.38 ± 0.37	$3.9\ e^{-5}$
20	1.85 ± 0.81	$2.0\ e^{-3}$	**36**	4.00 ± 0.38	$4.5\ e^{-5}$
21	3.81 ± 0.26	$7.9\ e^{-5}$	**37**	4.71 ± 0.42	$7.2\ e^{-6}$
22	3.74 ± 0.26	$7.9\ e^{-5}$	**38**	3.81 ± 0.26	$7.9\ e^{-5}$
23	2.77 ± 0.30	$1.6\ e^{-4}$	**39**	4.28 ± 0.28	$1.4\ e^{-5}$
27	3.89 ± 0.24	$2.0\ e^{-4}$	**40**	3.56 ± 0.26	$3.2\ e^{-4}$
28	4.66 ± 0.34	$1.3\ e^{-6}$	**41**	3.87 ± 0.26	$7.1\ e^{-5}$
29	3.15 ± 0.25	$2.3\ e^{-4}$	**42**	3.71 ± 0.37	$4.5\ e^{-5}$

Compound	logP[a]	Solubility[a,b] (mol/l)	Compound	logP[a]	Solubility[a,b] (mol/l)
43	2.41 ± 0.27	$1.8\ e^{-4}$	**55**	4.11 ± 0.34	$1.1\ e^{-4}$
44	2.53 ± 0.34	$2.9\ e^{-4}$	**56**	5.00 ± 0.33	$1.0\ e^{-4}$
45	5.05 ± 0.24	$1.0\ e^{-5}$	**57**	5.53 ± 0.33	$4.5\ e^{-5}$
46	2.41 ± 0.26	$9.3\ e^{-4}$	**58**	4.91 ± 0.33	$1.3\ e^{-4}$
47	2.58 ± 0.26	$6.0\ e^{-4}$	**59**	4.91 ± 0.33	$9.5\ e^{-5}$
48	1.68 ± 0.28	$1.5\ e^{-3}$	**60**	5.44 ± 0.33	$4.1\ e^{-5}$
50	4.05 ± 0.30	$6.7\ e^{-4}$	**61**	2.95 ± 0.57	$4.7\ e^{-4}$
51	4.41 ± 0.33	$2.3\ e^{-4}$	**62**	3.41 ± 0.57	$2.5\ e^{-4}$
52	3.99 ± 0.32	$2.0\ e^{-4}$	**63**	3.36 ± 0.58	$2.2\ e^{-4}$
53	4.36 ± 0.34	$7.1\ e^{-5}$	**64**	3.34 ± 0.27	$3.4\ e^{-3}$
54	4.39 ± 0.35	$6.8\ e^{-5}$	**65**	3.34 ± 0.27	$3.4\ e^{-3}$

[a] The predicted values were obtained using the ACD/I-Lab Web service (ACD/LogP 8.02 or ACD/Aqueous Solubility 8.02). [b] at pH 7.4.

Another important feature of candidate drugs is the solubility of the compound in water. The solubility largely dictates the route of drug administration and, quite often, the fate of drug candidates. Low solubility can limit *in vivo* bioavailability and therapeutic levels. Compounds **14-23, 27-48** and **50-65** showed solubility values in the range of $1.3\ e^{-6}$ and $3.4\ e^{-3}$ mol/l at pH 7.4, calculated using the ACD/Aqueous Solubility 8.02 program.

3.5.7. *In vivo* pharmacokinetic evaluation

3.5.7.1. Pharmacokinetic profiles of compounds 21 and 53.

It is the major purpose of *in vivo* pharmacokinetic studies to determine the relationship between dose and plasma concentration in order to obtain important information on drug absorption and elimination. Since the *in vitro* models (see 3.5.4. and 3.5.5.) were not able to explain the low *in vivo* potency of our CYP11B2 inhibitors **21** and **53**, the pharmacokinetic properties of these compounds were investigated in a rat model (cooperation with Pharmacelsus CRO, Saarbrücken).

Figure 32. Mean plasma profiles of **21** (MV23)**, 51** (MV18), **53** (MV45), SU11A and TS3 after po cassette dosing in 4 adult male rats (5 mg/kg)
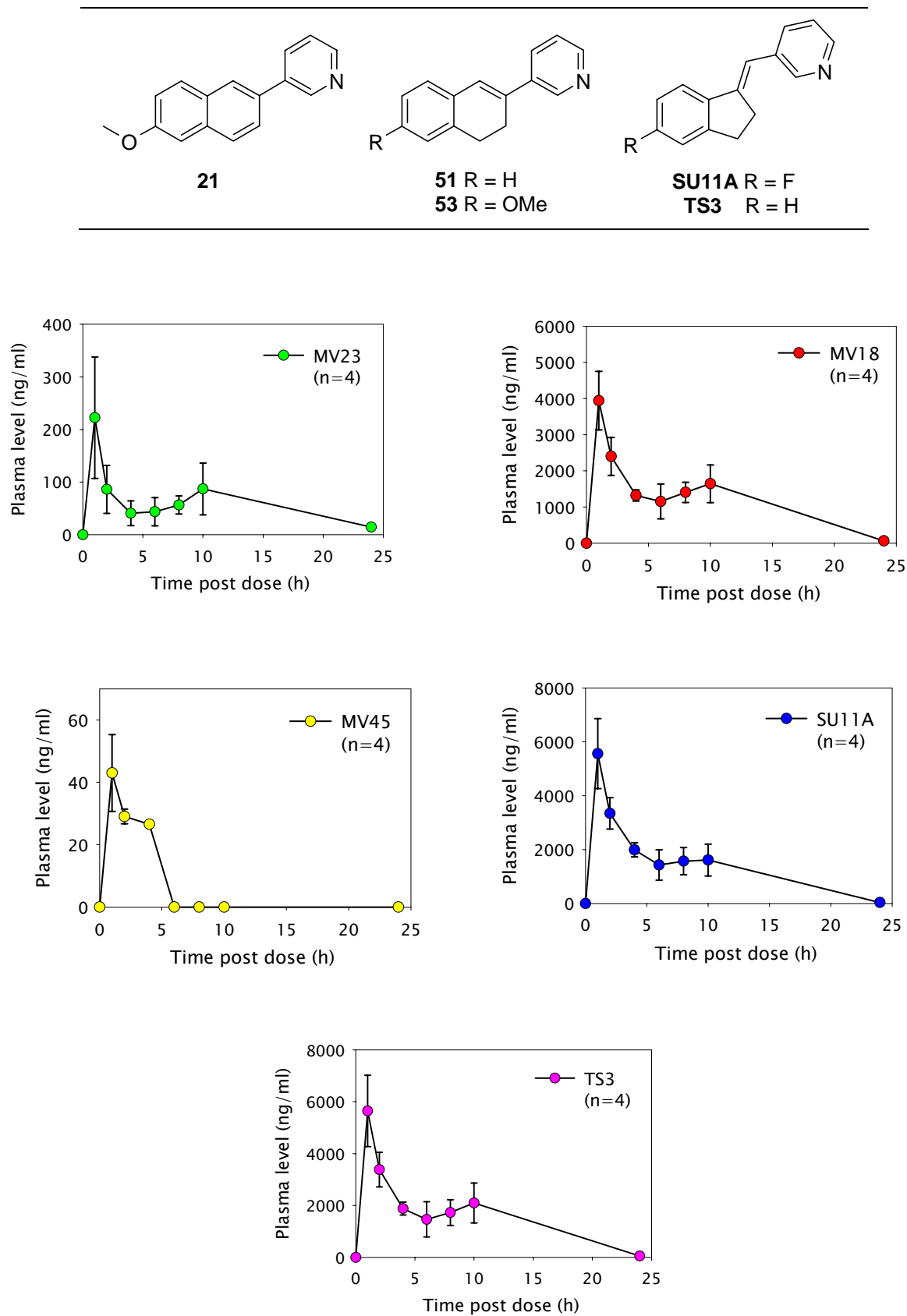
The pharmacokinetic profiles of **21** and **53**, together with **51**, SU11A and TS3, were determined after a peroral (po) dosing to adult male rats in a single cassette (N = 5). Blood samples were collected at different time points from the jugular vein. A HPLC-MS/MS method was established for quantification of the test compounds in rat plasma. The (pyridylmethylene)indanes SU11A and TS3 were described earlier in our working group as potent CYP11B2 inhibitors (Ulmschneider *et al.*, 2005b). *In vivo*, SU11A and TS3 showed a reduction of the aldosterone plasma level of 15 and 25 %, respectively. The mean profiles of the plasma levels (ng/ml) of the compounds after po administration at the dose of 5mg/kg are presented in Figure 32. The pharmacokinetic parameters are shown in Table 16.

Table 16: Pharmacokinetic parameters of the test compounds after oral dosing

Parameter	**51** (5mg/kg)	**21** (5mg/kg)	**53** (5mg/kg)	**SU11A** (5mg/kg)	**TS3** (5mg/kg)
C_{max} obs. (ng/ml)	3940.9	222.4	43.0	5562.1	5644.3
t_{max} obs. (h)	1	1	2	1	1
$t_{½\,\beta}$ (h)	3.00	5.42	15.40	2.58	2.60
Cl_{int} (l/kg/h)	0.17	3.24	6.76	0.148	0.131
$AUC_{o-\infty}$ (ng/mlxh)	29188.5	1543.5	739.5	33879.7	38191.6

C_{max} obs.: maximal concentration measured in the plasma; t_{max}: time point with the maximal plasma concentration measured; $t_{1/2\,\beta}$: terminal half-life; Cl_{int}: intrinsic hepatic clearance; $AUC_{o-\infty}$: area under the curve; E_h: hepatic extraction ratio

After po dosing, different C_{max} values in the range from 43 to 5644 ng/ml were measured. The lowest C_{max} was found for the 6-methoxy dihydronaphthalene compound **53** followed by **21** and **51**. The highest C_{max} (5644 ng/ml) was measured for TS3. After C_{max} was reached, plasma levels of the 5 tested compounds were cleared with different rates (0.17 to 6.76 l/kg/h) resulting in different plasma terminal half-life values from 2.6 to 15.4 h. TS3 is the compound with the highest AUC (38192 ng×h/ml), followed by SU11A, **51**, **21** and **53**.

Since the five compounds were given at the same dose, it is possible to compare their disposition in the body after po application. With regard to the area under the curve value, which indicates the total amount of compound absorbed, we can conclude that compounds TS3, SU11A and **51** are much more absorbed in the body than **21** and **53**. These latter compounds exhibit low compound disposition, which is in good correlation with their low maximal plasma concentration measured in this study. Keeping in mind the high metabolic stability of **21** and **53** in liver microsomes (see 3.5.4.), we conclude that the low disposition is

mainly due to lower absorption and not to rapid elimination of the compounds from the plasma. The low absorption of the 6-methoxy substituted compounds **21** and **53** could be the reason for the low activities exhibited in the *in vivo* experiment (see 3.4.3.).

3.5.7.2. Pharmacokinetic evaluation in search of suitable *in vivo* candidates

In order to find more suitable candidates for *in vivo* testing, the pharmacokinetic properties of other CYP11B2 inhibitors were investigated using the po cassette dosing approach. Test compounds with more favourable pharmacokinetic properties are expected to display better *in vivo* activity. Inhibitors, which displayed a selectivity factor > 100 *in vitro* and which were medium to highly permeable in the Caco-2 experiments, were administered perorally in rats in cassettes of 5 compounds at the time.

Pharmacokinetic evaluation of compounds 27, 29, 30, 50 and fadrozole

The naphthalene compounds **27**, **29** and **30**, the indene **50** and fadrozole were administered in a single cassette. After measurement of plasma drug levels (Figure 33) and calculation of the pharmacokinetic parameters, described in Table 17, the following observations could be made.

Table 17. Pharmacokinetic parameters of the compounds **27, 29, 30, 50** and fadrozole

Parameter	**Fadrozole** (5mg/kg)	**27** (5mg/kg)	**29** (5mg/kg)	**30** (5mg/kg)	**50** (5mg/kg)
C_{max} obs. (ng/ml)	486.90	373.80	13.20	10.90	339.00
t_{max} obs. (h)	1.00	1.00	1.00	1.00	1.00
$t_{\frac{1}{2}\beta}$ (h)	4.06	10.65	40.43	5.89	7.10
Cl_{int} (l/kg/h)	1.76	4.24	37.41	166.06	5.20
$AUC_{0-\infty}$ (ng/mlxh)	2838.60	1179.00	133.70	30.10	961.30

The compounds **29** and **30** show very low disposition in the body after po application. Their AUC values vary from 134 to only 30 ng/ml×h. In accordance, the C_{max} values range from 13 to 11 mg/kg. Compound **50** and **27** showed similar maximal plasma concentrations (339 and 374 ng/ml, respectively) and presented higher AUC values. The plasma levels were cleared with different rates resulting in different half-life values (4.06-40.4 h).

76

Figure 33. Mean plasma profiles of **27** (MV22)**, 29** (MV28), **30** (MV39), **50** (MV26), and fadrozole after po cassette dosing in 3 adult male rats at the dose of 5 mg/kg
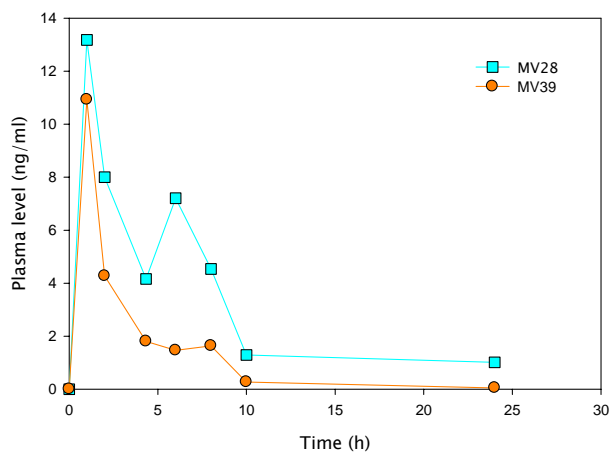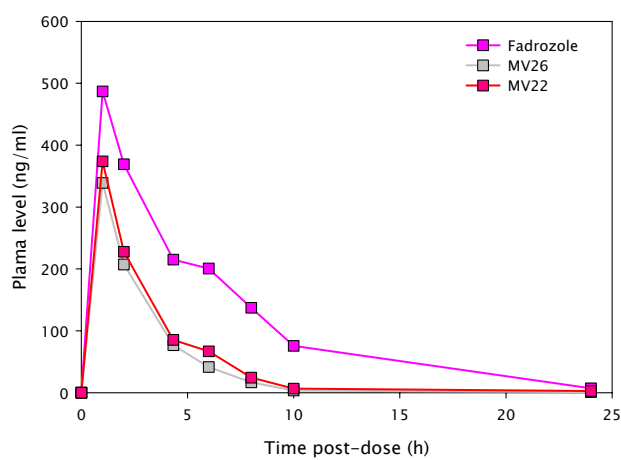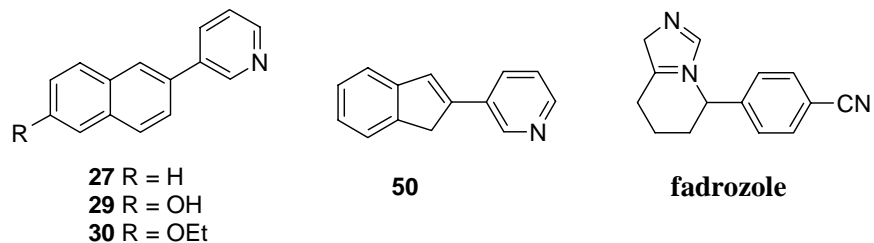
Pharmacokinetic evaluation of compounds 28, 56, SU1A, SU20A and fadrozole

In a third cassette dosing, a mixture of **28**, **56**, SU1A and SU20A was administered peroral to male adult rats. In this case, very low plasma drug levels could be detected for all the compounds. The different C_{max} values ranged from 7.6 to 138.1 ng/ml. The lowest C_{max} was measured for the 1-methyl substituted dihydronaphthalene **56**. Due to their low C_{max} values, the test compounds also presented low AUC (31.9-220.7 ng/ml×h) (Table 18).

Table 18. Pharmacokinetic parameters of compounds **28**, **56,** SU1A and SU20A
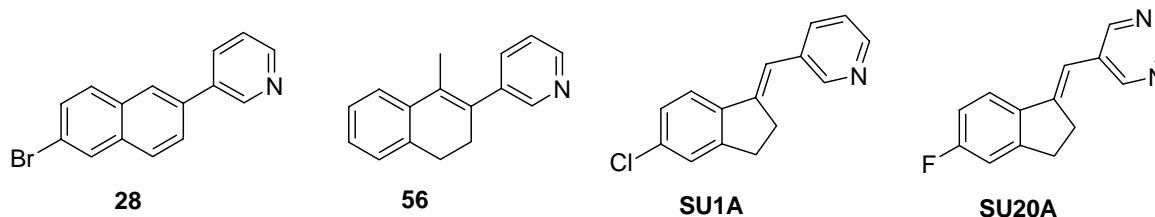
Parameter	28 (5mg/kg)	56 (5mg/kg)	SU1A (5mg/kg)	SU20A (5mg/kg)
C_{max} obs. (ng/ml)	39.10	7.60	54.30	138.10
t_{max} obs. (h)	1.00	1.00	2.00	1.00
$t_{½\,β}$ (h)	5.99	6.83	3.96	1.61
Cl_{int} (l/kg/h)	22.66	156.51	17.02	8.11
$AUC_{0-∞}$ (ng/mlxh)	220.70	31.90	293.8	616.20

Pharmacokinetic evaluation of compounds 37, 51, 52, 59 and fadrozole

In a last cassette dosing, the pharmacokinetic parameters of the inhibitors **37**, **51**, **52**, **59** and fadrozole were evaluated (Table 19). The lowest C_{max} was found for **37** followed by **52** and **59**. Compound **51** and fadrozole showed similar maximal plasma concentrations. Fadrozole was the compound with the highest AUC (3575 ng/ml×h), followed by **51**. Compound **52** showed the lowest absorption in the body with an AUC value of only 69.4 ng/ml×h. The results found for fadrozole are in good correlation with the results of a previous cassette dosing. The plasma concentrations of **51**, however, are much lower than the plasma levels measured in the first cassette dosing (see 3.5.7.1.).

Table 19. Pharmacokinetic parameters of compounds **37**, **51, 52, 59** and fadrozole.

Parameters	**Fadrozole** (5mg/kg)	**51** (5mg/kg)	**37** (5mg/kg)	**59** (5mg/kg)	**52** (5mg/kg)
C_{max} obs. (ng/ml)	453.90	440.40	19.00	161.20	22.80
t_{max} obs. (h)	1.00	1.00	1.00	1.00	1.00
$t_{\frac{1}{2}\beta}$ (h)	2.24	4.85	67.79	5.25	1.26
Cl_{int} (l/kg/h)	1.40	2.24	13.92	5.14	72.05
$AUC_{o-\infty}$ (ng/mlxh)	3575.10	2235.60	359.20	972.1	69.40

3.5.8. Discussion and conclusion

For testing the *in vivo* potency of our *in vitro* very active and highly selective CYP11B2 inhibitors, we used the rat model of Häusler *et al.* with slight modifications. After stimulation of the gluco- and mineralocorticoid biosynthesis with ACTH, the test compounds were administered intraperitoneally. Two hours later, the rats were sacrificed and the aldosterone and corticosterone serum levels were determined by RIA and compared with untreated controls.

The 6-methoxy substituted naphthalene **21** and dihydronaphthalene **53** were selected to be tested *in vivo* together with the reference compound fadrozole. The results showed that both of the *in vitro* highly active compounds were not able to decrease the serum aldosterone levels significantly. They showed *in vivo* only an inhibition of 17.1 and 13.1%, respectively. However, it might be possible to obtain a statistically significant inhibition by increasing the doses of the test compounds. Although the corticosterone serum level was not influenced by the compounds and thus some selectivity was noticeable, the *in vivo* results were disappointing. With IC_{50} values of 2 and 6 nM in the *in vitro* assay, the *in vivo* potency should have been much higher. In order to find out why the *in vitro* active CYP11B2 inhibitors

showed only little activity *in vivo,* some pharmacokinetic properties of the test compounds were investigated.

Metabolic stability studies provided information on the extent to which these compounds are metabolized. By using rat liver microsomes, the half-lifes of the test compounds were determined. With half-lifes of 67 and 93 minutes, the compounds showed to be metabolically stable. The fast metabolism of test compounds has negative influence on the *in vivo* activity. The results of the metabolic stability assay, however, showed that a fast hepatic metabolism of the test compounds is probably not the reason for the low *in vivo* activity. Additionally, possible metabolites of the test compounds were characterized by LC-MS/MS. One of the major metabolites of the 6-methoxy substituted naphthalene compound **21** was the hydroxylated naphthalene compound **29**, which exhibited high activity in the CYP11B2 expressing V79 cells assay as well (IC_{50} value = 22.6 nM).

The prediction of peroral drug absorption *in vivo* was performed by using a generally accepted *in vitro* model, Caco-2 monolayers (Yee, 1997). Permeability screening of the test compounds **21** and **53** and other active and selective inhibitors showed that almost all of the (dihydro)naphthalenes and indenes were medium to highly permeable. When halogens were introduced to the naphthalene core the permeability dropped substantially. With an ester group on the naphthalene ring, the permeability was completely gone.

Two physicochemical parameters have a very strong influence on drug-like properties of a compound: i.e. aqueous solubility, which is critical to drug delivery, and hydrophobicity (logP), which plays a key role in drug absorption, transport and distribution. The aqueous solubility of our inhibitors was in the range between 1.3 e^{-6} and 2.3 e^{-4} mol/l at pH 7.4. A good compound must be able to reach its target at effective concentrations. Therefore, the lowest acceptable solubility of a compound is related to its pharmacological potency and its permeability. The compounds **28, 32** and **34** had low solubility values ($< 1.0 \text{ e}^{-5}$). However, due to their very high potency towards CYP11B2, these inhibitors might still be possible drug candidates. All the CYP11B2 inhibitors exhibited favourable logP values lower than 5, except the benzyloxy naphthalene **32**, which was also poorly soluble in water (4.4 e^{-6}) and the dihydronaphthalenes **57** and **60**. Our most potent CYP11B2 inhibitors **33** and **53** had logP values of 3.3 and 4.4, respectively. The logP of the most selective inhibitor **52** (selectivity factor = 1421) was 4.

Based on the permeability and metabolic stability results, we can conclude that the test compounds **21** and **53** have some favourable pharmacokinetic properties: they display

metabolic stability and oral bioavailability. So what can be the reason for the low *in vivo* activity?

To answer this question, *in vivo* pharmacokinetic studies were performed with a series of *in vitro* highly active and selective inhibitors, including the compounds **21** and **53**. After peroral cassette dosing of five compounds to adult male rats, the plasma drug levels were measured using LC-MS/MS and pharmacokinetic parameters, like C_{max}, $t_{1/2}$, Cl and AUC were calculated. Since the compounds were given at the same dose, it is possible to compare their disposition in the body. Comparing the different AUC values, which indicate the total amount of compound absorbed, the best absorbed inhibitors could be determined. The compounds tested in the first *in vivo* assay, **21** and **53**, displayed very low AUC values and thus low disposition. As their metabolic stability was high in rat liver microsomes, the low disposition is mainly due to lower absorption and not to rapid elimination from the plasma. A possible explanation for the low activity *in vivo* could be the unfavourable absorption properties of compounds **21** and **53**. Based on the pharmacokinetic results obtained in the above described cassette dosing studies, it is possible to determine the most promising compounds for further *in vivo* testing. Because of their favourable pharmacokinetic properties the dihydronaphthalene compounds **51** and **59**, the unsubstituted indene **50** and naphthalene **27**, and SU20A should be more suitable compounds to test *in vivo* than the methoxy compounds **21** and **53**.

Another interesting point to mention is the difference in plasma concentrations of compound **51** in two different cassette dosing studies (C_{max} 1st study = 3940.9 ng/ml; C_{max} 2nd study = 440.4 ng/ml). Cytochrome P450 inhibition studies showed that compounds SU11A and TS3 are strong inhibitors of drug metabolizing enzymes (75-80% inhibition towards CYP2B6 (5 μM) and CYP2C19 (2 μM); 26-40% inhibition towards CYP2C9 (0.3 μM); unpublished results, U. Müller-Vieira). In the first cassette dosing, these compounds probably inhibited the metabolism of compound **51** leading to higher plasma concentrations. The indene **52**, one of the compounds in the second cassette, turned out to have only moderate activity towards these CYP enzymes (28 and 12% inhibition towards CYP2B6 (5 μM) and CYP2C19 (2 μM), respectively; no inhibition towards CYP2C9 (0.3 μM)) and could therefore not influence the metabolism process, explaining the lower C_{max} value. All the inhibitors tested in the drug metabolizing P450 inhibition assay showed only small activity towards CYP3A4. This P450 enzyme is the most important drug metabolizing enzyme in human liver, responsible for the metabolism of 40-50% of drugs in clinical use.

IV. Discussion

After having proposed aldosterone synthase as a novel pharmacological target as early as 1994 (Hartmann, 1994), our working group propagated more recently the blockade of aldosterone formation by inhibition of CYP11B2 for the treatment of hyperaldosteronism, congestive heart failure and myocardial fibrosis (Ehmer *et al.*, 2002). The treatment with CYP11B2 inhibitors should be a better therapeutic strategy than the use of aldosterone antagonists, like spironolactone and eplerenone. The latter compounds showed progestational and antiandrogenic side effects because of poor selectivity for the aldosterone receptor. Moreover, a correlation between the use of aldosterone antagonists and hyperkalemia-associated mortality was observed (Juurlink *et al.*, 2004). Non steroidal CYP11B2 inhibitors are preferred in order to minimize the risk of side effects caused by interference with steroid receptors.

A crucial point in the development of any CYP inhibitor is selectivity. This is especially true for CYP11B2: the inhibitors should not affect 11β-hydroxylase (CYP11B1), which is the key enzyme of glucocorticoid biosynthesis. Since both enzymes are very similar - there is an identity of 93% at the gene level (Taymans *et al.*, 1998) – this selectivity is not easy to reach.

Until now, only a few compounds are known to suppress aldosterone formation. Fadrozole, an aromatase inhibitor which is used for the treatment of breast cancer, reduced aldosterone and cortisol levels *in vitro* (Häusler *et al.*, 1989) and *in vivo* (Demers *et al.*, 1990). Ketoconazole, an antimycotic and unspecific CYP inhibitor (Bureik *et al.*, 2004), and the (imidazolylmethylene)tetrahydronaphthalenes and indanes (Ulmschneider *et al.*, 2005a) displayed moderate inhibitory activity towards CYP11B2. However, these compounds showed little or no selectivity towards other CYP enzymes and can therefore not be used in the treatment of congestive heart failure and myocardial fibrosis. The exchange of the imidazole ring by a pyridyl moiety led to another class of CYP11B2 inhibitors, the (pyridylmethylene)tetrahydronaphthalenes and indanes. These compounds turned out to be active and especially more selective inhibitors (Ulmschneider *et al.*, 2005b).

The emphasis of this work lays on one of the most used concepts in medicinal chemistry, the drug optimization process. With the aim of further increasing activity and selectivity, we used the previously described inhibitors as lead compounds. Since no X-ray crystal structure data of the target enzyme are available, we used the rational drug design approach. By modifying the lead compounds, the goal was to discover new classes of active and selective CYP11B2 inhibitors.

Synthesis and evaluation of CYP11B2 inhibitors

Guanabenz-related amidinohydrazones were described in the literature as potent non-azole inhibitors of aldosterone biosynthesis in rat adrenal gland fragments (Soll *et al.*, 1994). By combining the tetrahydronaphthalene or indane core with an amidinohydrazone moiety, we wanted to find out if these amidinohydrazones are able to inhibit our target enzyme CYP11B2. The compounds showed to be inactive towards CYP11B2 in the yeast assay as well as in experiments with the NCI-H295R cell line, which is able to produce all the adrenocortical steroids (Voets *et al.*, 2004). A plausible explanation is that the strong basic amidinohydrazones are not able to penetrate the cell membrane under physiological conditions. Thus, the aminoguanidine moiety is not a good alternative for a nitrogen containing heterocycle, which can complex with the heme iron of the CYP enzyme.

Supported by these results, we decided to focus again on compounds substituted with nitrogen containing heterocycles. Structural modifications of the core structure of the lead structure resulted in a new class of CYP11B2 inhibitors, the heteroaryl substituted naphthalenes. Comparative studies revealed that the 3-pyridine moiety is ideal with respect to activity and selectivity. The replacement of the 3-pyridine ring by 5-oxazole, 5-imidazole, 5-pyrimidine or 4-pyridine was disastrous for the activity. The bad influence of the 4-pyridine ring is in good correlation with previous results (Ulmschneider *et al.*, 2005b). For an optimal orbital overlap of the nitrogen of the inhibitor with the heme Fe, the pyridyl moiety should be located perpendicular to the heme group. In case of the 4-pyridine substituted naphthalene, the angle between the ligand and the plane of the heme is distorted. This change of geometry weakens the Fe-N interaction and leads to lower inhibitory potencies. Some 1-imidazole compounds showed high activity but the selectivity towards CYP11B2 was quite low (selectivity factor: 4-35).

Another important parameter which we evaluated was the impact of substitution of the naphthalene core on the inhibitory activity. Different substituents were introduced to investigate the influence of the position, size and chain length. The 6-position turned out to be appropriate for high activity and selectivity, as long as the substituents were not too big. The 6-propoxy and 6-benzyloxycompounds **31** and **32**, for instance, showed very low percent inhibition values (36 and 3%, respectively). A loss of activity was also observed for compounds with subsituents in 3- or 7-position.

The 3-pyridine substituted naphthalene compounds exhibited high inhibitory activities towards CYP11B2 and displayed better selecitivity profiles than the (pyridylmethylene)tetrahydronaphthalenes and indanes. The 6-cyano naphthalene **33** turned

out to be the most potent inhibitor with an IC_{50} value of 2.9 nM. The 6-ethoxy naphthalene **30** had a remarkable selectivity factor of 451.

In order to discover even more selective CYP11B2 inhibitors, we modified the 3-pyridine substituted napthalenes. Instead of introducing an unsaturated bridge into the ring, which yielded the aromatic naphthalene compounds, we introduced a saturated bridge to mimic the aliphatic ring in the tetrahydronapthalene and indane compounds. In this way, we found a new class of active and selective CYP11B2 inhibitors, the 3-pyridine substituted dihydronaphthalenes and indenes. The structure-activity relationships concerning the heme complexing heterocycles and substitution of the dihydronaphthalene core structure were similar to the ones described above. Most of the 3-pyridine substituted dihydronaphthalenes and indenes turned out to be very active and highly selective CYP11B2 inhibitors. The 6-methoxy substituted dihydronaphthalene **4** was the most active inhibitor with an IC_{50} value of 2 nM. The methoxy substituted indene **3** was a very potent (IC_{50} value = 4 nM) and the most selective compound with a remarkable selectivity factor of 1421. This compound displays the highest selectivity towards CYP11B2 described until now.

Docking and molecular dynamics studies using the homology modelled CYP11B2 structure

The 3D structure of the CYP11B2 enzyme has not been solved yet by X-ray crystallography. Therefore a homology protein model of CYP11B2 has been established (Ulmschneider *et al.*, 2005a-b). The recently resolved 3D structure of CYP2C9 was used as template. Several known inhibitors were docked and the binding pocket geometry was further refined through energy minimization and simulated annealing procedures. After optimization, docking and molecular dynamics studies were used to verify the homology modelled CYP11B2 structure and to explain some interesting structure-activity relationships.

CYP11B2 inhibitors are predominantly bound through hydrophobic interactions except for the nitrogen-metal interaction with the heme iron. The strongest interactions are formed with residues of the α-helix I. Former studies have shown that this I-helix is essential for the binding of the compounds (Rupasinghe *et al.*, 2003). These finding are also confirmed by site directed mutagenesis experiments, which indicate that the I-helix of CYP11B2 and CYP11B1 is important for substrate binding (Böttner *et al.*, 1996a-b).

Molecular dynamics (MD) calculations simulate the motion of the ligand in the binding pocket to obtain information about its time-dependent properties. The results of the MD study with some pairs of 3-pyridine and 1-imidazole substituted naphthalenes showed a good

correlation between the position of the docked compounds after 1ns of MD simulations and the potency of these inhibitors. Highly potent inhibitors remained stable throughout the simulations. Less active compounds reoriented themselves and moved away from the heme, breaking their Fe-N interactions. The 3-methoxy substituted 1-imidazole compound **18**, for instance, docked well in the active site of the protein model. Its 3-methoxy substituent fitted perfectly in a hydrophobic groove formed by hydrophobic amino acid residues. However, the methoxy substituent of the corresponding 3-pyridine compound **40** did not fit into this groove, due to the larger size of the pyridyl ring and the different geometry needed to form the coordinate bond with the heme group. This led to an energetically unfavourable position of the ligand close to the I-helix. During MD simulations, compound **40** tried to minimize the contacts of his aromatic region with the hydrophilic/hydrophobic amino acid residues of the I-helix and lost contact with the heme group.

Docking studies were able to explain the difference in potency of the 1-imidazole substituted naphthalene and dihydronaphthalene and showed the importance of hydrophobic interactions in the binding pocket. The highly active naphthalene compound **17** formed strong phenyl-CH_3 interactions with both aromatic rings of the naphthalene. The dihydronaphthalene compound **61**, on the other hand, contains only half of the aromatic rings and can make fewer interactions with its core. Therefore, it tries to enhance its binding affinity by forming additional aromatic-hydrophobic interactions via its imidazole ring. This leads to a shift of the imidazole with respect to the iron of the heme, weakening the Fe-N interactions, and explains the lower activity of **61** towards CYP11B2. These observations show that hydrophobic interactions play an important role for the positioning of inhibitors into the active site of the CYP11B2 enzyme.

At the start of the aldosterone synthase project, synthesized CYP11B2 inhibitors were used to optimize the homology modelled CYP11B2 structure. Now, this protein model demonstrates predictive value and could be used as a tool for drug optimization.

Evaluation of *in vivo* activity of CYP11B2 inhibitors

To test if our *in vitro* potent and highly selective CYP11B2 inhibitors exhibit the same potency and selectivity *in vivo*, the rat model of Häusler *et al.* was used. After stimulation of the gluco- and mineralocorticoid biosynthesis with ACTH, the test compounds were administered intraperitoneally and after two hours, the plasma aldosterone and corticosterone levels were determined. It is important to provide a stress-free environment for the test animals. Stress stimulates the glucocorticoid biosynthesis and this would lead to false-positive

results. The rats were applied with water *ad libitum*, as thirst leads also to false-positive aldosterone serum levels.

The results of the reference compound fadrozole were in good correlation with the published data (Häusler *et al.*, 1989). The *in vitro* very active 6-methoxy substituted naphthalene **21** and dihydronaphthalene **53**, on the other hand, turned out to reduce the aldosterone level with only 17.1 and 13.1 %, respectively. Although the corticosterone level was not influenced, exhibiting thus some selectivity, the test compounds did not show any significant effect on the aldosterone concentrations in the blood. By using higher doses of inhibitor, these results might improve in further experiments.

Determination of half-life values revealed that both of the test compounds had sufficient metabolic stability. The fast hepatic metabolism could be not the reason for the low *in vivo* activity. Additionally, permeability screening using Caco-2 cells showed that they were medium to highly permeable. We can thus assume that these compounds would be intestinal absorbed. The metabolic stability and oral bioavailability of compounds **21** and **53**, found by *in vitro* pharmacokinetic studies, could not explain the low *in vivo* activity.

Therefore, their pharmacokinetic profiles (absorption and clearance) were investigated *in vivo*. Experiments were carried out with male Wistar rats, which were dosed perorally (5 mg/kg) with the test compounds **21** and **53** and a series of other *in vitro* highly active and selective CYP11B2 inhibitors in cassettes (n = 5). Blood samples were collected at different time points from the jugular vein and plasma concentrations of the test compounds were measured by LC-MS/MS. Compounds **21** and **53** turned out to have a low compound disposition. Since the compounds display high metabolic stability in liver microsomes, we assume that the low disposition is mainly due to lower absorption. This is in good correlation with their low C_{max} and AUC values. This low absorption of the 6-methoxy compounds could be the reason for the low *in vivo* activity. Based on the pharmacokinetic results obtained in the cassette dosing studies, more promising *in vivo* candidates could be determined. The unsubstituted naphthalene **27**, the dihydronaphthalenes **51** and **59**, as well as the indene **50** exhibited more favourable pharmacokinetic properties and will be tested in further *in vivo* experiments.

Although the inhibitors **21** and **53** did not show significant reduction of the plasma aldosterone levels *in vivo* yet, we believe that the *in vivo* assay according to Häusler *et al.* is a useful tool to provide *proof of principle* for our treatment concept. Indeed, some previously tested unselective and selective CYP11B2 inhibitors were able to reduce the aldosterone and/or corticosterone levels in the rat (Müller-Vieira, 2005).

Future perspectives

➤ The *in vitro* activities of our test compounds **21** and **53** were measured in yeast and V79 cell assays expressing human CYP11B2. The rat CYP11B2 and human CYP11B2 have a homology of 69.6% (the homology between rat and human CYP11B1 is 64.5%). Therefore, it might be possible that due to interspecies differences active inhibitors towards human CYP11B2 are not able to exhibit the same potency towards rat CYP11B2. This could mean that a rat model is not useful to test our compounds *in vivo*. To check this hypothesis, an *in vitro* assay with rat adrenal glands (Häusler *et al.*, 1989) could be performed. The prepared rat adrenal fragments are incubated with test compound and ACTH. ACTH stimulates the corticosterone production; the aldosterone production is almost not stimulated by ACTH. The K^+-containing buffer used in the assay, however, is sufficient to stimulate aldosterone production. After incubation, the concentrations of aldosterone and corticosterone in the samples are measured using RIA. At the moment, experiments with fadrozole and compounds **21** and **53** are being performed to investigate their inhibitory activity towards rat CYP11B2 and CYP11B1.

➤ The 5-imidazole substituted naphthalene **14** and the (*Z*)-(phenylvinyl)pyridine **64** displayed selectivity factors of 0.7 and 0.4, respectively. These compounds are more active towards CYP11B1 than CYP11B2 and can be used as lead compounds in the search of CYP11B1 inhibitors. These inhibitors could be used in the treatment of diseases related to increased cortisol levels, like Cushing's syndrome and the metabolic syndrome. The drugs used in the treatment of pituitary-dependent Cushing's disease act at the hypothalamic-pituitary level and decrease corticotropin secretion. The neuromodulatory compounds used so far, like bromocriptine and somastatin are not so effective. The treatment of adrenal Cushing's disease, caused by a cortisol producing tumour in the adrenal cortex, is either the surgical removal of the tumour, or using steroid biosynthesis inhibitors. The most common inhibitors used are aminoglutethimide, metyrapone and ketoconazole and they reduce cortisol secretion by blocking one or more steroidogenic P450s. This mode of action has little selectivity and results in extra-adrenal side effects. Thus, the development of highly selective CYP11B1 inhibitors would be major improvement for the treatment of patients suffering from Cushing's syndrome.

V. Summary

The aim of this work was to design and synthesize potent and highly selective CYP11B2 inhibitors, which could be used for the treatment of congestive heart failure and myocardial fibrosis. Our efforts were focused on non steroidal compounds, which were evaluated *in vitro* and *in vivo* to determine their biological activity and selectivity towards CYP11B2.

In Chapter 3.1., the synthesis and biological evaluation of a series of amidinohydrazones **1-13** is described (Figure 33). These compounds were synthesized by condensation of the appropriate ketones with aminoguanidine nitrate or sulfate in the presence of sulfuric acid. They showed almost no inhibitory effect towards human CYP11B2. Compound **11** was tested in the adrenocortical tumour cell line NCI-H295R, but was not able to influence the formation of the adrenocorticoid steroids, aldosterone, cortisol, androstenedione and DHEA, produced by these tumour cells (Figure 33). The amidinohydrazones are strong bases and are probably not able to permeate the cell membrane under physiological conditions.

Figure 33. General structures

1-13 n = 0,1

11

Based on several reports, which support the positive effects of nitrogen containing heterocycles as suitable groups to form the necessary coordinate bond with the heme of CYP enzymes, we have synthesized different heteroaryl substituted naphthalenes **14-23** as described in Chapter 3.2. (Figure 34). This new class of CYP11B2 inhibitors was found by modifying the core of the lead structure, e.g. the (imidazolylmethylene)tetrahydronaphthalene. The 5-azole substituted naphthalenes **14-16** were prepared either by condensation of bromoacetonaphthone **14a** with formamide at high temperature or by treating naphthaldehyde **16a** and its corresponding *N*-methyl imine **15a** with tosylmethylisocyanide. The 1-imidazolyl compounds **17-20** were obtained by a copper salt catalyzed cross-coupling reaction of imidazole with arylboronic acids. The Suzuki reaction of 2-bromo-6-methoxynaphthalene **21a**

with pyri(mi)dylboronic acids yielded the pyri(mi)dine substituted compounds **21-23**. The compounds were tested for inhibitory activity towards human CYP11B2 and the active inhibitors were also tested towards CYP11B1 to obtain information about selectivity. The best compound was the 3-(6-methoxy-2-naphthyl)pyridine **21** exhibiting an IC_{50} value of 6 nM and a selectivity factor of 263 (Figure 34). It represents a new lead structure for the development of selective CYP11B2 inhibitors.

Figure 34. General structures

14-23   **21**
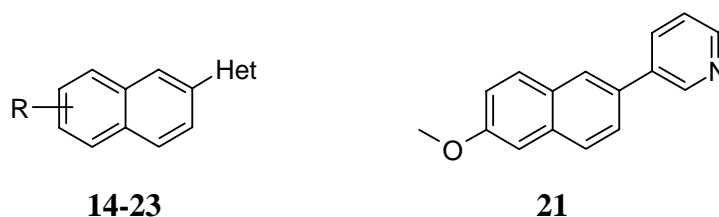
Chapter 3.3. dealt with the rational optimization of the new lead compound **21**. Different substituents were introduced on the naphthalene ring to investigate the influence of the chain length, size and position of these substituents on the inhibitory activity. The quino(xa)lines **46-48** were synthesized as well to check the influence of the naphthalene core (Figure 35). The key step in the reaction of these compounds was the Pd-catalyzed Suzuki coupling of bromo- or triflate naphthalenes with 3-pyridylboronic acid in the presence of potassium carbonate. The triflates **33,37-39a** were prepared by reacting the corresponding naphthols **33,37-39b** with Tf$_2$O. Demethylation of the methoxy compound **21** with BBr$_3$ gave the hydroxylated compound **29** and the treatment of the methyl ester **41** with formamide and NaOMe yielded the amides **43** and **44**. The compounds were tested for activity towards CYP11B2 and CYP11B1. Selectivity towards other steroidogenic CYP enzymes, CYP19 and CYP17, was evaluated as well.

The structure-activity relationships revealed that substitution in the 6-position is ideal in order to obtain highly active and selective CYP11B2 inhibitors. However, the available space in the binding pocket seems to be limited, since bigger substituents like propoxy or benzyloxy decrease the activity drastically. The quino(xa)line structure turned out to be not a good alternative for the naphthalene core. The 6-cyano compound **33** was the most potent CYP11B2 inhibitor with an IC_{50} value of 3 nM. The 6-ethoxy naphthalene **30** was the most

selective inhibitor with a remarkable selectivity factor 451 (Figure 35). Additionally, CYP19 and CYP17 were almost not affected.

Figure 35. General structures

27-48 (III)

30 R=6-EtO

IC_{50} CYP11B2=12 nM
IC_{50} CYP11B1=5419 nM
selectivity factor = 451

33 R=6-CN

IC_{50} CYP11B2=3 nM
IC_{50} CYP11B1=691 nM
selectivity factor = 238
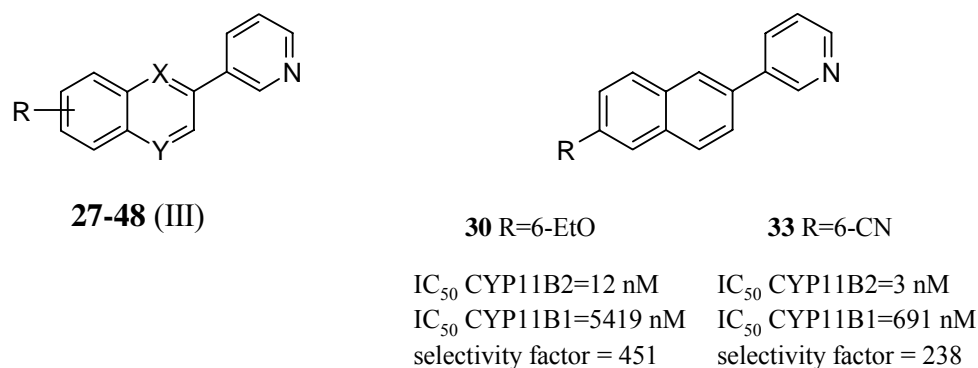
The synthesis of a series of heteroaryl substituted dihydronaphthalenes and indenes as new CYP11B2 inhibitors has been described in Chapter 3.4. (Figure 36). Two alternative pathways for the synthesis of the 3-pyridine substituted dihydronaphthalenes and indenes **50-55,58-60** are reported. The Grignard reaction of the 3-pyridine substituted tetralone **56b**, followed by dehydration with HCl, yielded the 1-alkyl substituted analogues **56-57**. The 1-imidazole substituted compounds **61-63** were prepared by treating the bromo compounds **50-51,53c** with imidazole, followed by reduction and dehydration.

Figure 36. General structures

50-55
61-63

56-60
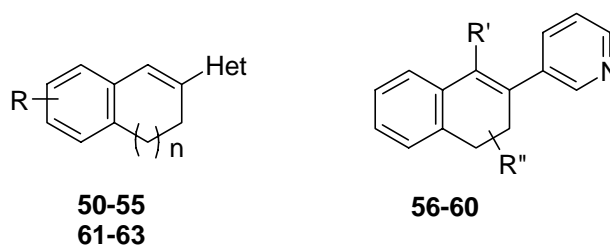
The 3-pyridine substituted dihydronaphthalenes and indenes **50-60** turned out to be more potent than the imidazole compounds **61-63**. Substitution in the 6-position was more favourable than the 7-position, but small alkyl groups in 1,3 or 4-position did not influence the high activity of this class of compounds. The 6-methoxy dihydronaphthalene **53** showed

91

the best potency (IC$_{50}$ CYP11B2 = 2 nM); the 5-methoxy indene **52**, on the other hand, was very active (IC$_{50}$ CYP11B2 = 4 nM) and had an exceptional selectivity factor of 1421, displaying the best selectivity profile described until now.

Docking and molecular dynamics studies using the homology modelled CYP11B2 protein model were performed to explain some very interesting structure-activity relationships. In Chapter 3.3., a correlation was found between the stability of the docked poses during molecular dynamics simulations and the IC$_{50}$ values. The docking studies in Chapter 3.4. showed that hydrophobic interactions play an important role for the positioning of inhibitors into the active site of the CYP11B2 enzyme.

The potent and selective compounds **21** and **53** were tested in adult male rats after stimulation with ACTH (see 3.5.). Despite their good *in vitro* profile, they decreased the blood aldosterone levels only marginally. Permeability screening using Caco-2 cells and metabolic stability studies with rat liver microsomes could not explain this lower *in vivo* activity. However, *in vivo* pharmacokinetic studies in rats indicated that compounds **21** and **53** were not optimally absorbed. Therefore, the absorption of other CYP11B2 inhibitors was evaluated and compounds with good pharmacokinetic properties were selected as possible candidates for future *in vivo* experiments.

VI. Zusammenfassung

Das Ziel dieser Arbeit war das Design und die Synthese potenter und hochselektiver CYP11B2 Inhibitoren, potentielle Therapeutika zur Behandlung von Herzinsuffizienz und Myokardfibrose. Die Bemühungen hatten nichtsteroidale Verbindungen zum Gegenstand, die *in vitro* und *in vivo* evaluiert wurden, um ihre biologische Aktivität und Selektivität gegenüber CYP11B2 zu bestimmen.

In Kapitel 3.1. wird die Synthese und biologische Testung einer Serie von Amidinohydrazonen **1-13** beschrieben (Abb. 33). Diese Verbindungen wurden durch Kondensation der entsprechenden Ketone mit Aminoguanidinnitrat oder -sulfat in Gegenwart von Schwefelsäure hergestellt. Sie zeigten beinahe keine Hemmpotenz gegenüber humanem CYP11B2. Verbindung **11** wurde an der adrenokortikalen Tumorzelllinie NCI-H295R getestet. Allerdings stellte sich heraus, dass die Verbindung nicht in der Lage war, die Bildung der adrenocorticoiden Steroide Aldosteron, Cortisol, Androstendion und DHEA zu beeinflussen, die von diesen Tumorzellen produziert werden. Die Amidinohydrazone sind starke Basen, liegen als solche protoniert vor und sind vermutlich nicht befähigt die Zellmembran unter physiologischen Bedingungen zu permeieren.

Abbildung 33. Allgemeine Strukturen

1-13   **11**
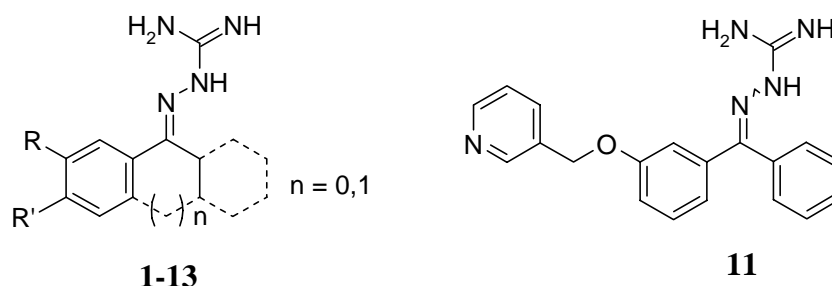
Aufgrund der breiten Erfahrungen im Arbeitskreis über positive Effekte von stickstoffhaltigen Heterozyklen als geeigneten Gruppen um das Hämeisen von CYP-Enzymen zu komplexieren, wurden in Kapitel 3.2. (Abb. 34) verschiedene Heteroaryl-substituierte Naphthaline **14-23** hergestellt. Diese neue Klasse an CYP11B2 Hemmstoffen wurde durch die Modifizierung der Kern-Leitstruktur gefunden, nämlich von (Imidazolylmethylen)tetrahydronaphthalin. Die 5-Azol-substituierten Naphthaline **14-16** wurden entweder durch Kondensation von Bromacetonaphthon **14a** mit Formamid bei hoher Temperatur hergestellt, oder durch

Behandlung von Naphthaldehyd **16a** und sein korrespondierendes *N*-Methyl Imin **15a** mit Tosylmethylisocyanid. Die 1-Imidazolyl Verbindungen **17-20** wurden durch eine kupfersalzkatalysierte Kupplungsreaktion von Imidazol mit Arylboronsäuren erhalten. Die Suzuki-Reaktion von 2-Brom-6-methoxynaphtalin **21a** mit Pyri(mi)dylboronsäuren führte zu den Pyri(mi)din-substituierten Verbindungen **21-23**. Diese Verbindung wurde auf Hemmaktivität gegenüber menschlichem CYP11B2 getestet und die aktiven Inhibitoren wurden ebenfalls gegenüber CYP11B1 evaluiert, um Informationen über die Selektivität zu erhalten. Die beste Verbindung war das 3-(6-Methoxy-2-naphthyl)pyridin **21**, das einen IC_{50}-Wert von 6 nM und einen Selektivitätsfaktor von 263 (Abb. 34) aufwies. Diese Verbindung stellt eine neue Leitstruktur für die Entwicklung von selektiven CYP11B2 Inhibitoren dar.

Abbildung 34. Allgemeine Strukturen

14-23   **21**
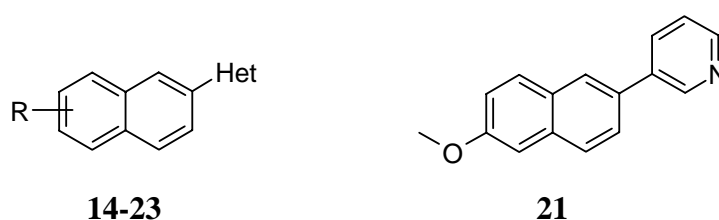
Kapitel 3.3. handelt von der rationalen Optimierung der neuen Leitverbindung **21**. Unterschiedliche Substituenten wurden in den Naphthalinring eingeführt, um den Einfluss der Kettenlänge zu erforschen, sowie Größe und Position dieser Substituenten auf die Hemmaktivität. Die Chino(xa)line **46-48** wurden auch synthetisiert, um den Einfluss des Naphthalinkerns zu überprüfen (Abb. 35). Der Schlüsselschritt in der Reaktion dieser Verbindungen war eine Pd-katalysierte Suzuki-Kupplung von Brom- oder Triflatnaphthalinen mit 3-Pyridinboronsäure in Gegenwart von Kaliumcarbonat. Die Triflate **33,37-39a** wurden durch Reaktion der korrespondierenden Naphthole **33,37-39b** mit Tf_2O hergestellt. Demethylierung der Methoxyverbindung **21** mit BBr_3 ergab die hydroxylierte Verbindung **29** und die Behandlung des Methylesters **41** mit Formamid und NaOMe führte zu den Amiden **43** und **44**. Die Verbindungen wurden auf Aktivität gegenüber CYP11B2 und CYP11B1 getestet. Selektivität gegenüber anderen steroidogenen CYP Enzymen, CYP19 und CYP17, wurde ebenfalls ermittelt.

Die Untersuchungen zu den Strukturwirkungsbeziehungen zeigten, dass Substitution in 6-Position ideal ist, um hochaktive und selektive CYP11B2 Hemmstoffe zu erhalten. Jedoch

scheint der verfügbare Raum in der Bindungstasche limitiert zu sein, da größere Substituenten wie Propoxy oder Benzyloxy die Aktivität drastisch vermindern. Die Chino(xa)lin-Struktur stellte sich als keine gute Alternative für den Naphthalinkern heraus. Die 6-Cyano-Verbindung **33** war der potenteste CYP11B2 Hemmstoff mit einem IC_{50}-Wert von 3 nM. Das 6-Ethoxy Naphthalin **30** war der selektivste Hemmstoff mit einem bemerkenswerten Selektivitätsfaktor von 451 (Abb. 35). Festzustellen bleibt ferner, dass die Enzyme CYP19 und CYP17 durch die Verbindung praktisch nicht beeinflusst wurden.

Abbildung 35. Allgemeine Strukturen
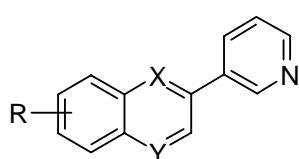
27-48 (III)
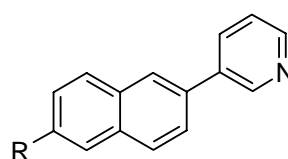
30 R=6-EtO

IC_{50} CYP11B2=12 nM
IC_{50} CYP11B1=5419 nM
Selektivitätsfaktor = 451

33 R=6-CN

IC_{50} CYP11B2=3 nM
IC_{50} CYP11B1=691 nM
Selektivitätsfaktor = 238

Die Synthese einer Serie von Heteroaryl-substituierten Dihydronaphthalinen und Indenen als neue CYP11B2 Inhibitoren wurde in Kapitel 3.4. beschrieben (Abb. 36). Zwei alternative Routen für die Synthese der 3-Pyridin-substituierten Dihydronaphthaline und Indene **50-55,58-60** wurden beschrieben. Die Grignard-Reaktion des 3-Pyridin-substituierten Tetralons **56b**, gefolgt von Wasserabspaltung mit HCl, ergab die 1-Alkyl-substituierten Analoga **56-57**. Die 1-Imidazol-substituierten Verbindungen **61-63** wurden durch Behandlung der Bromverbindungen **50-51,53c** mit Imidazol gefolgt von Reduktion und Dehydrierung hergestellt.

Die 3-Pyridin-substituierten Dihydronaphthaline und Indene **50-60** erwiesen sich als stärker wirksam als die Imidazolverbindungen **61-63**. Substitution in 6-Position war günstiger als in 7-Position. Kleine Alkylgruppen in 1,3 oder 4-Position beeinflussten nicht die hohe Aktivität dieser Verbindungsklasse. Das 6-Methoxy-Dihydronaphthalin **53** zeigte die beste Potenz (IC_{50} CYP11B2 = 2 nM); das 5-Methoxy-Inden **52**, war auf der anderen Seite sehr aktiv (IC_{50} CYP11B2 = 4 nM) und hatte einen extrem hohen Selektivitätsfaktor von 1421. Diese Verbindung ist somit die selektivste Verbindung, die bislang entwickelt wurde.

Abbildung 36. Allgemeine Strukturen
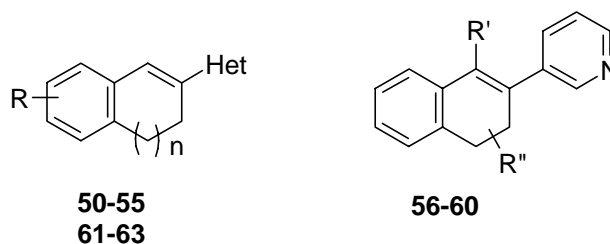
Docking und Moleküldynamikstudien wurden mit einer Homologie modellierten CYP11B2 Proteinstruktur durchgeführt, um einige der interessanten Strukturwirkungsbeziehungen zu erklären. In Kapitel 3.3. wurde eine Korrelation zwischen der Stabilität der gedockten Verbindungen während einer Molekulardynamiksimulation und den IC_{50}-Werten festgestellt. Die Dockingstudien in Kapitel 3.4. zeigten, dass hydrophobe Wechselwirkungen eine bedeutende Rolle für die Bindung der Hemmstoffe im aktiven Zentrum des CYP11B2 Enzyms spielt.

Die potenten und selektiven Hemmstoffe **21** und **53** wurden an erwachsenen männlichen Ratten nach Stimulation mit ACTH getestet (siehe 3.5.). Trotz ihres guten *in vitro* Profils reduzierten sie die Blutaldosteronspiegel nur geringfügig. Ein Permeabilitätsscreening unter Verwendung von CaCo-2-Zellen und Studien zum Metabolismus mit Rattenlebermikrosomen konnten die niedrige *in vivo* Aktivität nicht erklären. Jedoch zeigten *in vivo* Pharmakokinetikstudien an Ratten, dass die Verbindungen **21** und **53** nicht optimal resorbiert wurden. Deshalb wurde die Absorption von anderen CYP11B2 Inhibitoren bestimmt und Verbindungen mit einem guten pharmakokinetischen Profil wurden als mögliche Kandidaten für zukünftige *in vivo* Experimente ausgewählt.

VII. Experimental section

A. General description

^{1}H NMR spectra were recorded on a Bruker DRX-500 (500 MHz) instrument in DMSO-d_6 or CDCl$_3$. Chemical shifts are given in parts per million. All coupling constants (J) are given in Hz. The abbreviations of the signals are: s (singlet), br s (broad singlet), d (doublet), dd (double doublet), t (triplet), q (quartet), m (multiplet).

Elemental analyses were performed at the Department of Instrumental analysis and Bioanalysis, University of the Saarland.

IR spectra were measured neat on a Bruker Vector 33FT-infrared spectrometer. The absorption bands are expressed in cm^{-1} (v).

Mass spectra (electron spray ionization (ESI)) were measured on a TSQ quantum (Thermo Finnigan) instrument.

Melting points were measured on a Mettler FP1 melting point apparatus and are uncorrected.

Column chromatography (CC) was performed using silica gel (70-200 μm), and the reaction progress was followed by TLC analyses on ALUGRAM SIL G/UV$_{254}$ (Macherey-Nagel).

Reagents and solvents were used as obtained from commercial suppliers (Acros, Aldrich, Fluka and others) without further purification.

A.I. Synthetic procedure and characterization

Method 1

2-(2,3-Dihydro-1H-inden-1-ylidene)hydrazinecarboximidamide nitrate (1).

To a mixture of 1-indanone **1a** (800 mg, 6.05 mmol) and aminoguanidine nitrate (830 mg, 6.05 mmol) in methanol was added conc. sulphuric acid (0.33 mL, 6.05 mmol). The reaction

was stirred at 50°C for 3 hours. The precipitate was filtered off, washed thoroughly with water and diethyl ether and dried in open air.

Yield: 91%.
White solid, mp 261-262 °C.

^{1}H NMR (DMSO-d_6) : δ 2.79-2.82 (m, 2H, H-3), 3.12-3.14 (m, 2H, H-2), 7.34 (td, 1H, ^3J = 7.6 Hz, ^4J = 1.9 Hz, Ar H), 7.42-7.45 (m, 2H, Ar H), 7.88 (d, 1H, ^3J = 7.6 Hz, Ar H), 10.35 (br s, 1H, NH).

IR: ν_{max} = 3449, 3328, 3166, 1676, 1609 cm^{-1}.
MS: m/z = 189 (MH$^+$), 130, 101, 79.

$C_{10}H_{12}N_4$ (188.24)

2-(3,4-Dihydronaphthalen-1-ylidene)hydrazinecarboximidamide (2)

Synthesized from 1-tetralone **2a** as described in the literature (Pitzele *et al.*, 1988).

Yield: 23%.
Red solid, mp 183-185 °C.

^{1}H-NMR (CDCl$_3$): δ 1.90-1.92 (m, 2H, H-3), 2.77 (t, 2H, ^3J = 6.0 Hz, H-4), 2.85 (t, 2H, ^3J = 6.3 Hz, H-2), 5.68 (br s, 1H, NH), 7.12 (d, 1H, ^3J = 7.6 Hz, Ar H), 7.17-7.23 (m, 2H, Ar H), 8.07 (d, 1H, ^3J = 7.6 Hz, Ar H).

IR: ν_{max} = 3438, 3403, 3277, 3108, 1656, 1571 cm^{-1}.
MS: m/z = 203 (MH$^+$), 144, 101, 79.

$C_{11}H_{14}N_4$ (202.26)

2-(5-Methoxy-2,3-dihydro-1*H*-inden-1-ylidene)hydrazinecarboximidamide sulfate (3)

Synthesized from 5-methoxy-1-indanone **3a**. The reaction was stirred at 50°C overnight.

Yield: 78%.

White solid, mp 243-244 °C.

^{1}H-NMR (DMSO-d_6): δ 2.72-2.73 (m, 2H, H-3), 3.01-3.03 (m, 2H, H-2), 3.73 (s, 3H, OCH$_3$), 6.85 (dd, 1H, ^3J = 8.5 Hz, ^4J = 2.5 Hz, Ar H), 6.91 (d, 1H, ^4J = 2.5 Hz, Ar H), 7.70 (d, 1H, ^3J = 8.5 Hz, Ar H), 10.17 (br s, 1H, NH).

IR: $ν_{max}$ = 3459, 3357, 3192, 2838, 1656 cm^{-1}.

MS: m/z = 219 (MH$^+$), 160, 101, 79.

C$_{11}$H$_{14}$N$_4$O (218.26)

2-(6-Methoxy-3,4-dihydronaphthalen-1(2H)-ylidene)hydrazinecarboximidamide sulfate (4)

Synthesized from 6-methoxy-1-tetralone **4a**. The reaction was stirred for 3 hours at room temperature. The solution was diluted with diethyl ether to obtain the precipitated product.

Yield: 45%.

White solid, mp 212-213 °C.

^{1}H-NMR (DMSO-d_6): δ 1.84-1.86 (m, 2H, H-3), 2.58 (t, 2H, ^3J = 6.4 Hz, H-4), 2.74 (t, 2H, ^3J = 6.3 Hz, H-2), 3.78 (s, 3H, OCH$_3$), 6.77-6.80 (m, 2H, Ar H), 8.26 (d, 1H, ^3J = 8.5 Hz, Ar H), 10.36 (br s, 1H, NH).

IR: $ν_{max}$ = 3449, 3310, 3213, 2837, 1667, 1586 cm^{-1}.

MS: m/z = 233 (MH$^+$), 174, 101, 79.

C$_{12}$H$_{16}$N$_4$O (232.29)

2-(7-Methoxy-3,4-dihydronaphthalen-1(2*H*)-ylidene)hydrazinecarboximidamide sulfate (5)

Synthesized from 7-methoxy-1-tetralone **5a**. The reaction was stirred overnight at room temperature. The solution was diluted with diethyl ether to obtain the precipitated product.

Yield: 25%.
White solid, mp 176-178 °C.

^{1}H-NMR (DMSO-d_6): δ 2.01-2.05 (m, 2H, H-3), 2.81 (m, 2H, H-4), 2.90 (m, 2H, H-2), 4.00 (s, 3H, OCH$_3$), 7.13 (d, 1H, ^3J = 8.2 Hz, Ar H), 7.34 (d, 1H, ^3J = 8.2 Hz, Ar H), 8.00 (d, 1H, ^4J = 2.2 Hz, Ar H), 10.63 (br s, 1H, NH).

IR: ν_{max} = 3436, 3320, 3207, 2833, 1683, 1592 cm^{-1}.
MS: *m/z* = 233 (MH$^+$), 174, 101, 79.

C$_{12}$H$_{16}$N$_4$O (232.29)

2-[5-(Pyridin-3-ylmethoxy)-2,3-dihydro-1*H*-inden-1-ylidene) hydrazinecarboximidamide sulfate (6)

Synthesized from 5-(pyridin-3-ylmethoxy)indan-1-one **6a**. The reaction was stirred overnight at 50°C.

Yield: 77%.
White solid, mp 225-226 °C.

^{1}H-NMR (DMSO-d_6): δ 2.79-2.82 (m, 2H, H-3), 3.08-3.10 (m, 2H, H-2), 5.32 (s, 2H, O-CH$_2$), 7.05 (dd, 1H, ^3J = 8.5 Hz, ^4J = 2.2 Hz, Ar H), 7.11 (d, 1H, ^4J = 2.2 Hz, Ar H), 7.80-7.84 (m, 2H, Pyr.H-5, Ar H), 8.33 (d, 1H, ^3J = 7.9 Hz, Pyr.H-4), 8.76 (dd, 1H, ^3J = 5.4 Hz, ^4J = 1.6 Hz, Pyr.H-6), 8.89 (d, 1H, ^4J = 1.6 Hz, Pyr.H-2), 10.32 (br s, 1H, NH).

IR: ν_{max} = 3418, 3187, 1673, 1616.
MS: *m/z* = 296 (MH$^+$), 237, 93.

C$_{16}$H$_{17}$N$_5$O (295.35)

2-(6-(3-Pyridin-3-ylmethoxy)-3,4-dihydronaphthalen-1(2*H*)-ylidene) hydrazinecarboximidamide sulfate (7)

Synthesized from 6-(pyridin-3-ylmethoxy)-3,4-dihydronaphthalen-1(2*H*)-one **7a**. The reaction was stirred overnight at 50°C.

Yield: 76%.
White solid, mp 208-210 °C.

^{1}H-NMR (DMSO-d_6): δ 1.86-1.88 (m, 2H, H-3), 2.60 (t, 2H, ^3J = 6.3 Hz, H-4), 2.77 (t, 2H, ^3J = 5.7 Hz, H-2), 5.36 (s, 2H, OCH$_2$), 6.93-6.95 (m, 2H, Ar H), 7.97-8.00 (m, 1H, Pyr.H-5), 8.32 (d, 1H, ^3J = 8.8 Hz, Ar H), 8.50 (d, 1H, ^3J = 7.9 Hz, Pyr.H-4), 8.86 (d, 1H, ^3J = 5.4 Hz, Pyr.H-6), 8.98 (s, 1H, Pyr.H-2), 10.37 (br s, 1H, NH).

IR: ν$_{max}$ = 3421, 3326, 2939, 1668, 1592 cm^{-1}.
MS: m/z = 310 (MH$^+$), 101, 79.

C$_{17}$H$_{19}$N$_5$O (309.37)

2-(7-(3-Pyridin-3-ylmethoxy)-3,4-dihydronaphthalen-1(2*H*)-ylidene) hydrazinecarboximidamide sulfate (8)

Synthesized from 7-(pyridin-3-ylmethoxy)-3,4-dihydronaphthalen-1(2*H*)-one **8a**. The reaction was stirred overnight at 50°C.

Yield: 45%.
Red solid, mp 174-176 °C.

^{1}H-NMR (DMSO-d_6): δ 1.84 (m, 2H, H-3), 2.60 (m, 2H, H-4), 2.70 (m, 2H, H-2), 5.33 (s, 2H, OCH$_2$), 7.04 (d, 1H, ^3J = 8.2 Hz, Ar H), 7.17 (d, 1H, ^3J = 8.2 Hz, Ar H), 7.85 (m, 1H, Pyr.H-5), 7.94 (s, 1H, Ar H), 8.36 (d, 1H, ^3J = 7.2 Hz, Pyr.H-4), 8.87 (d, 1H, ^3J = 5.4 Hz, Pyr.H-6), 8.90 (s, 1H, Pyr.H-2), 10.44 (br s, 1H, NH).

IR: ν_{max} = 3422, 3185, 2946, 2869, 1662 cm^{-1}.

MS: m/z = 310 (MH$^+$), 101, 79.

$C_{17}H_{19}N_5O$ (309.37)

2-[bis(3-methoxyphenyl)methylene]hydrazinecarboximidamide nitrate (10)

Synthesized from bis(3-methoxy-phenyl)methanone **10a**. The reaction was stirred overnight at 50°C. The solution was diluted with diethyl ether to obtain the precipitated product.

Yield: 36%.

White solid, mp 194 °C.

^{1}H-NMR (DMSO-d_6): δ 3.93 (s, 3H, OCH$_3$), 3.97 (s, 3H, OCH$_3$), 7.02 (d, 1H, ^3J = 7.8 Hz, Ar H), 7.07 (s, 1H, Ar H), 7.17-7.20 (m, 2H, Ar H), 7.34 (dd, 1H, ^3J = 8.5 Hz, ^4J = 2.5 Hz, Ar H), 7.44-7.47 (m, 2H, Ar H), 7.72 (t, 1H, ^3J = 8.2 Hz, Ar H), 9.82 (br s, 1H, NH).

IR: ν_{max} = 3506, 3314, 3151, 2834, 1668.

MS: m/z = 299 (MH$^+$), 240.

$C_{16}H_{18}N_4O_2$ (298.35)

2-(9*H*-Fluoren-9-ylidene)hydrazinecarboximidamide sulfate (12)

Synthesized from 9*H*-fluorenone **12a**. The reaction was stirred overnight at 60°C.

Yield: 55%.

Yellow solid, mp 124-126 °C.

^{1}H-NMR (DMSO-d_6): δ 7.38 (t, 1H, ^3J = 7.2 Hz, Ar H), 7.46-7.49 (m, 2H, Ar H), 7.59 (t, 1H, ^3J = 7.5 Hz, Ar H), 7.84 (d, 1H, ^3J = 7.2 Hz, Ar H), 7.94 (d, 1H, ^3J = 7.5 Hz, Ar H), 8.09 (d, 1H, ^3J = 7.5 Hz, Ar H), 8.23 (d, 1H, ^3J = 7.5 Hz, Ar H), 10.78 (br s, 1H, NH).

IR: $\nu_{max.}$ = 3436, 3318, 3166, 1684, 1570 cm^{-1}.

MS: m/z = 237 (MH$^+$), 178, 101, 79.

C$_{14}$H$_{12}$N$_4$ (236.28)

Method 2

5-Hydroxy-1-indanone (6b)

Compounds **6b-8b** were prepared according to the literature (Woo *et al.*, 1998).

A suspension of AlCl$_3$ (2.04 g, 13.35 mmol) in dry toluene (40 mL) was stirred at room temperature under nitrogen atmosphere. 5-Methoxy-1-indanone **3a** (1 g, 6.14 mmol) was slowly added. After reflux for 2 hours, the reaction was cooled and cautiously quenched with water. The resulting mixture was extracted with ethyl acetate. The organic layer was washed with water exhaustively, dried (MgSO$_4$), filtered and evaporated *in vacuo*. The residue was washed with ethyl acetate and the resulting solid was air-dried.

Used without purification.
Yield: 66%.
White solid.

^{1}H-NMR (DMSO-*d$_6$*): δ 2.52-2.54 (m, 2H, H-3), 2.98 (t, 2H,^{3}*J* =6.0 Hz, H-2), 6.79 (dd, 1H, ^{3}*J* = 8.5 Hz, ^{4}*J* = 1.6 Hz, Ar H), 6.84 (s, 1H, Ar H), 7.47 (d, 1H, ^{3}*J* = 8.5 Hz, Ar H), 10.45 (s, 1H, OH).

IR: ν$_{max.}$ = 3130, 2927, 1675, 1597, 1270 cm^{-1}.

C$_9$H$_8$O$_2$ (148.16)

6-Hydroxy-3,4-dihydronaphthalen-1(2*H*)-one (7b)

Synthesized from 6-methoxy-1-tetralone **4a**.
Used without purification.

Yield: 60%.

White solid.

^{1}H-NMR (DMSO-d_6): δ 1.95-2.00 (m, 2H, H-3), 2.48 (t, 2H, ^3J = 6.3 Hz, H-4), 2.83 (t, 2H, ^3J = 6.3 Hz, H-2), 6.65 (s, 1H, Ar H), 6.71 (dd, 1H, ^3J = 8.5 Hz, ^4J = 2.2 Hz, Ar H), 7.74 (d, 1H, ^3J = 8.5 Hz, Ar H), 10.29 (s, 1H, OH).

IR: $\nu_{max.}$ = 3130, 3026, 2936, 1645, 1574, 1248 cm^{-1}.

C$_{10}$H$_{10}$O$_2$ (162.19)

7-Hydroxy-3,4-dihydronaphthalen-1(2*H*)-one (8b)

Synthesized from 7-methoxy-1-tetralone **5a**.

Used without purification.

Yield: 70%.

Beige solid.

^{1}H-NMR (DMSO-d_6): δ 1.96-2.01 (m, 2H, H-3), 2.53 (t, 2H, ^3J = 6.3 Hz, H-4), 2.81 (t, 2H, ^3J = 6.0 Hz, H-2), 6.95 (dd, 1H, ^3J = 8.5 Hz, ^4J = 2.5 Hz, Ar H), 6.15 (d, 1H, ^3J = 8.5 Hz, Ar H), 7.23 (d, 1H, ^4J = 2.5 Hz, Ar H), 9.54 (s, 1H, OH).

IR: $\nu_{max.}$ = 3191, 2943, 1650, 1574, 1298 cm^{-1}.

C$_{10}$H$_{10}$O$_2$ (162.19)

Method 3

5-(Pyridin-3-ylmethoxy)indan-1-one (6a)

A mixture of 5-hydroxy-1-indanone **6b** (600 mg, 4.05 mmol) and K$_2$CO$_3$ (1.40 g, 10.13 mmol) in DMF (20 mL) was stirred under nitrogen atmosphere. After 10 min, picolyl chloride

hydrochloride (665 mg, 4.05 mmol) was added in portions. The reaction was stirred for 3 hours at 100°C. Water was added and the mixture was extracted with dichloromethane. The organic layer was dried (MgSO$_4$), filtered and evaporated *in vacuo*.

Purification: CC (dichloromethane/methanol 97:3).

Yield: 73%.

White solid.

^{1}H-NMR (CDCl$_3$): δ 2.67-2.70 (m, 2H, H-3), 3.10 (t, 2H, ^3J = 6.0 Hz, H-2), 5.20 (s, 2H, OCH$_2$), 6.98-6.99 (m, 2H, Ar H), 7.44 (m, 1H, Pyr. H-5), 7.72 (d, 1H, ^3J = 7.5 Hz, Ar H), 7.88 (d, 1H, ^3J = 7.5 Hz, Pyr. H-4), 8.65 (d, 1H, ^3J = 5.0 Hz, Pyr. H-6), 8.76 (s, 1H, Pyr. H-2).

IR: ν$_{max.}$ = 3052, 2954, 2932, 1698, 1610, 1260 cm^{-1}.

C$_{15}$H$_{13}$NO$_2$ (239.28)

6-(Pyridin-3-ylmethoxy)-3,4-dihydronaphthalen-1(2*H*)-one (7a)

Synthesized from 6-hydroxy-3,4-dihydronaphthalen-1(2*H*)-one **7b**.

Purification: CC (dichloromethane/methanol 90:10).

Yield: 75%.

White solid.

^{1}H-NMR (CDCl$_3$): δ 2.12-2.15 (m, 2H, H-3), 2.63 (t, 2H, ^3J = 6.4 Hz, H-4), 2.95 (t, 2H, ^3J = 6.0 Hz, H-2), 5.20 (s, 2H, OCH$_2$), 6.81 (d, 1H, ^4J = 2.0 Hz, Ar H), 6.91 (dd, 1H, ^3J = 8.8 Hz, ^4J = 2.2 Hz, Ar H), 7.50 (m, 1H, Pyr. H-5), 7.95 (d, 1H, ^3J = 8.3 Hz, Ar H), 8.03 (d, 1H, ^3J = 3.5 Hz, Pyr. H-4), 8.66 (d, 1H, ^3J = 4.4 Hz, Pyr. H-6), 8.78 (s, 1H, Pyr. H-2).

IR: ν$_{max.}$ = 3057, 2946, 2877, 1672, 1596, 1267 cm^{-1}.

C$_{16}$H$_{15}$NO$_2$ (253.30)

7-(Pyridin-3-ylmethoxy)-3,4-dihydronaphthalen-1(2*H*)-one (8a)

Synthesized from 7-hydroxy-3,4-dihydronaphthalen-1(2*H*)-one **8b**.

Purification: CC (dichloromethane/methanol 95:5).
Yield: 76%.
White solid.

^{1}H-NMR (CDCl$_3$): δ 2.10-2.15 (m, 2H, H-3), 2.65 (t, 2H, ^3J = 6.6 Hz, H-4), 2.92 (t, 2H, ^3J = 6.1 Hz, H-2), 5.14 (s, 2H, OCH$_2$), 7.13 (dd, 1H, ^3J = 8.5 Hz, ^4J = 2.8 Hz, Ar H), 7.20 (d, 1H, ^3J = 8.2 Hz, Ar H), 7.41 (m, 1H, Pyr. H-5), 7.60 (d, 1H, ^4J = 2.8 Hz, Ar H), 7.87 (d, 1H, ^3J = 7.9 Hz, Pyr. H-4), 8.61 (d, 1H, ^3J = 3.8 Hz, Pyr. H-6), 8.72 (s, 1H, Pyr. H-2).

IR: ν$_{max.}$ = 2990, 2922, 1680, 1608, 1494, 1276 cm^{-1}.

C$_{16}$H$_{15}$NO$_2$ (253.30)

Phenyl[3-(pyridin-3-ylmethoxy)phenyl]methanone (11a)

Synthesized from (3-hydroxyphenyl)(phenyl)methanone **11b**.

Purification: CC (dichloromethane/methanol 99:1).
Yield: 42%.
Brown oil.

^{1}H-NMR (CDCl$_3$): δ 5.16 (s, 2H, OCH$_2$), 7.22 (dt, 1H, ^3J = 7.2 Hz, ^4J = 2.2 Hz, Ar H), 7.40-7.44 (m, 4H, Ar H, Pyr. H-5), 7.48 (t, 2H, ^3J = 7.2 Hz, Ar H), 7.60 (t, 1H, ^3J = 7.2 Hz, Ar H), 7.79 (d, 2H, ^3J = 7.2 Hz, Ar H), 7.87 (d, 1H, ^3J = 7.8 Hz, Pyr. H-4), 8.62 (dd, 1H, ^3J = 4.7 Hz, ^4J = 1.6 Hz, Pyr. H-6), 8.73 (d, 1H, ^4J = 1.6 Hz, Pyr. H-2).

IR: ν$_{max.}$ = 3061, 2928, 2872, 1657, 1595, 1278 cm^{-1}.

C$_{19}$H$_{15}$NO$_2$ (289.34)

Method 4

(3-Hydroxyphenyl)(phenyl)methanone (11b)

BBr_3 (2.17 mL, 22.92 mmol) was slowly added to (3-methoxyphenyl)(phenyl) methanone **9a** (Negash *et al.*, 1997) (2 g, 10.42 mmol) in dry CH_2Cl_2 at -78°C under nitrogen atmosphere. After 30 min of stirring, the cooling was stopped and the reaction was stirred at room temperature overnight. The reaction was slowly quenched with methanol and then washed with water. The organic layer was dried ($MgSO_4$), filtered, evaporated *in vacuo*.

Purification: CC (dichloromethane/methanol 93:7).

Yield: 86%.

White solid.

^{1}H-NMR (DMSO-d_6): δ 5.45 (br s, 1H, OH), 7.09 (dt, 1H, ^3J = 7.3 Hz, Ar H), 7.33-7.35 (m, 3H, Ar H), 7.48 (t, 2H, ^3J = 8.2 Hz, Ar H), 7.80 (d, 2H, ^3J = 8.2 Hz, Ar H).

IR: $\nu_{max.}$ = 3341, 3062, 2958, 1643, 1595, 1288 cm^{-1}.

$C_{13}H_{10}O_2$ (198.22)

Method 5

2-[(3-methoxyphenyl)(phenyl)methylene]hydrazinecarboximidamide (9)

To a mixture of (3-methoxyphenyl)phenyl methanone **9a** (820 mg, 3.87 mmol) and aminoguanidine hemisulfate (950 mg, 3.87 mmol) in methanol (20 mL), conc. sulphuric acid (0.21 mL, 3.87 mmol) was added. After stirring overnight at reflux, extra aminoguanidine hemisulfate (470 mg, 1.91 mmol) was added to the reaction and stirring was continued for 1 day at reflux. The reaction was basified with sodium hydroxide solution (6%) and then extracted with dichloromethane. The organic layer was dried ($MgSO_4$), filtered and evaporated *in vacuo*.

Purification: CC (dichloromethane/methanol/NH$_4$OH 84:14:2).

Yield: 88% (mixture of isomers).

White crystals, mp 96-97 °C.

^{1}H-NMR (CDCl$_3$): δ 3.77 (s, 6H, OCH$_3$, OCH$_3$'), 5.90 (br s, 2H, NH, NH'), 6.75 (m, 1H, Ar H), 6.80 (d, 1H, ^3J = 7.3 Hz, Ar H), 6.87 (dd, 1H, ^3J = 8.2 Hz, ^4J = 2.7 Hz, Ar H), 6.96 (dd, 1H, ^3J = 8.2 Hz, ^4J = 2.7 Hz, Ar H), 7.02 (d, 1H, ^3J = 7.9 Hz, Ar H), 7.09 (m, 1H, Ar H), 7.18-7.45 (m, 10H, Ar H), 7.50 (d, 2H, ^3J = 8.2 Hz, Ar H).

IR: ν$_{max.}$ = 3452, 3354, 2988, 1571 cm^{-1}.

MS: m/z = 269 (MH$^+$), 210, 101, 79.

C$_{15}$H$_{16}$N$_4$O (268.36)

2-{Phenyl[3-(pyridin-3ylmethoxy)phenyl]methylene}hydrazinecarboximidamide (11)

Synthesized from phenyl[3-(pyridin-3-ylmethoxy)phenyl]methanone **11a**.

Purification: CC (dichloromethane/methanol/NH$_4$OH 84:14:2).

Yield: 72% (mixture of isomers).

Yellow solid, mp 89-91 °C.

^{1}H-NMR (CDCl$_3$): δ 5.04 (d, 4H, OCH$_2$, OCH$_2$'), 5.54 (br s, 2H, NH, NH'), 6.84 (d, 1H, ^3J = 7.5 Hz, Ar H), 6.88 (m, 1H, Ar H), 6.92 (dd, 1H, ^3J = 7.5 Hz, ^4J = 2.5 Hz, Ar H), 7.00 (dd, 1H, ^3J = 7.5 Hz, ^4J = 2.5 Hz, Ar H), 7.04 (d, 1H, ^3J = 7.5 Hz, Ar H), 7.16-7.43 (m, 13H, Ar H), 7.48-7.49 (m, 2H, Ar .H), 7.73 (dd, 2H, ^3J = 7.8 Hz, ^4J = 1.9 Hz, Pyr.H-4), 8.51 (dd, 1H, ^3J = 4.7 Hz, ^4J = 1.9 Hz, Pyr.H-6), 8.55 (dd, 1H, ^3J = 4.7 Hz, ^4J = 1.9 Hz, Pyr.H-6), 8.63 (br s, 2H, Pyr.H-2).

IR: ν$_{max.}$ = 3454, 3308, 3081, 1570, 1528 cm^{-1}.

MS: m/z = 346 (MH$^+$), 287, 195, 167.

C$_{20}$H$_{19}$N$_5$O (345.41)

Method 6

9*H*-Fluoren-9-one semicarbazone hydrochloride (13)

A mixture of semicarbazide hydrochloride (280 mg, 2.5 mmol), sodium acetate (205 mg, 2.5 mmol) and water (2.5 mL) was added slowly to a stirred solution of 9*H*-fluorenone **12a** (450 mg, 2.5 mmol) in ethanol (10 mL). The reaction mixture was stirred at room temperature overnight. The precipitate was collected, washed with water and diethyl ether and air-dried.

Yield: 73%.
Yellow solid, mp 232-234 °C.

^{1}H-NMR (DMSO-d_6): δ 7.34 (t, 1H, ^3J = 7.2 Hz, ^4J = 0.9 Hz, Ar H), 7.41 (q, 2H, ^3J = 7.2 Hz, ^4J = 0.9 Hz, Ar H), 7.51 (t, 1H, ^3J = 7.5 Hz, Ar H), 7.82 (d, 1H, ^3J = 7.5 Hz, Ar H), 7.90 (d, 1H, ^3J = 7.5 Hz, Ar H), 8.00 (d, 1H, ^3J = 7.5 Hz, Ar H), 8.25 (d, 1H, ^3J = 7.5 Hz, Ar H), 10.00 (br s, 1H, NH).

IR: $v_{max.}$ = 1700, 1670, 1573 cm^{-1}.
MS: m/z = 238 (MH$^+$), 179.

$C_{14}H_{11}N_3O$ (237.26)

Method 7

2-bromo-1-(2-naphthyl)ethanone (14a)

To a solution of 2'-acetonaphthone **14b** (2 g, 11.75 mmol) in dichloromethane/methanol (140 mL/56 mL) was added TBA Br$_3$ (6.23 g, 12.92 mmol) at room temperature. The mixture was stirred until decoloration of the orange solution took place. The solvent was removed *in vacuo* and the obtained precipitate was extracted with diethyl ether. The ether layer was dried (MgSO$_4$), filtered and evaporated *in vacuo*.

Purification: CC (dichloromethane/hexane 45:55).

Yield: 78%.

White solid.

^{1}H NMR (CDCl$_3$): δ 4.58 (s, 1H, CH$_2$), 7.89 (d, 1H, ^3J = 8.2 Hz, Ar H), 7.92 (d, 1H, ^3J = 8.2 Hz, Ar H), 7.98 (d, 1H, ^3J = 8.2 Hz, Ar H), 8.02 (dd, 1H, ^3J = 8.8 Hz, ^4J = 1.9 Hz, Ar H), 8.51 (d, 1H, ^4J = 1.2 Hz, Ar H).

IR: ν$_{max}$ = 3002, 2950, 1689 cm^{-1}.

C$_{12}$H$_9$BrO (249.11)

2-Bromoindan-1-one (50c)

Synthesized from 1-indanone **1a**.

Purification: CC (dichloromethane).

Yield: 78%.

Yellow oil.

^{1}H NMR (CDCl$_3$): δ 3.44 (dd, 1H, ^2J = 18.0 Hz, ^3J = 3.0 Hz, H-3), 3.86 (dd, 1H, ^2J = 18.0 Hz, ^3J = 7.6 Hz, H-3'), 4.67 (dd, 1H, ^3J = 7.6 Hz, ^3J = 3.0 Hz, H-2), 7.44-7.48 (m, 2H, Ar H), 7.68 (t, 1H, ^3J = 7.6 Hz, Ar H), 7.86 (d, 1H, ^3J = 7.6 Hz, Ar H).

IR: ν$_{max}$ = 3061, 1721, 1604, 1464, 1426, 1272 cm^{-1}.

C$_9$H$_7$BrO (211.06)

2-Bromo-3,4-dihydro-2*H*-naphthalen-1-one (51c)

Synthesized from 1-tetralone **2a**.

Purification: CC (dichloromethane).

Yield: 50%.

Yellow oil.

^{1}H NMR (CDCl$_3$): δ 2.45-2-57 (m, 2H, H-4), 2.92 (dt, 1H, ^2J = 17.0 Hz, ^3J = 4.4 Hz, H-3), 3.29-3.36 (m, 1H, H-3'), 4.73 (t, 1H, ^3J = 4.4 Hz, H-2), 7.28 (d, 1H, ^3J = 7.6 Hz, Ar H), 7.36 (t, 1H, ^3J = 7.6 Hz, Ar H), 7.52(td, 1H, ^3J = 7.6 Hz, ^4J = 1.3 Hz, Ar H), 8.10 (dd, 1H, ^3J = 7.9 Hz, ^4J = 1.3 Hz, Ar H).

IR: ν$_{max}$ = 3069, 2933, 1665, 1595 cm^{-1}.

C$_{10}$H$_9$BrO (225.09)

2-Bromo-6-methoxy-3,4-dihydro-2*H*-naphthalen-1-one (53c)

Synthesized from 6-methoxy-1-tetralone **4a**.

Used without further purification.
Yield: 95%.
Yellow oil.

^{1}H NMR (CDCl$_3$): δ 2.42-2-54 (m, 2H, H-4), 2.86 (dt, 1H, ^2J = 17.0 Hz, ^3J = 4.4 Hz, H-3), 3.27-3.32 (m, 1H, H-3'), 3.87 (s, 3H, OCH$_3$), 4.69 (t, 1H, ^3J = 4.4 Hz, H-2), 6.72 (d, 1H, ^4J = 2.3 Hz, Ar H), 6.87 (dd, 1H, ^3J = 8.8 Hz, ^{4}J = 2.3 Hz, Ar H), 8.06 (d, 1H, ^3J = 8.8 Hz, Ar H).

IR: ν$_{max}$ = 2944, 2837, 1674, 1596, 1495, 1258 cm^{-1}.

C$_{11}$H$_{11}$BrO$_2$ (255.11)

2-Bromo-7-methoxy-3,4-dihydro-2*H*-naphthalen-1-one (54c)

Synthesized from 7-methoxy-1-tetralone **5a**.

Purification: CC (dichloromethane).
Yield: 60%.
Beige solid.

^{1}H NMR (CDCl$_3$): δ 2.43-2-54 (m, 2H, H-4), 2.86 (dt, 1H, ^2J = 16.7 Hz, ^3J = 4.4 Hz, H-3), 3.21-3.27 (m, 1H, H-3'), 3.84 (s, 3H, OCH$_3$), 4.72 (t, 1H, ^3J = 4.4 Hz, H-2), 7.11 (dd, 1H, ^3J = 8.5 Hz, ^4J = 2.8 Hz, Ar H), 7.19 (d, 1H, ^3J = 8.5 Hz, Ar H), 7.55(d, 1H, ^4J = 2.8 Hz, Ar H).

IR: ν$_{max}$ = 2940, 2837, 1681, 1609, 1497, 1243 cm^{-1}.

C$_{11}$H$_{11}$BrO$_2$ (255.11)

2-Bromo-4-methyl-3,4-dihydronaphthalen-1(2*H*)-one (59c)

Synthesized from 4-methyl-1-tetralone **59d**.

Used without further purification.
Yield: 96% (mixture of two isomers).
Brown oil.

^{1}H NMR (CDCl$_3$): δ = 1.47 (d, 3H, ^{3}J = 7.0 Hz, CH$_3$), 1.49 (d, 3H, ^{3}J = 7.0 Hz, CH$_3$'), 2.16-2.25 (m, 2H, H-3), 2.35-2.40 (m, 1H, H-3), 2.62-2.69 (m, 1H, H-3'), 3.29 (m, 2H, H-4, H-4'), 4.78 (dd, 1H, ^{3}J = 14.2 Hz, ^{3}J = 4.7 Hz, H-2), 4.91 (dd, 1H, ^{3}J = 13.5 Hz, ^{3}J = 4.7 Hz, H-2'), 7.36 (t, 2H, ^{3}J = 7.9 Hz, Ar H), 7.41 (d, 2H, ^{3}J = 7.9 Hz, Ar H), 7.58 (td, 2H, ^{3}J = 7.9 Hz, ^{4}J = 1.6 Hz, Ar H), 8.11 (d, 2H, ^{3}J = 7.9 Hz, Ar H).

IR: ν$_{max}$ = 2965, 1688, 1601, 1458 cm^{-1}.

C$_{11}$H$_{11}$BrO (239.11)

Method 8

5-(2-Naphthyl)-1*H*-imidazole (14)

A solution of 2-bromo-1-(2-naphthyl)ethanone **14a** (500 mg, 2.01 mmol) in formamide (2.4 mL) was stirred at 185°C for 2 hours. After cooling, the mixture was poured into hot, diluted HCl solution (12 mL) and active charcoal was added. After stirring for 15 min, the mixture

was filtered and basified with an aqueous ammonia solution and extracted with ethyl acetate. The organic layer was dried (MgSO$_4$), filtered and evaporated *in vacuo*.

Purification: CC (dichloromethane).
Yield: 9%.
White solid, mp 171 ºC.

^{1}H NMR (CDCl$_3$): δ 7.38 (s, 1H, Im. H-4), 7.39-7.45 (m, 2H, Ar H), 7.73 (dd, 1H, ^3J = 8.5 Hz, ^4J = 1.9 Hz, Ar H), 7.74-7.81 (m, 4H, Ar H, Im. H-2), 8.13 (s, 1H, Ar H).

IR: ν$_{max}$ = 3125, 3044, 2852 cm^{-1}.
MS: *m/z* = 195 (MH$^+$), 168, 141.

C$_{13}$H$_{10}$N$_2$ (194.24)·0.05H$_2$O

	C	H	N
Calc.	79.99	5.22	14.35
Obs.	80.00	5.64	14.13

Method 9

1-Methyl-5-(2-naphthyl)-1*H*-imidazole (15)

A mixture of methyl-naphthalen-2-ylmethylene-amine **15a** (300 mg, 1.77 mmol), tosylmethyl isocyanide (570 mg, 2.95 mmol) and K$_2$CO$_3$ (490 mg, 3.55 mmol) in absolute methanol (30 mL) was stirred at room temperature overnight. Methanol was evaporated *in vacuo* and dichloromethane was added to the crude product. After washing with water, the organic layer was dried (MgSO$_4$), filtered and evaporated *in vacuo*.

Purification: CC (dichloromethane/methanol 97:3).
Yield: 18%.
White solid, mp 103 ºC.

^{1}H NMR (CDCl$_3$): δ 3.75 (s, 3H, CH$_3$), 7.22 (s, 1H, Im. H-4), 7.49-7.53 (m, 3H, Ar H), 7.68 (s, 1H, Im. H-2), 7.85-7.87 (m, 3H, Ar H), 7.91 (d, 1H, ^3J = 8.5 Hz, Ar H).

IR: ν_{max} = 3083, 3053, 2952, 1600, 1490 cm^{-1}.
MS: m/z = 209 (MH$^+$), 167, 139, 115.

C$_{14}$H$_{12}$N$_2$ (208.27)·0.19H$_2$O

	C	H	N
Calc.	79.41	5.90	13.23
Obs.	79.39	5.74	12.90

5-(2-naphthyl)-1,3-oxazole (16)

Synthesized from 2-naphthaldehyde **16a**.

Purification: CC (dichloromethane/methanol 97:3).
Yield: 28%.
White solid, mp 121 ºC.

^{1}H NMR (CDCl$_3$): δ 7.47 (s, 1H, Im. H-4), 7.49-7.54 (m, 2H, Ar H), 7.73 (dd, 1H, ^3J = 8.5 Hz, ^4J = 1.6 Hz, Ar H), 7.83-7.90 (m, 3H, Ar H), 7.97 (s, 1H, Im. H-2), 8.14 (s, 1H, Ar H).

IR [1]: ν_{max} = 3128, 3055, 2952, 1630, 1497 cm$^-$.
MS: m/z = 196 (MH$^+$), 167, 139, 115.

C$_{13}$H$_9$NO (195.22)·0.08H$_2$O

	C	H	N
Calc.	79.38	4.70	7.12
Obs.	79.37	4.80	7.22

Method 10

2-Methoxy-3-naphthylboronic acid (18a)

To a mixture of 2-methoxynaphthalene **18b** (1.58 g, 10 mmol) in dry THF (20 mL) under nitrogen atmosphere at –20°C, *n*BuLi (2.5 M in hexane, 4 mL, 10 mmol) was slowly added. After stirring for 2.5 hours at room temperature, the mixture was cooled to –60°C and trimethylborate (1.37 mL, 12 mmol) was slowly added. After 1 hour at –60°C and overnight at room temperature, a HCl solution (2M) was added and the reaction was stirred for 30 min. The mixture was extracted with ethyl acetate, dried ($MgSO_4$), filtered and evaporated *in vacuo*.

No further purification necessary.

Yield: 45%.

Light brown solid.

^1H NMR ($CDCl_3$): δ 4.30 (s, 3H, OCH_3), 7.16 (s, 1H, Ar H), 7.37 (td, 1H, ^3J = 8.2 Hz, ^4J = 1.3 Hz, Ar H), 7.50 (td, 1H, ^3J = 8.2 Hz, ^4J = 1.3 Hz, Ar H), 7.74 (d, 1H, ^3J = 8.2 Hz, Ar H), 7.84 (d, 1H, ^3J = 8.2 Hz, Ar H), 8.41 (s, 1H, Ar H).

IR: v_{max} = 3375, 2926, 2839, 1598, 1469, 1346 cm^{-1}.

$C_{14}H_{12}N_2O$ (224.26)

Method 11

(2-Naphthyl)-1*H*-imidazole (17)

A mixture of 2-naphthyl boronic acid **17a** (420 mg, 2.44 mmol), imidazole (200 mg, 2.93 mmol) and a catalytic amount of copper(I)iodide in dry methanol (20 mL) was refluxed for 3 hours under an atmosphere of air. Subsequently, the reaction mixture was evaporated *in vacuo*.

Purification: CC (dichloromethane/methanol 98:2).

Yield: 51%.

White solid, mp 123 ºC.

^{1}H NMR (CDCl$_3$): δ 7.26 (s, 1H, Im. H-4), 7.40 (s, 1H, Im. H-5), 7.51-7.58 (m, 3H, Ar H), 7.82 (d, 1H, ^4J = 1.5 Hz, Ar H), 7.88 (t, 2H, ^3J = 7.6 Hz, Ar H), 7.96 (d, 1H, ^3J = 7.6 Hz, Ar H), 8.05 (s, 1H, Im. H-2).

IR: ν$_{max}$ = 3116, 3058, 1688, 1602, 1493 cm^{-1}.
MS: m/z = 195 (MH$^+$), 167, 139, 115, 77, 51.

C$_{13}$H$_{10}$N$_2$ (194.24)·0.08H$_2$O

	C	H	N
Calc.	79.80	5.23	14.32
Obs.	79.79	5.13	14.28

1-(3-Methoxynaphthalen-2-yl)-1*H*-imidazole (18)

Synthesized from 2-methoxy-3-naphthaleneboronic acid **18a**.

Purification: CC (dichloromethane/methanol 97:3).

Yield: 13%.

White solid, mp 217 °C.

^{1}H NMR (CDCl$_3$): δ = 3.97 (s, 3H, OCH$_3$), 7.21 (s, 1H, Im. H-4), 7.30 (s, 2H, Ar H, Im. H-5), 7.24 (td, 1H, ^3J = 8.2 Hz, ^4J = 1.3 Hz, Ar H), 7.51 (td, 1H, ^3J = 8.2 Hz, ^4J = 1.3 Hz, Ar H), 7.74 (s, 1H, Ar H), 7.79 (d, 2H, ^3J = 8.5 Hz, Ar H), 7.87 (s, 1H, Im. H-2).

IR: ν$_{max}$ = 3059, 2940, 2839, 1506 cm^{-1}.
MS: m/z = 225 (MH$^+$).

C$_{14}$H$_{12}$N$_2$O (224.26)·HCl·0.22H$_2$O

	C	H	N
Calc.	63.54	5.14	10.59
Obs.	63.53	5.03	10.50

Method 12

1-(6-Methoxynaphthalen-2-yl)-1*H*-imidazole (19)

A mixture of 6-methoxy-2-naphthyl boronic acid **19a** (260 mg, 1.29 mmol), imidazole (50 mg, 0.75 mmol), copper(II)acetate (170 mg, 0.96 mmol), pyridine (100 mg, 1.29 mmol) and 4Å molecular sieve in anhydrous dichloromethane (5 mL) was stirred at room temperature for two days. The mixture was filtered over celite and evaporated *in vacuo*.

Purification: CC (dichloromethane/methanol 99:1).
Yield: 13%.
White solid, mp 85 ºC.

^{1}H NMR (CDCl$_3$): δ 3.95 (s, 3H, OCH$_3$), 7.18 (d, 1H, ^4J = 2.5 Hz, Ar H), 7.24 (dd, 1H, ^3J = 8.5 Hz, ^4J = 2.5 Hz, Ar H), 7.28 (s, 1H, Im. H-4), 7.38 (s, 1H, Im. H-5), 7.48 (dd, 1H, ^3J = 8.5 Hz, ^4J = 2.5 Hz, Ar H), 7.76 (s, 1H, Ar H), 7.77 (d, 1H, ^3J = 8.5 Hz, Ar H), 7.85 (d, 1H, ^3J = 8.5 Hz, Ar H), 8.07 (s, 1H, Im. H-2).

IR: ν$_{max}$ = 3113, 3003, 2962, 2842, 1607 cm^{-1}.
MS: *m/z* = 225 (MH$^+$), 210, 126.

C$_{14}$H$_{12}$N$_2$O (224.26)·0.13H$_2$O

	C	H	N
Calc.	74.21	5.45	12.36
Obs.	74.20	5.96	11.97

Method 13

3-Imidazol-1-yl-quinoline (20)

A mixture of 3-bromoquinoline **20a** (0.50 g, 2.40 mmol), imidazole (0.17 g, 2.56 mmol), K_2CO_3 (0.32 g, 2.30 mmol) and Cu(II)O (13 mg, 0.16 mmol) in nitrobenzene (4 mL) was refluxed for 24 hours with heavy stirring. After cooling, the mixture was extracted with chloroform and the organic layer was dried ($MgSO_4$), filtered and evaporated *in vacuo*.

Purified by CC (dichloromethane/methanol 97:3).
Yield: 18%.
White solid, mp 146 °C.

^{1}H NMR (CDCl$_3$): δ = 7.34 (t, 1H, ^4J = 1.3 Hz, Im. H-4), 7.44 (t, 1H, ^4J = 1.5 Hz, Im. H-5), 7.66 (td, 1H, ^3J = 8.2 Hz, ^4J = 1.3 Hz, Ar H), 7.79 (td, 1H, ^3J = 8.2 Hz, ^4J = 1.5 Hz, Ar H), 7.90 (dd, 1H, ^3J = 8.2 Hz, ^4J = 1.6 Hz, Ar H), 8.17 (s, 1H, Im. H-2), 8.18-8.19 (m, 2H, Ar H), 9.04 (d, 1H, ^4J = 1.8 Hz, Ar H).

IR: ν_{max} = 3102, 2962, 1608, 1497 cm^{-1}.
MS: *m/z* = 196 (MH$^+$), 169, 77, 51.

$C_{12}H_9N_3$ (195.23)·0.14H$_2$O

	C	H	N
Calc.	72.88	4.73	21.25
Obs.	72.86	4.76	21.07

Method 14

3-(6-Methoxy-2-naphthyl)pyridine (21)

A mixture of substituted 2-bromo-6-methoxy naphthalene **21a** (480 mg, 2.02 mmol), 3-pyridylboronic acid **24** (373 mg, 3.04 mmol), aqueous Na$_2$CO$_3$ (451 mg, 4.25 mmol) and Pd(PPh$_3$)$_4$ (0.02 eq) in ethylene glycol dimethyl ether or toluene was stirred overnight at 80°C

under nitrogen. The reaction was cooled to room temperature and water was added. The mixture was extracted with ethyl acetate, dried ($MgSO_4$), filtered and evaporated *in vacuo*.

Purification: CC (dichloromethane/methanol 97:3).
Yield: 77%.
White solid, mp 120 ºC.

^{1}H NMR ($CDCl_3$): δ 3.95 (s, 1H, OCH_3), 7.17 (d, 1H, ^4J = 2.5 Hz, Ar H), 7.22 (dd, 1H, ^3J = 8.8 Hz, ^4J = 2.2 Hz, Ar H), 7.45-7.47 (m, 1H, Pyr. H-5), 7.67 (dd, 1H, ^3J = 8.5 Hz, ^4J = 1.8 Hz, Ar H), 7.81 (d, 1H, ^3J = 8.5 Hz, Ar H), 7.85 (d, 1H, ^3J = 8.5 Hz, Ar H), 7.98 (s, 1H, Ar H), 8.04-8.06 (m, 1H, Pyr. H-4), 8.61 (dd, 1H, ^3J = 4.7 Hz, ^4J = 1.3 Hz, Pyr. H-6), 8.97 (s, 1H, Pyr. H-2).

IR: ν_{max} = 3058, 2938, 1605, 1489 cm^{-1}.
MS: *m/z* = 236 (MH$^+$).

$C_{16}H_{13}NO$ (235.29)·0.04H_2O

	C	H	N
Calc.	81.68	5.57	5.95
Obs.	81.10	5.37	5.62

4-(6-Methoxy-2-naphthyl)pyridine (22)

Synthesized from 2-bromo-6-methoxy naphthalene **21a** and 4-pyridylboronic acid **25**.

Purification: CC (dichloromethane/methanol 97:3).
Yield: 60%.
White solid, mp 159 ºC.

^{1}H NMR ($CDCl_3$): δ 3.97 (s, 3H, OCH_3), 7.19 (d, 1H, ^4J = 2.5 Hz, Ar H), 7.25 (dd, 1H, ^3J = 8.8 Hz, ^4J = 2.5 Hz, Ar H), 7.76 (dd, 1H, ^3J = 8.5 Hz, ^4J = 1.9 Hz, Ar H), 7.86 (d, 1H, ^3J = 8.5 Hz, Ar H), 7.90 (d, 1H, ^3J = 8.5 Hz, Ar H), 7.94 (dd, 1H, ^3J = 6.6 Hz, ^4J = 1.6 Hz, Pyr. H-3,

Pyr. H-5), 8.15 (d, 1H, ^4J = 1.9 Hz, Ar H), 8.75 (dd, 1H, ^{3}J = 6.3 Hz, ^4J = 1.3 Hz, Pyr. H-2, Pyr. H-6).

IR: ν_{max} = 3040, 2938, 2840, 1699, 1621, 1488, 1210 cm^{-1}.
MS: m/z = 236 (MH$^+$).

C$_{16}$H$_{13}$NO (235.29)

	C	H	N
Calc.	81.68	5.57	5.95
Obs.	81.59	6.20	5.91

5-(6-Methoxy-2-naphthyl)pyrimidine (23)

Synthesized from 2-bromo-6-methoxy naphthalene **21a** and 5-pyrimidylboronic acid **26**.

Purification: CC (dichloromethane/methanol 97:3).
Yield: 24%.
White solid, mp 155 ºC.

^{1}H NMR (CDCl$_3$): δ 3.96 (s, 3H, OCH$_3$), 7.19 (d, 1H, ^4J = 2.5 Hz, Ar H), 7.24 (dd, 1H, ^3J = 8.8 Hz, ^4J = 2.5 Hz, Ar H), 7.67 (dd, 1H, ^3J = 8.5 Hz, ^4J = 1.9 Hz, Ar H), 7.84 (d, 1H, ^3J = 8.5 Hz, Ar H), 7.90 (d, 1H, ^3J = 8.5 Hz, Ar H), 8.02 (d, 1H, ^4J = 1.9 Hz, Ar H), 9.15 (s, 2H, Pyr. H-4, Pyr. H-6), 9.26 (s, 1H, Pyr. H-2).

IR: ν_{max} = 3034, 2940, 1694, 1626, 1606, 1487, 1210 cm^{-1}.
MS: m/z = 237 (MH$^+$).

C$_{15}$H$_{12}$N$_2$O (236.28)·0.13H$_2$O, C,H,N.

	C	H	N
Calc.	75.48	5.18	11.74
Obs.	75.47	5.36	11.91

3-(2-Naphthyl)pyridine (27)

Synthesized from 2-bromonaphthalene **27a** and 3-pyridylboronic acid **24**.

Purification: CC (dichloromethane/methanol 97:3).
Yield: 82%.
White solid, mp 101 ºC.

^{1}H NMR (CDCl$_3$): δ 7.43-7.45 (m, 1H, Pyr. H-5), 7.51-7.56 (m, 2H, Ar H), 7.71 (dd, 1H, $^{3}J =$ 8.5 Hz, $^{4}J =$ 1.6 Hz, Ar H), 7.88-7.90 (m, 2H, Ar H), 7.96 (d, 1H, $^{3}J =$ 8.5 Hz, Ar H), 8.03-8.05 (m, 2H, Ar H, Pyr. H-4), 8.63 (dd, 1H, $^{3}J =$ 4.7 Hz, $^{4}J =$ 1.6 Hz, Pyr. H-6), 8.99 (dd, 1H, $^{4}J =$ 1.6 Hz, Pyr. H-2).

IR: ν$_{max}$ = 3392, 3051, 3029, 1599, 1484 cm^{-1}.
MS: $m/z =$ 206 (MH^{+}), 178, 151, 77, 51.

C$_{15}$H$_{11}$N (205.26)·0.04H$_2$O

	C	H	N
Calc.	87.77	5.40	6.82
Obs.	87.44	5.63	6.68

3-(6-Bromo-2-naphthyl)pyridine (28)

Synthesized from 2,6-dibromonaphthalene **28a** and 3-pyridylboronic acid **24**.

Purification: CC (dichloromethane/methanol 98:2).
Yield: 21%.
White solid, mp 105 ºC.

^{1}H NMR (CDCl$_3$): δ 7.53 (m, 1H, Pyr. H-5), 7.62 (dd, 1H, $^{3}J =$ 8.5 Hz, $^{4}J =$ 1.6 Hz, Ar H), 7.73 (dd, 1H, $^{3}J =$ 8.5 Hz, $^{4}J =$ 1.6 Hz, Ar H), 7.79 (d, 1H, $^{3}J =$ 8.5 Hz, Ar H), 7.89 (d, 1H, $^{3}J =$ 8.5 Hz, Ar H), 8.02 (d, 1H, $^{4}J =$ 1.5 Hz, Ar H), 8.06 (d, 1H, $^{4}J =$ 1.5 Hz, Ar H), 8.11 (dt, 1H,

^3J = 7.9 Hz, ^4J = 1.6 Hz, Pyr. H-4), 8.65 (dd, 1H, ^3J = 5.0 Hz, ^4J = 1.6 Hz, Pyr. H-6), 8.99 (d, 1H, ^4J = 1.6 Hz, Pyr. H-2).

IR: ν_{max} = 3032, 2963, 1482 cm^{-1}.

MS: m/z = 286-284 (MH$^+$).

C$_{15}$H$_{10}$BrN (284.16)·0.36H$_2$O

	C	H	N
Calc.	61.99	3.72	4.82
Obs.	61.95	3.75	4.83

3-(6-Ethoxy-2-naphthyl)pyridine (30)

Synthesized from 2-ethyloxy-6-bromonaphthalene **30a** and 3-pyridylboronic acid **24**.

Purification: CC (dichloromethane/methanol 98:2).

Yield: 86%.

White solid, mp 106 ºC.

^{1}H NMR (CDCl$_3$): δ 1.51 (t, 3H, ^3J = 6.9 Hz, CH$_3$), 4.18 (q, 2H, ^3J = 6.9 Hz, CH$_2$), 7.17 (d, 1H, ^4J = 2.5 Hz, Ar H), 7.21 (dd, 1H, ^3J = 8.8 Hz, ^4J = 2.5 Hz, Ar H), 7.54-7.56(m, 1H, Pyr. H-5), 7.66 (dd, 1H, ^3J = 8.5 Hz, ^4J = 1.9 Hz, Ar H), 7.82 (d, 1H, ^3J = 8.8 Hz, Ar H), 7.85 (d, 1H, ^3J = 8.8 Hz, Ar H), 7.98 (d, 1H, ^4J = 1.9 Hz, Ar H), 8.16 (dt, 1H, ^3J = 7.9 Hz, ^4J = 1.6 Hz, Pyr. H-4), 8.61 (dd, 1H, ^3J = 5.0 Hz, ^4J = 1.6 Hz, Pyr. H-6), 8.99 (d, 1H, ^4J = 2.5 Hz, Pyr. H-2).

IR: ν_{max} = 3021, 2995, 1601, 1489, 1252 cm^{-1}.

MS: m/z = 250 (MH$^+$), 221.

C$_{17}$H$_{15}$NO (249.32)

	C	H	N
Calc.	81.90	6.06	5.62
Obs.	81.56	5.91	5.58

3-(6-Propoxy-2-naphthyl)pyridine (31)

Synthesized from 2-propyloxy-6-bromonaphthalene **31a** and 3-pyridylboronic acid **24**.

Purification: CC (dichloromethane/methanol 98:2).

Yield: 84%.

White solid, mp 116 ºC.

^{1}H NMR (CDCl$_3$): δ 1.10 (t, 3H, ^3J = 7.2 Hz, CH$_3$), 1.89 (q, 2H, ^3J = 6.6 Hz, CH$_2$), 4.07 (t, 2H, ^3J = 6.6 Hz, CH$_2$), 7.17 (d, 1H, ^4J = 2.5 Hz, Ar H), 7.21 (dd, 1H, ^3J = 8.8 Hz, ^4J = 2.5 Hz, Ar H), 7.38-7.40 (m, 1H, Pyr. H-5), 7.67 (dd, 1H, ^3J = 8.5 Hz, ^4J = 1.9 Hz, Ar H), 7.82 (d, 1H, ^3J = 8.5 Hz, Ar H), 7.83 (d, 1H, ^3J = 8.8 Hz, Ar H), 7.97 (d, 1H, ^4J = 1.9 Hz, Ar H), 7.98 (dt, 1H, ^3J = 7.9 Hz, ^4J = 1.6 Hz, Pyr. H-4), 8.60 (dd, 1H, ^3J = 4.7 Hz, ^4J = 1.6 Hz, Pyr. H-6), 8.96 (d, 1H, ^4J = 2.5 Hz, Pyr. H-2).

IR: ν$_{max}$ = 2967, 2934, 2878, 1629, 1604, 1491, 1389, 1254 cm^{-1}.

MS: m/z = 264 (MH$^+$).

C$_{18}$H$_{17}$NO (263.34)

	C	H	N
Calc.	82.10	6.51	5.32
Obs.	81.88	6.62	5.23

3-[6-(Benzyloxy)-2-naphthyl]pyridine (32)

Synthesized from 2-benzyloxy-6-bromonaphthalene **32a** and 3-pyridylboronic acid **24**.

Purification: CC (dichloromethane/methanol 97:3).

Yield 76%

White solid, mp 130 ºC.

^{1}H NMR (CDCl$_3$): δ 5.22 (s, 2H, CH$_2$), 7.26 (d, 1H, ^4J = 2.5 Hz, Ar H), 7.30 (dd, 1H, ^3J = 7.6 Hz, ^4J = 2.5 Hz, Ar H), 7.36 (t, 1H, ^3J = 7.6 Hz, Ar H), 7.42 (t, 2H, ^3J = 7.6 Hz, Ar H), 7.48-

7.51 (m, 1H, Pyr. H-5, Ar H), 7.67 (dd, 1H, ^3J = 8.5 Hz, ^4J = 1.9 Hz, Ar H), 7.84 (d, 1H, ^3J = 8.5 Hz, Ar H), 7.85 (d, 1H, ^3J = 8.5 Hz, Ar H), 7.99 (s, 1H, Ar H), 8.10 (dt, 1H, ^3J = 7.8 Hz, ^4J = 1.6 Hz, Pyr. H-4), 8.62 (dd, 1H, ^3J = 5.0 Hz, ^4J = 1.6 Hz, Pyr. H-6), 8.98 (d, 1H, ^4J = 1.6 Hz, Pyr. H-2).

IR: ν_{max} = 3040, 1604, 1490 cm^{-1}.

MS: m/z = 312 (MH$^+$), 221.

C$_{22}$H$_{17}$NO (311.39)

	C	H	N
Calc.	86.86	5.50	4.50
Obs.	86.58	5.66	4.44

6-Pyridin-3-yl-2-naphthonitrile (33)

Synthesized from 6-cyano-2-naphthyl trifluoromethanesulfonate **33a** and 3-pyridylboronic acid **24**. The reaction was stirred for 2.5 hours.

Purification: CC (dichloromethane/methanol 98:2).

Yield. 71%.

White solid, mp 122 ºC.

^{1}H NMR (CDCl$_3$): δ 7.53-7.56 (m, 1H, Pyr. H-5), 7.68 (dd, 1H, ^3J = 8.5 Hz, ^4J = 1.6 Hz, Ar H), 7.84 (dd, 1H, ^3J = 8.5 Hz, ^4J = 1.6 Hz, Ar H), 8.01 (d, 1H, ^3J = 8.5 Hz, Ar H), 8.04 (d, 1H, ^3J = 8.5 Hz, Ar H), 8.10 (d, 1H, ^4J = 1.6 Hz, Ar H), 8.12 (dt, 1H, ^3J = 7.9 Hz, ^4J = 1.5 Hz, Pyr. H-4), 8.28 (s, 1H, Ar H), 8.70 (dd, 1H, ^3J = 4.9 Hz, ^4J = 1.5 Hz, Pyr. H-6), 9.01 (d, 1H, ^4J = 2.4 Hz, Pyr. H-2).

IR: ν_{max} = 3032, 2224, 1629, 1469, 1424 cm^{-1}.

MS: m/z = 231 (MH$^+$).

C$_{16}$H$_{10}$N$_2$ (230.17)

	C	H	N
Calc.	83.46	4.38	12.17
Obs.	83.27	4.54	12.14

3-(5-Chloro-6-methoxy-2-naphthyl)pyridine (34)

Synthesized from 6-bromo-1-chloro-2-methoxynaphthalene **34a** and 3-pyridylboronic acid **24**.

Purification: CC (dichloromethane/methanol 97:3).
Yield: 93%.
White solid, mp 150 ºC.

^{1}H NMR (CDCl$_3$): δ 4.07 (s, 3H, OCH$_3$), 7.39 (d, 1H, ^3J = 9.1 Hz, Ar H), 7.63-7.66 (m, 1H, Pyr. H-5), 7.79 (dd, 1H, ^3J = 8.8 Hz, ^4J = 2.2 Hz, Ar H), 7.89 (d, 1H, ^3J = 8.8 Hz, Ar H), 8.04 (d, 1H, ^4J = 1.9 Hz, Ar H), 8.26 (dt, 1H, ^3J = 8.1 Hz, ^4J = 1.6 Hz, Pyr. H-4), 8.36 (d, 1H, ^3J = 8.8 Hz, Ar H), 8.65 (dd, 1H, ^3J = 5.0 Hz, ^4J = 1.6 Hz, Pyr. H-6), 9.02 (d, 1H, ^4J = 2.2 Hz, Pyr. H-2).

IR: ν_{max} = 3033, 2955, 2844, 1602, 1490, 1275 cm^{-1}.
MS: m/z = 272-270 (MH$^+$), 255, 227, 192.

C$_{16}$H$_{12}$ClNO (269.73)

	C	H	N
Calc.	71.25	4.48	5.19
Obs.	71.19	4.18	5.18

3-(5-Bromo-6-methoxy-2-naphthyl)pyridine (35)

Synthesized from 1,6-dibromo-2-methoxynaphthalene **35a** and 3-pyridylboronic acid **24**.

Purification: CC (dichloromethane/methanol 98:2).
Yield: 66%.
White solid, mp 162 ºC.

^{1}H NMR (CDCl$_3$): δ 4.07 (s, 3H, OCH$_3$), 7.36 (d, 1H, ^3J = 8.8 Hz, Ar H), 7.60-7.63 (m, 1H, Pyr. H-5), 7.79 (dd, 1H, ^3J = 8.8 Hz, ^4J = 2.2 Hz, Ar H), 7.92 (d, 1H, ^3J = 8.8 Hz, Ar H), 8.02 (d, 1H, ^4J = 1.9 Hz, Ar H), 8.22 (dt, 1H, ^3J = 7.9 Hz, ^4J = 2.2 Hz, Pyr. H-4), 8.36 (d, 1H, ^3J = 8.8 Hz, Ar H), 8.65 (dd, 1H, ^3J = 5.0 Hz, ^4J = 1.6 Hz, Pyr. H-6), 9.01 (d, 1H, ^4J = 2.2 Hz, Pyr. H-2).

IR: ν$_{max}$ = 3045, 2955, 2832, 1601, 1488, 1272 cm^{-1}.
MS: m/z = 317-314 (MH$^+$), 270, 227, 191, 163.

C$_{16}$H$_{12}$BrNO (314.18)

	C	H	N
Calc.	61.17	3.85	4.46
Obs.	61.57	4.18	4.35

3,3'-(2-methoxynaphthalene-1,6-diyl)dipyridine (36)

Synthesized from 1,6-dibromo-2-methoxynaphthalene **35a** and 3-pyridylboronic acid **24** (3 eq).

Purification: CC (dichloromethane/methanol 98:2).
Yield: 5%.
White solid, mp 173 ºC.

^{1}H NMR (CDCl$_3$): δ 3.89 (s, 3H, OCH$_3$), 7.43-7.46 (m, 2H, Ar H, Pyr. H-5), 7.54-7.56 (m, 2H, Ar H, Pyr. H-5), 7.62 (dd, 1H, ^3J = 8.8 Hz, ^4J = 1.9 Hz, Ar H), 7.86 (dt, 1H, ^3J = 7.9 Hz, ^4J = 1.9 Hz, Pyr. H-4), 8.01-8.04 (m, 2H, Ar H, Pyr.H-4), 8.07 (d, 1H, ^4J = 1.6 Hz, Ar H), 8.62 (d, 1H, ^3J = 5.0 Hz, Pyr. H-6), 8.68 (s, 1H, Pyr. H-2), 8.70 (d, 1H, ^3J = 5.0 Hz, Pyr. H-6), 8.97 (s, 1H, Pyr. H-2).

IR: ν$_{max}$ = 3031, 2950, 2842, 1599, 1488, 1258 cm^{-1}.
MS: m/z = 313 (MH$^+$).

C$_{11}$H$_8$Br$_2$O (315.99)

3-(1,5-Dichloro-6-methoxy-2-naphthyl)pyridine (37)

Synthesized from 1,5-dichloro-6-methoxy-2-naphthyl trifluoromethanesulfonate **37a** and 3-pyridylboronic acid **24**.

Purification: CC (dichloromethane/methanol 98:2).
Yield: 41%.
White solid, mp 153 ºC.

^{1}H NMR (CDCl$_3$): δ 4.10 (s, 3H, OCH$_3$), 7.48 (d, 1H, ^3J = 9.1 Hz, Ar H), 7.50 (d, 1H, ^3J = 8.8 Hz, Ar H), 7.69-7.71 (m, 1H, Pyr. H-5), 8.18 (dt, 1H, ^3J = 7.9 Hz, ^4J = 1.6 Hz, Pyr. H-4), 8.30 (d, 1H, ^3J = 8.8 Hz, Ar H), 8.37 (d, 1H, ^3J = 9.1 Hz, Ar H), 8.73 (dd, 1H, ^3J = 5.3 Hz, ^4J = 1.6 Hz, Pyr. H-6), 8.85 (d, 1H, ^4J = 1.6 Hz, Pyr. H-2).

IR: ν_{max} = 3060, 2940, 2830, 1617, 1487 cm^{-1}.
MS: m/z = 307-304 (MH$^+$), 270, 227, 191, 163.

C$_{16}$H$_{11}$Cl$_2$NO (304.18)·0.07H$_2$O

	C	H	N
Calc.	62.93	3.77	4.59
Obs.	62.93	4.16	4.54

3-(7-Methoxy-2-naphthyl)pyridine (38)

Synthesized from 7-methoxy-2-naphthyl trifluoromethanesulfonate **38a** and 3-pyridylboronic acid **24**. The reaction was stirred for 8 hours.

Purification: CC (dichloromethane/methanol 97:3).
Yield: 31%.
White solid, mp 100 ºC.

^{1}H NMR (CDCl$_3$): δ 3.95 (s, 3H, OCH$_3$), 7.18-7 21 (m, 2H, Ar H), 7.47-7.49 (m, 1H, Pyr. H-5), 7.54 (dd, 1H, ^3J = 8.2 Hz, ^4J = 1.6 Hz, Ar H), 7.78 (d, 1H, ^3J = 8.2 Hz, Ar H), 7.88 (d, 1H,

^3J = 8.2 Hz, Ar H), 7.95 (d, 1H, ^4J = 1.8 Hz, Ar H), 8.08 (dt, 1H, ^3J = 7.8 Hz, ^4J = 1.6 Hz, Pyr. H-4), 8.63 (dd, 1H, ^3J = 5.0 Hz, ^4J = 1.6 Hz, Pyr. H-6), 8.99 (d, 1H, ^4J = 2.5 Hz, Pyr. H-2).

IR: ν_{max} = 3030, 2973, 2835, 1626 cm^{-1}.
MS: m/z = 236 (MH$^+$), 221.

C$_{16}$H$_{13}$NO (235.29)

	C	H	N
Calc.	81.68	5.57	5.95
Obs.	81.40	5.71	5.78

3-(1-Chloro-7-methoxy-2-naphthyl)pyridine (39)

Synthesized from 1-chloro-7-methoxy-2-naphthyl trifluoromethanesulfonate **39a** and 3-pyridylboronic acid **24**.

Purification: CC (hexane/ethyl acetate, 80:20).
Yield: 18%.
White solid, mp 95 ºC.

^{1}H NMR (CDCl$_3$): δ 4.00 (s, 3H, OCH$_3$), 7.26-7.29 (m, 2H, Ar H), 7.58-7.60 (m, 1H, Pyr. H-5), 7.64 (d, 1H, ^4J = 2.5 Hz, Ar H), 7.80 (d, 1H, ^3J = 8.8 Hz, Ar H), 7.82 (d, 1H, ^3J = 8.8 Hz, Ar H), 8.06 (dt, 1H, ^3J = 7.9 Hz, ^4J = 1.6 Hz, Pyr. H-4), 8.70 (d, 1H, ^3J = 5.0 Hz, Pyr. H-6), 8.82 (s, 1H, Pyr. H-2).

IR: ν_{max} = 3020, 2932, 2878, 1677, 1506, 1225 cm^{-1}.
MS: m/z = 272-270 (MH$^+$), 255, 191.

C$_{16}$H$_{12}$ClNO (269.73)·0.13H$_2$O

	C	H	N
Calc.	70.61	4.54	5.15
Obs.	70.60	4.58	5.06

3-(3-Methoxy-2-naphthyl)pyridine (40)

Synthesized from 3-bromopyridine **24a** and 2-methoxy-3-naphthylboronic acid **18a**. The reaction was stirred at 90°C for 4 hours.

Purification: (dichloromethane/methanol 98:2).

Yield: 31%.

White solid, mp 189 ºC.

^{1}H NMR (CDCl$_3$): δ 3.94 (s, 3H, OCH$_3$), 7.25 (s, 1H, Ar H), 7.35-7.40 (m, 2H, Ar H, Pyr. H-5), 7.48 (td, 1H, ^3J = 8.2 Hz, ^4J = 1.3 Hz, Ar H), 7.77 (s, 1H, Ar H), 7.78 (d, 1H, ^3J = 8.2 Hz, Ar H), 7.81 (d, 1H, ^3J = 8.2 Hz, Ar H), 7.93 (dt, 1H, ^3J = 7.9 Hz, ^4J = 1.9 Hz, Pyr. H-4), 8.60 (dd, 1H, ^3J = 4.9 Hz, ^4J = 1.8 Hz, Pyr. H-6), 8.85 (s, 1H, Pyr. H-2).

IR: ν_{max} = 3054, 2962, 2832, 1631, 1599, 1504, 1466, 1410, 1254 cm^{-1}.

MS: m/z = 236 (MH$^+$).

C$_{16}$H$_{13}$NO (235.29)·HCl·0.26H$_2$O

	C	H	N
Calc.	69.54	5.29	5.15
Obs.	69.52	5.43	5.07

Methyl 6-pyridin-3-yl-2-naphthoate (41)

Synthesized from methyl 6-bromo-2-naphthoate **41a** and 3-pyridylboronic acid **24**.

Purification: CC (dichloromethane/methanol 98:2).

Yield: 10%.

White solid, mp 147 ºC.

^{1}H NMR (CDCl$_3$): δ 3.93 (s, 3H, OCH$_3$), 7.35-7.37 (m, 1H, Pyr. H-5), 7.71 (dd, 1H, ^3J = 8.5 Hz, ^4J = 1.9 Hz, Ar H), 7.89 (d, 1H, ^3J = 8.5 Hz, Ar H), 7.94 (dt, 1H, ^3J = 7.9 Hz, ^4J = 1.6 Hz, Pyr. H-4), 8.00 (d, 1H, ^3J = 8.5 Hz, Ar H), 8.01 (s, 1H, Ar H), 8.05 (dd, 1H, ^3J = 8.5 Hz, ^4J =

1.9 Hz, Ar H), 8.58 (s, 1H, Ar H), 8.59 (dd, 1H, ^3J = 5.0 Hz, ^4J = 1.6 Hz, Pyr. H-6), 8.92 (d, 1H, ^4J = 2.2 Hz, Pyr. H-2).

IR: ν_{max} = 3052, 2952, 1718, 1598, 1499, 1292 cm^{-1}.

MS: m/z = 264 (MH$^+$).

C$_{17}$H$_{13}$NO$_2$ (263.30)·0.20H$_2$O

	C	H	N
Calc.	76.50	5.06	5.25
Obs.	76.49	4.96	5.41

Methyl 3-methoxy-7-pyridin-3-yl-2-naphthoate (42)

Synthesized from methyl 7-bromo-3-methoxy-2-naphthoate **42a** and 3-pyridylboronic acid **24**.

Purification: CC (dichloromethane/methanol 98:2).

Yield: 15%.

Yellow solid, mp 95 ºC.

^{1}H NMR (CDCl$_3$): δ 3.97 (s, 3H, OCH$_3$), 4.03 (s, 3H, OCH$_3$), 7.25 (s, 1H, Ar H), 7.40-7.42 (m, 1H, Pyr. H-5), 7.76 (dd, 1H, ^3J = 8.5 Hz, ^4J = 1.6 Hz, Ar H), 7.85 (d, 1H, ^3J = 8.8 Hz, Ar H), 7.97 (dt, 1H, ^3J = 7.9 Hz, ^4J = 1.6 Hz, Pyr. H-4), 8.01 (d, 1H, ^4J = 1.6 Hz, Ar H), 8.37 (s, 1H, Ar H), 8.62 (dd, 1H, ^3J = 4.7 Hz, ^4J = 1.6 Hz, Pyr. H-6), 8.95 (d, 1H, ^4J = 2.2 Hz, Pyr. H-2).

IR: ν_{max} = 3005, 2946, 1714, 1699, 1607, 1483, 1212 cm^{-1}.

MS: m/z = 294 (MH$^+$).

C$_{18}$H$_{15}$NO$_3$ (293.33)

	C	H	N
Calc.	73.71	5.15	4.78
Obs.	73.48	5.40	4.75

3-(9-Phenanthryl)pyridine (45)

Synthesized from 9-bromophenanthrene **45a** and 3-pyridylboronic acid **24**.

Purification: CC (dichloromethane/methanol 98:2).

Yield: 94%.

White solid, mp 129 ºC.

^{1}H NMR (CDCl$_3$): δ 7.56-7.61 (m, 2H, Ar H, Pyr. H-5), 7.66 (td, 1H, ^3J = 8.2 Hz, ^4J = 1.3 Hz, Ar H), 7.70-7.74 (m, 3H, Ar H), 7.77 (dd, 1H, ^3J = 8.2 Hz, ^4J = 0.9 Hz, Ar H), 7.92 (dd, 1H, ^3J = 7.9 Hz, ^4J = 1.6 Hz, Ar H), 8.03 (dt, 1H, ^3J = 7.9 Hz, ^4J = 1.9 Hz, Pyr. H-4), 8.73-8.76 (m, 2H, Ar H, Pyr. H-6), 8.81 (d, 1H, ^3J = 8.5 Hz, Ar H), 8.85 (d, 1H, ^4J = 2.2 Hz, Pyr. H-2).

IR: ν$_{max}$ = 3055, 1659, 1535, 1456, 1247 cm^{-1}.

MS: m/z = 256 (MH$^+$).

C$_{19}$H$_{13}$N (255.32)

	C	H	N
Calc.	89.38	5.13	5.49
Obs.	89.23	5.02	5.55

3-Pyridin-3-yl-quinoline (46)

Synthesized from 3-bromoquinoline **46a** and 3-pyridylboronic acid **24**.

Purification: CC (dichloromethane/methanol 97:3).

Yield: 3%.

Beige solid, mp 103 ºC.

^{1}H NMR (CDCl$_3$): δ 7.45-7.48 (m, 1H, Pyr. H-5), 7.62 (td, 1H, ^3J = 8.2 Hz, ^{4}J = 1.6 Hz, Ar H), 7.77 (td, 1H, ^3J = 8.5 Hz, ^4J = 1.6 Hz, Ar H), 7.91 (d, 1H, ^3J = 7.6 Hz, Ar H), 8.02 (dt, 1H, ^3J = 7.9 Hz, ^4J = 2.2 Hz, Pyr. H-4), 8.16 (d, 1H, ^3J = 8.2 Hz, Ar H), 8.33 (d, 1H, ^4J = 2.2 Hz,

Ar H), 8.69 (dd, 1H, ^3J = 4.7 Hz, ^4J = 1.3 Hz, Pyr. H-6), 8.98 (d, 1H, ^4J = 2.5 Hz, Pyr. H-2), 9.16 (d, 1H, ^4J = 2.2 Hz, Ar H).

IR: ν_{max} = 3055, 2930, 1494 cm^{-1}.
MS: m/z = 207 (MH$^+$).

$C_{14}H_{10}N_2$ (206.25)

2-Pyridin-3-yl-quinoline hydrochloride salt (47)

Synthesized from 2-bromoquinoline **47a** and 3-pyridylboronic acid **24**. After purification, the product was dissolved in of diethyl ether (4 mL) and one equivalent of HCl in diethyl ether (1M) was added. The resulting precipitate was filtered and washed thoroughly with diethyl ether.

Purification: CC (dichloromethane/methanol 99:1).
Yield: 43%.
White solid, mp 180 ºC.

^{1}H NMR (CDCl$_3$): δ 7.68 (td, 1H, ^3J = 7.9 Hz, ^4J = 0.9 Hz, Ar H), 7.86 (td, 1H, ^3J = 8.5 Hz, ^4J = 1.6 Hz, Ar H), 7.95 (dd, 1H, ^3J = 8.2 Hz, ^4J = 0.9 Hz, Ar H), 8.11-8.14 (m, 1H, Pyr. H-5), 8.17 (d, 1H, ^3J = 8.5 Hz, Ar H), 8.34 (d, 1H, ^3J = 8.5 Hz, Ar H), 8.57 (d, 1H, ^3J = 8.5 Hz, Ar H), 8.87 (d, 1H, ^3J = 5.4 Hz, Pyr. H-4), 9.34 (d, 1H, ^3J = 8.2 Hz, Pyr. H-6), 9.67 (s, 1H, Pyr. H-2).

IR: ν_{max} = 3053, 2931, 1596, 1548, 1506 cm^{-1}.
MS: m/z = 207 (MH$^+$).

$C_{14}H_{10}N_2$ (206.25)·HCl·0.83H$_2$O

	C	H	N
Calc.	65.27	4.95	10.87
Obs.	65.02	4.91	10.67

2-Pyridin-3-yl-quinoxaline hydrochloride salt (48)

Synthesized from 2-bromoquinoxaline **48a** and 3-pyridylboronic acid **24**. After purification, the product was dissolved in diethyl ether (4 mL) and one equivalent of HCl in diethyl ether (1M) is added. The resulting precipitate was filtered and washed thoroughly with diethyl ether.

Purification: CC (dichloromethane/methanol 99:1).

Yield: 44%.

White solid, mp 233 ºC.

^{1}H NMR (CDCl$_3$): δ 7.79-7.82 (m, 2H, Ar H), 8.07-8.12 (m, 2H, Ar H), 8.14-8.17 (m,1H, Pyr. H-5), 8.92 (d, 1H, ^3J = 5.0 Hz, Pyr. H-4), 9.33 (d, 1H, ^3J = 7.9 Hz, Pyr. H-6), 9.46 (s, 1H, Pyr. H-2), 9.71 (s, 1H, Ar H).

IR: ν_{max} = 3066, 1604, 1547, 1499, 1313 cm^{-1}.

MS: m/z = 208 (MH$^+$), 181, 102, 75, 51.

C$_{13}$H$_9$N$_3$ (207.24)·HCl·0.02H$_2$O

	C	H	N
Calc.	64.07	4.14	17.24
Obs.	63.98	4.74	16.97

3-(1*H*-Inden-2-yl)pyridine (50)

Synthesized from 2-bromo-1*H*-indene **50a** and 3-pyridylboronic acid **24**.

Purification: CC (dichloromethane/methanol 99:1).

Yield: 51%.

Beige solid, mp 102 ºC.

^{1}H NMR (CDCl$_3$): δ 3.81 (s, 2H, H-3), 7.23 (td, 1H, ^3J = 7.2 Hz, ^4J = 0.9 Hz, Ar H), 7.29-7.32 (m, 3H, H-1, Ar H, Pyr. H-5), 7.44 (d, 1H, ^3J = 7.2 Hz, Ar H), 7.50 (d, 1H, ^3J = 7.2 Hz,

Ar H), 7.89 (dt, 1H, ^3J = 8.1 Hz, ^4J = 1.9 Hz, Pyr. H-4), 8.50 (s, 1H, Pyr. H-6), 8.90 (s, 1H, Pyr. H-2).

IR: ν_{max} = 3054, 2916, 1533 cm^{-1}.

MS: m/z = 194 (MH$^+$).

$C_{14}H_{11}N$ (193.25)

	C	H	N
Calc.	87.01	5.74	7.25
Obs.	87.10	5.51	6.84

3-(3,4-Dihydronaphthalen-2-yl)pyridine (51)

Synthesized from 3-bromo-1,2-dihydronaphthalene **51a** and 3-pyridylboronic acid **24**.

Purification: CC (dichloromethane/methanol 97:3).

Yield: 62%.

White solid, mp 199 °C (HCl salt).

^{1}H NMR (CDCl$_3$): δ 2.73 (t, 2H, ^3J = 8.3 Hz, H-4), 2.97 (t, 2H, ^3J = 7.8 Hz, H-3), 6.89 (s, 1H, H-1), 7.13-7.19 (m, 4H, Ar H), 7.32-7.34 (m, 1H, Pyr H-5), 7.85 (td, 1H, ^3J = 8.1 Hz, ^4J = 1.5 Hz, Pyr H-4), 8.49 (dd, 1H, ^3J = 4.9 Hz, ^4J = 1.5 Hz, Pyr H-2), 8.79 (d, 1H, ^4J = 1.9 Hz, Pyr H-6).

IR: ν_{max} = 3022, 2935, 2885, 2831, 1485, 1421 cm^{-1}.

MS: m/z = 208 (MH$^+$), 179, 101, 79.

$C_{15}H_{13}N$ (207.28)·HCl·0.24H$_2$O

	C	H	N
Calc.	72.64	5.88	5.65
Obs.	73.04	6.28	5.56

3-(6-Methoxy-3,4-dihydronaphthalen-2-yl)pyridine (53)

Synthesized from 3-bromo-7-methoxy-1,2-dihydronaphthalene **53a** and 3-pyridylboronic acid **24**.

Purification: CC (dichloromethane/methanol 99:1).

Yield: 89%.

Yellow solid, mp 80 ºC.

^{1}H NMR (CDCl$_3$): δ 2.73 (t, 2H, ^3J = 8.5 Hz, H-3), 2.96 (t, 2H, ^3J = 8.5 Hz, H-4), 3.82 (s, 3H, OCH$_3$), 6.73-6.75 (m, 2H, Ar H), 6.88 (s, 1H, H-1), 7.10 (d, 1H, ^3J = 8.2 Hz, Ar H), 7.32-7.35 (m, 1H, Pyr. H-5), 7.86 (dt, 1H, ^3J = 8.2 Hz, ^{4}J = 1.6 Hz, Pyr. H-4), 8.48 (dd, 1H, ^3J = 4.7 Hz, ^4J = 1.6 Hz, Pyr. H-6), 8.79 (d, 1H, ^4J = 2.5 Hz, Pyr. H-2).

IR: ν_{max} = 3021, 2936, 2834, 1607, 1570, 1499, 1250 cm^{-1}.

MS: m/z = 238 (MH$^+$), 223, 194,165.

C$_{16}$H$_{15}$NO (237.30)·HCl·0.03H$_2$O

	C	H	N
Calc.	80.78	6.38	5.89
Obs.	80.77	6.82	5.84

3-(7-Methoxy-3,4-dihydronaphthalen-2-yl)pyridine (54)

Synthesized from 3-bromo-6-methoxy-1,2-dihydronaphthalene **54a** and 3-pyridylboronic acid **24**. The reaction was stirred for 2 hours.

Purification: CC (dichloromethane/methanol 99:1).

Yield: 79%.

Yellow solid, mp 168 °C (HCl salt).

^{1}H NMR (CDCl$_3$): δ 2.74 (t, 2H, ^3J = 8.2 Hz, H-3), 2.92 (t, 2H, ^3J = 8.2 Hz, H-4), 3.81 (s, 3H, OCH$_3$), 6.73-6.75 (m, 2H, Ar H), 6.87 (s, 1H, H-1), 7.09 (d, 1H, ^3J = 8.2 Hz, Ar H), 7.35-7.38

(m, 1H, Pyr. H-5), 7.88 (dt, 1H, ^3J = 7.8 Hz, ^4J = 1.9 Hz, Pyr. H-4), 8.51 (dd, 1H, ^3J = 5.0 Hz, ^4J = 1.6 Hz, Pyr. H-6), 8.80 (d, 1H, ^4J = 1.6 Hz, Pyr. H-2).

IR: ν_{max} = 3025, 2934, 2833, 1604, 1571, 1497, 1255, 1040 cm^{-1}.

MS: m/z = 238 (MH$^+$).

C$_{16}$H$_{15}$NO (237.30)·HCl·0.79H$_2$O

	C	H	N
Calc.	66.64	6.14	4.86
Obs.	66.56	6.06	4.82

4-(6-Methoxy-3,4-dihydronaphthalen-2-yl)pyridine (55)

Synthesized from 3-bromo-7-methoxy-1,2-dihydronaphthalene **53a** and 4-pyridylboronic acid **25**. The reaction was stirred for 2 hours.

Purification: CC (dichloromethane/methanol 97:3).

Yield: 51%.

Yellow solid, mp 108 ºC.

^{1}H NMR (CDCl$_3$): δ 2.66 (t, 2H, ^3J = 8.5 Hz, H-3), 2.91 (t, 2H, ^3J = 8.5 Hz, H-4), 3.77 (s, 3H, OCH$_3$), 6.69-6.71 (m, 2H, Ar H), 7.09-7.11 (m, 2H, H-1, Ar H), 7.53 (dd, 1H, ^3J = 6.6 Hz, ^4J = 1.6 Hz, Pyr. H-3, Pyr. H-5), 8.49 (dd, 1H, ^3J = 6.6 Hz, ^4J = 1.6 Hz, Pyr. H-2, Pyr. H-6).

IR: ν_{max} = 3040, 2939, 2835, 1599, 1504, 1209 cm^{-1}.

MS: m/z = 238 (MH$^+$).

C$_{16}$H$_{15}$NO (237.30)

	C	H	N
Calc.	80.98	6.37	5.90
Obs.	80.93	6.33	5.83

3-(4-Methyl-3,4-dihydronaphthalen-2-yl)pyridine (59)

Synthesized from 3-bromo-1-methyl-1,2-dihydronaphthalene **59a** and 3-pyridylboronic acid **24**. The reaction was stirred for 3 hours.

Purification: CC (dichloromethane/methanol 97:3).

Yield: 68%.

Yellow solid, mp 189 °C (HCl salt).

^{1}H NMR (CDCl$_3$): δ 1.32 (d, 3H, ^3J = 6.9 Hz, CH$_3$), 2.54 (ddd, 1H, ^2J = 16.1 Hz, ^3J = 7.6 Hz, ^4J = 0.9 Hz, H-3), 2.87 (ddd, 1H, ^2J = 16.1 Hz, ^3J = 6.6 Hz, ^4J = 1.6 Hz, H-3'), 3.11-3.17 (m, 1H, H-4), 6.89 (s, 1H, H-1), 7.16-7.24 (m, 4H, Ar H), 7.33-7.35 (m, 1H, Pyr. H-5), 7.86 (td, 1H, ^3J = 8.1 Hz, ^4J = 1.5 Hz, Pyr. H-4), 8.52 (dd, 1H, ^3J = 4.7 Hz, ^4J = 1.6 Hz, Pyr. H-6), 8.82 (d, 1H, ^4J = 2.0 Hz, Pyr. H-2).

IR: ν$_{max}$ = 2963, 2854, 1613, 1518, 1231 cm^{-1}

MS: m/z = 222 (MH$^+$),203, 178, 77.

C$_{16}$H$_{15}$N (221.30)·HCl·0.18H$_2$O

	C	H	N
Calc.	73.62	6.32	5.37
Obs.	73.61	6.50	5.46

Method 15

Compounds **24-26** were prepared according to the literature (Li *et al.*, 2002).

3-Pyridylboronic acid (24)

A three-necked flask was charged with 3-bromopyridine **24a** (3.86 mL, 40.0 mmol) and triisopropyl borate (11.08 mL, 48.00 mmol) in toluene (64 mL) and THF (16 mL) and put under a nitrogen atmosphere. The mixture was cooled to -40°C using a dry ice/acetone bath. *n*-Butyllithium (2.5 M in hexanes, 19.2 mL, 48.0 mmol) was added dropwise via a septum

and the mixture was stirred for an additional 0.5 h while the temperature was held at -40°C. The reaction was allowed to warm to -20°C before a 2N HCl solution (40 mL) was added. When the mixture reached room temperature, the aqueous layer was separated and its pH was adjusted to 7 using a 5N NaOH solution. A white solid product precipitated as the pH approached 7. This mixture was saturated with NaCl (10 g) and extracted three times with THF. The THF extracts were evaporated *in vacuo* to provide a solid. This solid was taken up in acetonitrile (16 mL) for crystallization. The resulting slurry was heated to 70°C, stirred for 30 min and allowed to cool slowly to room temperature. After the slurry was stirred at 0°C for 30 min, the solid was filtered off, washed with cold acetonitrile and dried in a desiccator.

Yield: 85%.
White solid.

^{1}H NMR (CH$_3$OD): δ 7.74 (br s, 1H, Ar H), 8.44 (br s, 1H, Ar H), 8.55 (dd, 1H, ^3J = 8.5 Hz, ^4J = 1.9 Hz, Ar H), 8.67 (br s, 1H, Ar H).

IR: ν$_{max}$ = 3356, 1608, 1352, 1310 cm^{-1}.

C$_5$H$_6$BNO$_2$ (122.92)

4-Pyridylboronic acid (25)

Synthesized from 4-bromopyridine **25a**.

Yield: 70%.
White solid.

^{1}H NMR (CH$_3$OD): δ 8.07 (d, 2H, ^3J = 6.3 Hz, Ar H), 8.53 (d, 2H, ^3J = 6.6 Hz, Ar H).

IR: ν$_{max}$ = 3312, 1621, 1312 cm^{-1}.

C$_5$H$_6$BNO$_2$ (122.92)

5-Pyrimidylboronic acid (26)

Synthesized from 5-bromopyrimidine **26a**.

Yield: 64%.
Brown solid.

^{1}H NMR (CH$_3$OD): δ 8.71 (s, 2H, Ar H), 8.65 (s, 1H, Ar H).

IR: ν_{max} = 3315, 2959, 1667, 1406 cm^{-1}.

C$_4$H$_5$BN$_2$O$_2$ (123.91)

Method 16

6-Cyano-2-naphthyl trifluoromethanesulfonate (33a)

To a solution of 6-cyano-2-naphthol **33b** (0.5 g, 2.96 mmol) and pyridine (0.39 mL, 4.73 mmol) in dichloromethane/acetonitrile (15 mL/10 mL) at 0°C under nitrogen atmosphere was added slowly trifluoromethanesulfonic anhydride (0.65 mL, 3.84 mmol). The solution was allowed to slowly warm to room temperature and stirred overnight. The solution was cooled to 0°C and stirred with ice water to decompose excess anhydride. The mixture was made slightly basic with saturated NaHCO$_3$ solution. The aqueous layer was extracted with dichloromethane and the combined organic layers were washed with water, dried (MgSO$_4$), filtered and evaporated *in vacuo*.

Purification: CC (hexane/ethyl acetate 80:20).
Yield: 60%.
Yellow oil.

^{1}H NMR (CDCl$_3$): δ 7.52 (dd, 1H, ^3J = 8.8 Hz, ^4J = 2.5 Hz, Ar H), 7.73 (dd, 1H, ^3J = 8.5 Hz, ^4J = 1.6 Hz, Ar H), 7.83 (d, 1H, ^4J = 2.5 Hz, Ar H), 7.99 (d, 1H, ^3J = 8.5 Hz, Ar H) 8.02 (d, 1H, ^3J = 8.8 Hz, Ar H), 8.30 (s, 1H, Ar H).

IR: ν_{max} = 2232, 1632, 1427, 1216, 1140 cm^{-1}.

C$_{12}$H$_6$F$_3$NO$_3$S (301.25)

1,5-Dichloro-6-methoxy-2-naphthyl trifluoromethanesulfonate (37a)

Synthesized from 1,5-dichloro-6-methoxy-2-naphthalen-2-ol **37b**.

Purification: CC (hexane/ethyl acetate 80:20).
Yield: 30%.
Yellow oil.

^{1}H NMR (CDCl$_3$): δ 4.08 (s, 3H, OCH$_3$), 7.48 (d, 1H, ^3J = 8.8 Hz, Ar H), 7.50 (d, 1H, ^3J = 8.8 Hz, Ar H), 8.24 (d, 1H, ^3J = 8.8 Hz, Ar H), 8.26 (d, 1H, ^3J = 8.8 Hz, Ar H).

IR: ν_{max} = 3025, 2942, 2835, 1599, 1427, 1216, 1139 cm^{-1}.

C$_{12}$H$_8$ClF$_3$O$_4$S (340.71)

7-Methoxy-2-naphthyl trifluoromethanesulfonate (38a)

Synthesized from 7-methoxy-2-naphthol **38b**.

Purification: CC (hexane/ethyl acetate 90:10).
Yield: 88%.
Colorless oil.

^{1}H NMR (CDCl$_3$): δ 3.94 (s, 3H, OCH$_3$), 7.14 (d, 1H, ^4J = 2.5 Hz, Ar H), 7.21 (dd, 1H, ^3J = 9.1 Hz, ^4J = 2.5 Hz, Ar H), 7.22 (dd, 1H, ^3J = 9.1 Hz, ^4J = 2.5 Hz, Ar H), 7.64 (d, 1H, ^4J = 2.5 Hz, Ar H), 7.77 (d, 1H, ^3J = 9.1 Hz, Ar H), 7.83 (d, 1H, ^3J = 9.1 Hz, Ar H).

IR: ν_{max} = 3011, 2946, 2840, 1633, 1420, 1208, 1139 cm^{-1}.

C$_{12}$H$_9$F$_3$O$_4$S (306.26)

1-Chloro-7-methoxy-2-naphthyl trifluoromethanesulfonate (39a).

Synthesized from 1-chloro-7-methoxy-naphthalen-2-ol **39b**

Purification: CC (hexane/ethyl acetate 90:10).

Yield: 52%.

Colorless oil.

^{1}H NMR (CDCl$_3$): δ 3.99 (s, 3H, OCH$_3$), 7.26 (dd, 1H, ^3J = 8.8 Hz, ^4J = 2.5 Hz, Ar H), 7.30 (d, 1H, ^3J = 8.8 Hz, Ar H), 7.54 (d, 1H, ^4J = 2.5 Hz, Ar H), 7.76 (d, 1H, ^3J = 9.1 Hz, Ar H), 7.78 (d, 1H, ^3J = 8.8 Hz, Ar H).

IR: ν$_{max}$ = 3009, 2945, 2834, 1628, 1423, 1206 cm^{-1}.

C$_{12}$H$_8$ClF$_3$O$_4$S (340.71)

Method 17

1,5-Dichloro-6-methoxy-2-naphthalen-2-ol (37b)

Compound **37b** was prepared according to the literature (Mewshaw *et al.*, 2003).

A suspension of 6-methoxy-2-naphthol **37c** (0.48 g, 2.77 mmol) and *N*-chlorosuccinimide (0.41 g, 3.05 mmol) in acetonitrile (15 mL) was stirred at room temperature overnight. Extra *N*-chlorosuccinimide (0.19 g, 1.50 mmol) was added and the reaction was further stirred at room temperature for 4 hours. The resulting solution was evaporated *in vacuo*.

Purification: CC (hexane/ethyl acetate 80:20).

Yield: 36%.

White solid.

^{1}H NMR (CDCl$_3$): δ 4.03 (s, 3H, OCH$_3$), 7.34 (d, 1H, ^3J = 9.4 Hz, Ar H), 7.38 (d, 1H, ^3J = 9.4 Hz, Ar H), 8.01 (d, 1H, ^3J = 9.4 Hz, Ar H), 8.12 (d, 1H, ^3J = 9.4 Hz, Ar H).

IR: ν_{max} = 3317, 1601, 1501, 1344, 1278, 1252 cm^{-1}.

MS: m/z = 244 (MH$^+$), 242, 240, 225, 112.

C$_{11}$H$_8$Cl$_2$O$_2$ (243.09)

Method 18

1-Chloro-7-methoxy-naphthalen-2-ol (39b)

A suspension of 7-methoxy-2-naphthol **39c** (0.75 g, 4.30 mmol) and *N*-chlorosuccinimide (0.63 g, 4.73 mmol) in acetonitrile (15 mL) was heated to reflux for 3 h. The resulting solution was evaporated *in vacuo*.

Purification: CC (hexane/ethyl acetate 90:10).

Yield: 46%.

White solid.

^{1}H NMR (CDCl$_3$): δ 3.97 (s, 3H, OCH$_3$), 7.04 (dd, 1H, ^3J = 8.8 Hz, ^4J = 2.4 Hz, Ar H), 7.11 (d, 1H, ^3J = 8.8 Hz, Ar H), 7.33 (d, 1H, ^4J = 2.4 Hz, Ar H), 7.62 (d, 1H, ^3J = 8.8 Hz, Ar H), 7.67 (d, 1H, ^3J = 8.8 Hz, Ar H).

IR: ν_{max} = 3379, 2832, 1609, 1174 cm^{-1}.

C$_{11}$H$_9$ClO$_2$ (208.61)

Method 19

2-Ethyloxy-6-bromonaphthalene (30a).

To a solution of 6-bromo-2-naphthol **49** (2.0 g, 8.58 mmol) in DMF (100 mL) under nitrogen atmosphere was added K$_2$CO$_3$ (2.96 g, 21.45 mmol). After 10 minutes, ethyl bromide (1.03 g, 9.44 mmol) was added and the mixture was stirred at 100°C for 3.5 h. After cooling, water

was added and the resulting precipitate was filtered off, washed with water and dried in the dessicator.

Used without further purification.

Yield: 96%.

Yellow solid.

^{1}H NMR (CDCl$_3$): δ 1.48 (t, 3H, ^3J = 6.9 Hz, CH$_3$), 4.14 (q, 2H, ^3J = 6.9 Hz, CH$_2$), 7.08 (d, 1H, ^4J = 2.5 Hz, Ar H), 7.16 (dd, 1H, ^3J = 8.8 Hz, ^4J = 2.5 Hz, Ar H), 7.48 (dd, 1H, ^3J = 8.8 Hz, ^4J = 2.2 Hz, Ar H), 7.58 (d, 1H, ^3J = 8.8 Hz, Ar H), 7.64 (d, 1H, ^3J = 8.8 Hz, Ar H), 7.91 (d, 1H, ^4J = 1.9 Hz, Ar H).

IR: ν$_{max}$ = 2981, 1624, 1589, 1207 cm^{-1}.

C$_{12}$H$_{11}$BrO (251.12)

2-Propyloxy-6-bromonaphthalene (31a).

Synthesized from 6-bromo-2-naphthol **49** and propyl bromide.

Used without further purification.

Yield: 70%.

Yellow solid.

^{1}H NMR (CDCl$_3$): δ 1.08 (t, 3H, ^3J = 7.2 Hz, CH$_3$), 1.87 (q, 2H, ^3J = 6.9 Hz, CH$_2$), 4.03 (t, 2H, ^3J = 6.9 Hz, CH$_2$), 7.08 (d, 1H, ^4J = 2.5 Hz, Ar H), 7.16 (dd, 1H, ^3J = 8.8 Hz, ^4J = 2.5 Hz, Ar H), 7.48 (dd, 1H, ^3J = 8.5 Hz, ^4J = 1.9 Hz, Ar H), 7.58 (d, 1H, ^3J = 8.8 Hz, Ar H), 7.64 (d, 1H, ^3J = 8.8 Hz, Ar H), 7.91 (d, 1H, ^4J = 1.9 Hz, Ar H).

IR: ν$_{max}$ = 2926, 1628, 1591, 1208, 913, 742 cm^{-1}.

C$_{13}$H$_{13}$BrO (265.15)

2-Benzyloxy-6-bromonaphthalene (32a).

Synthesized from 6-bromo-2-naphthol **49** and benzyl chloride.

Used without further purification.

Yield: 86%.

Beige solid.

^{1}H NMR (CDCl$_3$): δ 5.17 (s, 2H, CH$_2$), 7.19 (d, 1H, ^4J = 2.5 Hz, Ar H), 7.25 (dd, 1H, ^3J = 8.9 Hz, ^4J = 2.5 Hz, Ar H), 7.35 (t, 1H, ^3J = 7.6 Hz, Ar H), 7.41 (t, 2H, ^3J = 7.6 Hz, Ar H), 7.48 (t, 2H, ^3J = 8.2 Hz, Ar H), 7.59 (d, 1H, ^3J = 8.8 Hz, Ar H), 7.63 (d, 1H, ^3J = 9.1 Hz, Ar H), 7.67 (d, 1H, ^3J = 8.8 Hz, Ar H), 7.92 (d, 1H, ^4J = 2.2 Hz, Ar H).

IR: ν$_{max}$ = 3042, 2962, 1586, 1257, 1203 cm^{-1}.

C$_{17}$H$_{13}$BrO (313.20)

Method 20

6-Bromo-1-chloro-2-methoxynaphthalene (34a).

A suspension of 2-bromo-6-methoxynaphthalene **21a** (0.50 g, 2.11 mmol) and freshly recrystallized *N*-chlorosuccinimide (0.39 g, 2.91 mmol) in THF (15 ml) was heated to reflux for 3 h. Extra *N*-chlorosuccinimide (0.15 g, 1.00 mmol) was added and the reaction was further refluxed for 3 h. After evaporation of the solvent, ethyl acetate was added to the crude product. The precipitate was filtered off and the filtrate was evaporated *in vacuo*.

Purification: CC (hexane/ethyl acetate 90:10).

Yield: 94%.

Yellow solid.

^{1}H NMR (CDCl$_3$): δ 4.03 (s, 3H, OCH$_3$), 7.31 (d, 1H, ^3J = 9.1 Hz, Ar H), 7.61 (dd, 1H, ^3J = 9.1 Hz, ^4J = 2.2 Hz, Ar H), 7.68 (d, 1H, ^3J = 9.1 Hz, Ar H), 7.94 (d, 1H, ^4J = 2.0 Hz, Ar H), 8.08 (d, 1H, ^3J = 9.1 Hz, Ar H).

IR: ν$_{max}$ = 2924, 2841, 1586, 1494, 1274 cm^{-1}.

C$_{11}$H$_8$BrClO (271.54)

2,5-Dibromo-6-methoxynaphthalene (35a).

Synthesized from 2-bromo-6-methoxynaphthalene **21a** and *N*-bromosuccinimide. The reaction was stirred at room temperature for 2 h. The resulting solution was partly evaporated *in vacuo*. By adding hexane, the wanted compound precipitated and was filtered off, washed and dried at open air.

Used without further purification.
Yield: 70%.
Yellow solid.

^{1}H NMR (CDCl$_3$): δ 4.03 (s, 3H, OCH$_3$), 7.29 (d, 1H, ^3J = 8.8 Hz, Ar H), 7.61 (dd, 1H, ^3J = 9.1 Hz, ^4J = 1.9 Hz, Ar H), 7.73 (d, 1H, 1H, ^3J = 8.8 Hz, Ar H), 7.94 (d, 1H, ^4J = 1.9 Hz, Ar H), 8.09 (d, 1H, ^3J = 9.1 Hz, Ar H).

IR: ν$_{max}$ = 3060, 2939, 2841, 1587, 1272 cm^{-1}.

C$_{11}$H$_8$Br$_2$O (315.99)

Method 21

4,7-Dibromo-3-hydroxy-2-naphthoic acid (42c)

3-Hydroxy-2-naphthoic acid **42d** (5.0 g, 26.57 mmol) was suspended in glacial acetic acid (50 mL) and cooled to 0°C. To this stirred mixture was added dropwise a solution of bromine

(10.62 g, 66.42 mmol) in glacial acetic acid (25 mL) while keeping the reaction temperature below 5°C. The reaction was refluxed for 2 h, cooled and poured into ice water (500 mL). The product was filtered off, washed with water and ether and air-dried.

Used without further purification.

Yield: 75%.

Yellow solid.

^{1}H NMR (CD$_3$OD): δ 7.77 (dd, 1H, ^3J = 9.1 Hz, ^4J = 1.8 Hz, Ar H), 8.08 (d, 1H, ^3J = 9.1 Hz, Ar H), 8.16 (d, 1H, ^4J = 1.8 Hz, Ar H), 8.57 (s, 1H, Ar H).

IR: ν_{max} = 3394, 3061, 1671, 1280 cm^{-1}.

C$_{11}$H$_6$Br$_2$O$_3$ (345.98)

Method 22

7-Bromo-3-hydroxy-2-naphthoic acid (42b)

The dibromo acid **42c** (6.90 g, 19.94 mmol) was suspended in glacial acetic acid (100 mL) and 10 N HCl (30 mL) and tin powder (2.37 g, 19.94 mmol) were added. The reaction mixture was refluxed for 3h, cooled and diluted with water (100 mL). The yellow product was filtered off, washed with water and air-dried.

Used without further purification.

Yield: 75%.

Yellow solid.

^{1}H NMR (CD$_3$OD): δ 7.47 (s, 1H, Ar H), 7.77 (dd, 1H, ^3J = 8.8 Hz, ^4J = 1.9 Hz, Ar H), 7.84 (d, 1H, ^3J = 8.8 Hz, Ar H), 8.26 (s, 1H, Ar H), 8.69 (s, 1H, Ar H).

IR: ν_{max} = 3259, 3062, 1661, 1504, 1269 cm^{-1}.

C$_{11}$H$_7$BrO$_3$ (267.08)

Method 23

Methyl 7-bromo-3-methoxy-2-naphthoate (42a)

The bromo acid **42b** (4.00 g, 14.98 mmol), K_2CO_3 (9.94 g, 71.91 mmol) and dimethyl sulfate (4.31 g, 34.16 mmol) in dry acetone (100 mL) were refluxed for 4 hours. The reaction was cooled, water (10 mL) was added and the mixture was stirred for 2 hours at 30°C to destroy any remaining dimethyl sulfate. The precipitate was filtered off and the acetone was evaporated *in vacuo*. The residue was taken up in dichloromethane, washed several times with water, dried ($MgSO_4$), filtered and evaporated *in vacuo*.

Purification: CC (dichloromethane).
Yield: 77%.
White solid.

^{1}H NMR (CDCl$_3$): δ 3.96 (s, 3H, OCH$_3$), 3.99 (s, 3H, OCH$_3$), 7.17 (s, 1H, Ar H), 7.57 (dd, 1H, ^3J = 8.8 Hz, ^4J = 1.9 Hz, Ar H), 7.61 (d, 1H, ^3J = 8.8 Hz, Ar H), 7.96 (d, 1H, ^4J = 1.9 Hz, Ar H), 8.18 (s, 1H, Ar H).

IR: ν_{max} = 2951, 2839, 1733, 1627, 1586, 1494 cm^{-1}.

$C_{13}H_{11}BrO_3$ (295.13)

Method 24

6-Pyridin-3-yl-naphthalen-2-ol (29)

BBr$_3$ (2.55 mL, 2.55 mmol) was slowly added to compound **21** (150 mg, 0.64 mmol) in dry CH$_2$Cl$_2$ (25 mL) at -78°C under nitrogen atmosphere. After 30 min stirring, the cooling was stopped and the reaction was stirred at room temperature overnight. The reaction was slowly quenched with methanol and then washed with a saturated NaHCO$_3$ solution. The organic layer was dried ($MgSO_4$), filtered and evaporated *in vacuo*.

Purification: CC (dichloromethane/methanol 99:1).

Yield: 65%.

White solid, mp 253 ºC.

^{1}H NMR (CDCl$_3$): δ 7.20 (dd, 1H, ^3J = 8.8 Hz, ^4J = 1.9 Hz, Ar H), 7.23 (d, 1H, ^4J = 1.9 Hz, Ar H), 7.60-7.62 (m, 1H, Pyr. H-5), 7.83 (dd, 1H, ^3J = 8.5 Hz, ^4J = 1.6 Hz, Ar H), 7.87 (d, 1H, ^3J = 8.8 Hz, Ar H), 7.92 (d, 1H, ^3J = 8.8 Hz, Ar H), 8.24 (s, 1H, Ar H), 8.29 (dt, 1H, ^3J = 7.9 Hz, ^4J = 1.9 Hz, Pyr. H-4), 8.65 (d, 1H, ^3J = 4.7 Hz, Pyr. H-6), 9.08 (d, 1H, ^4J = 1.6 Hz, Pyr. H-2), 9.95 (s, 1H, OH).

IR: ν_{max} = 3634, 3021, 1594, 1489, 1308, 793 cm^{-1}.

MS: m/z = 222 (MH$^+$).

C$_{15}$H$_{11}$NO (221.26)·0.24H$_2$O

	C	H	N
Calc.	79.86	5.13	6.21
Obs.	79.80	5.13	5.80

Method 25

Compounds **43** and **44** were prepared according to the literature (Jagdmann *et al.*, 1990).

6-Pyridin-3-yl-2-naphthamide (43)

A stirred mixture of the ester compound **41** (150 mg, 0.57 mmol) and formamide (86 mg, 1.90 mmol) under nitrogen was charged with anhydrous DMF (3 mL) and heated at 100°C. Methanolic sodium methoxide (21 mg, 0.40 mmol) was added and stirring was continued for 1 h. The mixture was cooled and water was added (2 mL), then extracted with ethyl acetate, dried (MgSO$_4$), filtered and evaporated *in vacuo*.

Purification: CC (dichloromethane/methanol 95:5).

Yield: 61%.

White solid, mp 227 ºC.

^{1}H NMR (CDCl$_3$): δ 7.42-7.45 (m, 1H, Pyr. H-5), 7.75 (dd, 1H, ^3J = 8.5 Hz, ^4J = 1.9 Hz, Ar H), 7.90 (dd, 1H, ^3J = 8.5 Hz, ^4J = 1.9 Hz, Ar H), 7.96 (d, 1H, ^3J = 8.8 Hz, Ar H), 8.01-8.04 (m, 2H, Ar H, Pyr. H-4), 8.06 (d, 1H, ^4J = 1.3 Hz, Ar H), 8.38 (d, 1H, ^4J = 1.3 Hz, Ar H), 8.59 (dd, 1H, ^3J = 4.7 Hz, ^4J = 1.6 Hz, Pyr. H-6), 8.92 (d, 1H, ^4J = 1.9 Hz, Pyr. H-2).

IR: ν_{max} = 3335, 3066, 1664, 1590, 1426 cm^{-1}.
MS: m/z = 249 (MH$^+$).

C$_{16}$H$_{12}$N$_2$O (248.29)

	C	H	N
Calc.	77.40	4.87	11.28
Obs.	77.15	5.14	11.08

N-Methyl-6-pyridin-3-yl-2-naphthamide (44)

Synthesized from methyl 6-pyridin-3-yl-2-naphthoate **41** and *N*-methylformamide.

Purification: CC (dichloromethane/methanol 95:5).
Yield: 83%.
White solid, mp 158 ºC.

^{1}H NMR (CDCl$_3$): δ 3.10 (s, 3H, OCH$_3$), 6.33 (s, 1H, NH), 7.42-7.44 (m, 1H, Pyr. H-5), 7.77 (dd, 1H, ^3J = 8.5 Hz, ^4J = 1.8 Hz, Ar H), 7.87 (dd, 1H, ^3J = 8.5 Hz, ^4J = 1.8 Hz, Ar H), 7.96-8.07 (m, 4H, Ar H, Pyr. H-4), 8.33 (s, 1H, Ar H), 8.65 (dd, 1H, ^3J = 4.6 Hz, ^4J = 1.5 Hz, Pyr. H-6), 8.98 (d, 1H, ^4J = 1.5 Hz, Pyr. H-2).

IR: ν_{max} = 3316, 3059, 2929, 1644, 1549, 1313 cm^{-1}.
MS: m/z = 263 (MH$^+$).

C$_{17}$H$_{14}$N$_2$O (262.31)·0.15H$_2$O

	C	H	N
Calc.	77.34	5.44	10.57
Obs.	77.04	5.84	10.54

Method 26

2-Bromoquinoline (47a)

POBr$_3$ (1.30 g, 4.55 mmol) was added to quinolin-2-ol **47b** (0.28 g, 1.96 mmol) in a flask with air condenser and CaCl$_2$-tube. The reaction was heated at 155°C for 4 hours. After cooling to room temperature, some water was added and the resulting red solution was neutralised with solid sodium bicarbonate and basified with 10% sodium hydroxide solution. The solution was extracted with diethyl ether and active charcoal was added to the organic layer. After filtration, the organic layer was dried (MgSO$_4$), filtered and evaporated *in vacuo*.

Purification: CC (dichloromethane).
Yield: 78%.
Beige solid.

^{1}H NMR (CDCl$_3$): δ 7.53 (d, 1H, ^3J = 8.5 Hz, Ar H), 7.58 (td, 1H, ^3J = 8.1 Hz, ^4J = 1.3 Hz, Ar H), 7.75 (td, 1H, ^3J = 8.5 Hz, ^4J = 1.6 Hz, Ar H), 7.81 (dd, 1H, ^3J = 8.2 Hz, ^4J = 1.3 Hz, Ar H), 8.01 (d, 1H, ^3J = 8.5 Hz, Ar H), 8.07 (d, 1H, ^3J = 8.5 Hz, Ar H).

IR: ν$_{max}$ = 3068, 1583, 1082 cm^{-1}.

C$_9$H$_6$BrN (208.06)

2-Bromoquinaxoline (48a)

Synthesized from to quinoxalin-2-ol **48b**.

Purification: CC (dichloromethane).
Yield: 83%.
Yellow solid.

^{1}H NMR (CDCl$_3$): δ 7.80-7.82 (m, 2H, Ar H), 8.04-8.06 (m, 1H, Ar H), 8.10-8.12 (m, 1H, Ar H), 8.63 (s, 1H, Ar H).

IR cm^{-1}: ν_{max} = 3064, 2936, 1537.

C$_8$H$_5$BrN$_2$ (209.05)

Method 27

2-Bromo-1,2,3,4-tetrahydro-naphthalen-1-ol (51b)

A solution of the 2-bromo-3,4-dihydro-2*H*-naphthalen-1-one **51c** (400 mg, 1.77 mmol) in anhydrous methanol/tetrahydrofuran (1:1, 6 mL) was stirred under nitrogen in an icebad. NaBH$_4$ (47 mg, 1.24 mmol) was added portionwise. After stirring for 15 minutes at 0°C and 0.5 hour at room temperature, the mixture was poured into water and extracted with diethyl ether. The organic layer was dried (MgSO$_4$), filtered and evaporated *in vacuo*.

Used for further reaction without purification.
Yield: 88%.
White solid.

^{1}H NMR (CDCl$_3$) δ 2.28-2.34 (m, 1H, H-3), 2.50-2.57 (m, 1H, H-3'), 2.86-2.92 (m, 1H, H-4), 3.01-3.15 (m, 1H, H-4'), 4.71-4.74 (m, 1H, H-2), 4.81 (d, 1H, ^3J = 3.5 Hz, H-1), 7.12-7.14 (m, 1H, Ar H), 7.25-7.28 (m, 2H, Ar H), 7.49-7.50 (m, 1H, Ar H).

IR: ν_{max} = 3413, 3022, 2955, 2923, 2849, 1603, 1490, 1455, 1225 cm^{-1}.

C$_{10}$H$_{11}$BrO (227.10)

5-Methoxy-2-pyridin-3-yl-indan-1-ol (52a)

Synthesized from 5-methoxy-2-pyridin-3-yl-indan-1-one **52b**.

Used without purification.
Yield: 53 %.
White solid.

^{1}H NMR (CDCl$_3$): δ 2.98 (dd, 1H, ^2J = 15.8 Hz, ^3J = 8.2 Hz, H-3), 3.21 (dd, 1H, ^2J = 15.8 Hz, ^3J = 7.9 Hz, H-3), 3.29-3.44 (m, 3H, H-3, H-3, H-2), 3.69-3.73 (m, 1H, H-2), 5.17 (d, 1H, ^{3}J = 6.6 Hz, H-1), 5.23 (d, 1H, ^3J = 5.6 Hz, H-1), 6.79-6.86 (m, 4H, Ar H, Ar H), 7.26-7.29 (m, 1H, Pyr. H-5), 7.32-7.34 (m, 2H, Pyr. H-5, Ar H), 7.36 (d, 1H, ^3J = 8.5 Hz, Ar H), 7.68 (dt, 1H, ^3J = 7.9 Hz, ^4J = 1.9 Hz, Pyr. H-4), 7.76 (dt, 1H, ^3J = 7.9 Hz, ^4J = 1.9 Hz, Pyr. H-4), 8.41-8.43 (m, 2H, Pyr. H-6, Pyr. H-6), 8.53 (d, 1H, ^4J = 2.2 Hz, Pyr. H-2), 8.54 (d, 1H, ^4J = 2.2 Hz, Pyr. H-2).

IR: ν$_{max}$ = 3226, 2940, 1609, 1492, 1252 cm^{-1}.

C$_{15}$H$_{15}$NO$_2$ (241.29)

2-Bromo-6-methoxy-1,2,3,4-tetrahydro-naphthalen-1-ol (53b)

Synthesized from 2-bromo-6-methoxy-3,4-dihydro-2*H*-naphthalen-1-one **53c**.

Used for further reaction without purification.
Yield: 86%.
White solid.

^{1}H NMR (CDCl$_3$): δ 2.25-2.29 (m, 1H, H-3), 2.49-2.53 (m, 1H, H-3'), 2.82-2.87 (m, 1H, H-4), 3.03-3.08 (m, 1H, H-4'), 3.79 (s, 3H, OCH$_3$), 4.65-4.68 (m, 1H, H-2), 4.75 (d, 1H, ^3J = 3.2 Hz, H-1), 6.63 (d, 1H, ^4J = 2.4 Hz, Ar H), 6.80 (dd, 1H, ^3J = 8.5 Hz, ^4J = 2.4 Hz, Ar H), 7.37 (d, 1H, ^3J = 8.5 Hz, Ar H).

IR: ν$_{max}$ = 3305, 2830, 1610, 1499, 1248 cm^{-1}.

C$_{11}$H$_{13}$BrO$_2$ (257.13)

2-Bromo-7-methoxy-1,2,3,4-tetrahydro-naphthalen-1-ol (54b)

Synthesized from 2-bromo-7-methoxy-3,4-dihydro-2*H*-naphthalen-1-one **54c**.

Used for further reaction without purification.

Yield: 84%.

White solid.

^{1}H NMR (CDCl$_3$): δ 2.17-2.23 (m, 1H, H-3), 2.38-2.44 (m, 1H, H-3'), 2.69-2.75 (m, 1H, H-4), .94-3.00 (m, 1H, H-4'), 3.73 (s, 3H, OCH$_3$), 4.64-4.67 (m, 1H, H-2), 4.68 (d, 1H, ^3J = 3.5 Hz, H-1), 6.81 (dd, 1H, ^3J = 8.5 Hz, ^4J = 2.5 Hz, Ar H), 7.02-7.04 (m, 2H, Ar H).

IR: ν$_{max}$ = 3441, 2945, 2838, 1612, 1502, 1244 cm^{-1}.

C$_{11}$H$_{13}$BrO$_2$ (257.13)

3-Methyl-2-pyridin-3-yl-1,2,3,4-tetrahydronaphthalen-1-ol (58a)

Synthesized from 3-methyl-2-pyridin-3-yl-3,4-dihydro-*2H*-naphthalen-1-one **58b**.

Used without purification.

Yield: 72%.

White solid.

IR: ν$_{max}$ = 3183, 2935, 1483, 1429 cm^{-1}.

C$_{16}$H$_{17}$NO (239.32)

2-Bromo-4-methyl-1,2,3,4-tetrahydronaphthalen-1-ol (59b)

Synthesized from 2-bromo-4-methyl-3,4-dihydronaphthalen-1(2*H*)-one **59c**.

Used for further reaction without purification.

Yield: 91%.

Yellow solid.

IR: ν$_{max}$ = 3395, 2960, 2871.

C$_{11}$H$_{13}$BrO (241.13)

153

4-Ethyl-2-pyridin-3-yl-1,2,3,4-tetrahydronaphthalen-1-ol (60a)

Synthesized from 4-ethyl-2-pyridin-3-yl-3,4-dihydronaphthalen-1(2*H*)-one **60b**.

Used without purification.

Yield: 100%.

Yellow oil.

IR: ν_{max} = 3355, 3063, 2961, 2928, 2873, 1578, 1484, 1428 cm^{-1}.

$C_{17}H_{19}NO$ (253.35)

2-(1*H*-imidazol-1-yl)indan-1-ol (61a)

Synthesized from 2-(1*H*-imidazol-1-yl)indan-1-one **61b**.

Used without purification.

Yield: 96%.

Yellow oil.

IR: ν_{max} = 3541, 3032, 1660, 1504, 1276, 1084 cm^{-1}.

$C_{12}H_{12}N_2O$ (200.24)

2-(1*H*-imidazol-1-yl)-1,2,3,4-tetrahydronaphthalen-1-ol (62a)

Synthesized from 2-(1*H*-imidazol-1-yl)-3,4-dihydronaphthalen-1(2*H*)-one **62b**.

Used without purification.

Yield: 91%.

Yellow oil.

IR: ν_{max} = 3114, 2932, 1676, 1504, 1231, 1084 cm^{-1}.

$C_{13}H_{14}N_2O$ (214.17)

2-(1*H*-imidazol-1-yl)-6-methoxy-1,2,3,4-tetrahydronaphthalen-1-ol (63a)

Synthesized from 2-(1*H*-imidazol-1-yl)-6-methoxy-3,4-dihydronaphthalen-1(2*H*)-one **63b**.

Used without purification.

Yield: 83%.

White solid.

IR: ν_{max} = 3104, 2955, 2838, 1598, 1031 cm^{-1}.

$C_{14}H_{16}N_2O_2$ (244.30)

Method 28

2-Bromo-1*H*-indene (50a)

A mixture of 2-bromoindan-1-ol **50b** (5.20 g, 24.40 mmol) and *p*-toluenesulphonic acid (464 mg, 2.44 mmol) in toluene was heated at reflux (with Dean-Starktrap) for 2 hours to remove any water. The mixture was washed with saturated sodium bicarbonate and water. The organic layer was dried (MgSO$_4$), filtered and evaporated *in vacuo*.

Purification: CC (hexane).

Yield: 47%.

Colorless oil.

^{1}H NMR (CDCl$_3$): δ 3.61 (s, 2H, H-3), 6.94 (t, 1H, ^4J = 1.9 Hz, H-1), 7,17 (td, 1H, ^3J = 7.6 Hz, ^4J = 1.3 Hz, Ar H), 7.24 (t, 1H, ^3J = 7.6 Hz, ArH), 7.31 (d, 1H, ^3J = 7.6 Hz, Ar H), 7.38 (d, 1H, ^3J = 7.6 Hz, Ar H).

IR: ν_{max} = 3072, 2897, 1556 cm^{-1}.

C_9H_7Br (195.06)

3-Bromo-1,2-dihydronaphthalene (51a)

Synthesized from 2-bromo-1,2,3,4-tetrahydro-naphthalen-1-ol **51b**.

Purification: CC (hexane).
Yield: 81%.
Colorless oil.

^{1}H NMR (CDCl$_3$): δ 2.77 (t, 2H, ^3J = 8.2 Hz, H-3), 2.95 (t, 2H, ^3J = 8.2 Hz, H-4), 6.79 (s, 1H, H-1), 6.96-6.98 (m, 1H, Ar H), 7.08-7.10 (m, 1H, Ar H), 7.14-7.16 (m, 2H, Ar H).

IR: ν_{max} = 3017, 2943, 2890, 2833, 1662, 1485 cm^{-1}.

C$_{10}$H$_9$Br (209.09)

3-Bromo-7-methoxy-1,2-dihydronaphthalene (53a)

Synthesized from 2-bromo-6-methoxy-1,2,3,4-tetrahydro-naphthalen-1-ol **53b**.

Purification: CC (hexane/ethyl acetate 80:20).
Yield: 60%.
Beige oil.

^{1}H NMR (CDCl$_3$): δ 2.73 (t, 2H, ^3J = 8.5 Hz, H-3), 2.92 (t, 2H, ^3J = 8.5 Hz, H-4), 3.79 (s, 3H, OCH$_3$), 6.67-6.69 (m, 2H, Ar H), 6.74 (s, 1H, H-1), 6.91 (d, 1H, ^3J = 7.9 Hz, Ar H).

IR: ν_{max} = 3000, 2939, 2833, 1607, 1498, 1247 cm^{-1}.

C$_{11}$H$_{11}$BrO (239.11)

3-Bromo-6-methoxy-1,2-dihydronaphthalene (54a)

Synthesized from 2-bromo-7-methoxy-1,2,3,4-tetrahydro-naphthalen-1-ol **54b**.

Purification: CC (hexane/ethyl acetate 80:20).

Yield: 58%.

Yellow oil.

^{1}H NMR (CDCl$_3$): δ 2.75 (t, 2H, ^3J = 8.5 Hz, H-3), 2.88 (t, 2H, ^3J = 8.5 Hz, H-4), 3.78 (s, 3H, OCH$_3$), 6.54 (d, 1H, ^4J = 2.5 Hz Ar H), 6.69 (dd, 1H, ^3J = 8.2 Hz, ^{4}J = 2.5 Hz, Ar H), 6.74 (s, 1H, H-1), 6.99 (d, 1H, ^3J = 8.2 Hz, Ar H).

IR: ν$_{max}$ = 3000, 2938, 2831, 1604, 1498, 1254 cm^{-1}.

C$_{11}$H$_{11}$BrO (239.11)

3-Bromo-1-methyl-1,2-dihydronaphthalene (59a)

Synthesized from 2-bromo-4-methyl-1,2,3,4-tetrahydronaphthalen-1-ol **59b**.

Purification: CC (hexane/dichloromethane 90:10).

Yield: 59%.

Yellow oil.

^{1}H NMR (CDCl$_3$): δ 1.29 (d, 3H, ^3J = 6.9 Hz, Me), 2.54 (ddd, 1H, ^2J = 17.3 Hz, ^3J = 6.9 Hz, ^4J = 1.3 Hz, H-3), 2.93 (ddd, 1H, ^2J = 17.0 Hz, ^3J = 6.9 Hz, ^4J = 1.6 Hz, H-3'), 3.09 (m, 1H, H-4), 6.79 (s, 1H, Ar H), 6.98 (dd, 1H, ^3J = 6.9 Hz, ^4J = 1.6 Hz, Ar H), 7.14-7.20 (m, 3H, Ar H).

IR: ν$_{max}$ = 3066, 2963, 1629, 1447 cm^{-1}.

C$_{11}$H$_{11}$Br (223.11)

Method 29

3-(3-Methoxy-phenyl)-2-pyridin-3-yl-propionitrile (52d)

To a suspension of NaNH$_2$ (408 mg, 9.40 mmol) in anhydrous DMF (20 mL) (three-neckflask, refluxcooler, gasinlet and droppingfunnel with septum) under nitrogen was added

157

dropwise 3-pyridyl acetonitrile (1.0 g, 8.46 mmol) while stirring and cooling with anicebad. After stirring for 1 hour at room temperature and 1 hour at 80°C, the mixture was cooled with an icebad and 3-methoxybenzyl chloride **52e** (1.25 g, 7.99 mmol) was added dropwise. The reaction was stirred for 3 hours at room temperature and then 1 hour at 80°C. After cooling, an excess of water was added and the mixture was extracted exhaustively with diethyl ether. The organic layer was washed with water, dried (MgSO$_4$), filtered and evaporated *in vacuo*.

Purification: CC (dichloromethane/methanol 99:1).

Yield: 26%.

Yellow oil.

^{1}H NMR (CDCl$_3$): δ 3.13-3.25 (m, 2H, H-3), 3.76 (s, 3H, OCH$_3$), 4.20 (t, 1H, ^3J = 7.2 Hz, H-2), 6.65 (t, 1H, ^4J = 2.2 Hz, Ar H), 6.67 (d, 1H, ^3J = 7.6 Hz, Ar H), 6.82 (dd, 1H, ^3J = 8.2 Hz, ^4J = 2.2 Hz, Ar H), 7.21 (t, 1H, ^3J = 8.2 Hz, Ar H), 7.43-7.46 (m, 1H, Pyr. H-5), 7,74 (dt, 1H, ^3J = 8.2 Hz, ^4J = 1.9 Hz, Pyr. H-4), 8.61 (d, 1H, ^4J = 2.5 Hz, Pyr. H-2), 8.62 (dd, 1H, ^3J = 5.0 Hz, ^4J = 1.6 Hz, Pyr. H-6).

IR: ν$_{max}$ = 3030, 2938, 2837, 2244, 1602, 1491, 1264 cm^{-1}.

C$_{15}$H$_{14}$N$_2$ (238.29)

4-Phenyl-2-pyridin-3-yl-butyronitrile (56d)

Synthesized from phenethyl bromide **56e**.

Purification: CC (dichloromethane/methanol 99:1)

Yield: 14%.

Orange oil.

^{1}H NMR (CDCl$_3$): δ 2.15-2.22 (m, 1H, H-3), 2.69-2.34 (m, 1H, H-3'), 2.80-2.90 (m, 2H, H-4), 3.81 (dd, 1H, ^3J = 9.5 Hz, ^3J = 5.7 Hz, H-2), 7.20 (d, 2H, ^3J = 7.9 Hz, Ar H), 7.25 (d, 1H, ^3J = 7.9 Hz, Ar H), 7.32 (t, 2H, ^3J = 7.9 Hz, Ar H), 7.38-7.41 (m, 1H, Pyr. H-5), 7.77 (dt, 1H, ^3J = 7.9 Hz, ^4J = 2.2 Hz, Pyr. H-4), 8.58 (d, 1H, ^4J = 2.5 Hz, Pyr. H-2), 8.61(dd, 1H, ^3J = 5.0 Hz, ^4J = 1.6 Hz, Pyr. H-6).

IR: ν_{max} = 3029, 2971, 2242, 1603, 1577, 1496, 1426 cm^{-1}.

$C_{15}H_{14}N_2$ (222.29)

3-Methyl-4-phenyl-2-pyridin-3-yl-butyronitrile (58d)

Synthesized from 2-bromo-1-phenylpropane **58e**.

Purification: CC (dichloromethane/methanol 99:1).
Yield: 29% (mixture of two isomers).
Brown oil.

^{1}H NMR (CDCl$_3$): δ 0.97-1.01 (m, 6H, CH$_3$), 1.88-1.97 (m, 1H, H-4), 2.19-2.26 (m, 1H, H-4), 2.30-2.40 (m, 1H, H-4), 2.80-2.83 (m, 2H, H-3), 2.89-2.94 (m, 1H, H-4), 3.85-3.88 (m, 2H, H-2), 7.10 (d, 2H, ^3J = 7.6 Hz, Ar H), 7.23-7.29 (m, 6H, Ar H), 7.35 (t, 2H, ^3J = 7.6 Hz, Ar H), 7.38-7.41 (m, 2H, Pyr. H-5), 7.72 (m, 1H, Pyr. H-4), 7.78 (m, 1H, Pyr. H-4), 8.50 (d, 2H, ^4J = 2.2 Hz, Pyr. H-2), 8.59 (dd, 1H, ^3J = 4.7 Hz, ^4J = 1.6 Hz, Pyr. H-6), 8.63 (dd, 1H, ^3J = 4.7 Hz, ^4J = 1.6 Hz, Pyr. H-6).

IR: ν_{max} = 3030, 2968, 2875, 2241, 1577, 1426 cm^{-1}.

$C_{16}H_{16}N_2$ (236.32)

4-Phenyl-2-pyridin-3-yl-hexanenitrile (60d)

Synthesized from 1-(bromomethyl)propyl]benzene **60e**.

Purification: CC (dichloromethane/methanol 98:2).
Yield: 59%.
Brown oil.

^{1}H NMR (CDCl$_3$): δ 0.71 (d, 3H, ^3J = 7.2 Hz, CH$_3$), 0.83 (d, 3H, ^3J = 7.2 Hz, CH$_3$), 1.64-1.71 (m, 4H, CH$_2$), 1.96-2.02 (m, 2H, H-3), 2.25-2.31 (m, 2H, H-3), 2.39-2.41 (m, 1H, H-4), 2.84-2.90 (m, 1H, H-4), 3.42 (dd, 1H, ^2J = 12.0 Hz, ^3J = 4.4 Hz, H-2), 3.57 (m, 1H, H-2), 7.07 (d,

1H, ^3J = 7.6 Hz, Ar H), 7.16-7.40 (m, 11H, Ar H, Pyr. H-5), 7.64 (dt, 1H, ^3J = 8.2 Hz, ^4J = 1.9 Hz, Pyr. H-4), 7.67 (dt, 1H, ^3J = 8.2 Hz, ^4J = 1.9 Hz, Pyr. H-4), 8.41 (d, 1H, ^4J = 2.2 Hz, Pyr. H-2), 8.42 (d, 1H, ^4J = 2.2 Hz, Pyr. H-2), 8.56 (dd, 1H, ^3J = 5.0 Hz, ^4J = 1.6 Hz, Pyr. H-6), 8.60 (dd, 1H, ^3J = 5.0 Hz, ^4J = 1.6 Hz, Pyr. H-6).

IR: ν_{max} = 3059, 2961, 2242, 1654, 1599, 1455, 1252 cm^{-1}.

C$_{17}$H$_{18}$N$_2$ (250.35)

Method 30

3-(3-Methoxy-phenyl)-2-pyridin-3-yl-propionic acid (52c)

To a solution of 3-(3-methoxy-phenyl)-2-pyridin-3-yl-propionitrile **52d** (486 mg, 2.04 mmol) in ethanol (3 mL) was added NaOH (898 mg, 22.46 mmol) in water (1 mL). After reflux for 24 hours, some water was added and the pH was adjusted to 5 with 2N HCl solution and aqueous acetic acid. The mixture was extracted with ethyl acetate and, after drying (MgSO$_4$) and filtration, evaporated *in vacuo*.

Used without purification.
Yield: 86%.
Yellow oil.

IR: ν_{max} = 2939, 2836, 2526, 1721, 1585, 1491 cm^{-1}.

C$_{15}$H$_{15}$NO$_3$ (257.29)

4-Phenyl-2-pyridin-3-yl-butyric acid (56c)

Synthesized from 4-phenyl-2-pyridin-3-yl-butyronitrile **(56d)**.

Used without purification.
Yield: 74%.
White oil.

^{1}H NMR (CDCl$_3$): δ 2.06-2.14 (m, 1H, H-3), 2.49-2.55 (m, 1H, H-3'), 2.59-2.68 (m, 2H, H-4), 3.66-3.69 (m, 1H, CH), 7.14 (d, 2H, ^3J = 7.9 Hz, Ar H), 7.17-7.20 (m, 1H, Ar H), 7.26-7.29 (m, 2H, Ar H), 7.45-7.48 (m, 1H, Pyr. H-5), 7.92 (dt, 1H, ^3J = 7.9 Hz, ^4J = 2.2 Hz, Pyr. H-4), 8.54 (d, 1H, ^3J = 4.4 Hz, Pyr. H-6), 8.68 (s, 1H, Pyr. H-2).

IR: ν$_{max}$ = 3028, 2952, 1717 cm^{-1}.

MS: m/z = 242 (MH$^+$), 179, 101, 79.

C$_{15}$H$_{15}$NO$_2$ (241.29)

3-Methyl-4-phenyl-2-pyridin-3-yl-butyric acid (58c)

Synthesized from 3-methyl-4-phenyl-2-pyridin-3-yl-butyronitrile **58d**.

Used without purification.

Yield: 99%.

Brown oil.

IR: ν$_{max}$ = 3028, 2967, 2930, 2479, 1676, 1427 cm^{-1}.

C$_{16}$H$_{17}$NO$_2$ (255.32)

4-Phenyl-2-pyridin-3-yl-hexanoic acid (60c)

Synthesized from 4-phenyl-2-pyridin-3-yl-hexanenitrile **60d**.

Used without purification.

Yield: 99%.

Yellow oil.

MS: m/z = 268 (M-H$^+$).

C$_{17}$H$_{19}$NO$_2$ (269.35)

Method 31

5-Methoxy-2-pyridin-3-yl-indan-1-one (52b)

A mixture of polyphosphoric acid (2.2 g) and 3-(3-methoxy-phenyl)-2-pyridin-3-yl-propionic acid **52c** (0.53 g, 2.05 mmol) was stirred at 110°C for 20 minutes. The reaction was poured into ice water and neutralized with 6% NaOH solution. The pH was adjusted to 8 with sodium bicarbonate, and the solution was extracted with diethyl ether. The organic layer was dried (MgSO$_4$), filtered and evaporated *in vacuo*.

Purification: CC (dichloromethane/methanol 97:3).
Yield: 48%.
Colorless oil.

^{1}H NMR (CDCl$_3$): δ 3.20 (dd, 1H, ^2J = 17.3 Hz, ^3J = 4.1 Hz, H-3), 3.67 (dd, 1H, ^2J = 17.3 Hz, ^3J = 8.5 Hz, H-3'), 3.90-3.92 (m, 4H, OCH$_3$, H-2), 6.96-6.98 (m, 2H, Ar H), 7.28-7.31 (m, 1H, Pyr. H-5), 7,57 (dt, 1H, ^3J = 8.2 Hz, ^4J = 1.9 Hz, Pyr. H-4), 7.74 (d, 1H, ^3J = 8.2 Hz, Ar H), 8.50-8.51 (m, 2H, Pyr. H-6, Pyr. H-2).

IR: ν_{max} = 2945, 2841, 1702, 1599, 1261 cm^{-1}.

C$_{15}$H$_{13}$NO$_2$ (239.28)

2-Pyridin-3-yl-3,4-dihydro-*2H*-naphthalen-1-one (56b)

Synthesized from 4-phenyl-2-pyridin-3-yl-butyric acid **(56c)**.

Purification: CC (dichloromethane/methanol 97:3).
Yield: 90%.
Colorless oil.

^{1}H NMR (CDCl$_3$): δ 2.42-2.47 (m, 2H, H-4), 3.10 (dt, 1H, ^2J = 16.6 Hz, ^3J = 3.9 Hz, H-3); 3.17-3.24 (m, 1H, H-3'), 3.85 (t, 1H, ^3J = 8.3 Hz, H-2), 7.31 (d, 1H, ^3J = 7.8 Hz, Ar H), 7.34-7,37 (m, 2H, Ar H, Pyr. H-5), 7.53 (td, 1H, ^3J = 7.8 Hz, ^4J = 1.5 Hz, Ar H), 7.61 (dt, 1H, ^3J =

7.8 Hz, ^4J = 1.9 Hz, Pyr. H-4), 8.08 (dd, 1H, ^3J = 7.8 Hz, ^4J = 1.5 Hz, Ar H), 8.51 (d, 1H, ^4J = 1.9 Hz, Pyr. H-2), 8.55 (dd, 1H, ^3J = 4.9 Hz, ^4J = 1.5 Hz, Pyr. H-6).

IR: ν_{max} = 3057, 2933, 1682, 1599, 1425, 1226 cm^{-1}.

C$_{15}$H$_{13}$NO (223.28)

3-Methyl-2-pyridin-3-yl-3,4-dihydro-*2H*-naphthalen-1-one (58b)

Synthesized from 3-methyl-4-phenyl-2-pyridin-3-yl-butyric acid **58c**.

Purification: CC (dichloromethane/methanol 96:4).
Yield: 38%.
Yellow oil.

^{1}H NMR (CDCl$_3$): δ 0.97 (d, 3H, ^3J = 6.7 Hz, CH$_3$), 2.53-2.61 (m, 1H, H-4), 2.95 (dd, 1H, ^2J = 16.5 Hz, ^3J = 11.5 Hz, H-3), 3.12 (dd, 1H, ^2J = 16.5 Hz, ^3J = 4.0 Hz, H-3'), 3.46 (d, 1H, ^3J = 12.0 Hz, H-2), 7.30 (d, 1H, ^3J = 7.6 Hz, Ar H), 7.35 (t, 1H, ^3J = 7.6 Hz, Ar H), 7.40 (m, 1H, Pyr. H-5), 7.54 (td, 1H, ^3J = 7.6 Hz, ^4J = 1.2 Hz, Ar H), 7.57 (dt, 1H, ^3J = 7.9 Hz, ^4J = 1.8 Hz, Pyr. H-4), 8.04 (dd, 1H, ^3J = 7.9 Hz, ^4J = 1.2 Hz, Ar H), 8.44 (d, 1H, ^4J = 1.8 Hz, Pyr. H-2), 8.57 (dd, 1H, ^3J = 4.9 Hz, ^4J = 1.5 Hz, Pyr. H-6).

IR: ν_{max} = 3028, 2970, 2927, 1682, 1602, 1270 cm^{-1}.

C$_{16}$H$_{15}$NO (237.30)

4-Ethyl-2-pyridin-3-yl-3,4-dihydronaphthalen-1(2*H*)-one (60b)

Synthesized from 4-phenyl-2-pyridin-3-yl-hexanoic acid **60c**.

Purification: CC (dichloromethane/methanol 97:3).
Yield: 63% (mixture of two isomers).
Colorless oil.

^{1}H NMR (CDCl$_3$): δ 1.00 (t, 3H, ^3J = 7.6 Hz, CH$_3$), 1.10 (t, 3H, ^3J = 7.6 Hz, CH$_3$), 1.82-1.92 (m, 4H, CH$_2$), 2.16-2.20 (m, 1H, H-3), 2.36-2.44 (m, 2H, H-3), 2.56-2.62 (m, 1H, H-3), 2.96-2.99 (m, 1H, H-4), 3.22-3.24 (m, 1H, H-4), 3.83 (dd, 1H, ^3J = 13.6 Hz, ^3J = 4.4 Hz, H-2), 4.00 (dd, 1H, ^3J = 13.6 Hz, ^{3}J = 4.4 Hz, H-2), 7.17 (m, 2H, Ar H), 7.24-7.38 (m, 4H, Ar H, Pyr. H-5), 7.49-7.61 (m, 4H, Ar H, Pyr. H-4), 8.06 (dd, 1H, ^3J = 7.9 Hz, ^4J = 1.6 Hz, Ar H), 8.08 (dd, 1H, ^3J = 7.9 Hz, ^4J = 1.6 Hz, Ar H), 8.51 (d, 2H, ^4J = 1.8 Hz, Pyr. H-2), 8.54 (dd, 1H, ^3J = 4.7 Hz, ^4J = 1.6 Hz, Pyr. H-6), 8.57 (dd, 1H, ^3J = 4.7 Hz, ^4J = 1.6 Hz, Pyr. H-6).

IR: ν$_{max}$ = 3029, 2956, 1683, 1599, 1425, 1252, 1173 cm^{-1}.

C$_{17}$H$_{17}$NO (251.33)

Method 32

3-(6-Methoxy-1*H*-inden-2-yl)pyridine (52)

A mixture of acetic acid (4.60 mL), sulphuric acid (0.64 mL) and 5-methoxy-2-pyridin-3-yl-indan-1-ol **52a** (434 mg, 1.80 mmol) was stirred at 100°C for 1 hour. The reaction was poured in ice water and basified with a 6% NaOH solution. After extractions with dichloromethane, the organic layer was dried (MgSO$_4$), filtered and evaporated *in vacuo*.

Purification: CC (dichloromethane/methanol 98:2).
Yield: 45%.
Beige solid, mp 82 ºC.

^{1}H NMR (CDCl$_3$): δ 3.77 (s, 2H, H-3), 3 85 (s, 3H, OCH$_3$), 6.86 (dd, 1H, ^3J = 8.2 Hz, ^4J = 2.2 Hz, Ar H), 7.09 (d, 1H, ^4J = 1.5 Hz, Ar H), 7.30 (s, 1H, H-1), 7.34 (d, 1H, ^3J = 8.2 Hz, Ar H), 7.36-7.39 (m, 1H, Pyr. H-5), 7.94 (dt, 1H, ^3J = 7.9 Hz, ^4J = 1.5 Hz, Pyr. H-4), 8.46 (dd, 1H, ^3J = 4.9 Hz, ^4J = 1.5 Hz, Pyr. H-6), 8.85 (d, 1H, ^4J = 1.8 Hz, Pyr. H-2).

IR: ν$_{max}$ = 3059, 2905, 2836, 1685, 1607, 1493, 1259 cm^{-1}.
MS: *m/z* = 224 (MH$^+$).

$C_{15}H_{13}NO$ (223.28)·0.02H_2O

	C	H	N
Calc.	80.09	5.91	6.23
Obs.	80.08	6.15	6.13

3-(3-Methyl-3,4-dihydronaphthalen-2-yl)pyridine (58)

Synthesized from 3-methyl-2-pyridin-3-yl-1,2,3,4-tetrahydronaphthalen-1-ol **58a**.

Purification: CC (dichloromethane/methanol 98:2).

Yield 63%.

White solid, mp 169 °C (HCl salt).

^{1}H NMR (CDCl$_3$): δ 1.03 (d, 3H, ^3J = 6.9 Hz, CH$_3$), 2.76 (dd, 1H, ^2J = 15.4 Hz, ^3J = 2.2 Hz, H-4), 3.00-3.06 (m, 1H, H-3), 3.23 (dd, 1H, ^2J = 15.4 Hz, ^3J = 6.9 Hz, H-4'), 6.86 (s, 1H, H-1), 7.16-7.22 (m, 2H, Ar H), 7.36 (m, 1H, Pyr. H-5), 7.92 (dt, 1H, ^3J = 7.9 Hz, ^4J = 1.6 Hz, Pyr. H-4), 8.52 (dd, 1H, ^3J = 4.7 Hz, ^4J = 1.9 Hz, Pyr. H-6), 8.85 (d, 1H, ^4J = 1.9 Hz, Pyr. H-2).

IR: ν_{max} = 3020, 2962, 2924, 1564, 1453, 1216 cm^{-1}.

MS: m/z = 222 (MH$^+$).

$C_{16}H_{15}N$ (221.30)·HCl·0.43H_2O

	C	H	N
Calc.	72.45	6.41	5.28
Obs.	72.30	6.00	5.31

3-(4-Ethyl-3,4-dihydronaphthalen-2-yl)pyridine (60)

Synthesized from 4-ethyl-2-pyridin-3-yl-1,2,3,4-tetrahydronaphthalen-1-ol **60a**.

Purification: CC (dichloromethane/methanol 98:2).

Yield 55%.

Beige solid, mp 174 °C (HCl salt).

^{1}H NMR (CDCl$_3$): δ 0.92 (t, 3H, ^3J = 7.6 Hz, CH$_3$), 1.56-1.69 (m, 2H, CH$_2$), 2.68 (dd, 1H, ^2J = 16.4 Hz, ^3J = 3.8 Hz, H-3), 2.83-2.86 (m, 1H, H-4), 2.93 (dd, 1H, ^2J = 16.4 Hz, ^3J = 2.5 Hz, H-3'), 6.86 (d, 1H, ^4J = 2.5 Hz, H-1), 7.16-7.22 (m, 4H, Ar H), 7.32-7.34 (m, 1H, Pyr. H-5), 7.84 (dt, 1H, ^3J = 7.9 Hz, ^4J = 1.6 Hz, Pyr. H-4), 8.52 (dd, 1H, ^3J = 4.7 Hz, ^4J = 1.6 Hz, Pyr. H-6), 8.82 (d, 1H, ^4J = 1.9 Hz, Pyr. H-2).

IR: ν_{max} = 3035, 2962, 2931, 1682, 1569, 1486, 1456, 1022 cm^{-1}.
MS: m/z = 236 (MH$^+$).

C$_{17}$H$_{17}$N (235.33)·HCl·0.19H$_2$O

	C	H	N
Calc.	74.21	6.73	5.09
Obs.	74.20	7.36	4.98

1-(1*H*-inden-2-yl)-1*H*-imidazole (61)

Synthesized from 2-(1*H*-imidazol-1-yl)indan-1-ol **61a**. The reaction was stirred for 4 hours.

Purification: CC (dichloromethane/methanol 97:3).
Yield: 70%.
Beige solid, mp 64 °C.

^{1}H NMR (CDCl$_3$): δ 3.87 (s, 2H, H-3), 6.78 (s, 1H, H-1), 7.22-7.24 (m, 2H, Im. H-4, Ar H), 7.30-7.33 (m, 2H, Im. H-5, Ar H), 7.38 (d, 1H, ^3J = 7.6 Hz, Ar H), 7.45 (d, 1H, ^3J = 7.6 Hz, Ar H), 8.09 (s, 1H, Im. H-2).

IR: ν_{max} = 2940, 1707, 1616, 1498, 1264, 1238 cm^{-1}.
MS: m/z = 183 (MH$^+$).

C$_{12}$H$_{10}$N$_2$ (182.23)

1-(3,4-dihydronaphthalen-2-yl)-1*H*-imidazole (62)

Synthesized from 2-(1*H*-imidazol-1-yl)-1,2,3,4-tetrahydronaphthalen-1-ol **62a**. The reaction was stirred for 4 hours.

Purification: CC (dichloromethane/methanol 98:2).

Yield: 96%.

Brown solid, mp 186 °C (HCl salt).

^{1}H NMR (CDCl$_3$): δ 2.83 (t, 2H, ^3J = 8.2 Hz, H-4), 3.08 (t, 1H, ^3J = 8.2 Hz, H-3), 6.57 (s, 1H, H-1), 7.12 (d, 1H, ^3J = 7.8 Hz, Ar H), 7.18-7.22 (m, 4H, Im. H-4, Ar H), 7.28 (s, 1H, Im. H-5), 7.95 (s, 1H, Im. H-2).

IR: ν$_{max}$ = 3006, 3990, 1650, 1484, 1295, 1045 cm^{-1}.

MS: *m/*z = 197 (MH$^+$).

C$_{13}$H$_{12}$N$_2$ (196.25)·HCl·0.82H$_2$O

	C	H	N
Calc.	63.08	5.96	11.32
Obs.	62.82	6.51	10.98

1-(6-methoxy-3,4-dihydronaphthalen-2-yl)-1*H*-imidazole (63)

Synthesized from 2-(1*H*-imidazol-1-yl)-6-methoxy-1,2,3,4-tetrahydronaphthalen-1-ol **63a**. The reaction was stirred for 4 hours.

Purification: CC (dichloromethane/methanol 98:2).

Yield: 54%.

White solid, mp 106 °C.

^{1}H NMR (CDCl$_3$): δ 2.79 (t, 2H, ^3J = 8.2 Hz, H-4), 2.96 (t, 1H, ^3J = 8.2 Hz, H-3), 3.75 (s, 3H, OCH$_3$), 6.76-6.77 (m, 2H, Ar H), 6.81 (s, 1H, H-1), 7.04 (s, 1H, Im. H-4), 7.07 (d, 1H, ^3J = 8.2 Hz, Ar H), 7.64 (s, 1H, Im. H-5), 8.10 (s, 1H, Im. H-2).

IR: v_{max} = 2924, 1729, 1646, 1604, 1495, 1459, 1298, 1253 cm^{-1}.

MS: m/z = 227 (MH$^+$).

$C_{14}H_{14}N_2O$ (226.28)·0.36H$_2$O

	C	H	N
Calc.	72.22	6.38	12.03
Obs.	72.16	6.63	11.68

Method 33

1-Methyl-2-pyridin-3-yl-1,2,3,4-tetrahydronaphthalen-1-ol (56a)

To a solution of 2-pyridin-3-yl-3,4-dihydronaphthalen-1-one **56b** (0.15 g, 0.65 mmol) in dry toluene (15 mL) was added methylmagnesium chloride, 3M in THF (0.44 mL, 1.31 mmol) dropwise under nitrogen atmosphere. After stirring at reflux for 3 hours and at room temperature overnight, an NH$_4$Cl solution was added. The mixture was extracted with ethyl acetate, dried (MgSO$_4$), filtered and evaporated *in vacuo*.

Purification: CC (dichloromethane/methanol 98:2).
Yield: 41%.
Colorless oil.

^{1}H NMR (CDCl$_3$): δ 1.07 (s, 3H, CH$_3$), 2.04-2.08 (m, 1H, H-3), 2.25-2.31 (m, 1H, H-3'), 2.96-2.30 (m, 2H, H-4), 3.28-3.31 (m, 2H, H-2, OH), 7.03 (d, 1H, ^3J = 7.9 Hz, Ar H), 7.12 (t, 1H, ^3J = 7.9 Hz, Ar H), 7.17 (t, 1H, ^3J = 7.9 Hz, Ar H), 7.56 (d, 1H, ^3J = 7.9 Hz, Ar H), 7.69-7.71 (m, 1H, Pyr. H-5), 8.14 (d, 1H, ^3J = 7.9 Hz, Pyr. H-4), 8.54 (d, 1H, ^3J = 5.4 Hz, Pyr. H-6), 8.65 (s, 1H, Pyr. H-2).

IR: v_{max} = 3316, 3065, 2934, 1687, 1603, 1428 cm^{-1}.

$C_{16}H_{17}NO$ (239.32)

1-Ethyl-2-pyridin-3-yl-1,2,3,4-tetrahydronaphthalen-1-ol (57a)

Synthesized from 2-pyridin-3-yl-3,4-dihydronaphthalen-1-one **56b** and ethylmagnesium bromide, 1M in THF.

Purification: CC (dichloromethane/methanol 99:1).

Yield: 20%.

Colorless oil.

^{1}H NMR (CDCl$_3$): δ 0.79 (t, 3H, CH$_3$), 1.58-1.65 (m, 1H, CH$_2$), 1.92-1.95 (m, 1H, H-3), 2.03-2.08 (m, 1H, CH$_2$), 2.32-2.37 (m, 1H, H-3), 2.91-2.93 (m, 2H, H-4), 3.15 (dd, 1H, ^3J = 11.6 Hz, ^3J = 3.0 Hz, H-2), 7.16 (d, 1H, ^3J = 7.6 Hz, Ar H), 7.22-7.28 (m, 3H, Ar H, Pyr. H-5), 7.51 (dd, 1H, ^3J = 7.6 Hz, ^4J = 1.8 Hz, Ar H), 7.70 (dt, 1H, ^3J = 7.6 Hz, ^4J = 1.8 Hz, Pyr. H-4), 8.49 (dd, 1H, ^3J = 4.9 Hz, ^4J = 1.8 Hz, Pyr. H-6), 8.54 (d, 1H, ^4J = 1.8 Hz, Pyr. H-2).

IR: ν_{max} = 3268, 2927, 1574, 1428,1262 cm^{-1}.

C$_{17}$H$_{19}$NO (253.35)

Method 34

3-(1-Methyl-3,4-dihydronaphthalen-2-yl)-pyridine (56)

A mixture of 1-methyl-2-pyridin-3-yl-1,2,3,4-tetrahydronaphthalen-1-ol **56a** (60 mg, 0.25 mmol) and HCl (1 mL) was stirred at 100°C for 2 hours. The reaction was poured in ice water and basified with a 6% NaOH solution. After extractions with dichloromethane, the organic layer was dried (MgSO$_4$), filtered and evaporated *in vacuo*.

Purification: CC (dichloromethane/methanol 97:3).

Yield: 63%.

Yellow solid, mp 174 °C (HCl salt).

^{1}H NMR (CDCl$_3$): δ 2.05 (s, 3H, CH$_3$), 2.57 (td, 2H, ^3J = 8.2 Hz, ^4J = 1.6 Hz, H-3), 2.92 (t, 2H, ^3J = 8.2 Hz, H-4), 7.19-7.23 (m, 2H, Ar H), 7.27 (t, 1H, ^3J = 7.6 Hz, Ar H), 7.38 (d, 1H, ^3J = 7.6 Hz, Ar H), 7.41-7.45 (m, 1H, Pyr. H-5), 7.72 (td, 1H, ^3J = 7.92 Hz, ^4J = 1.6 Hz, Pyr. H-4), 8.54 (dd, 1H, ^3J = 5.0 Hz, ^4J = 1.6 Hz, Pyr. H-6), 8.57 (s, 1H, Pyr. H-2).

IR: ν$_{max}$ = 3024, 2937, 2831, 1602, 1487, 1408, 1250 cm^{-1}.
MS: m/z = 222 (MH$^+$).

C$_{16}$H$_{15}$N (221.30)·HCl·0.19H$_2$O

	C	H	N
Calc.	73.59	6.32	5.36
Obs.	73.58	6.40	5.05

3-(1-Ethyl-3,4-dihydronaphthalen-2-yl)-pyridine (57)

Synthesized from 1-ethyl-2-pyridin-3-yl-1,2,3,4-tetrahydronaphthalen-1-ol **57a**.

Purification: CC (dichloromethane/methanol 99:1).
Yield 60%.
White solid, mp 141 °C (HCl salt).

^{1}H NMR (CDCl$_3$): δ 1.05 (t, 3H, ^3J = 7.6 Hz, CH$_3$), 2.47-2.54 (m, 4H, CH$_2$, H-3), 2.87 (t, 2H, ^3J = 7.6 Hz, H-4), 7.18-7.20 (m, 2H, Ar H), 7.24-7.27 (m, 1H, Ar H), 7.30-7.33 (m, 1H, Pyr. H-5), 7.38 (d, 1H, ^3J = 7.6 Hz, Ar H), 7.56 (dt, 1H, ^3J = 7.6 Hz, ^4J = 1.8 Hz, Pyr. H-4), 8.51-8.53 (m, 2H, Pyr. H-6, Pyr. H-2).

IR: ν$_{max}$ = cm^{-1}.
MS: m/z = 236 (MH$^+$).

C$_{17}$H$_{17}$N (235.33)·HCl·0.53H$_2$O

	C	H	N
Calc.	72.57	6.83	4.98
Obs.	72.48	6.79	4.86

Method 35

2-(1*H*-imidazol-1-yl)indan-1-one (61b)

A solution of 2-bromoindan-1-one **50c** (1.01 g, 4.79 mmol) and imidazole (1.63 g, 23.94 mmol) in DMF (20 mL) was stirred overnight at room temperature. The mixture was poured into ice water and extracted with dichloromethane. After washing exhaustively with water, the organic layer was dried (MgSO$_4$), filtered and evaporated *in vacuo*.

Purification: CC (dichloromethane/methanol 98:2).
Yield: 39%.
Yellow oil.

^{1}H NMR (CDCl$_3$): δ 3.32 (dd, 1H, ^2J = 17.2 Hz, ^3J = 5.4 Hz, H-3), 3.87 (dd, 1H, ^2J = 17.2 Hz, ^3J = 8.6 Hz, H-3), 5.06 (dd, 1H, ^3J = 8.6 Hz, ^3J = 5.4 Hz, H-2), 6.91 (s, 1H, Im. H-4), 7.12 (s, 1H, Im. H-5), 7.49 (t, 1H, ^3J = 7.6 Hz, Ar H), 7.54 (d, 1H, ^3J = 7.6 Hz, Ar H), 7.70 (s, 1H, Im. H-2), 7.73 (t, 1H, ^3J = 7.6 Hz, Ar H), 7.84 (d, 1H, ^3J = 7.6 Hz, Ar H).

IR: ν$_{max}$ = 3009, 1722, 1603, 1262 cm^{-1}.

C$_{12}$H$_{10}$N$_2$O (198.23)

2-(1*H*-imidazol-1-yl)-3,4-dihydronaphthalen-1(2*H*)-one (62b)

Synthesized from 2-bromo-3,4-dihydro-2*H*-naphthalen-1-one **51c**.

Purification: CC (dichloromethane/methanol 98:2).
Yield. 65%.
Yellow solid.

^{1}H NMR (CDCl$_3$): δ 2.62-2.69 (m, 2H, H-3), 3.22 (dt, 1H, ^2J = 17.0 Hz, ^3J = 3.8 Hz, H-4), 3.34-3.41 (m, 1H, H-4), 5.21 (dd, 1H, ^3J = 7.2 Hz, ^3J = 5.4 Hz, H-2), 7.22 (s, 1H, Im. H-4), 7.28 (s, 1H, Im. H-5), 7.34 (d, 1H, ^3J = 7.6 Hz, Ar H), 7.40 (t, 1H, ^3J = 7.9 Hz, Ar H), 7.59 (tt, 1H, ^3J = 7.6 Hz, ^4J = 1.6 Hz, Ar H), 8.04 (s, 1H, Im. H-2), 8.09 (d, 1H, ^3J = 7.9 Hz, Ar H).

IR cm^{-1}: ν_{max} 3061, 2959, 1700.

$C_{13}H_{12}N_2O$ (212.25)

2-(1*H*-imidazol-1-yl)-6-methoxy-3,4-dihydronaphthalen-1(2*H*)-one (63b)

Synthesized from 2-bromo-6-methoxy-3,4-dihydro-2*H*-naphthalen-1-one **53c**.

Purification: CC (dichloromethane/methanol 98:2).

Yield: 50%.

Yellow oil.

^{1}H NMR (CDCl$_3$): δ 2.59-2.63 (m, 2H, H-3), 3.14 (dt, 1H, ^2J = 16.7 Hz, ^3J = 3.8 Hz, H-4), 3.26-3.31 (m, 1H, H-4), 3.91 (s, 3H, OCH$_3$), 5.01 (m, 1H, H-2), 6.77 (s, 1H, Ar H), 6.91 (dd, 1H, ^3J = 8.8 Hz, ^4J = 2.2 Hz, Ar H), 6.98 (s, 1H, Im. H-4), 7.18 (s, 1H, Im. H-5), 7.78 (s, 1H, Im. H-2), 8.06 (d, 1H, ^3J = 8.5 Hz, Ar H).

IR cm^{-1}: ν_{max} = 3006, 2963, 2835, 1710.

$C_{14}H_{14}N_2O_2$ (242.28)

Method 36

Benzyl phosphonium salt (64a)

A mixture of benzylalcohol **64b** (0.50 g, 4.62 mmol) and triphenylphosphonium bromide (1.59 g, 4.62 mmol) in toluene (40 mL) was refluxed for 12 h under a nitrogen atmosphere. After cooling, the phosphonium salt **64a** was filtered off, washed with diethyl ether and air-dried. The salt was used for further reaction without purification.

Method 37

(*E*)/(*Z*)-3-Styrylpyridine (64-65)

A suspension of the phosphonium salt **64a** (0.76 g, 1.75 mmol), K_2CO_3 (2.42 g, 17.50 mmol), pyridine-3-carbaldehyde **67** (0.19 g, 1.75 mmol) and a few milligrams of 18-crown-6 in anhydrous dichloromethane (50 mL) was refluxed for 12 h. After washing with water, the organic layer was dried ($MgSO_4$), filtered and evaporated *in vacuo*. The two resulting isomers **64** and **65** were separated by column chromatography.

3-[(*E*)-2-phenylvinyl]pyridine (64)

Purification: CC (hexane/ethyl acetate 1:1).
Yield: 38%.
White solid, mp 81 °C.

^{1}H NMR (CDCl$_3$): δ 7.08 (d, 1H, ^3J = 16.4 Hz, CH-Ph), 7.20 (d, 1H, ^3J = 16.4 Hz, CH-Pyr), 7.31 (tt, 1H, ^3J = 7.6 Hz, ^4J = 1.3 Hz, Ar H), 7.35-7.40 (m, 3H, Pyr. H-5, Ar H), 7.54 (d, 2H, ^3J = 8.8 Hz, Ar H), 7,91 (dt, 1H, ^3J = 7.9 Hz, ^4J = 1.6 Hz, Pyr. H-4), 8.50 (dd, 1H, ^3J = 4.7 Hz, ^4J = 1.6 Hz, Pyr. H-6), 8.75 (d, 1H, ^4J = 1.9 Hz, Pyr. H-2).

IR: ν_{max} = 3022, 962 cm^{-1}.
MS: *m/z* = 182 (MH$^+$), 167, 115, 77, 51.

$C_{13}H_{11}N$ (181.24)

	C	H	N
Calc.	86.15	6.12	7.73
Obs.	86.26	6.03	7.10

3-[(*Z*)-2-phenylvinyl]pyridine (65)

Purification: CC (hexane/ethyl acetate 1:1).
Yield: 52%.

Colorless oil.

^{1}H NMR (CDCl$_3$): δ 6.48 (d, 1H, ^3J = 12.3 Hz, CH-Ph), 6.72 (d, 1H, ^3J = 12.3 Hz, CH-Pyr), 7.10-7.20 (m, 6H, Pyr. H-5, Ar H), 7.51 (dt, 1H, ^3J = 8.2 Hz, ^4J = 1.6 Hz, Pyr. H-4), 8.35 (dd, 1H, ^3J = 5.0 Hz, ^4J = 1.3 Hz, Pyr. H-6), 8.41 (d, 1H, ^4J = 1.6 Hz, Pyr. H-2).

IR: ν$_{max}$ = 3079, 3026, 704 cm^{-1}.
MS: m/z = 182 (MH$^+$), 167, 115, 77, 51.

C$_{13}$H$_{11}$N (181.24)·HCl

	C	H	N
Calc.	71.72	5.56	6.43
Obs.	71.69	5.75	6.08

B. Biological section

B.I. Materials and reagents

B.I.1. Apparatus

Cell counter CASY Model TT, from Schärfe System, Reutlingen

Phosphoimager system Fuji FLA-3000, from Raytest, Straubenhardt

Shaking incubator Unitron 25, from Infors, Stuttgart

Cell culture incubator Biosafe, from Revco, Ashville (USA)

Centrifuge universal 30 RF, from Hettich GmbH, Tuttlingen

Table centrifuge Micro 24-48 R, from Hettich GmbH, Tuttlingen

Ultracentrifuge 2330 Ultraspin 55 Hitachi, from Pharmacia LKB, Freiburg

Ultrasonic bath Sonsorex RK 106 Transistor, from Bandelin, Berlin

Mixer Krups Promix 200, from Electro Meyer, Saarbrücken

Sonicator Sonopuls HD60, from Bandelin, Berlin

Ultra-turrax T25, from IKA-Labortechnik, Staufen

HPLC system Agilent 1100:

 Agilent 1100 autosampler

 PDA detector

 ChemStation software, from Agilent, Waldbronn

 Nucleodur C18ec column (120-3,3 × 12.5 mm), from Macherey Nagel, Düren

LC-MS/MS:

 Surveyor autosampler

 Surveyor MS pump

 TSQ quantum triple quadrupole mass spectrometer, from ThermoFinnigan,

 San Jose, (USA)

 Gravity C_{18} column (3 μm, 125×3.0 mm)

 Gravity C_{18} column (3 μm, 10×3.0 mm), from Macherey-Nagel, Düren

β-counter type 1209 Rackbeta Wallac, from Pharmacia LKB, Freiburg

γ-counter Wallac CliniGamma 1272, from Wallac, Turku (Finnland)

B.I.2. Materials

24-Well cell culture plates, from Nunc International, Roskilde (Denmark)

HPTLC plates 20 cm×10 cm, Silicagel 60F$_{254}$, from Merck, Darmstadt

[^{14}C]-imaging plate BAS-MS2340, from Raytest, Straubenhardt

Corticosterone and aldosterone RIA, from DRG Instruments GmbH, Marburg

Androstenedione and DHEA ELISA, from ibl-hamburg, Hamburg

Cortisol EIA, from Cayman Chemical, Ann Arbor (USA)

B.I.3. Chemicals and reagents

ACTH$_{1-24}$, from Synacthen Depot$^{®}$, Novartis, Basel (Switzerland)

[^{14}C]11-deoxycorticosterone, from NEN, Boston (USA)

Progesterone, from Sigma, Deisenhofen

NADPH, NADP^{+}, from Sigma, Deisenhofen

Glucose-6-phosphate, from Sigma, Deisenhofen

Glucose-6-phosphate dehydrogenase, from Serva, Heidelberg

[1β-^{3}H]androstenedione, from Perkin Elmer Life & Analytical Sciences, Boston (USA)

Fadrozole, from Ciba-Geigy, Basel (Switzerland)

DMEM:Ham's F12 medium, from c.c. pro, Neustadt

Streptomycin, from c.c. pro, Neustadt

ITS^{+}Premix, from BD Biosciences, Bedford (USA)

Ultroser SF, from Ciphergen, Cergy-Saint-Christophe (France)

B.I.4. Biological material

Male Sprague-Dawley rats, from Harlan Winkelmann, Borchen

Male Wistar rats, from Harlan Winkelmann, Borchen

Rat microsomes (male pool), from Gentest, Woburn, (USA)

B.II. In vitro methods

B.II.1. CYP11B2 inhibition assay in fission yeast (Ehmer *et al.*, 2002)

Screening Assay in Fission Yeast.

To test the inhibitory activity of compounds towards human CYP11B2, fission yeast *Schizosaccheromyces pombe* PE1, recombinantly expressing the target enzyme, was used. A fission yeast suspension (diluted to cellular density 3 x 10^7 cells/ml) was prepared from a freshly grown culture using a modified EMMG (EMM: Edinburgh Minimal Medium) medium at pH 7.4. A 500 µl-aliquot of the yeast suspension was preincubated with the potential inhibitor dissolved in ethanol, in a final concentration of 500 nM for 15 min at 32 °C. Control samples contained 1% ethanol. The enzymatic reaction was started by addition of [^{14}C]-deoxycorticosterone (60 mCi/mmol) in a final concentration of 100 nM. Sample tubes were shaken horizontally at 32 °C for 6 h. The enzyme reaction was quenched by the addition of the same volume of ethyl acetate to extract the steroids. The organic layer was pipetted into a fresh cup and evaporated to dryness. The residue was dissolved in 10 µl chloroform and the conversion of the substrate into corticosterone was analyzed by HPTLC as described below.

HPTLC Analysis and phosphoimaging of radiolabeled steroids.

The redissolved steroids were transferred onto an HPTLC plate (20 cm x 10 cm, silica gel 60F$_{254}$) with concentrating zone and developed two times using the solvent chloroform/methanol/water (300:20:1). For the CYP11B2 reaction, 11-deoxycorticosterone, corticosterone, 18-hydroxycorticosterone and aldosterone were used as reference. Subsequently, imaging plates (BAS MS2340) were exposed to the HPTLC plates for 48 h. The imaging plates were scanned using the phosphoimager system Fuji FLA 3000 and the steroids were quantified.

B.II.2. CYP11B2 and CYP11B1 inhibition assay in V79 cells (Ehmer *et al.*, 2002)

V79 MZh 11B1 and V79 MZh 11B2 cells were grown on 24-well cell culture plates with 1.9 cm^2 culture area per well until confluence. Before testing, the DMEM culture medium was removed and 400 µl of fresh DMEM, containing the inhibitor in at least three different concentrations for determining the IC$_{50}$ value, was added to each well. After a preincubation step of 60 min at 37°C, the reaction was started by the addition of 100 µl of DMEM

containing the substrate 11-deoxycorticosterone (20 µM, containing 6 nCi of $[4\text{-}^{14}C]$11-deoxycorticosterone, dissolved in ethanol). The V79 MZh 11B1 cells were incubated for 120 min, whereas the V79 MZh 11B2 cells were incubated for 40 min. Controls were treated in the same way without inhibitor. Enzyme reactions were stopped by extracting the supernatant with ethyl acetate. Samples were centrifuged and the solvent was pipetted into fresh cups. The solvent was evaporated, and the steroids were redissolved in 10 µl of chloroform and analyzed by HPTLC as described above.

B.II.3. Assay using the adrenocortical tumor cell line NCI-H295R

NCI-H295R cells were obtained from the American Type Culture Collection (CRL-2128). The cells were maintained in 90 mm culture dishes in DMEM:Ham's F12 medium supplemented with 2% Ultroser SF, 100 units/ml penicillin, 0.1 mg/ml streptomycin and 1% ITS$^+$ Premix (containing 6.25 µg/ml insulin, 6.25 µg/ml transferrin, 6.25 ng/ml selenium, 1.25 mg/ml BSA and 5.35 g/ml linoleic acid). Cells were grown at 37°C under an atmosphere of 95% air/5% CO_2. All cells used for the experiments were between passages 10 and 40.

For testing compounds, cells were seeded at a cellular density of 1 x 10^6 cells per well in 24-well plates. After 48 h, the monolayers were confluent. To determine the effect of the compounds, medium was removed and replaced by fresh DMEM:Ham's F12. Aldosterone secretion was stimulated by the addition of 20 mM K$^+$ in presence of the potential inhibitor in a final concentration of 1 µM. At the end of the 6 h incubation time, the medium was removed to fresh tubes and stored at - 20 °C until assayed. Aldosterone, cortisol, androstenedione and DHEA contents were quantified using commercially available ELISA kits according to the manufacturer's instructions. Each experiment was performed in triplicate.

B.II.4. CYP17 *E. coli* inhibition assay (Ehmer *et al.*, 2000)

Enzyme preparation

Recombinant *E. coli* pJL17/OR coexpressing human CYP17 and rat NADPH-P450-reductase were grown and stored as described (Ehmer *et al.*, 2000). For isolation of membrane fractions, 5 mL of bacterial suspension with an OD$_{578}$ of 50 were washed using phosphate buffer (0.05 M, pH 7.4, 1 mM MgCl$_2$, 0.1 mM EDTA and 0.1 mM dithiothreitol). Bacteria were harvested by centrifugation (2,000 × g) and the pellet was resuspended in 10 mL of ice cold TES buffer (0.1 M tris-acetate, pH 7.8, 0.5 mM EDTA, 0.5 M sucrose). Lysozyme was added with 10 mL

of ice cold water resulting in a concentration of 0.2 mg/mL followed by incubation for 30 min on ice with continuous shaking. Spheroplasts were harvested by centrifugation (12,000 × g for 10 min), and resuspended in 4 mL of ice cold phosphate buffer (the same as described above plus 0.5 mM phenylmethylsulfonyl fluoride (PMSF)).

After freezing and thawing, samples were sonicated on ice (pulse 20s on, 30s off, five times), using a sonicator Sonopuls HD60 at maximum power. Unbroken cells and debris were pelleted at 3,000 × g for 7 min, and the supernatant was centrifuged at 50,000 × g for 20 min at 4°C. The membrane pellet was resuspended in 2 mL of phosphate buffer (the same as described above) with 20% glycerol using and ultra-turrax T25. Protein content was determined by the method of Lowry. (Lowry et al., 1951) Aliquots of this preparation, which generally had a content of about 5 mg protein per mL, were stored at -70°C until used.

Determination of the inhibitory activity towards CYP17

The 17α-hydroxylase activity of CYP17 was determined by measuring the conversion of progesterone into 17α-hydroxyprogesterone and the byproduct 16α-hydroxyprogesterone. The assay was performed as follows: A solution of 6.25 nmol progesterone (in 5 µL methanol) in 140 µL phosphate buffer (0.05 M, pH 7.4, 1 mM $MgCl_2$, 0.1 mM EDTA and 0.1 mM dithiothreitol), 50 µL NADPH generating system (in phosphate buffer with 10 mM $NADP^+$, 100 mM glucose-6-phosphate and 2.5 units of glucose-6-phosphate dehydrogenase) and inhibitor (in 5 µL DMSO) was preincubated at 37°C for 5 min. Control cups were supplemented with 5 µL DMSO without inhibitor. The reaction was started by adding 50 µL of 1:5 diluted membrane suspension in phosphate buffer (0.8-1 mg protein per mL). After mixing, incubation was performed for 30 min at 37°C. Subsequently the reaction was stopped with 50 µL 1 N HCL.

Extraction of steroids was performed by addition of 1 mL ethyl acetate and vigorous shaking for 1 min. After a centrifugation step (2,500 × g for 5 min) the organic phase (0.9 mL) was transferred into a cup containing 0.25 mL of incubation buffer and 50 µL 1 N HCl and mixed again. After centrifugation, 0.8 mL ethyl acetate solution was evaporated to dryness in a fresh cup. Samples were dissolved in 50 µL water and methanol (1:1) and analyzed by HPLC.

HPLC was performed using an Agilent 1100 HPLC system with PDA detector and a Nucleodur C18ec column (120-3,3 × 12.5 mm), which was run at 40°C. The steroids were eluted under isocratic conditions using 10 mM sodium acetate buffer (adjusted to pH 4.0 with acetic acid):methanol (30:70; V/V) at a flow rate of 0.70 ml/min and pressure of about 25 MPa. For each analysis 25 µL were injected by an Agilent 1100 autosampler, which was

thermostated at 4°C. UV absorbance was monitored at 240 and 254 nm. The products 17α-hydroxyprogesterone and 16α-hydroxyprogesterone eluted with retention times of 1.8 and 2.8 min, respectively. Elution time for the substrate progesterone was 4.7 min. Peak areas were determined by integration of the resulting chromatograms using ChemStations software. Substrate conversion was determined by product versus substrate peak areas. The inhibitory potencies were calculated using the diminished substrate conversion by the inhibitors.

$$\%Inhibition = \left[\left[\frac{\sum Peakareas(inhibitorincubation)}{\sum Peakareas(controlincubation)}\right]-1\right]\cdot(-100)$$

B.II.5. CYP19 inhibition assay

Preparation of aromatase CYP19

The enzyme was obtained from the microsomal fraction of freshly delivered human term placental tissue according to the procedure of Thompson and Siiteri. (Thompson and Siiteri, 1974) The isolated microsomes were suspended in a minimum volume of phosphate buffer (0.05 M, pH 7.4, 20% glycerol). Additionally, DTT (dithiothreitol, 10 mM) and EDTA (1 mM) was added to protect the enzyme from degradation. Protein concentration was determined by the method of Lowry et al. (Lowry et al., 1951) and usually was about 35 mg/mL.

Determination of IC$_{50}$ values for CYP19

This assay was performed similar to the described methods (Graves *et al.*, 1979; Foster *et al.*, 1983), monitoring enzyme activity by measuring the ^3H_2O formed from [1β-^3H]androstenedione during aromatization. Each incubation tube contained 15 nM [1β-^3H]androstenedione (0.08 µCi), 485 nM unlabeled androstenedione, 2 mM NADPH, 20 mM glucose-6-phosphate, 0.4 units of glucose-6-phosphate dehydrogenase and inhibitor (0-100 µM) in phosphate buffer (0.05 M, pH 7.4). The test compounds were dissolved in DMSO and diluted with buffer. The final DMSO concentration in the control and inhibitor incubation was 2%. Each tube was preincubated for 5 min at 30°C in a water bath. Microsomal protein was added to start the reaction (0.1 mg). The total volume for each incubation was 0.2 mL. The reaction was terminated by the addition of 200 µL of a cold aqueous dextran-coated charcoal (DCC) suspension (2%), the vials were shaken for 20 min and centrifuged at 1.500 × g for 5

min to separate the charcoal absorbed steroids. The supernatant was assayed for ^3H_2O by counting in a scintillation mixture using a LKB-Wallac β-counter. The calculation of the IC_{50} values was performed by plotting the percent inhibition versus the concentration of inhibitor on a semi-log plot. From this the molar concentration causing 50% inhibition was calculated.

B.II.6. Permeability screening in Caco-2 transport experiments.

Caco-2 cell culture and transport experiments were performed according to Yee (Yee, 1997) with small modifications. Cell culture time was reduced to 10 days by increasing seeding density from $6.3 \cdot 10^4$ to $1.65 \cdot 10^5$ cells per well. Four reference compounds, atenolol, ketoprofene, testosterone and erythromycin, were used in each assay for validation of the transport properties of the Caco-2 cells. The compounds were applied to the cells as mixtures (cassette dosing) to increase the throughput of the permeability tests. The starting concentration of the compounds in the donor compartment was 50 μM in buffer containing either 1% ethanol or DMSO. After a preincubation step of 20 min at 37°C, the reaction was started. The 12-well Transwell plates (Corning Costar) were stirred (20 rpm) at 37°C. Samples were taken from the acceptor side after 60, 120 and 180 minutes and from the donor side after 0 and 180 minutes. Each experiment was run in triplicate. Monolayer integrity was checked by measuring the transepithelial electrical resistance (TEER) before the transport experiments and by measuring lucifer yellow permeability after each assay. All samples were analyzed by LS-MS/MS after 1:1 dilution with buffer of the opposite transwell chamber containing 2% acetic acid. The apparent permeability coefficients (P_{app}) were calculated using the equation $P_{app} = dQ/dt \cdot A \cdot c_0$, where dQ/dt is the mass appearance rate in the acceptor compartment, A is the surface area of the transwell membrane, and c_0 is the initial concentration in the donor compartment.

B.II.7. Metabolic stability assay.

The assay was performed with rat microsomes. The incubation solution contained a microsomal suspension of 0.15 mg of protein per ml in phosphate buffer 0.1 M, pH 7.4 and a NADPH-regenerating system (NADP 1 mM, glucose-6-phosphate 5 mM, glucose-6-phosphate dehydrogenase 5U/ml, $MgCl_2$ 5 mM). After pre-incubation at 37°C, the reaction was initiated by the addition of the test compound (a stock solution of 10 mM in 100% DMSO, diluted in phosphate buffer 0.1 mM, pH7.4 to reach the final concentration of 5 μM

with 2% of final DMSO concentration). After 0, 30, 60, 120 and 180 minutes, 200 μl from the incubation was removed, added to ethyl acetate, containing the internal standard (I.S.) methoxyverapamil (5 μM), to stop the reaction and vortexed for 5 min. A negative control was run in addition, to which the microsomes were boiled and inactivated with ethyl acetate prior to addition of the test compound.

For each test compound, appropriate dilutions of the stock solutions were prepared with phosphate-buffer (0.1 M, pH 7.4) containing rat microsomes to reach the working solutions of 0.5, 2.5 and 5 μM. Ethyl acetate containing the I.S. was added.

Subsequently, the water layer was frozen in a bath of acetone/dry ice for each sample and standard. The organic layer was removed and evaporated in under nitrogen stream. The residue was reconstituted in 200 μL mixture of acetonitrile and 10 mM ammonium acetate/2% methanol (1:1, v:v).

Sample quantification was performed by LC-MS/MS: 20 μL of each sample was separated on a Xterra^{TM}MS C$_{18}$ (5 μm, 50x2.1 mm, Waters) analytical column with a pre-column (Xterra^{TM}MS C$_{18}$ 5 μm, 50x2.1 mm, Waters) using a gradient elution with 10 mM ammonium acetate/2% methanol as aqueous phase (A) and acetonitrile as organic phase (B). The following gradient was applied: %B (t (min)), 20(0)-90(3)-20(3.5-6). The most intensive product ion of the [M+H]$^{+}$ was used to quantify the compounds in the selected reaction monitoring mode (SRM). A second product ion was taken as a qualifier.

Table 1. Overview of MS conditions used for quantification

Compound	Mw (g/mol)	[M+H]$^{+}$ (m/z)	Monitoring ion (m/z)	Qualifier ion (m/z)	Collision energy (V)
21	271.7	236.2	214.1	199.1	10/35
53	273.7	238.2	216.1	201.1	10/35
I.S.	484.6	485.2	311.1	143.0	25/25

For the metabolite identification the gradient time was extended and the eluent mix gradient set as follows: %B (t (min)), 20(0)-85(6-7)-20(7.5-10). The data acquisition was performed in the auto scan mode switching between the full scan mode (80-500 Da) and MS^{2} dependent scan mode (collision energy 20V) by selection of the most intensive ion. In a second step, MS^{2} spectra (collision energy 35V) were taken from the parent compounds and the putative metabolite signals assigned in the first step.

Calibration curves, represented by the plot of the peak area ratios of the compound to I.S. (Y axis) versus the concentration of the calibration standards (0.5, 2.5 and 5 μM) were generated using quadratic regression. Sample concentrations were calculated from the resulting peak area of the compound to I.S. and the regression equation of the calibration curve. The percentage of the remaining test compound was plotted against the corresponding time points, and the half-life time derived by a standard fit of the data.

B.III. *In vivo* methods

B.III.1. Determination of aldosterone and corticosterone in rats (adapted from Häusler *et al.*, 1989).

Male Sprague Dawley rats, weighting 200-300g, were housed in a temperature-controlled room (20-22°C) and maintained in a 12h light/12h dark cycle for 14 days in absolute quietness. The animals were divided into 4 groups, 2 control groups (unstimulated and ACTH-stimulated animals) and 2 test groups. On the first day of the experiment, the animals received at 16.00 h a subcutaneous injection of 1 mg/kg of a depot preparation of $ACTH_{1-24}$; the unstimulated test group received a physiological NaCl solution. At 8.00 h on the second day of the experiment, the test groups received the test solution of fadrozole or the inhibitor intraperitoneally. The 2 control groups received only a NaCl solution. The test compounds were dissolved in physiological NaCl solution (maximum of 25% DMSO for solubility). Two hours later, all animals were killed through cervical dislocation and blood was collected by heart punction. The blood samples were left at room temperature for 60 min and plasma was obtained by centrifugation (5000 rpm for 30 min). The supernatans (serum) was then pipetted and aliquoted. For the analysis of the samples, an aldosterone RIA and corticosterone RIA were performed and subsequently, the samples were measured using the γ-counter.

For the determination of the inhibitory effect of the inhibitor on the aldosterone and corticosterone level in rat, the following group divisions were made:

Group	Amount of rats	ACTH application	Inhibitor application
Unstimulated control	7	NaCl sol., s.c.	NaCl sol., i.p.
ACTH stimulated control	8	ACTH, s.c.	NaCl sol., i.p.
Inhibitor (0.4 mg/kg/KG)	7	ACTH, s.c.	Inhibitor, i.p.
Inhibitor (4.0 mg/kg/KG)	7	ACTH, s.c.	Inhibitor, i.p.

The doses of the selected compounds were calculated by comparing their IC_{50} values with the IC_{50} value of fadrozole. A dose of 4mg/kg of test compound pro 1 nM of its IC_{50} value was used in the animal test.

B.III.2. *In vivo* pharmacokinetic evaluation in catheterized rats (peroral cassette dosing)

Preparation and administration of cassette dosing solutions

Male Wistar rats, weighting 260-305 g, were housed in a temperature-controlled room (20-22°C) and maintained in a 12h light/12h dark cycle. Twelve hours prior to compound application food was removed, water was available *ad libitum*. The rats were anaesthetised with a ketamine (135mg/kg)/xylazine (10mg/kg) mixture, and cannulated with silicone tubing via the right jugular vein. Prior to the first blood sampling, animals were connected to a counterbalanced system and tubing to perform blood sampling in the freely moving rat.

Immediately before application, the cassette dosing solution was prepared by adding equal volumes of stock solutions (5mg/ml in DMSO:NaCl (10:90)) of 5 test compounds to end up with a final concentration of 1mg/ml for each compound. This cassette dosing solution was perorally applied to 4 rats with an injection volume of 5ml/kg. Blood samples (0.2 ml) were taken at -1h, 1h, 2h, 4h, 6h, 8h, 10h and 24h after application. Blood samples collected in heparinised tubes were centrifuged at 3000 g for 10 min at 4°C and plasma was harvested and kept at -20°C until LC-MS analysis.

Measurement of plasma drug levels

The HPLC system consisted of a MS pump (Surveyor) and an autosampler (Surveyor). Mass spectrometry was performed on a TSQ quantum triple quadrupole mass spectrometer equipped with an electrospray (ESI) interface (Thermo-Finnigan) and connected to a PC running the standard software Xcalibur. Pump flow rate was set at 350μl/min and the compounds were separated on a Gravity C_{18} (3 μm, 125×3.0 mm, Macherey-Nagel) analytical column with a pre-column (Gravity C_{18}, 3 μm, 10×3.0 mm) in gradient mode. A gradient elution with 10 mM ammonium acetate/0.1% formic acid as aqueous phase (A) and acetonitrile as organic phase (B) was used. The following gradient was applied: %B (t (min)), 90(0)-97(3-4.4)-90(4.5-7). The most intensive product ion of the $[M+H]^+$ was used to quantify the compounds in the selected reaction monitoring mode (SRM). Compound **57** was used as an internal standard.

100µl acetonitrile containing the internal standard (**57**, 150ng/ml) was added to 50µl of rat plasma sample to precipitate plasma proteins. Samples were then vigorously shaken and, after 5 min at room temperature, centrifuged for 10 min at 6000g and 20°C. An aliquot of the particle-free supernatant was transferred to 200µl sampler vials and subsequently subjected to LC-MS/MS.

The system was calibrated in the operating range of 4 to 3200 ng/ml using quadratic least squares regression as mathematical model. To improve the accuracy of determined plasma drug levels, the 1/X weighted regression equations were used. The regression was fitted on the group mean profiles and the pharmacokinetic parameters were calculated using a non compartment model software (PK solutions 2.0, Summit Research Services, Montrose, USA).

C. Protein modelling and docking.

Using the recently resolved human cytochrome CYP2C9 structure (PDB code: 1OG5) (Williams *et al.*, 2003) as template, a homology model was build and refined for CYP11B2. Selected compounds were docked into the refined homology model using FlexX-Pharm (Hindle *et al.*, 2002). Pharmacophore constraints were applied to ensure the right binding mode of the inhibitors (a Fe(heme)-N(inhibitor) interaction was required). Based on the docked protein-inhibitor complex structures, molecular dynamics simulations were performed using the GROMOS96 force field (Scott *et al.*, 1999) and the GROMACS program (Lindahl *et al.*, 2001). A cut-off of 14Å was used for the non-bonded interactions and a time step of 1fs was applied. The temperature was maintained by weak coupling to an external bath with a temperature coupling relaxation time of 0.1ps. Throughout the simulations the bond lengths were constrained to ideal values using the LINCS procedure. No explicit solvent was included, because of the mainly hydrophobic character of the binding pocket. Potential solvent molecules were approximated through a dielectric constant of 4.0. Harmonic restraints were applied to all backbone atoms outside the binding pocket (all residues, except residues 106-133, 212-221, 244-262, 305-332, 372-384, and 483-494). The systems were heated from 0-300K over 200ps and afterwards 800ps of molecular dynamics were performed at 300K.

VIII. References

Aktories, K.; Förstermann, U.; Hofmann, F. B.; Starke, K. *Allgemeine und Spezielle Pharmakologie und Toxikologie.* W. Forth, W.; Henschler, D.; Rummel, W., Eds.; Urban & Fischer Verlag, **2005**.

Belkina, N. V.; Lisurek, M.; Ivanov, A. S.; Bernhardt, R. Modelling of three-dimensional structures of cytochromes P450 11B1 and 11B2. *J. Inorg. Biochem.* **2001**, *87*, 197-207.

Böttner, B.; Bernhardt, R. Changed ratios of glucocorticoids/mineralocorticoids caused by point mutations in the putative I-helix regions of CYP11B1 and CYP11B2. *Endocr. Res.* **1996**, *22*, 455-461.

Böttner, B.; Schrauber, H.; Bernhardt, R. Engineering a mineralocorticoid- to a glucocorticoid-synthesizing cytochrome P450. *J. Biol. Chem.* **1996**, *271*, 8028-8033.

Bredereck, H.; Theilig, G. Imidazolsynthesen mit Formamid. *Chem. Ber.* **1953**, *86*, 88-96.

Brilla, C. G.; Matsubara, L. S.; Weber, K. T. Anti-aldosterone treatment and the prevention of myocardial fibrosis in primary and secondary hyperaldosteronism. *J. Mol. Cell. Cardiol.* **1993**, *25*, 563-575.

Brilla, C. G. Renin-angiotensin-aldosterone system and myocardial fibrosis. *Cardiovasc. Res.* **2000a**, *47*, 1-3.

Brilla, C. G. Aldosterone and myocardial fibrosis in heart failure. *Herz* **2000b**, *25*, 299-306.

Bureik, M.; Lisurek, M.; Bernhardt, R. The human steroid hydroxylases CYP11B1 and CYP11B2. *Biol. Chem.* **2002a**, *383*, 1537-1551.

Bureik, M.; Schiffler, B.; Hiraoka, Y.; Vogel, F.; Bernhardt, R. Functional expression of human mitochondrial CYP11B2 in fission yeast and identification of a new internal electron transfer protein, etp1. *Biochemistry* **2002b**, *41*, 2311-2321.

Bureik, M.; Hubel, K.; Dragan, C. A.; Scher, J.; Becker, H.; Lenz, N.; Bernhardt, R. Development of test systems for the discovery of selective human aldosterone synthase (CYP11B2) and 11beta-hydroxylase (CYP11B1) inhibitors. Discovery of a new lead compound for the therapy of congestive heart failure, myocardial fibrosis and hypertension. *Mol. Cell. Endocrinol.* **2004**, *217*, 249-254.

Cheng, Y.; Prusoff, W. H. Relationship between the inhibition constant (K_i) and the concentration of inhibitor which causes 50 per cent inhibition (IC_{50}) of an enzymatic reaction. *Biochem. Pharmacol.*, **1973**, *22*, 3099-3108.

Defaye, G.; Piffeteau, A.; Delorme, C.; Marquet, A. Specific inhibition of the last steps of aldosterone biosynthesis by 18-vinylprogesterone in bovine adrenocortical cells. *J. Steroid Biochem. Mol. Biol.* **1996**, *57*, 141-147.

Demers, L. M.; Melby, J. C.; Wilson, T. E.; Lipton, A.; Harvey, H. A.; Santen, R. J. The effects of CGS 16949A, an aromatase inhibitor on adrenal mineralocorticoid biosynthesis. *J. Clin. Endocrinol. Metab.* **1990**, *70*, 1162-1166.

Denner, K.; Doehmer, J.; Bernhardt, R. Cloning of CYP11B1 and CYP11B2 from normal human adrenal and their functional expression in COS-7 and V79 chinese hamster cells. *Endocr. Res.* **1995a**, *21*, 443-448.

Denner, K.; Vogel, R.; Schmalix, W.; Doehmer, J.; Bernhardt, R. Cloning and stable expression of the human mitochondrial cytochrome P45011B1 cDNA in V79 chinese hamster cells and their application for testing of potential inhibitors. *Pharmacogenetics* **1995b**, *5*, 89-96.

Ehmer, P. B.; Jose, J.; Hartmann, R. W. Development of a simple and rapid assay for the evaluation of inhibitors of human 17α-hydroxylase-$C_{17,20}$-lyase (P450c17) by coexpression of P450c17 with NADPH-cytochrome-P450-reductase in *Escherichia coli*. *J. Steroid Biochem. Mol. Biol.* **2000**, *75*, 57-63.

Ehmer, P. B.; Bureik, M.; Bernhardt, R.; Müller, U.; Hartmann, R. W. Development of a test system for inhibitors of human aldosterone synthase (CYP11B2): screening in fission yeast and evaluation of selectivity in V79 cells. *J. Steroid Biochem. Mol. Biol.* **2002**, *81*, 173-179.

Foster, A. B.; Jarman, M.; Leung, C. S.; Rowlands, M. G.; Taylor, G. N. Analogues of aminoglutethimide: selective inhibition of cholesterol side-chain cleavage. *J. Med. Chem.* **1983**, *26*, 50-4.

Gazdar, A. F.; Oie, H. K.; Shackleton, C. H.; Chen, T. R.; Triche, T. J.; Myers, C. E.; Chrousos, G. P.; Brennan, M. F.; Stein, C. A.; La Rocca, R. V. Establishment and characterization of a human adrenocortical carcinoma cell line that expresses multiple pathways of steroid biosynthesis. *Cancer Res.* **1990**, *50*, 5488-5496.

Gomez-Sanchez, C. E.; Zhou, M. Y.; Cozza, E. N.; Morita, H.; Foecking, M. F.; Gomez-Sanchez, E. P. Aldosterone biosynthesis in the rat brain. *Endocrinology* **1997a**, *138*, 3369-3373.

Gomez-Sanchez, C. E.; Gomez-Sanchez, E. P.; Foecking, M. F.; Zhou, M. Y. Inhibition of steroidogenesis in rat adrenal cells by 18-ethynyldeoxycorticosterone: evidence for an alternative pathway of aldosterone biosynthesis. *J. Steroid Biochem. Mol. Biol.* **1997b**, *62*, 207-212.

Graves, P. E.; Salhanick, H. A. Stereoselective inhibition of aromatase by enantiomers of aminoglutethimide. *Endocrinology* **1979**, *105*, 52-7.

Hartmann, R. W.; Batzl, C. Aromatase inhibitors. Synthesis and evaluation of mammary tumor inhibiting activity of 3-alkylated 3-(4-aminophenyl)piperidine-2,6-diones. *J. Med. Chem.* **1986**, *29*, 1362-1369.

Hartmann, R. W. Selective inhibition of steroidogenic P450 enzymes: current status and future perspectives. *Eur. J. Pharm. Sci.* **1994**, *2*, 15-16.

Hartmann, R. W.; Bayer, H.; Grün, G.; Sergejew, T.; Bartz, U.; Mitrenga, M. Pyridyl-substituted tetrahydrocyclopropa[a]naphthalenes: highly active and selective inhibitors of P450 arom. *J. Med. Chem.* **1995**, *38*, 2103-2111.

Hartmann, R. W.; Müller, U.; Ehmer, P. B. Discovery of selective CYP11B2 (aldosterone synthase) inhibitors for the therapy of congestive heart failure and myocardial fibrosis. *Eur. J. Med. Chem.* **2003**, *38*, 363-366.

Hatakeyama, H.; Miyamori, I.; Fujita, T.; Takeda, Y.; Takeda, R.; Yamamoto, H. Vascular aldosterone. Biosynthesis and a link to angiotensin II-induced hypertrophy of vascular smooth muscle cells. *J. Biol. Chem.* **1994**, *269*, 24316-24320.

Häusler, A.; Monnet, G.; Borer, C.; Bhatnagar, A. S. Evidence that corticosterone is not an obligatory intermediate in aldosterone biosynthesis in the rat adrenal. *J. Steroid Biochem.* **1989**, *34*, 567-570.

Hindle, S. A.; Rarey, M.; Buning, C.; Lengauer, T. Flexible docking under pharmacophore type constraints. *J. Comput. Aided Mol. Des.* **2002**, *16*, 129-49.

Hutschenreuter, T. U.; Ehmer, P. B.; Hartmann, R. W. Synthesis of hydroxy derivatives of highly potent non-steroidal CYP 17 inhibitors as potential metabolites and evaluation of their activity by a non cellular assay using recombinant human enzyme. *J. Enzyme Inhib. Med. Chem.* **2004**, *19*, 17-32.

Jagdmann, G. E.; Munson, H. R.; Gero, T. W. A mild efficient procedure for the conversion of carboxylic acid esters to primary amides using formamide/methanolic sodium methoxide. *Synth. Commun.* **1990**, *20*, 1203-1208.

Juurlink, D. N.; Mamdani, M. M.; Lee, D. S.; Kopp, A.; Austin, P. C.; Laupacis, A.; Redelmeier, D. A. Rates of hyperkalemia after publication of the Randomized Aldactone Evaluation Study. *New Engl. J. Med.* **2004**, *351*, 543-551.

Kauffmann, T.; Tigler, D.; Woltermann, A. Kondensation von 3-(1-Imidazolyl)-und-(1-Benzimidazolyl)-chinolin zu Heterocyclotetraaromaten. *Chem. Ber.* **1982**, *115*, 452-458.

Kawamoto, T.; Mitsuuchi, Y.; Toda, K.; Yokoyama, Y.; Miyahara, K.; Miura, S.; Ohnishi, T.; Ichikawa, Y.; Nakao, K.; Imura, H.; et al. Role of steroid 11 beta-hydroxylase and steroid 18-hydroxylase in the biosynthesis of glucocorticoids and mineralocorticoids in humans. *Proc. Natl. Acad. Sci. USA* **1992**, *89*, 1458-1462.

Khan, N. U.; Movahed, A. The role of aldosterone and aldosterone-receptor antagonists in heart failure. *Rev. Cardiovasc. Med.* **2004**, *5*, 71-81.

Kirton, S. B.; Kemp, C. A.; Tomkinson, N. P.; St-Gallay, S.; Sutcliffe, M. J. Impact of incorporating the 2C5 crystal structure into comparative models of cytochrome P450 2D6. *Proteins* **2002**, *49*, 216-231.

Lam, P. Y. S.; Clark, C. G.; Saubern, S.; Adams, J.; Winters, M. P.; Chan, D. M. T.; Combs, A. New aryl/heteroaryl C-N bond cross-coupling reactions via arylboronic acid/cupric acetate arylation. *Tetrahedron Lett.* **1998**, *39*, 2941-2944.

Lan, J.; Chen, L.; Yu, X.; You, J.; Xie, R. A simple copper salt catalysed the coupling of imidazole with arylboronic acids in protic solvent. *Chem. Commun.* **2004**, *2*, 188-189.

Li, W.; Nelson, D. P.; Jensen, M. S.; Hoerrner, R. S.; Cai, D.; Larsen, R. D.; Reider, P. J. An improved protocol for the preparation of 3-pyridyl- and some arylboronic acids. *J. Org. Chem.* **2002**, *67*, 5394-5397.

Lijnen, P.; Petrov, V. Induction of cardiac fibrosis by aldosterone. *J. Mol. Cell. Cardiol.* **2000**, *32*, 865-879.

Lindahl, E.; Hess, B.; van der Spoel, D. GROMACS 3.0: a package for molecular simulation and trajectory analysis. *J. Mol. Mod.* **2001**, *7*, 306-317.

Lipinski, C. A.; Lombardo, F.; Dominy, B. W.; Feeney, P. J. Experimental and computational approaches to estimate solubility and permeability in drug discovery and development settings. *Adv. Drug Del. Rev.* **1997**, *23*, 3-25.

Lowry, O. H.; Rosebrough, N. J.; Farr, A. L.; Randall, R. J. Protein measurement with the Folin phenol reagent. *J. Biol. Chem.* **1951**, *193*, 265-75.

MacFadyen, R. J.; Barr, C. S.; Struthers, A. D. Aldosterone blockade reduces vascular collagen turnover, improves heart rate variability and reduces early morning rise in heart rate in heart failure patients. *Cardiovasc. Res.* **1997**, *35*, 30-34.

Meunier, B.; de Visser, S. P.; Shaik, S. Mechanism of oxidation reactions catalyzed by cytochrome p450 enzymes. *Chem. Rev.* **2004**, *104*, 3947-3980.

Mewshaw, R. E.; Edsall, R. J.; Yang, C.; Harris, H. A.; Keith, J. C.; Albert, L. M. (Wyeth). Substituted phenyl naphthalenes as estrogenic agents. PCT Int. Appl. WO03051805, 2003.

Miyaura, N.; Suzuki, N. Palladium-catalyzed cross-coupling reactions of organoboron compounds. *Chem. Rev.* **1995**, *95*, 2457-2483.

Müller-Vieira, U. Selektive Inhibition der Aldosteronsynthase (CYP11B2) als neues Therapiekonzept bei Herzinsuffizienz und Myokard-Fibrose: Entwicklung und Evaluierung einer Teststrategie unter besonderer Berücksichtigung der adrenocorticalen Tumorzelllinie NCI-H295R, Dissertationsschrift, Universität des Saarlandes, **2005**.

Murphy, R. A.; Kung, H. F.; Kung, M. P.; Billings, J. Synthesis and characterization of iodobenzamide analogues: potential D-2 dopamine receptor imaging agents. *J. Med. Chem.* **1990**, *33*, 171-178.

Negash, K.; Nichols, D. E.; Watts, V. J.; Mailman, R. B. Further definition of the D1 dopamine receptor pharmacophore: synthesis of trans-6,6a,7,8,9,13b-hexahydro-5H-benzo[d]naphth[2,1-b]azepines as rigid analogues of beta-phenyldopamine. *J. Med. Chem.* **1997**, *40*, 2140-2147.

Ngarmukos, C.; Grekin, R. J. Nontraditional aspects of aldosterone physiology. *Am. J. Physiol. Endocrinol. Metab.* **2001**, *281*, E1122-1227.

Omura, T.; Sato, R. The Carbon Monoxide-Binding Pigment of Liver Microsomes. I. Evidence for its hemoprotein nature. *J. Biol. Chem.* **1964**, *239*, 2370-2378.

Pitt, B.; Zannad, F.; Remme, W. J.; Cody, R.; Castaigne, A.; Perez, A.; Palensky, J.; Wittes, J. The effect of spironolactone on morbidity and mortality in patients with severe heart failure. *New Engl. J. Med.* **1999**, *341*, 709-717.

Pitt, B.; Remme, W.; Zannad, F.; Neaton, J.; Martinez, F.; Roniker, B.; Bittman, R.; Hurley, S.; Kleiman, J.; Gatlin, M. Eplerenone, a selective aldosterone blocker, in patients with left ventricular dysfunction after myocardial infarction. *New Engl. J. Med.* **2003**, *348*, 1309-1321.

Pitzele, B. S.; Moormann, A. E.; Gullikson, G. W.; Albin, D.; Bianchi, R. G.; Palicharla, P.; Sanguinetti, E. L.; Walters, D. E. Potential antisecretory antidiarrheals. 1. Alpha 2-adrenergic aromatic aminoguanidine hydrazones. *J. Med. Chem.* **1988**, *31*, 138-144.

Raff, H.; Findling, J. W. A physiologic approach to diagnosis of the Cushing syndrome. *Ann. Intern. Med.* **2003**, *138*, 980-991.

Rainey, W. E.; Bird, I. M.; Mason, J. I. The NCI-H295 cell line: a pluripotent model for human adrenocortical studies. *Mol. Cell. Endocrinol.* **1994**, *100*, 45-50.

Riechers, H.; Albrecht, H. P.; Amberg, W.; Baumann, E.; Bernard, H.; Bohm, H. J.; Klinge, D.; Kling, A.; Muller, S.; Raschack, M.; Unger, L.; Walker, N.; Wernet, W. Discovery and optimization of a novel class of orally active nonpeptidic endothelin-A receptor antagonists. *J. Med. Chem.* **1996**, *39*, 2123-2128.

Rupasinghe, S.; Baudry, J.; Schuler, M. A. Common active site architecture and binding strategy of four phenylpropanoid P450s from Arabidopsis thaliana as revealed by molecular modeling. *Protein Eng.* **2003**, *16*, 721-731.

Sani, M. Chronic heart failure. Diagnosis of the disease. *Hospital Pharmacist* **2004**, *11*, 87-91.

Satoh, M.; Nakamura, M.; Saitoh, H.; Satoh, H.; Akatsu, T.; Iwasaka, J.; Masuda, T.; Hiramori, K. Aldosterone synthase (CYP11B2) expression and myocardial fibrosis in the failing human heart. *Clin. Sci. (Lond.)* **2002**, *102*, 381-386.

Scott, W. R. P.; Hünenberger, P. H.; Tironi, I. G.; Mark, A. E.; Billeter, S. R.; Fennen, J.; Torda, A. E.; Huber, T.; Krüger, P.; and van Gunsteren W. F. The GROMOS Biomolecular Simulation Program Package. *J. Phys. Chem. A* **1999,** *103*, 3596-3607.

Shupnik, M.; Chrousos, G. P.; Siragy, H. Chapter 37: Glucocorticoids and mineralocorticoids. In *Human pharmacology: Molecular to clinal*. Brody, T.; Larner, J.; Minneman, K., Eds.; Mosby. **1998**, 485-497.

Silvestre, J. S.; Robert, V.; Heymes, C.; Aupetit-Faisant, B.; Mouas, C.; Moalic, J. M.; Swynghedauw, B.; Delcayre, C. Myocardial production of aldosterone and corticosterone in the rat. *J. Biol. Chem.* **1998**, *273*, 4883-4891.

Silvestre, J. S.; Heymes, C.; Oubénaissa, A.; Robert, V.; Aupetit-Faisant, B.; Carayon, A.; Swynghedauw, B.; Delcayre, C. Activation of cardiac aldosterone production in rat myocardial infarction. *Circulation* **1999**, *99*, 2694-2701.

Soll, R. M.; Dollings, P. M.; Mitchell, R. D.; Hafner, D. A. Guanabenz-related amidinohydrazones: potent non-azole inhibitors of aldosterone biosynthesis. *Eur. J. Med. Chem.* **1994**, *29*, 223-232.

Stewart, P. Chapter III: Adrenal cortex: renin-angiotensin-aldosterone axis and hypertension. In *Comprehensive clinical endocrinology*. Besser, G.; Thorner, M., Eds., Mosby. **2002**, 1-10.

Stewart, P. M. Tissue-specific Cushing's syndrome, 11beta-hydroxysteroid dehydrogenases and the redefinition of corticosteroid hormone action. *Eur. J. Endocrinol.* **2003**, *149*, 163-8.

Struthers, A. D. Aldosterone escape during angiotensin-converting enzyme inhibitor therapy in chronic heart failure. *J. Card. Fail.* **1996**, *2*, 47-54.

Takeda, Y.; Miyamori, I.; Yoneda, T.; Iki, K.; Hatakeyama, H.; Blair, I. A.; Hsieh, F. Y.; Takeda, R. Production of aldosterone in isolated rat blood vessels. *Hypertension* **1995**, *25*, 170-173.

Taymans, S. E.; Pack, S.; Pak, E.; Torpy, D. J.; Zhuang, Z.; Stratakis, C. A. Human CYP11B2 (aldosterone synthase) maps to chromosome 8q24.3. *J. Clin. Endocrinol. Metab.* **1998**, *83*, 1033-1036.

Thompson, E. A., Jr.; Siiteri, P. K. Utilization of oxygen and reduced nicotinamide adenine dinucleotide phosphate by human placental microsomes during aromatization of androstenedione. *J. Biol. Chem.* **1974**, *249*, 5364-5372.

Ulmschneider, S.; Müller-Vieira, U.; Mitrenga, M.; Hartmann, R. W.; Oberwinkler-Marchais, S.; Klein, C. D.; Bureik, M.; Bernhardt, R.; Antes, I.; Lengauer, T. Synthesis and evaluation of imidazolylmethylenetetrahydronaphthalenes and imidazolylmethyleneindanes: potent inhibitors of aldosterone synthase. *J. Med. Chem.* **2005a**, *48*, 1796-1805.

Ulmschneider, S.; Müller-Vieira, U.; Klein, C. D.; Antes, I.; Lengauer, T.; Hartmann, R. W. Synthesis and evaluation of (pyridylmethylene)tetrahydronaphthalenes/-indanes and structurally modified derivatives: potent and selective inhibitors of aldosterone synthase. *J. Med. Chem.* **2005b**, *48*, 1563-1575.

Voets, M.; Müller-Vieira, U.; Marchais-Oberwinkler, S.; Hartmann, R. W. Synthesis of amidinohydrazones and evaluation of their inhibitory effect towards aldosterone synthase (CYP11B2) and the formation of selected steroids. *Arch. Pharm. Pharm. Med. Chem.* **2004**, *337*, 411-416.

Voets, M.; Antes, I.; Scherer, C.; Müller-Vieira, U.; Biemel, K.; Barassin, C.; Marchais-Oberwinkler, S.; Hartmann, R. W. Heteroaryl-substituted naphthalenes and structurally modified derivatives: Selective inhibitors of CYP11B2 for the treatment of congestive heart failure and myocardial fibrosis. *J. Med. Chem.* **2005**, *48*, 6632-6642.

Wächter, G. A.; Hartmann, R. W.; Sergejew, T.; Grun, G. L.; Ledergerber, D. Tetrahydronaphthalenes: influence of heterocyclic substituents on inhibition of steroid enzymes P450 arom and P450 17. *J. Med. Chem.* **1996**, *39*, 834-841.

Weber, K. T.; Janicki, J. S.; Pick, R.; Capasso, J.; Anversa, P. Myocardial fibrosis and pathological hypertrophy in the rat with renovascular hypertension. *Am. J. Cardiol.* **1990**, *65*, 1-7.

Weber, K. T. Aldosterone in congestive heart failure. *New Engl. J. Med.* **2001**, *345*, 1689-1697.

Weindel, K.; Lewicka, S.; Vecsei, P. Inhibitory effects of the novel anti-aldosterone compound mespirenone on adrenocortical steroidogenesis in vitro. *Arzneimittelforschung* **1991**, *41*, 946-949.

Williams, P. A.; Cosme, J.; Ward, A.; Angove, H. C.; Matak Vinkovic, D.; Jhoti, H. Crystal structure of human cytochrome P450 2C9 with bound warfarin. *Nature* **2003**, *424*, 464-468.

Woo, L. W.; Howarth, N. M.; Purohit, A.; Hejaz, H. A.; Reed, M. J.; Potter, B. V. Steroidal and nonsteroidal sulfamates as potent inhibitors of steroid sulfatase. *J. Med. Chem.* **1998**, *41*, 1068-1083.

Yee, S. In vitro permeability across Caco-2 cells (colonic) can predict in vivo (small intestinal) absorption in men – fact or myth. *Pharm. Res.* **1997**, *14*, 763-766.

Young, T. E.; Amstutz, E. D. Halogen reactivities. Certain heterocyclic iminohalide systems. *J. Am. Chem. Soc.* **1951**, 4773-4775.

Zannad, F.; Alla, F.; Dousset, B.; Perez, A.; Pitt, B. Limitation of excessive extracellular matrix turnover may contribute to survival benefit of spironolactone therapy in patients with congestive heart failure: insights from the randomized aldactone evaluation study (RALES). Rales Investigators. *Circulation* **2000**, *102*, 2700-2706.